VOL 11
ISSUE 2
MAR 2026

eMetN METEOR JOURNAL

eJournal for meteor observers www.emetn.net

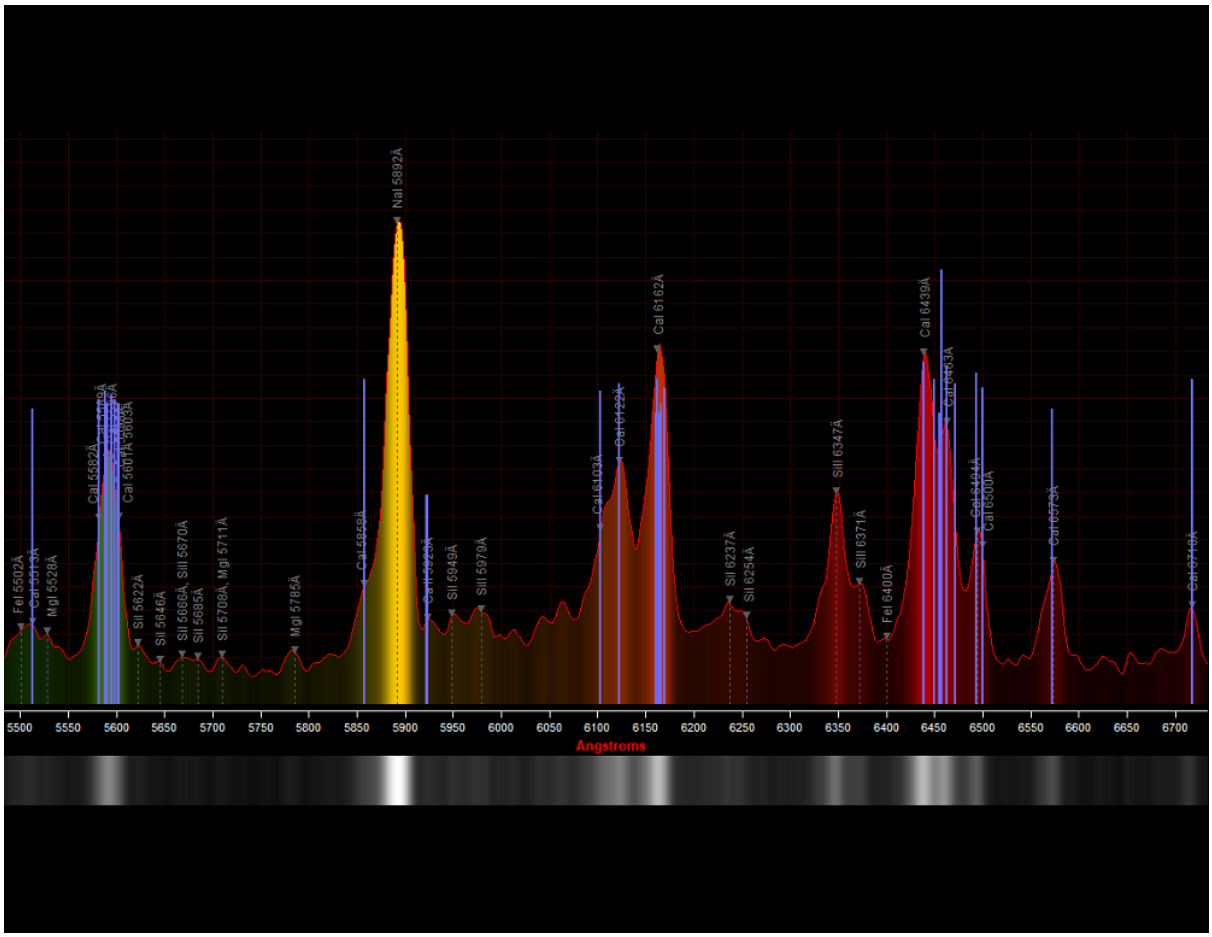

On 16 January 2024, the cameras of the Belarusian Meteor Network recorded a meteor spectrum with exceptionally intense calcium emission lines. Spectroscopic analysis confirms the meteoroid's affiliation with the HED clan (Howardites–Eucrites–Diogenites), most likely classifying it as a eucrite. Author: Harachka Yury.

ISSN 3041 - 4261

Contents

Global Meteor Network report 2025

Paul Roggemans[1], Peter Campbell-Burns[2], Milan Kalina[3], Mark McIntyre[4], James M. Scott[5], Damir Šegon[6], and Denis Vida[7]

[1] **Pijnboomstraat 25, 2800 Mechelen, Belgium**
paul.roggemans@gmail.com

[2] **UK Meteor Observation Network, Cavendish Gardens, Fleet, Hampshire, United Kingdom**
peter@campbell-burns.com

[3] **Czech Astronomical Society, Ondrejov, Czech Republic**
milank2010@gmail.com

[4] **UK Meteor Observation Network and Tackley Observatory, United Kingdom**
mark.jm.mcintyre@cesmail.net

[5] **Department of Geoscience, Aarhus University, Høegh-Guldbergs Gade 2. DK-8000 Aarhus C, Denmark**
jscott@geo.au.dk

[6] **Astronomical Society Istra Pula, Park Monte Zaro 2, 52100 Pula, Croatia**
Višnjan Observatory, Istarska 5, 52463 Višnjan, Croatia
damir@astro.hr

[7] **Department of Physics and Astronomy, University of Western Ontario, Richmond Street, London, N6A 3K7, Ontario, Canada**
Institute for Earth and Space Exploration, University of Western Ontario, Perth Drive, London, N6A 5B8, Ontario, Canada
dvida@uwo.ca

A status report is presented for the Global Meteor Network. Since the start of the network, 2847823 meteoroid orbits have been collected up to the end of 2025 and 418 different meteor showers have been identified among these orbits. During 2025, more than 236 new GMN cameras started contributing successfully paired meteors. 966063 orbits were collected in 2025. The development of the Global Meteor Network in different regions is described. The coverage of the camera fields of view is shown on maps.

1 Introduction

Over the past 20 years many video camera networks were created, both regional and national, with the aim of obtaining meteor trajectories through multi-station registrations. Most of these networks specialize in fireballs and meteorite droppers, others are dedicated to a fainter magnitude range comparable to what visual observers used to cover. The orbit data obtained by these networks brought a tremendous progress in our knowledge of meteoroid streams.

The Global Meteor Network is the most recent development in this domain. Its success builds on the many years of expertise of the Croatian Meteor Network, one of the pioneers in the field of video meteor observations and the origin of GMN (Gural and Šegon, 2009). Based on RMS, the significantly improved Raspberry Pi solution introduced by Zubović et al. (2015) and Vida et al. (2016), the Global Meteor Network began its operation at the end of 2018; its first six cameras located in New Mexico used IP cameras controlled by a Raspberry running its own dedicated software and reduction pipeline (Vida et al., 2021). GMN became the fastest growing meteor video network with 76 operational cameras at the end of 2019, 172 at the end of 2020, 390 at the end of 2021, 700 at the end of 2022, 1066 in 2023, 1213 by the end of 2024 and 1365 in 2025. In 2025 236 new cameras got operational, 12 non-active in 2024 resumed capturing, 96 cameras active in 2024 did no longer contribute in 2025, bringing the total number of decommissioned cameras at 254.

2 Joining the Global Meteor Network

More information about this project can be found in Vida et al. (2020a; 2020b; 2021; 2022) and on the GMN website[1]. An informative video presentation about the Global Meteor Network project can be watched online[2]. Many sites and participants are still waiting to find partners to improve the coverage on their cameras. New participants are welcome to expand the network.

To obtain a camera for participation you can either buy it plug&play from Istrastream[3], or you buy the components and build your own camera for about 250 US$ or ~200 €. The RMS cameras are easy to build and operate. If you are

[1] https://globalmeteornetwork.org/
[2] https://www.youtube.com/watch?v=MAGq-XqD5Po
[3] https://globalmeteornetwork.org/?page_id=136

interested in building your own camera you can find detailed instructions online[4].

The daily status of most (not all) meteor stations can be followed on the GMN weblog[5] or on the GMN status pages per country[6]. The GMN results and data are publicly available and daily updated online[7]. The UK meteor network maintains a comprehensive archive[8] and daily update[9] which may inspire others. Their Wiki-page[10] may be helpful to people outside the UK as well as their github repos[11,12].

The meteor map[13] is an online tool for visualizing meteor cameras and ground tracks of observed meteors. Each participant can check the results obtained with each camera, check the location of the meteor trajectories and combinations with other camera stations. The tool has been described in an article (Dijkema, 2022). Milan Kalina developed another tool, "Meteorview[14]" to map meteor trajectories with several extra functionalities described in an article (Kalina, 2024). Steve Matheson generated the GMN Status viewer that rapidly summarizes the nightly activity[15].

As the static maps of camera FoVs presented in this report sometimes become overcrowded, the aggregated kml files valid for end of 2025 can be downloaded[16]. The individual up-to-date kml-files for all GMN cameras can be downloaded from the GMN website[17]. Camera operators are encouraged to point new cameras in function of optimal coverage with other cameras. Opening the kml files in Google Earth allows to toggle cameras on and off to get a better view on the actual coverage. Make sure to compare kml files at the same elevation (e.g. 100 km) and prevent 3D perspective by changing the properties in the Google Earth graphical interface to "clamped to ground" instead of the default setting "absolute".

If you have a dark site with a free view and if you are looking to make a scientifically useful contribution, with just five RMS cameras with 3.6 mm lenses (FoV 88° × 47°) pointed at azimuths 0° (North), 70°, 140°, 220° and 290°, between 35° and 40° elevation, you cover all the sky except your zenith. Avoid pointing a camera at the meridian (180° azimuth) as the transit of the Full Moon will take full effect in this position. Also do not point lower than 35° elevation; there are no meteors in the local scenery, trees or buildings. If you use 6 mm lenses, recommended where light pollution is an issue, you need six RMS to cover the sky with a royal overlap between the camera edges. Six cameras with 6 mm lenses (FoV 54° × 30°) pointed at azimuths 30°, 90°, 150°, 210°, 270° and 330°, between 35° and 40° elevation, would make you a key video meteor hub in the network. Building the cameras at the cost of the purchased components, or bought plug & play, both remain a low-cost project, affordable to many amateurs, observatories and societies.

The unavailability of Raspberry Pi because of production limitations due to Covid in former years has been meanwhile solved, but inspired people to explore alternative systems for unavailable RPi's. A cheap Linux PC can handle multiple cameras and a system has been developed to operate multiple GMN cameras using a single PC. Read the article written by Harman et al. (2023) and check the Wiki pages for the latest updates.

3 Annual GMN meeting 2025 (online)

The annual meeting of the Global Meteor Network got more than 100 people participating online from around the globe. The meeting took place in two sessions on February 8–9, 2025 in order to allow people from all time zones to participate. 23 presentations were given with enough time for questions and discussions; each session ended with a Q&A workshop session. Both sessions can be viewed online:

- Session 1 – February 8, 16^h00^m – 21^h00^m UTC[18]
- Session 2 – February 9, 00^h00^m – 03^h00^m UTC[19]

4 GMN camera coverage

The aim of the GMN is to cover all latitudes and longitudes to assure a global coverage of meteor activity in order to let no unexpected meteor event pass unnoticed. This is an ambitious goal especially for a project that depends for most efforts entirely on volunteers' work. In this report we describe the progress that was made by GMN during 2025 in different regions of the world. The status of the camera coverage is illustrated with maps showing the fields of view intersected at an elevation of 100 km in the atmosphere, projected and clamped to the ground. This way the actual overlap between the camera fields is shown without any effects of 3D perspectives. Where possible the camera ID has been mentioned on the plots.

Many RMS cameras with 4 mm optics have the horizon at the bottom of their field of view, which results in a huge camera field at 100 km elevation. Rather few meteors will be bright enough to get registered near the horizon. The large distance between the camera station and the meteor also reduces the chances to obtain a useable triangulation. The number of paired meteors at the outskirts of these large camera fields is very small. However, cameras pointing so low towards the horizon turn out to be very useful regarding

[4] https://globalmeteornetwork.org/wiki/index.php?title=Build_A_Camera
[5] https://globalmeteornetwork.org/weblog/
[6] https://globalmeteornetwork.org/status/
[7] https://globalmeteornetwork.org/data/
[8] https://www.ukmeteornetwork.org
[9] https://www.ukmeteors.co.uk/live/index.html
[10] https://github.com/markmac99/ukmon-pitools/wiki
[11] https://github.com/markmac99/ukmon-pitools
[12] https://github.com/markmac99/UKmon-shared
[13] https://tammojan.github.io/meteormap/
[14] https://www.meteorview.net/
[15] https://globalmeteornetwork.org/status/
[16] https://www.emeteornews.net/wp-content/uploads/2026/01/all_kml_2025.zip
[17] https://globalmeteornetwork.org/data/kml_fov/
[18] https://www.youtube.com/watch?v=_tV7WBo0RrQ
[19] https://www.youtube.com/watch?v=z23aJeIg7wo

obtaining coverage at lower heights where meteorite dropping fireballs end their visible path. When looking for camera overlap, it is strongly recommended to look for an optimized overlap between cameras. An interesting study on this topic for the New Mexico Meteor Array has been published by Mroz (2021). Camera operators are encouraged to optimize their camera overlap.

The number of multi-station events mentioned per country corresponds to the number of orbits, unless an orbit was based on camera data from different countries, then it was counted once for each country. This can also be visualized on the MeteorMap[20] (Dijkema, 2022) or with MeteorView[21] (Kalina, 2024). The current camera coverage is presented per country or per region for reason of readability. To consider the real overlap for most European countries it is necessary to look at the camera coverage of neighboring countries. In several regions the camera coverage is too dense to visualize it in a single map. We strongly recommend to view the camera FoVs in Google Earth. The required kml-files have been grouped per country and can be downloaded for: Asia, Europe, North America, Africa and Southern hemisphere.

4.1 AQ – Antarctica

On 11 March 2025 the first seven cameras were installed on Antarctica. No multiple station meteors and thus no orbits were obtained yet as there isn't yet a partner station for coverage (*Figure 1*).

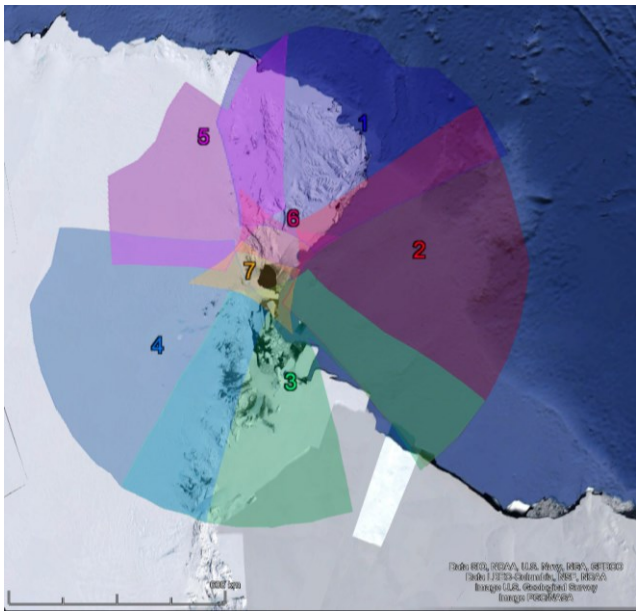

Figure 1 – GMN camera fields in 2025 intersected at 100 km elevation, for cameras active at Antarctica.

4.2 AT – Austria

Austria got its first RMS (AT0002), generating orbits since August 2024, and the second camera (AT0004) had its first orbits in October 2024, good for 1701 orbits in 2024. The two Austrian GMN cameras contributed 4819 orbits in 2025, most of which combined with GMN cameras in neighboring countries, see *Figure 2*.

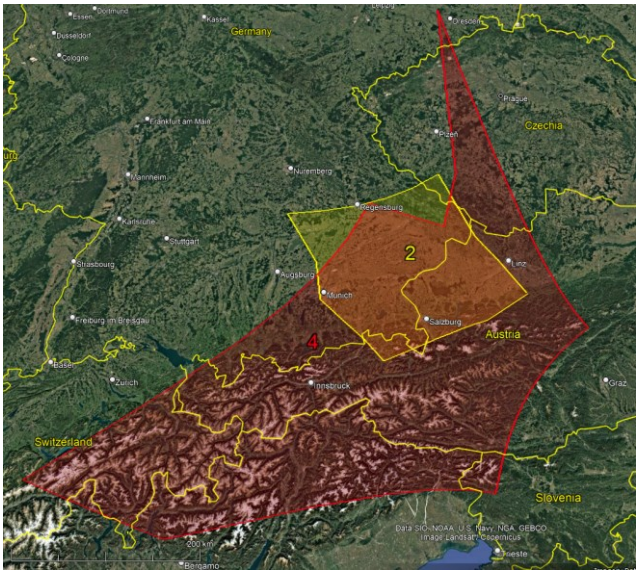

Figure 2 – GMN camera fields in 2025 intersected at 100 km elevation, for cameras active in Austria.

4.3 AU – Australia

The first 31 meteor orbits by Australian RMS cameras were registered in September 2021 when the first five cameras got ready to harvest meteors. By the end of 2021, twelve cameras managed to obtain 1871 orbits in the final 4 months of 2021. A first breakthrough was achieved in 2022 as the number of RMS cameras in Australia increased to 29, good for 12460 orbits in 2022. The expansion of the network accelerated even more in 2023 with 66 operational cameras contributing 40712 orbits making Australia one of the major contributors to GMN. Nine cameras active in 2023 were decommissioned, but 31 new cameras were added in 2024. This resulted in a major breakthrough in 2024 with 88 cameras contributing as many as 100044 orbits (see *Table 5*). Eleven cameras stopped capturing, while four new were installed and one resumed capture in 2025. With 82 cameras 111155 orbits were obtained. The all-time number of orbits is 266242 for Australia, twenty cameras were decommissioned so far.

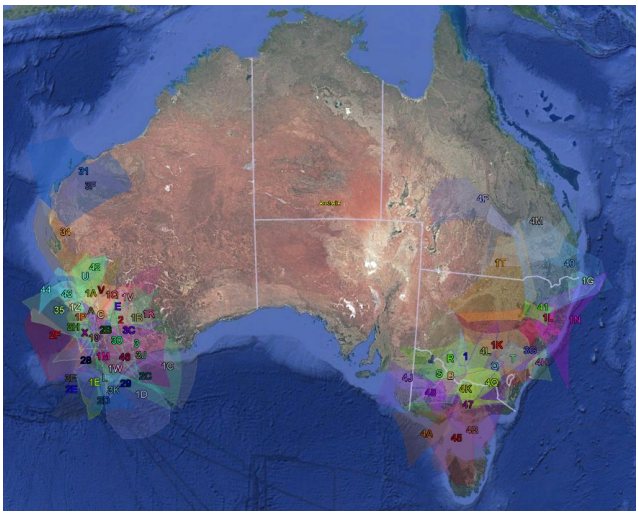

Figure 3 – GMN camera fields in 2025 intersected at 100 km elevation, for cameras active in Australia, global view.

[20] https://tammojan.github.io/meteormap/

[21] https://www.meteorview.net/

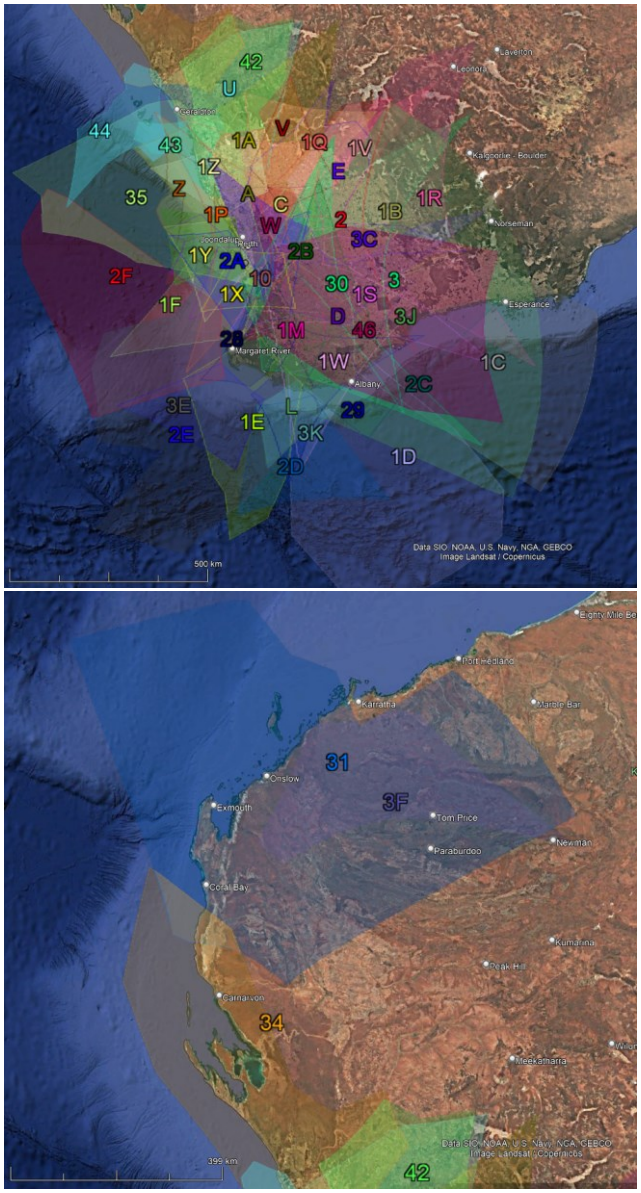

Figure 4 – GMN cameras in Western Australia in 2025 intersected at 100 km elevation. Note the expansion further north.

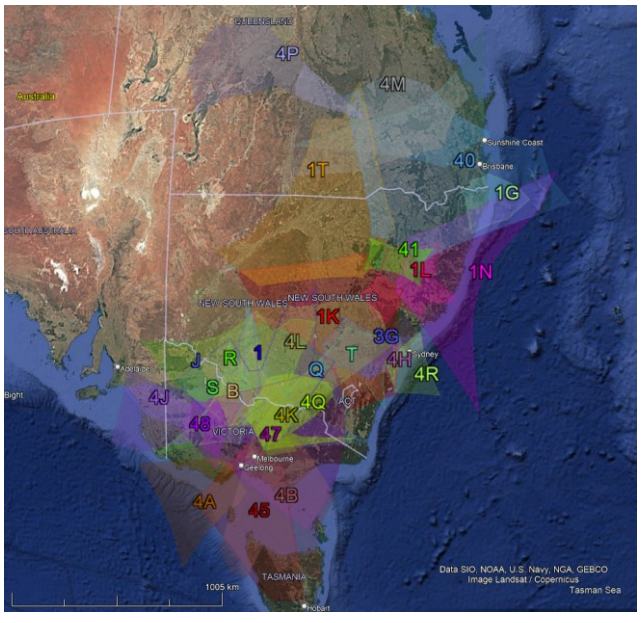

Figure 5 – GMN camera fields in 2025 intersected at 100 km elevation, for cameras active in Australia (eastern states).

Most cameras were installed in Western Australia (*Figure 4*) but there is also a dense network in the eastern states of Australia with more cameras in Victoria, Queensland and New South Wales (*Figure 5*). Australia being a very large country, describing its camera networks as a single network is a bit unfair as it is like considering all European countries as a single EU network.

4.4 BA – Bosnia and Herzegovina

In August 2025, five GMN cameras were installed in Bosnia and Herzegovina with a lot of overlap with cameras in Croatia and other countries in the region (*Figure 6*). In the final months of the year, these cameras contributed 6153 orbits to GMN.

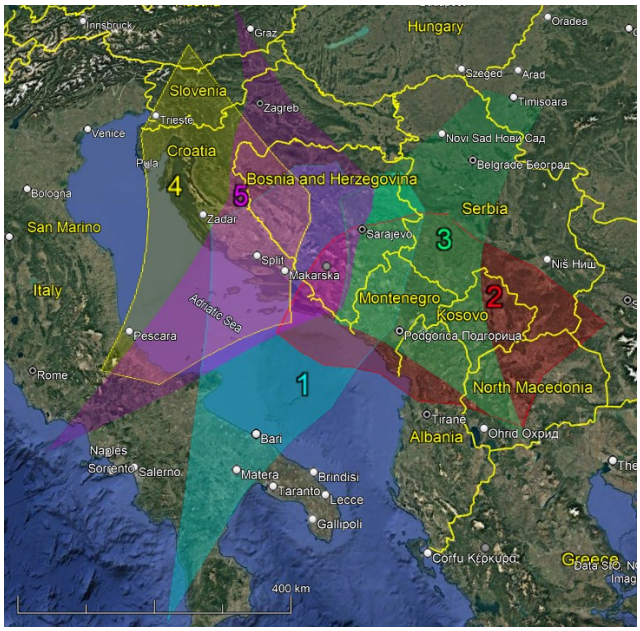

Figure 6 – GMN camera fields in 2025 intersected at 100 km elevation, for cameras active in Bosnia and Herzegovina.

4.5 BE – Belgium

Belgium had its first RMS cameras operational in early 2019. *Figure 7* shows the GMN coverage at the end of 2025 for Belgium. The map can be compared with the situation end of 2024 in the previous GMN annual report (Roggemans et al., 2025).

Most of the Belgian RMS cameras were installed for the reinforcement of the CAMS-BeNeLux. For this purpose, the 6 mm lenses are preferred which have less distortion than the 3.6 mm and detect more fainter meteors. GMN started in Belgium with four cameras in 2019 recording 921 orbits in 2019 and 5500 orbits in 2020. Six more cameras were installed in 2021, when 8582 orbits were collected. The network expanding to twenty cameras in 2022 when exceptional favorable weather resulted in 23174 orbits. In 2023, 23 cameras were active and had 25443 orbits. Although the weather was significantly less favorable in 2024, 34049 orbits were collected with 28 operational cameras. As many as 15 extra cameras were installed in 2025 and with 43 cameras, 53244 orbits were collected. The all-time number of orbits for Belgium is 150913. The only two decommissioned cameras so far will be hopefully reinstalled in 2026. Belgian cameras have many paired meteors with those in neighboring countries, France,

Germany, Netherlands and the United Kingdom. Especially the overlap from cameras of the largest and most successful network in the UK result in many good combinations. Some cameras in Belgium have been installed to improve the coverage on Northern France.

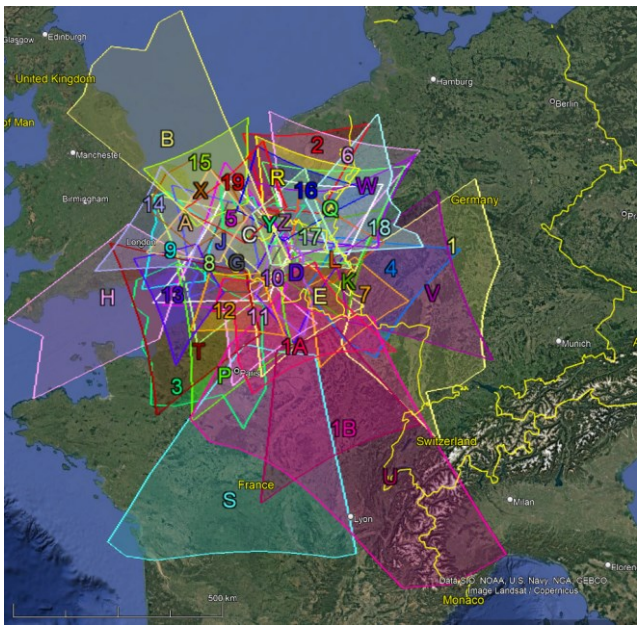

Figure 7 – GMN camera fields intersected at 100 km elevation, for 43 cameras installed in Belgium, status 2025.

4.6 BR – Brazil

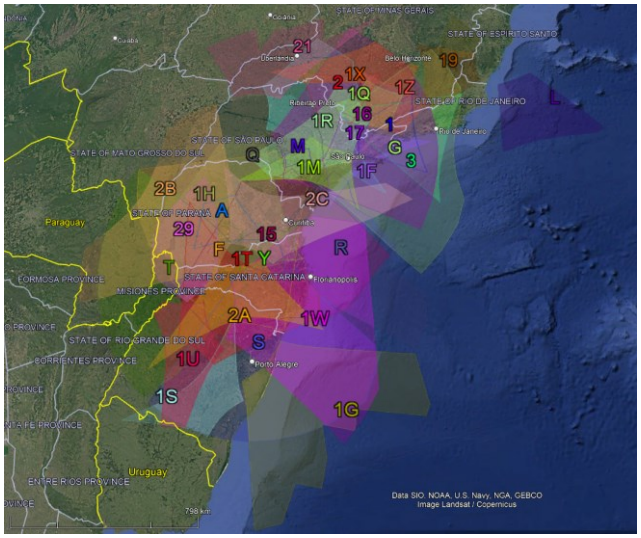

Figure 8 – GMN camera fields in 2025 intersected at 100 km elevation, for 36 cameras active in Brazil.

The BRAMON network had its first two RMS cameras getting paired meteors in October 2020 good for 40 orbits with two cameras in the last quarter of 2020. The network expanded to 13 operational cameras, good for 1645 orbits in 2021. In 2022 the number of cameras increased to 20 and 2760 orbits were obtained. In 2023 the number of cameras increased to 34 but the number of paired meteors dropped to 2331. With 37 cameras contributing to orbits in 2024, 4753 orbits were collected. In 2025, nine cameras were decommissioned and eight new cameras were installed. With 36 cameras 9949 meteoroid orbits were obtained, a record for Brazilian GMN cameras so far. The all-time number of orbits is 21478 for Brazil. This is a huge country and most RMS cameras are installed in the southern part (*Figure 8*). Some cameras are installed waiting for coverage from other cameras. Further optimization of the network could increase the number of orbits a lot as these longitudes need more observing capacity to cover southern hemisphere meteor activity.

4.7 BG – Bulgaria

Bulgaria had its first RMS camera operational in June 2021 and got three cameras installed by the end of 2021 of which two had 419 multi-station events. In April 2022 a 4th RMS and in July 2022, two extra cameras were installed. With 6 cameras in 2022, 3877 orbits could be collected. Seven operational cameras had 3530 orbits in 2023. As many as ten extra cameras were installed in 2024, good for 15058 meteor orbits. One camera was decommissioned in 2025, and with 16 cameras 12297 orbits were recorded. The Bulgarian RMS cameras also get paired meteors with cameras in Greece and in Romania (*Figure 8*).

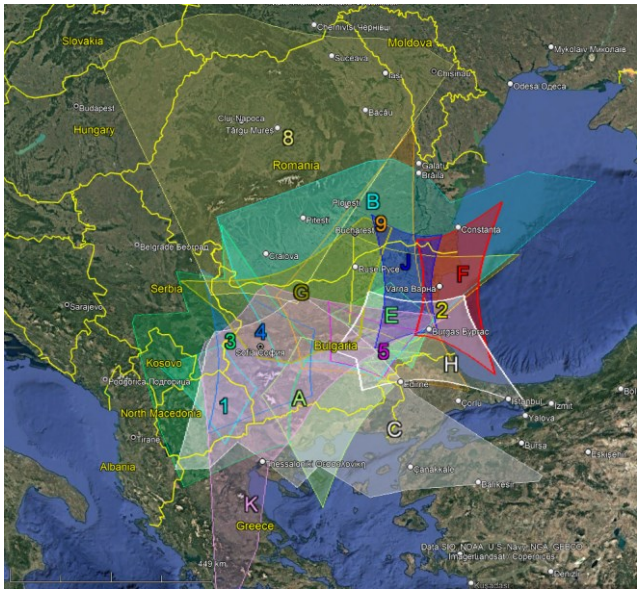

Figure 9 – GMN camera fields in 2025 intersected at 100 km elevation, for 16 cameras active in Bulgaria.

4.8 CA – Canada

The Canadian GMN network had its first five operational RMS cameras providing orbits in June 2019 and expanded to 11 cameras by the end of 2019, good for 3599 orbits. The number of cameras increased to 17 by the end of 2020 with 10815 orbits registered. During 2021, 15 new camera IDs appeared in the list and 8809 orbits were recorded with 29 cameras in 2021, less than the year before despite the extra cameras. The number of cameras doubled from 29 to 58 in 2022 resulting in 16232 orbits. In 2023 the number of contributing cameras increased to 67, resulting in 15023 orbits. The number of operating cameras dropped to 51 in 2024, good for 18508 orbits. In 2025, 13 cameras were decommissioned, one resumed and ten new installed. With 49 cameras, 20576 meteoroid orbits were collected. In total 50 Camera IDs that worked in previous years have been decommissioned since the start of the project.

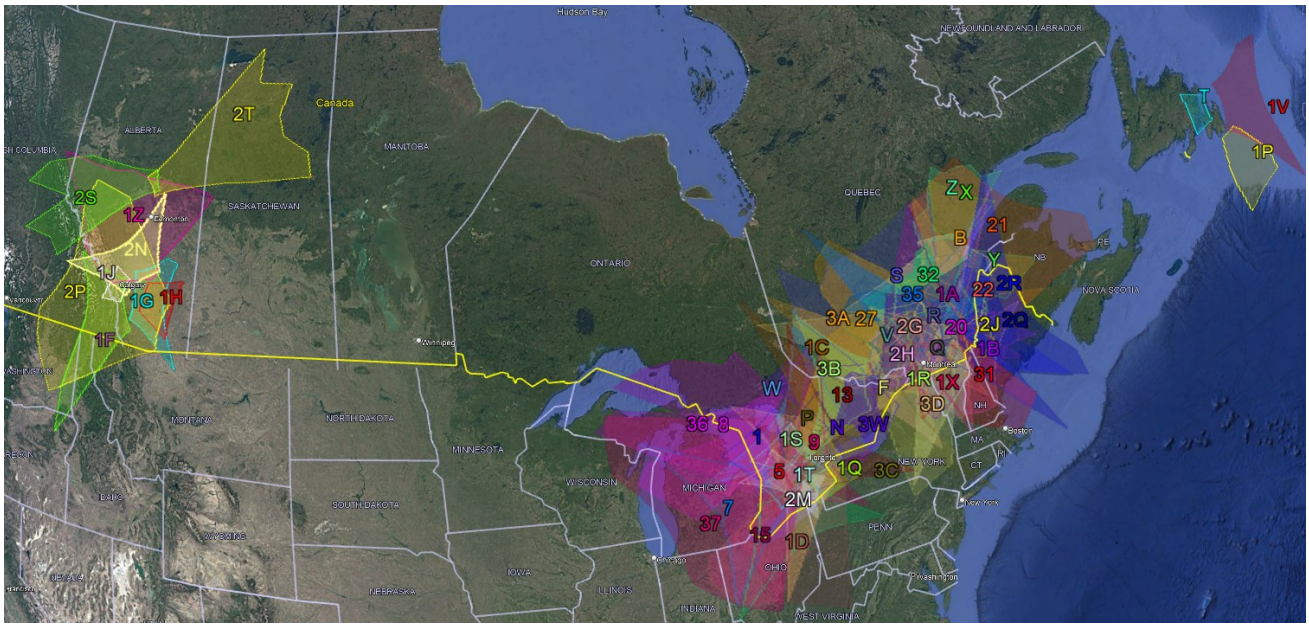

Figure 10 – GMN camera fields in 2025 intersected at 100 km elevation, for cameras active in Canada, overview.

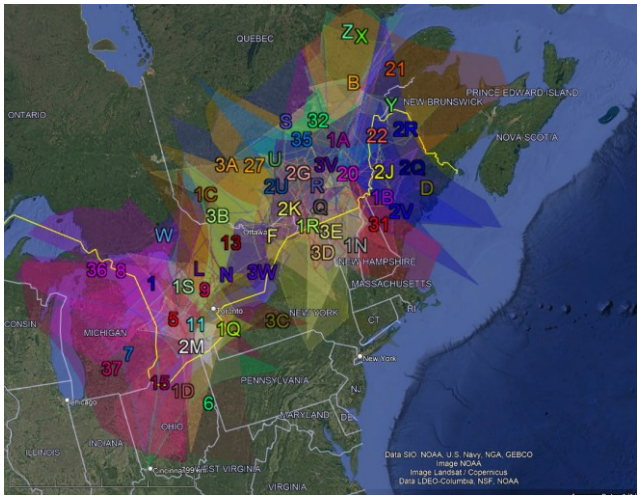

Figure 11 – GMN camera fields intersected at 100 km elevation, for cameras active in Canada, Quebec and Ontario in 2025.

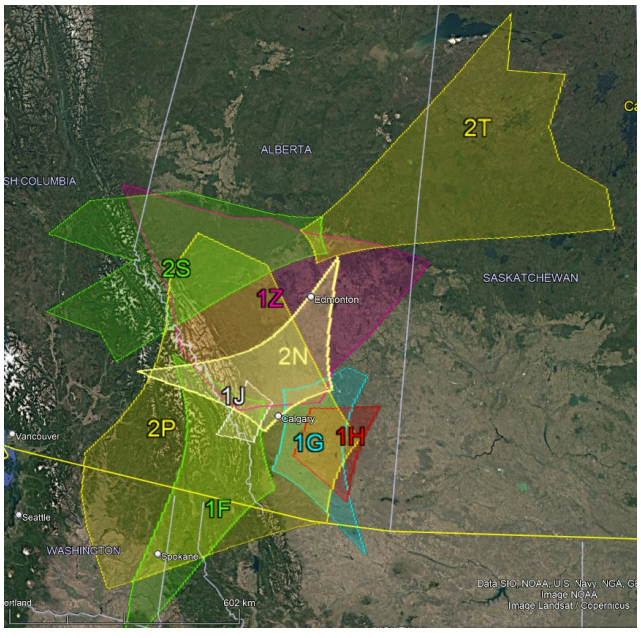

Figure 12 – GMN camera fields intersected at 100 km elevation, for cameras active in Canada, Alberta in 2025.

Two smaller sub-networks existed, CAWE (Elginfield) and CAWT (Tavistock). Each of both networks had eight cameras, but Tavistock stopped observing in 2023. Six new cameras were added at Elginfield in 2025. A small network in the Calgary region of Alberta had its first orbits in 2022 (*Figure 12*) and continued in 2025. Most cameras are installed in Quebec and Southern Ontario, ideal for volunteers south of the Canadian border in the US. Some cameras in New Found Land still wait for a multi-station partner (*Figure 10*).

4.9 HR – Croatia

Croatia was the first European country in May 2019 to harvest orbits with three RMS cameras. By the end of 2019 Croatia had already 23 cameras successfully contributing in triangulations, good for 12221 multi-station events. The number of cameras increased to 32 in 2020 resulting in 35099 orbits that year. 38370 multi-station events were recorded in 2021 with 48 cameras. 2022 was slightly less successful with 31329 orbits and 45 operational cameras. In 2023 the number of cameras slightly decreased at 41 contributing to 27721 orbits. In 2024, 35726 orbits were collected with 43 operational cameras. In 2025 six cameras were decommissioned, but 12 new installed and 13 inactive cameras from 2024 resumed capturing. With 50 cameras in 2025, 57060 orbits were collected. In total Croatia contributed 237526 orbits to the GMN orbit database. 22 cameras have been decommissioned since the start.

Croatia plays a major role in the coordination of GMN, maintaining the IstraStream service to produce and deliver new cameras for many countries and providing technical assistance to participants in the GMN project worldwide. The Croatian cameras provide a huge overlap on the neighboring countries (*Figure 13*). A number of Croatian cameras have a very small FoV to register fainter meteors with higher positional accuracy. To view these camera fields in detail we refer to the online KML files for consultation in Google Earth.

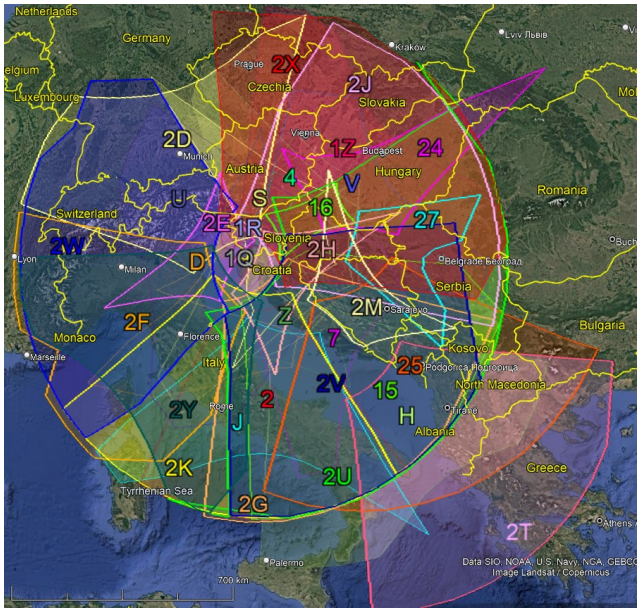

Figure 13 – GMN camera fields intersected at 100 km elevation, for cameras installed in Croatia, status 2025.

4.10 CK – Cook Island

The Cook Islands is a nation in the South Pacific and its 15 islands are scattered over a vast area. The Global Meteor Network got the first camera installed at this geographically interesting location. So far, we wait for multi station coverage.

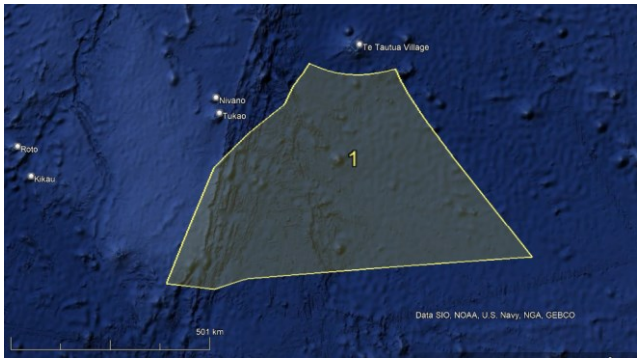

Figure 14 – GMN camera fields in 2025, intersected at 100 km elevation, for the camera active on the Cook Islands.

4.11 CL – Chile

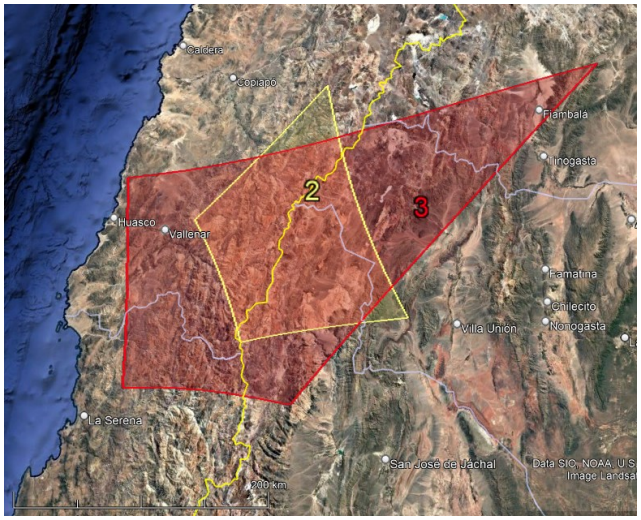

Figure 15 – GMN camera fields in 2025, intersected at 100 km elevation, for the camera active in Chile.

In June 2025, two GMN cameras were installed in Chile to cover strategic longitudes in the Southern Hemisphere. Thanks to a favorable climate, 1907 orbits were collected by these two cameras at observatories La Silla and El Sauce. Further camera enhancement and FOV optimization is planned in 2026.

4.12 CZ – Czech Republic

The first three RMS in the Czech Republic scored 163 orbits in 2020, with four cameras in 2021, 464 orbits were recorded and 2490 orbits with six cameras in 2022. A major breakthrough happened in 2023 as the number of cameras increased to twenty, good for 11269 orbits. In 2024, five more cameras were installed and a total of 18248 orbits were collected. In 2025 one camera was decommissioned and four new added, 28 cameras harvested 25668 orbits. In total Czech GMN cameras captured 58302 orbits.

Since the end of 2022, the Czech and Slovak GMN camera operators are grouped in the CSMON (Czech & Slovak Meteor Observation Network), which helps the new and current meteor enthusiasts to get on board. In addition to individual amateur astronomers, there is an increasing number of public observatories getting equipped by RMS cameras, thanks to public funding. Latest advances in the SBC (Pi5) technology allows to multiply the numbers of cameras on the same PC, i.e. make it even more accessible for low budgets.

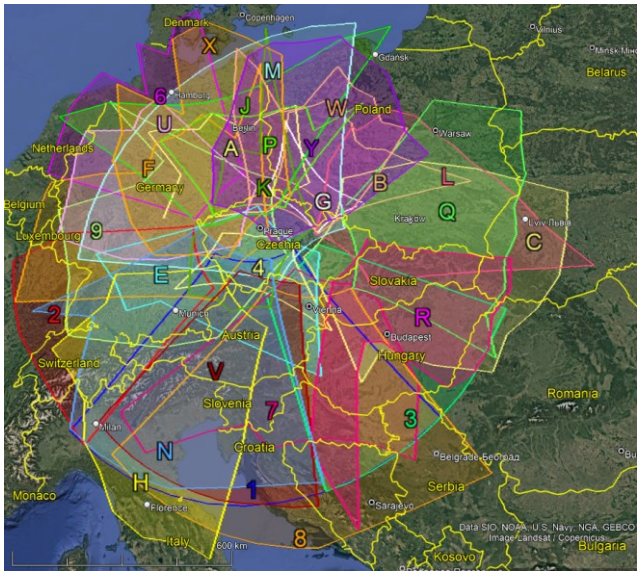

Figure 16 – GMN camera fields in 2025, intersected at 100 km elevation, for cameras active in the Czech Republic.

4.13 DK – Denmark

In October 2022 a first GMN camera was operational in Denmark, good for 55 orbits that year. In 2023 four cameras were active in Denmark, and these obtained 1386 orbits. A fifth camera was added in 2024 and 3360 orbits were collected. The GMN network underwent a spectacular expansion in Denmark in 2025 with 22 new GMN cameras being added and the establishment of the Nordic Meteor Network. With 27 cameras, 20522 orbits were collected bringing the all-time total to 25323 orbits for Danish cameras. These northern cameras create possibilities for

further camera coverage in southern Norway and Sweden as well as in Northern Germany (*Figure 17*).

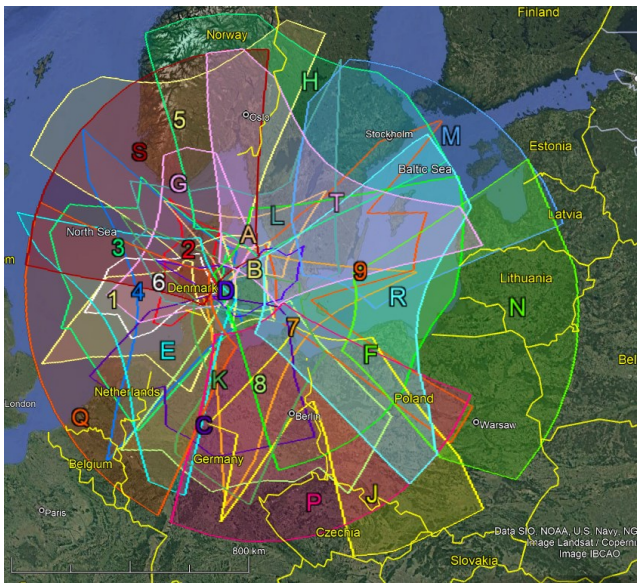

Figure 17 – GMN camera field in 2025 intersected at 100 km elevation, for cameras active in Denmark.

4.14 FI – Finland

In October 2022 the first GMN cameras became operational at two sites in Finland, with 41 orbits as a first result. In 2023 there were five cameras active which resulted in 90 orbits and in 2024 three more cameras were installed and 204 orbits obtained. In 2025 one new camera was added and with 8 of the 9 cameras 407 orbits were obtained (*Figure 18*).

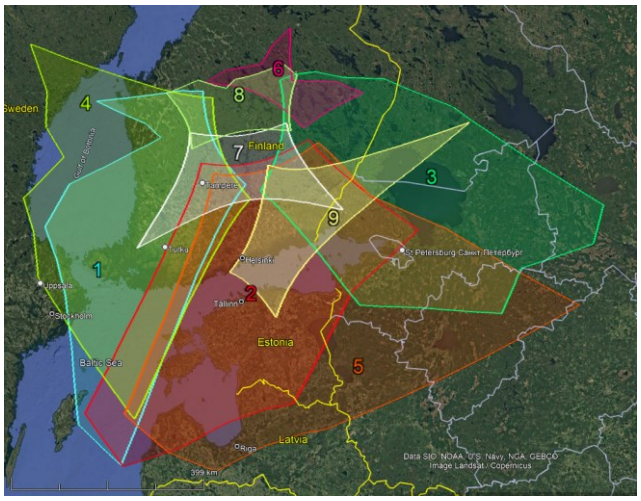

Figure 18 – GMN camera fields in 2025 intersected at 100 km elevation, for cameras active in Finland.

4.15 FR – France

The number of RMS cameras in France increased gradually from 10 in 2020 with 3176 orbits registered, to 14 devices in 2021 with 5601 orbits and 16 cameras in 2022 with 11990 orbits. More new cameras were installed in 2023 and 16682 orbits were obtained with 18 cameras. In 2024 there were 19 operational cameras in France contributing 20592 orbits to the GMN dataset. In 2025, 27617 orbits were collected with 20 cameras. In total 28 RMS cameras were installed since March 2020, but eight of them did not function anymore in 2025. The all-time total of orbits is 85658 for France. A large part of France, the entire south-western, is still without GMN coverage (*Figure 19*).

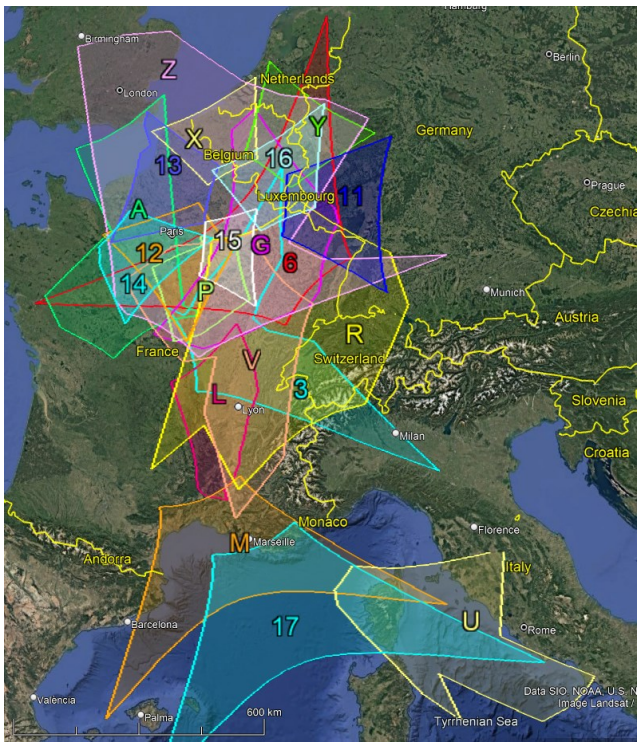

Figure 19 – GMN camera fields in 2025 intersected at 100 km elevation, for cameras active in France.

4.16 DE – Germany

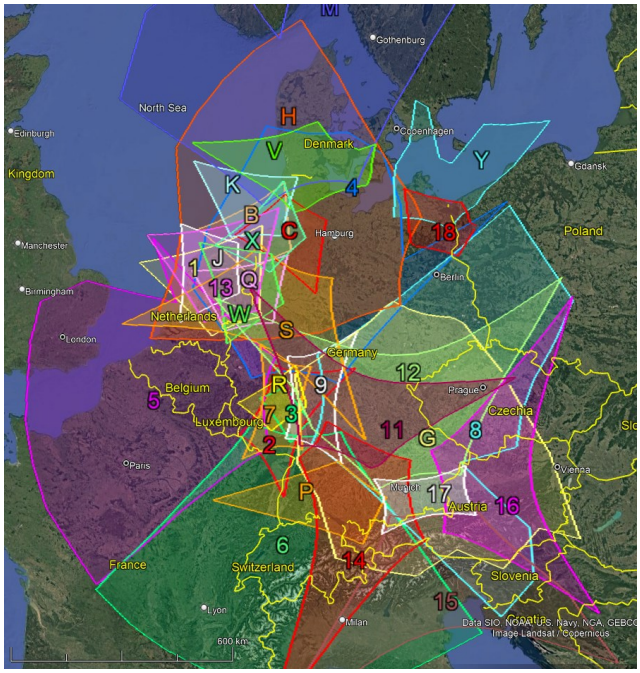

Figure 20 – GMN camera fields in 2025 intersected at 100 km elevation, for cameras active in Germany.

The first GMN camera in Germany had its first orbits in August 2019 with Belgian GMN cameras. By the end of 2019 there were four GMN cameras in Germany, good for 200 orbits. The number of cameras increased to 10 and the numbers of orbits to 3963 in 2020. With 12 cameras in 2021, 7009 orbits were collected, in 2022, with 18 cameras 9128 orbits were collected. In 2023 as many as 12194 orbits were recorded with 19 cameras. In 2024 the number of

cameras in Germany increased with 11 to 30, good for 23240 orbits. 32 cameras in 2025 resulted in 37570 orbits, bringing the total score at 93304 orbits for Germany. Two cameras were decommissioned so far. Some GMN cameras in the North-Western part of Germany also participate in the CAMS-BeNeLux network, supporting both GMN and CAMS (*Figure 20*).

4.17 GR – Greece

In September 2022 the first GMN camera got operational in Greece, ideally pointed to overlap with some Bulgarian GMN cameras and it was good for 977 paired meteors in the four last months of 2022. Three extra cameras were installed and with four cameras 3375 orbits were obtained in 2023. Four more cameras were installed in 2024 and with eight operational cameras 8998 orbits were obtained. The same number of cameras resulted in 16865 orbits in 2025 bringing the all-time total at 30215 orbits for Greece (*Figure 21*).

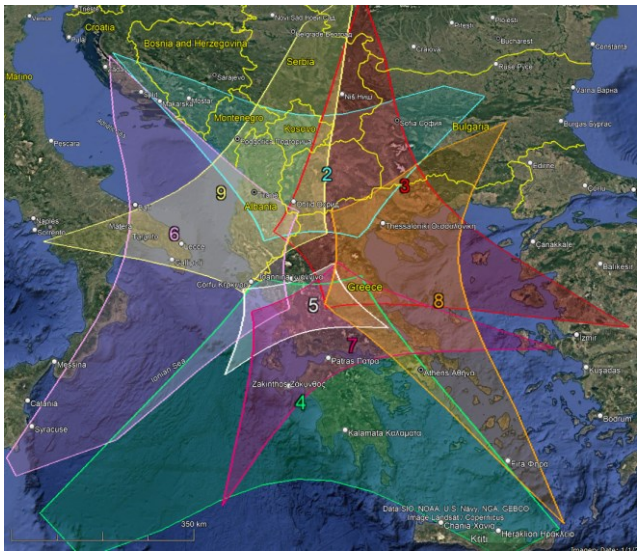

Figure 21 – GMN camera fields in 2025 intersected at 100 km elevation, for cameras active in Greece.

4.18 – Greenland

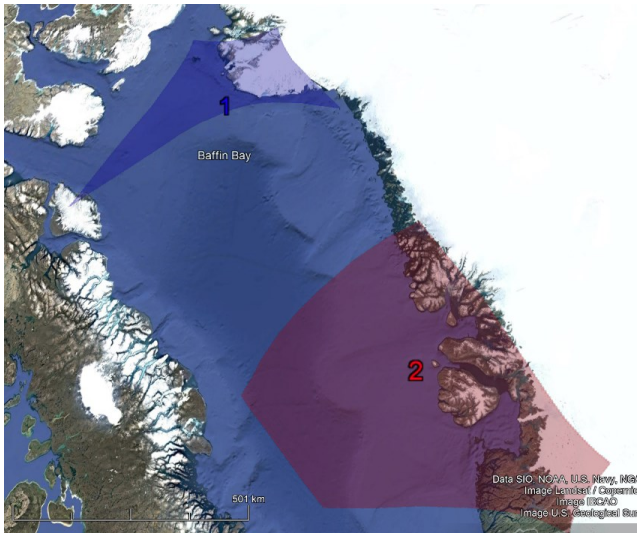

Figure 22 – GMN camera field in 2025 intersected at 100 km elevation in Greenland.

The most northern GMN camera, GL0001, installed in the North West of Greenland at 77°28' northern latitude. During the late autumn and winter months, this site has almost permanent night time. A second camera was installed in 2025. The possibilities are being considered to install more cameras at favorable distances for triangulations.

4.19 – Hungary

A first GMN camera was operational in March 2022 in Hungary and by end of 2022, two Hungarian cameras had obtained 2114 orbits. One new camera was added in 2023 and the Hungarian cameras contributed 7872 orbits. The number of cameras remained status quo in 2024 and produced 9626 orbits, mainly paired meteors with Croatian and Czech cameras. A break-through happened in 2025 when nine new cameras got installed and 19870 meteors were recorded bringing the all-time total for Hungary at 39482 orbits.

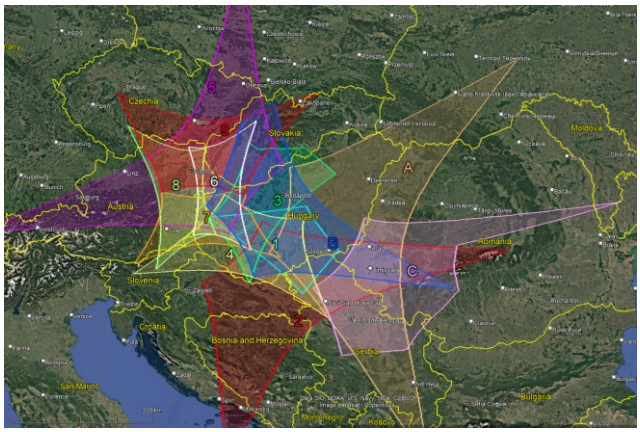

Figure 23 – GMN camera fields in 2025 intersected at 100 km elevation, for cameras active in Hungary.

4.20 IE – Ireland

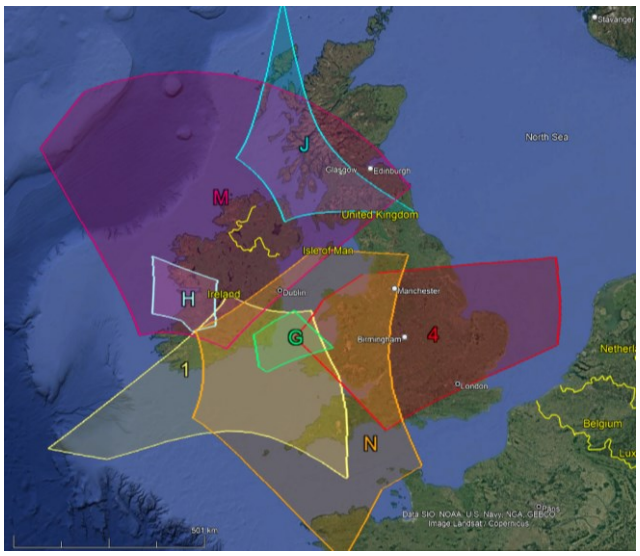

Figure 24 – GMN camera fields in 2025 intersected at 100 km elevation, for cameras active in Ireland.

Ireland got a first GMN operational in October 2020 and a second one a month later, good for 120 orbits in 2020. With three cameras in 2021 the number of orbits increased to 424. 3490 orbits were recorded in 2022 with five GMN cameras. In 2023 the number of cameras remained unchanged but the

number of orbits dropped to 1954. In 2024 two new cameras were added and one previously active RMS stopped uploading data. With six available cameras, 3706 orbits were obtained. In 2025 the number of cameras remained at six, but 6692 orbits were obtained, the best year so far for Ireland. The all-time total of orbits is 16386 for Ireland. Most of the paired meteors were obtained thanks to the overlap provided by GMN cameras in the UK.

4.21 IL – Israel

Israel had its first three GMN cameras installed in November 2020, good for 553 orbits that year. In 2021 with three extra cameras 2009 orbits were obtained. In 2022 the cameras did not provide orbits during some periods of time and one camera was discontinued, resulting in 975 orbits. In 2023, 1096 orbits were collected using six cameras. In 2024 an extra camera was installed and with seven cameras, 991 orbits were collected. In 2025 six cameras had 681 orbits. In total three cameras were decommissioned, the all-time number of orbits for Israel is 6305.

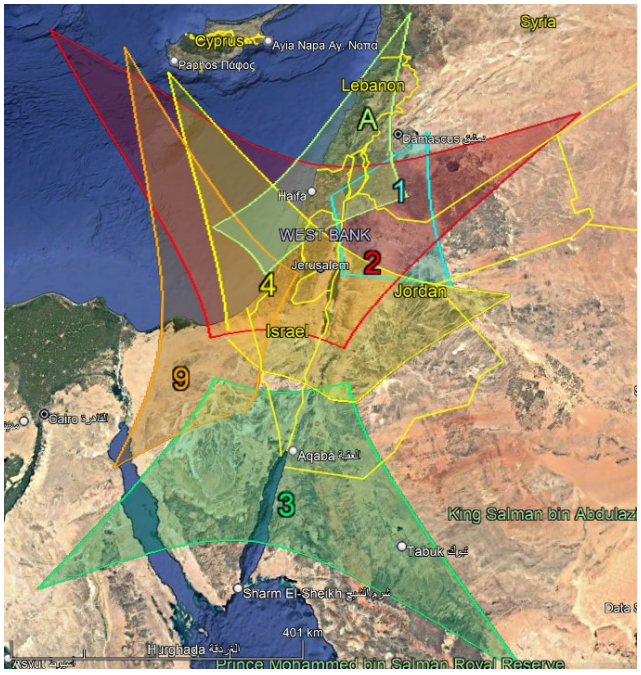

Figure 25 – GMN camera fields in 2025 intersected at 100 km elevation, for cameras active in Israel.

4.22 IT – Italy

Italy had its first GMN camera installed and contributed to orbits in October 2019, and was good for 862 orbits. Italy remained with one GMN camera in 2020, which had as many as 5384 paired meteors with Croatian and Slovenian cameras. Italy increased its number of cameras to five and these cameras were involved in 5447 multi-station events in 2021. An extra camera was added in Bologna in 2022 and 4943 orbits were collected. With seven cameras in 2023, 5064 orbits were obtained. In 2024, 6603 orbits were obtained with seven cameras. The number of cameras remained unchanged in 2025 and 9249 orbits were collected, so far the best year. Three cameras were decommisioned before 2025 and the all-time number of orbits is 37489 for Italy. More cameras in Italy would allow to cover much more of the atmosphere over the Mediterranean Sea.

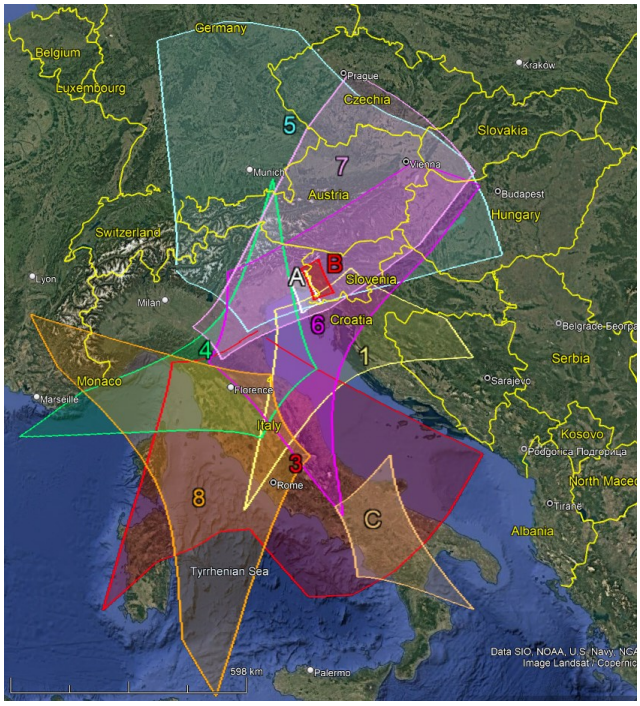

Figure 26 – GMN camera fields in 2025 intersected at 100 km elevation, for cameras active in Italy.

4.23 JP – Japan

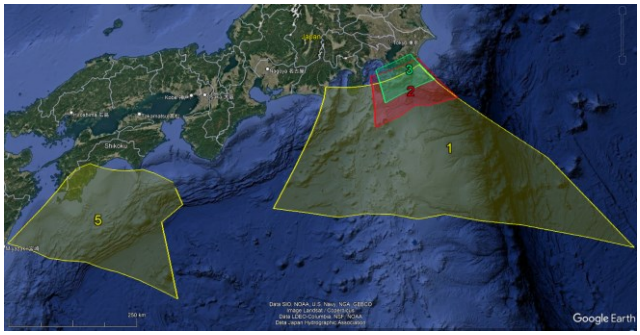

Figure 27 – GMN camera fields in 2025 intersected at 100 km elevation, for cameras active in Japan.

A first GMN camera was installed in Japan in 2022, waiting for some multi-station partners at suitable distance for triangulation. In 2023 a second camera was installed which allowed to obtain 629 orbits. The network remained status quo in 2024 with two cameras and 606 orbits. In 2025 a third camera was installed and 147 orbits recorded. The all-time number of orbits for GMN in Japan is 1382. Japan has the very active SonotaCo network which, uses analog Watec cameras. RMS cameras deliver UFO capture output which may offer opportunities for the SonotaCo network to include GMN cameras in its network.

4.24 KR – Korea (South)

A most impressive deployment of GMN cameras took place in 2022 in South Korea with a first few cameras obtaining orbits in September and as many as 47 GMN cameras installed in November and December 2022. The cameras were installed and pointed to obtain an optimal overlap resulting in 7711 orbits during the first year. In 2023 the number of cameras rapidly increased to 125 (!) collecting 34044 orbits. This fast deployment made the RMS network in South Korea a major contributor at a strategic geo-

location at the northern hemisphere for a 24 on 24-hour monitoring of meteor activity.

In 2024 three cameras were decommissioned, 122 operational cameras captured 42477 orbits. 123 operational cameras obtained 63284 orbits in 2025, the best year so far for South Korea. The all-time number of orbits stands at 147516. The dense coverage of overlapping camera fields in 2025 can be compared to the situation end of 2022 in *Figure 28*. If any RMS cameras are installed in South-Western Japan, these would generate many paired meteors with the Korean cameras.

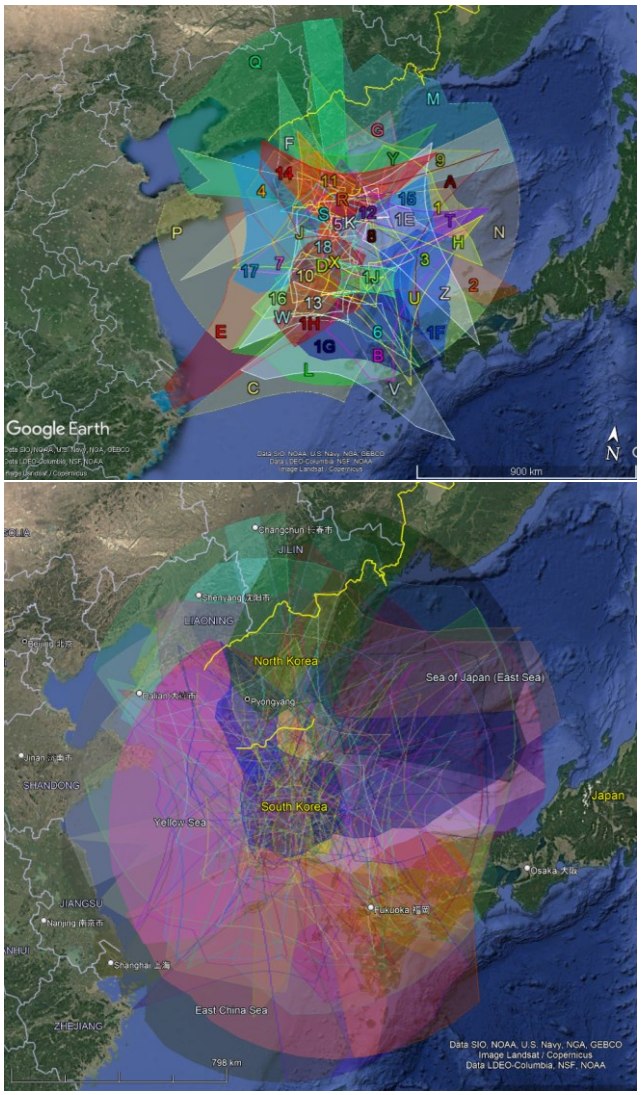

Figure 28 – GMN camera fields in 2022 (top) and in 2025 (bottom) intersected at 100 km elevation, for cameras active in South Korea.

4.25 – Luxembourg

In October 2022 a first GMN camera was installed in Luxembourg in combination contributing to 622 orbits with Belgian, Dutch, French, German and even Czech GMN cameras (*Figure 29*). In 2023 this camera had 2018 paired meteors with orbits and in 2024, 2194 orbits were obtained. In 2025 a second camera was installed in Luxembourg and 4133 orbits were recorded. The all-time number of orbits for Luxembourg stands at 8967. With many cameras in Belgium, France and Germany, extra cameras in Luxembourg can score many multi-station events.

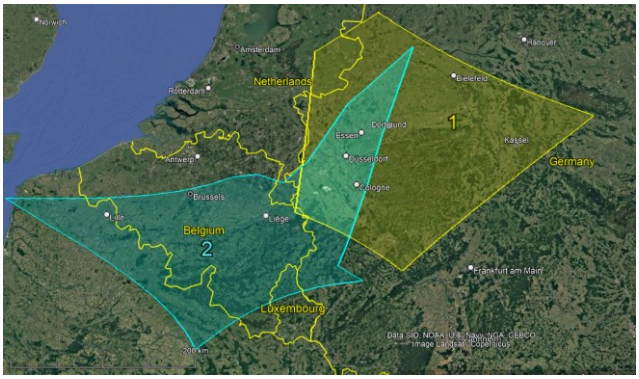

Figure 29 – GMN camera field in 2025 intersected at 100 km elevation, for cameras active in Luxembourg.

4.26 MY – Malaysia

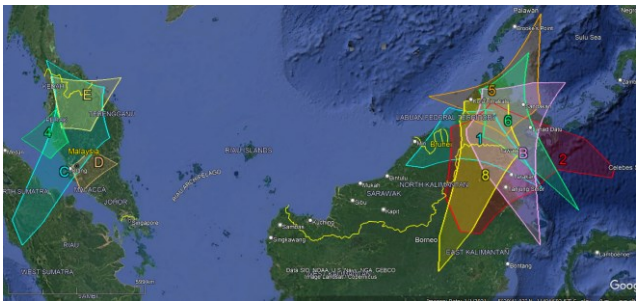

Figure 30 – GMN camera fields in 2025 intersected at 100 km elevation, for cameras active in Malaysia.

A first GMN camera was installed in Malaysia in 2021 but waited for coverage from cameras installed at suitable distances to get good triangulations. Some extra cameras were installed in 2022, and in June 2022 the first orbits were obtained. In total 50 orbits were collected in 2022 with three cameras. In 2023 a ten-fold of orbits, 501, were collected with five cameras. In 2024, 246 orbits were obtained with six cameras, two new cameras were added and two cameras were decommissioned. With 10 cameras, 258 orbits were obtained in 2025. The all-time total of orbits stands at 1055 for Malaysia. Further extensions of the Malaysian network are very welcome. Extra cameras in the western part of Malaysia could give coverage on the camera in Singapore.

4.27 MX – Mexico

An impressive deployment of GMN cameras took place in Mexico in 2022. The first few installed cameras obtained the first orbits in February 2022 and soon twelve cameras were installed with a good overlap. A total of 1769 meteor orbits were collected in 2022. The number of cameras increased to 15 in 2023 with 2953 orbits as a result. In 2024 13 cameras recorded 2871 orbits, two cameras were decommissioned. Eleven cameras remained in 2025 and recorded 1134 orbits. The all-time number of orbits is 8727 for Mexico. The efforts in Mexico are crucial in getting coverage for both the northern and especially the southern hemisphere at these longitudes (*Figure 31*).

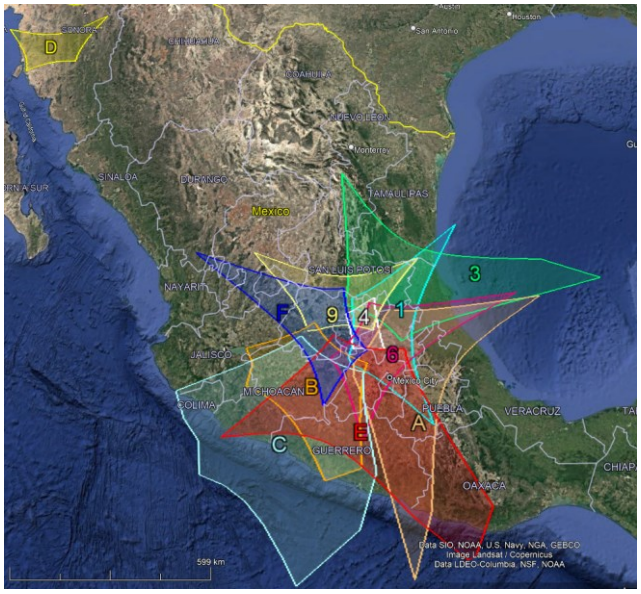

Figure 31 – GMN camera fields in 2025 intersected at 100 km elevation, for cameras active in Mexico.

4.28 MA – Morocco

The first two GMN cameras obtained their first meteor orbits in May 2024, and a third camera was added in July. The Moroccan GMN cameras collected 851 orbits in 2024 and 1312 in 2025, despite frequent technical issues that prevented recording meteors much of the time (*Figure 32*).

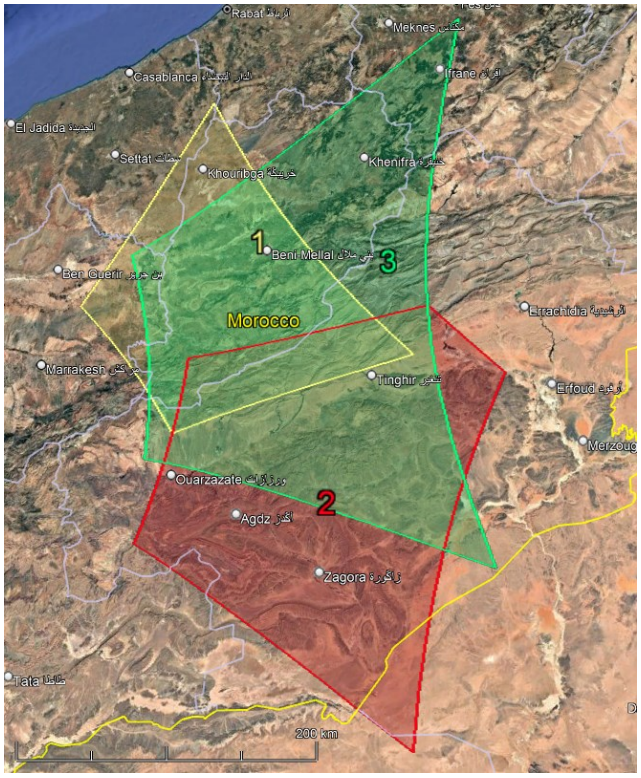

Figure 32 – GMN camera fields in 2025 intersected at 100 km elevation, for cameras active in Morocco.

4.29 NL – Netherlands

The Netherlands started collecting orbits within GMN in August 2019 with two cameras and had 278 orbits in this first year. The number of GMN cameras increased to eleven in 2020 with 4337 orbits as a result. The number of cameras remained unchanged in 2021 but the better overlap from neighboring countries resulted in 7605 orbits. Some cameras dropped off in 2022 and a few new ones were installed, resulting in 9139 orbits from 13 cameras. In 2023, 14 Dutch RMS cameras had 9421 orbits. In 2024 four new RMS cameras were installed, with a total of 18 cameras 17409 orbits were collected. A major breakthrough came in 2025 when 13 new GMN cameras were added, most of them built during a workshop where interested people could assemble their camera under supervision of experienced GMN camera operators. 33566 orbits were obtained with 31 cameras in 2025, the best year so far. The Netherlands have five decommissioned RMS cameras. Dutch cameras get mainly multi-station coverage from cameras in Belgium, Germany, the UK and Denmark (*Figure 33*). The all-time total number of orbits is 81755 for the Netherlands.

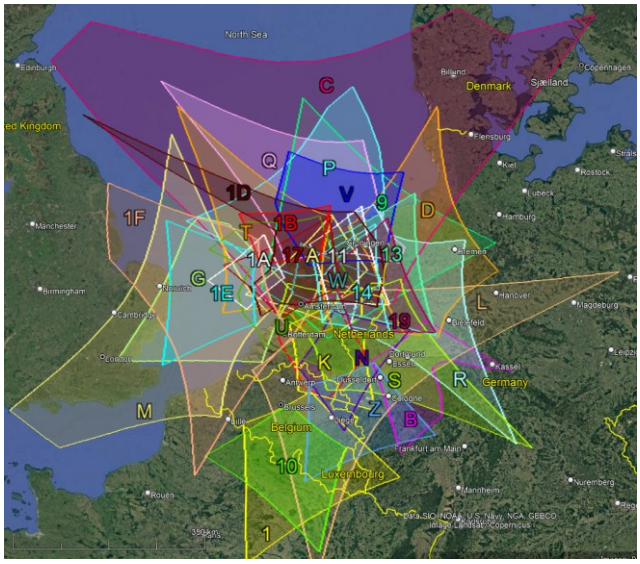

Figure 33 – GMN camera fields in 2025 intersected at 100 km elevation, for cameras active in the Netherlands.

4.30 NZ – New Zealand

The first two GMN cameras were installed in July 2021 in New Zealand and 1146 orbits were obtained that year. From March 2022 more cameras were installed month by month with an impressive deployment of strategically placed well pointed cameras covering the huge surface of the country. With 28 active cameras at the end of 2022, 6280 orbits were recorded. The New Zealand GMN network, known as Fireballs Aotearoa, was further expanded in 2023 and with a total of 111 cameras 47436 orbits were obtained, making New Zealand one of the most important providers of orbit data for the Southern Hemisphere. The density of the camera coverage can be seen in *Figure 34* and compared to the situation three years earlier. In 2024, 44 extra cameras became operational and three older cameras decommissioned. With a total of 152 cameras, 147831 meteor orbits were collected. In 2025, five cameras were decommissioned, one older camera resumed capturing, and 36 new cameras were added to the network. 182324 orbits were collected with the 184 available cameras. This makes New Zealand the greatest orbit contributor within the Global Meteor Network, doing better than the GMN network in the USA that covers a much larger volume of atmosphere to intercept meteoroids. The all-time number of collected orbits is 385017 for New Zealand, with seven cameras decommissioned.

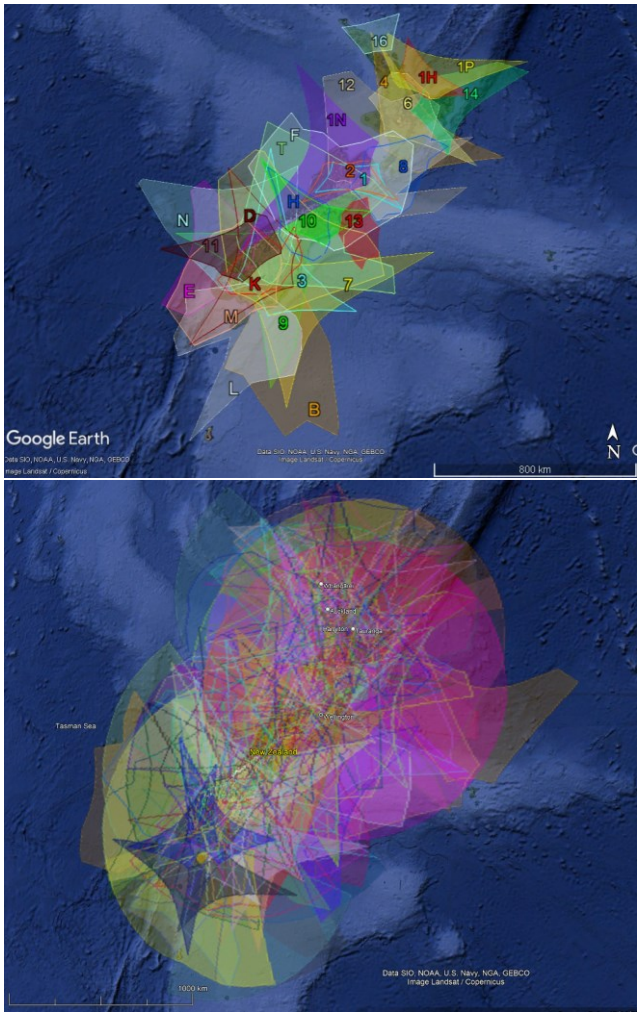

Figure 34 – GMN camera fields in 2022 (top) and in 2025 (bottom) intersected at 100 km elevation, for cameras active in New Zealand.

4.31 NO – Norway

The two first GMN cameras were installed in Norway in December 2024, but so far without paired meteors as calibration failed. The cameras are pointed south and should combine well with cameras in Denmark, Germany and the United Kingdom (*Figure 35*). Unfortunately, the cameras are currently listed as decommissioned.

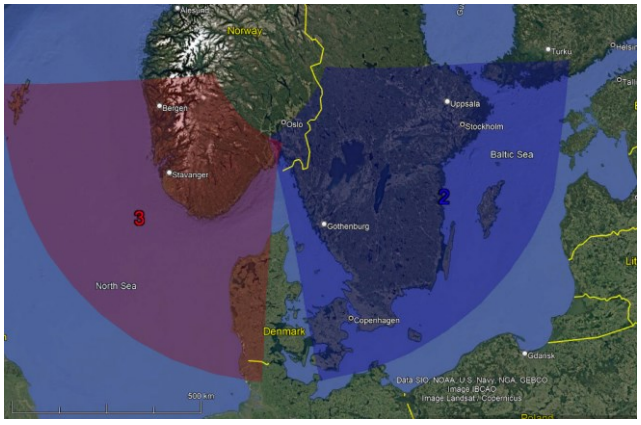

Figure 35 – GMN camera fields in 2025 intersected at 100 km elevation, for cameras active in Norway.

4.32 PL – Poland

The first GMN camera was installed in September 2020 and remained long the only Polish GMN camera with 35 orbits in 2020 and 67 orbits in 2021. In March 2022 two extra Polish GMN cameras got their first 35 orbits. The cameras didn't function all the time but the number of orbits obtained increased to 398 in 2022. In 2023 only two cameras were active and 456 orbits were collected. In 2024 two new cameras were installed and 1759 orbits obtained. Eight new cameras were added in 2025 and 7486 orbits collected with eleven operational cameras. The all-time number of orbits is 10201. Polish GMN cameras get mainly paired meteors with cameras installed in Czechia and Germany (*Figure 36*).

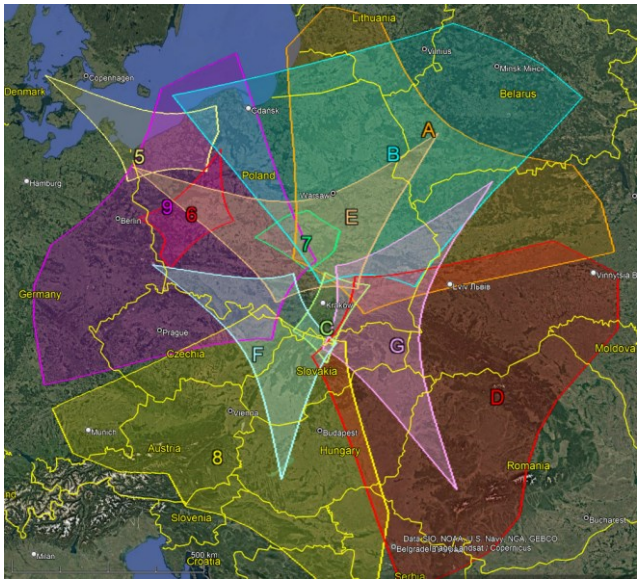

Figure 36 – GMN camera fields in 2025 intersected at 100 km elevation, for cameras active in Poland.

4.33 PT – Portugal

A first GMN camera got meteor orbits in September 2022 in Portugal. A vast coverage from GMN cameras in Spain guarantees many paired meteors (*Figure 37*). In 2022, 327 orbits were recorded, in 2023 the total increased to 3322 orbits. A second camera was installed in January 2024 and with two cameras, 4413 orbits were obtained. The two Portuguese cameras collected 4067 orbits in 2025, bringing the all-time total at 12129 for Portugal.

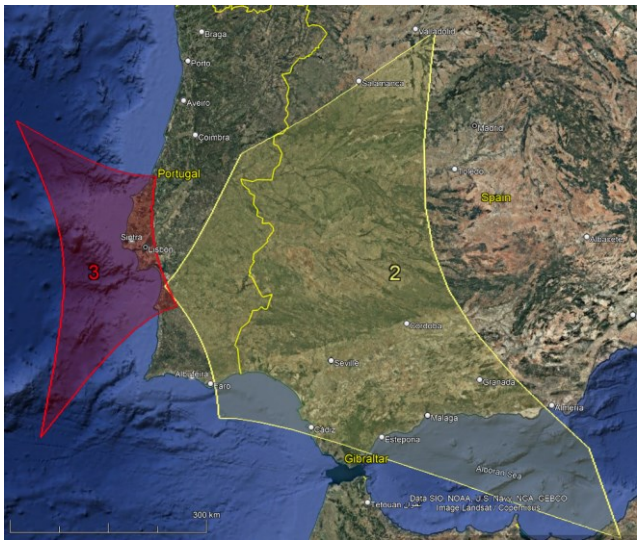

Figure 37 – GMN camera field in 2025 intersected at 100 km elevation, for cameras active in Portugal.

4.34 RO – Romania

Romania had its first three RMS cameras installed in 2023. Operational since October 2023 and despite unfavorable weather, 417 orbits were collected. The network in Romania remained status quo in 2024, but RO0003 failed functioning in February. With only two functioning cameras, 4361 meteor orbits were collected. In December 2025 three new cameras got installed and 4426 orbits were collected this year. The all-time number of orbits is 9204 for Romania. These cameras had many paired meteors with Bulgarian, Croatian, Czech and Hungarian cameras. Several new camera systems have been commissioned for installation in 2026.

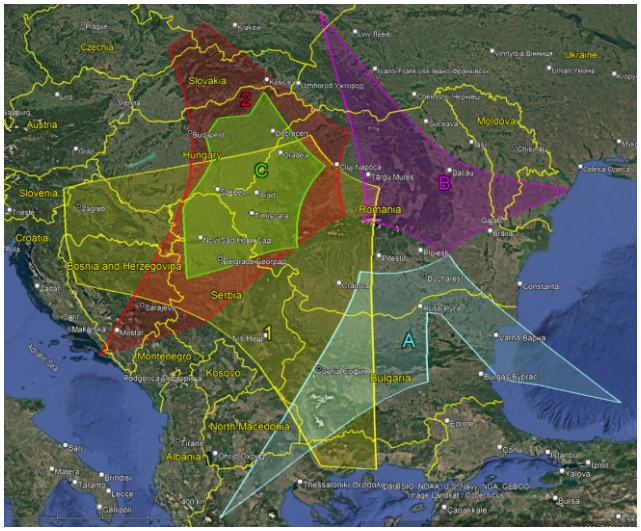

Figure 38 – GMN camera field in 2025 intersected at 100 km elevation, for cameras active in Romania.

4.35 RU – Russia

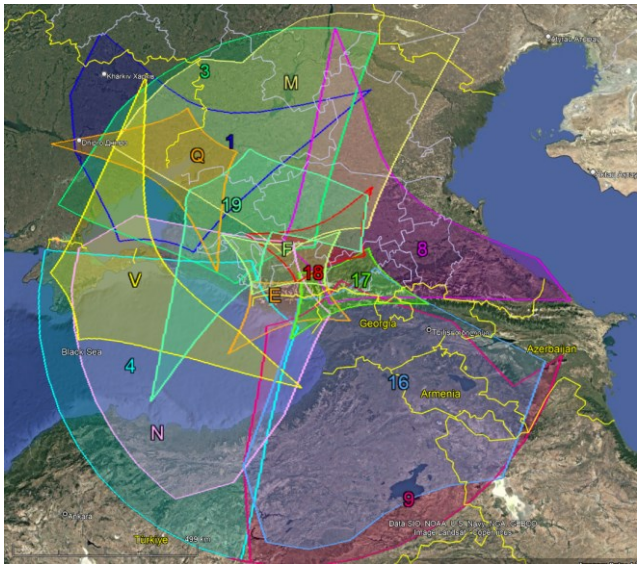

Figure 39 – GMN camera field in 2025 intersected at 100 km elevation, for cameras active in the South of Russia.

The first two GMN cameras in Russia had orbits in July 2019 in Southern Russia (*Figure 39*). The first year had already 5715 orbits with 10 cameras. In 2020 the number of cameras increased to 21, good for as many as 13438 orbits. The number of RMS cameras having paired meteors remained stable at 21, but the number of orbits decreased to 6208 in 2021. Problems with the maintenance of some meteor stations reduced the number of paired observations. In 2022, 19 cameras in Russia had 5437 orbits. The number of Russian GMN cameras decreased further to 15 in 2023 and the number of paired meteors dropped to 1992. In 2024 seven new cameras were installed and with 22 cameras, 10939 meteor orbits were obtained. In 2025 two cameras were decommissioned and one new added, good for 10553 orbits in 2025. The all-time number of orbits for Russia is 54282. In total 14 of the formerly active cameras were decommissioned.

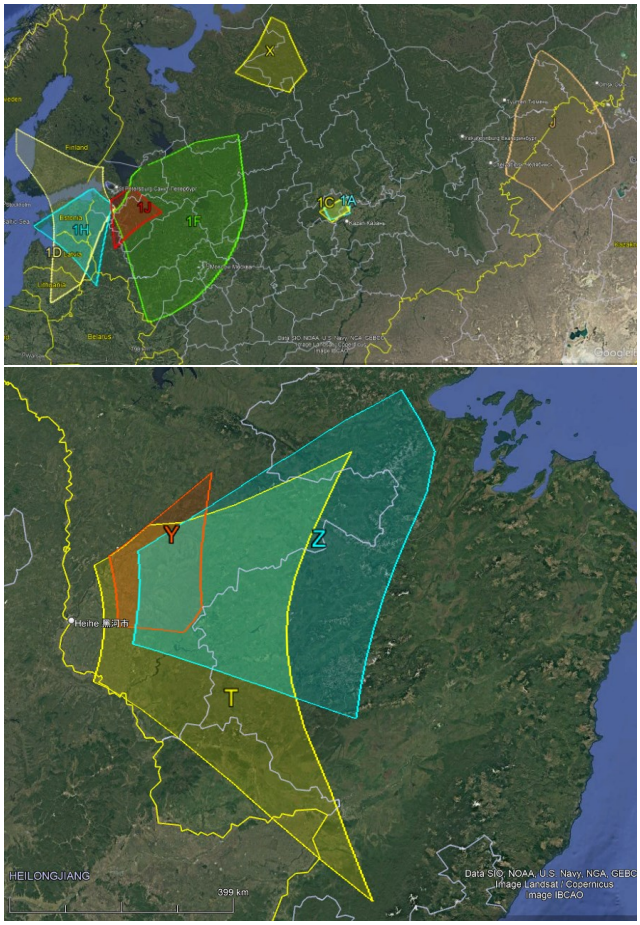

Figure 40 – GMN camera fields in 2025 intersected at 100 km elevation, for cameras active in Western Russia (top) and in the Russian Far East (bottom).

Some single RMS devices were installed elsewhere in Russia, like near St. Petersburg and Kazan, some other cameras are still waiting for coverage from other sites at a suitable distance. Some cameras are installed in the far east of Russia at longitude ~132° east and 50° north (*Figure 40*).

4.36 SG – Singapore

A first camera was installed in 2022 and is waiting for multi-station partners, no orbits could be obtained yet in 2025. Multi-station work should be possible with nearby cameras in Malaysia (*Figure 41*).

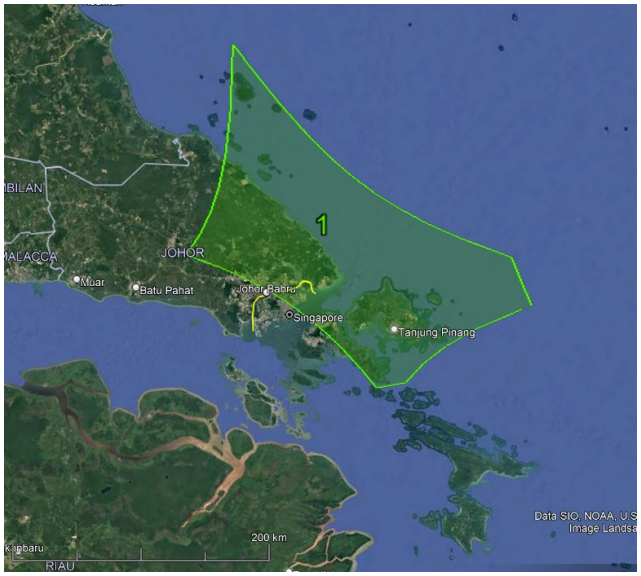

Figure 41 – GMN camera fields in 2025 intersected at 100 km elevation, for cameras active in Singapore.

4.37 SK – Slovakia

Slovakia got its first camera in November 2021 with 37 paired meteors. In 2022, three GMN cameras got operational good for 2026 orbits. The number of cameras increased to four in 2023 and 5535 paired meteors with orbits were recorded by Slovakian cameras. In March 2024 a fifth camera was installed and 7532 orbits were obtained. The five cameras recorded 6943 orbits in 2025 bringing the all-time number of orbits at 22073 for Slovakia (*Figure 42*). Since the end of 2022, the Czech and Slovak GMN camera operators are grouped in the CSMON (Czech & Slovak Meteor Observation Network), which helps the new and current meteor enthusiasts to get on board.

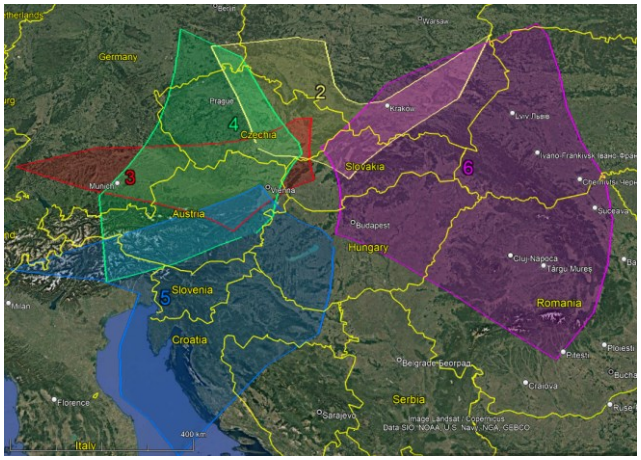

Figure 42 – GMN camera fields in 2025 intersected at 100 km elevation, for cameras active in Slovakia.

4.38 SI – Slovenia

Slovenia had its first RMS contributing in August 2019 and a second RMS in August 2021. The coverage with mainly cameras in neighboring Croatia, resulted in 2753 orbits in 2019, 3999 in 2020 and 6001 in 2021. The two Slovenian cameras contributed to 5887 orbits in 2022. In 2023, four extra cameras were installed and 6789 orbits were collected. The number of cameras remained status quo in 2024 with six, and 12209 orbits were obtained. A new camera was added in 2025 and 14741 orbits were collected. The all-time total of orbits for Slovenia is 52379 (*Figure 43*).

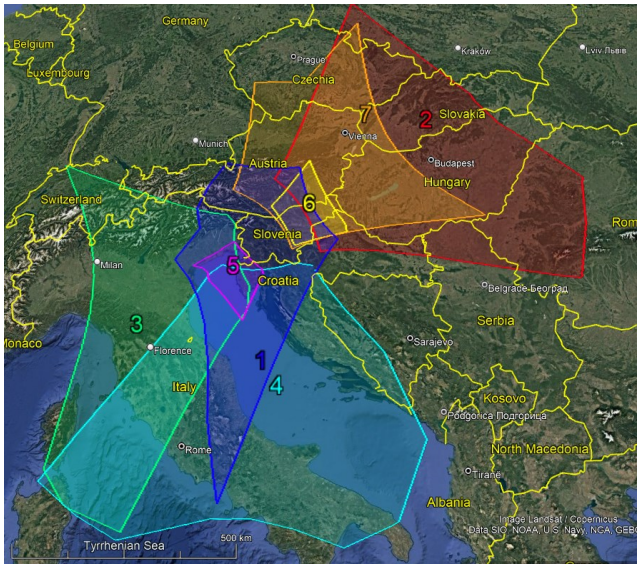

Figure 43 – GMN camera fields in 2025 intersected at 100 km elevation, for cameras active in Slovenia.

4.39 ES – Spain

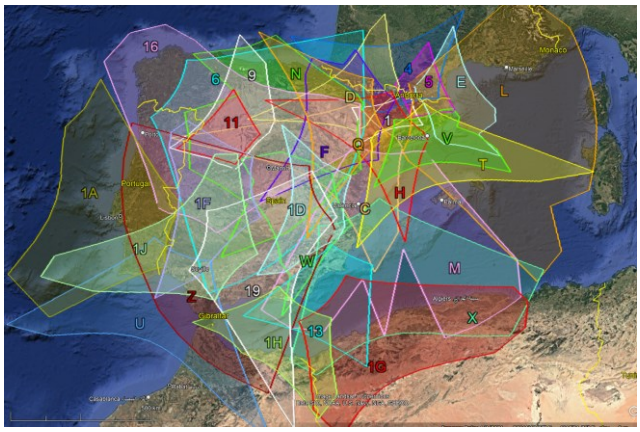

Figure 44 – GMN camera fields in 2025 intersected at 100 km elevation, for cameras active at the Canary Islands (Spain).

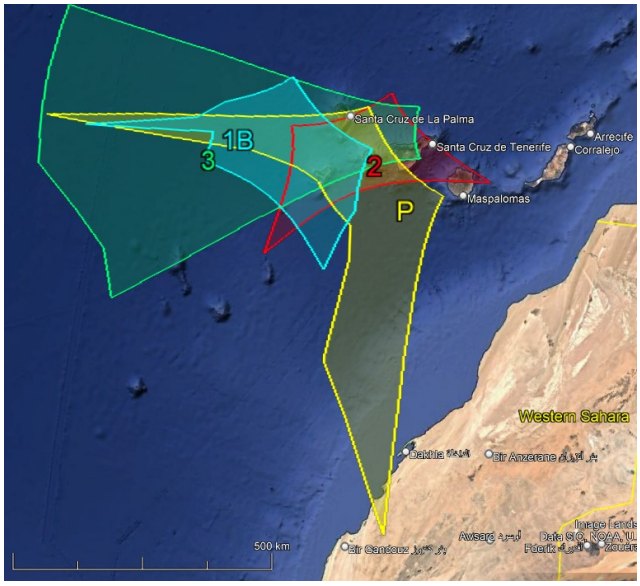

Figure 45 – GMN camera fields in 2025 intersected at 100 km elevation, for cameras active in Spain.

The GMN had its first orbits collected in Spain in April 2020. End of 2020, eight GMN cameras had collected 1207 orbits. A lot of progress was made in Spain in 2021 when the number of cameras increased from eight to 23. The 23

Spanish cameras were involved in 15113 multi-station events in 2021. The number of GMN cameras increased further to 30 in 2022 and resulted in 19301 orbits. In 2023, 22610 orbits were obtained with 35 cameras. In 2024 three new cameras were installed but six older cameras were decommissioned so that the number of operational cameras decreased to 32. 16771 meteor orbits were recorded in 2024. One camera was decommissioned and two new installed in 2025, resulting in 12599 orbits. Four cameras are installed at the Canary Islands (*Figure 45*). The all-time total of orbits is 87601 for Spain.

4.40 CH – Switzerland

The first orbits were obtained in August 2021 but it took until May 2022 before extra cameras were installed and more orbits recorded. With five operational cameras 3439 orbits were obtained in 2022. The central location of Switzerland is ideal to obtain multi-station events with GMN cameras in the neighboring countries. The number of cameras remained unchanged in 2023 and the number of paired meteors increased to 4352. In 2024 one camera was decommissioned and with the remaining four cameras, 2383 meteor orbits were obtained. In 2025 four cameras collected 3808 orbits. The all-time number of orbits is 13985 for Switzerland.

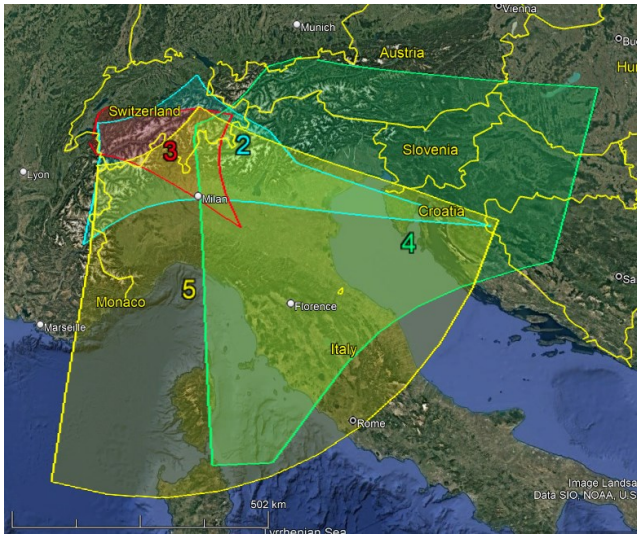

Figure 46 – GMN camera fields in 2025 intersected at 100 km elevation, for cameras active in Switzerland.

4.41 TJ – Tajikistan

The country has a long tradition in meteor astronomy and observations. In June 2024 two GMN cameras installed in Tajikistan had their first paired meteors. In total 411 meteor orbits were obtained despite technical issues that limited the time both cameras were operational. In 2025 the cameras collected 794 orbits. The all-time total of orbits stands at 1205 for Tajikistan (*Figure 47*).

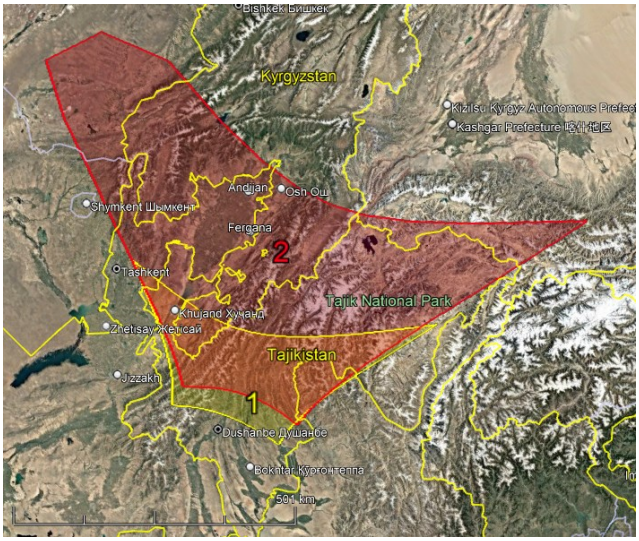

Figure 47 – GMN camera fields in 2025 intersected at 100 km elevation, for cameras active in Tajikistan.

4.42 UA – Ukraine

A first RMS camera contributes meteor data to Global Meteor Network in Ukraine in 2024 but no paired meteors were recorded. In 2025 five more cameras joined GMN and 1896 orbits were recorded. This is an amazing achievement in a country that suffers under war conditions.

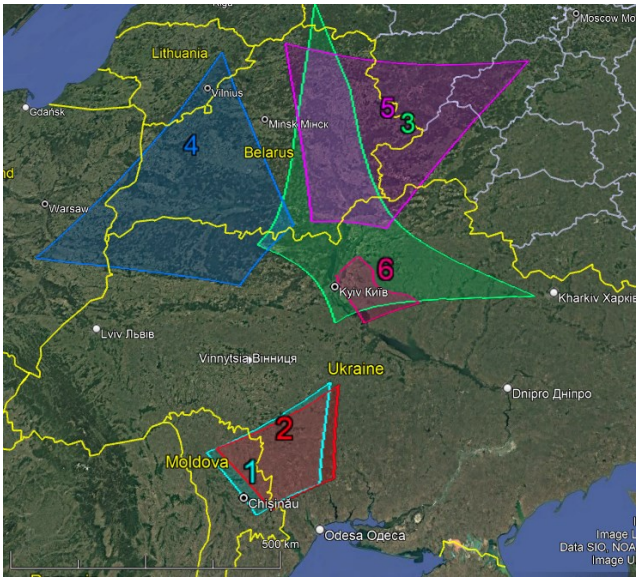

Figure 48 – GMN camera fields in 2025 intersected at 100 km elevation, for cameras active in Ukraine.

4.43 UK – United Kingdom

The GMN started with 13 cameras in 2020 in the UK, which contributed 1889 orbits. These numbers rapidly grew in 2021 to 97 cameras and 27430 orbits. The largest expansion came in 2022 when 191 cameras contributed 78652 paired meteors. The network continued to grow throughout 2023 when 261 cameras contributed 84688. In 2024 the UK had 95730 orbits with 283 cameras. 30 cameras quit, 24 new were installed and 2 resumed operations, with 279 cameras 139838 orbits were obtained in 2025, best result for the UK so far. The all-time total number of orbits for the U.K. is 428227, 56 cameras were decommissioned in past years. The vast majority of the UK cameras are part of the UK

Meteor Network which now provides complete coverage of the UK and Eire (*Figure 49*), see also the kml file[22].

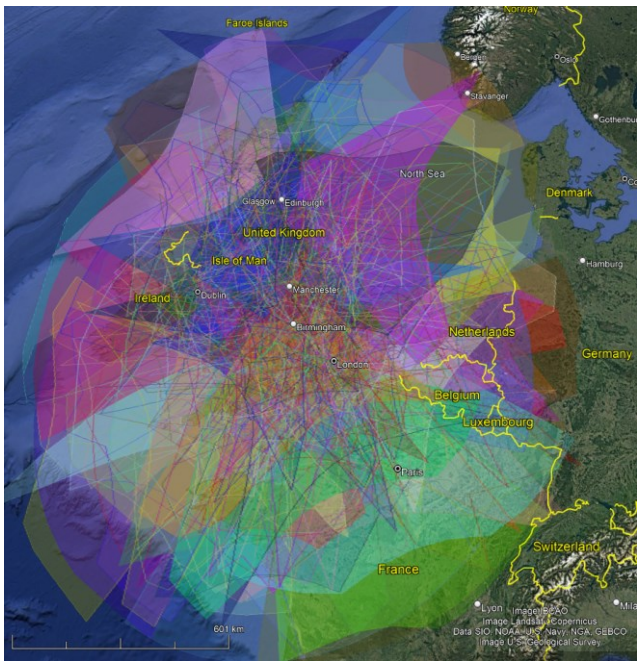

Figure 49 – GMN camera fields in 2025 intersected at 100 km elevation, for all cameras active in the United Kingdom.

Cameras

UK camera numbers have now more or less stabilized, with 279 different cameras contributing to trajectories during the year, slightly down from 2024. There were 242 active cameras in January and while around 40 new cameras came online during the year, the same number were decommissioned for various reasons. Almost all the cameras are contributing to UKMON.

The cameras along the eastern side of the UK overlap well with cameras in Europe, and 134 different non-UK cameras contributed to matches with UK cameras with the number per month increasing from around 50 to over 100 by the end of the year (*Figure 50*). There were contributions from cameras in Belgium, the Czech Republic, Croatia, Germany, Denmark, France, Ireland, Luxembourg and the Netherlands.

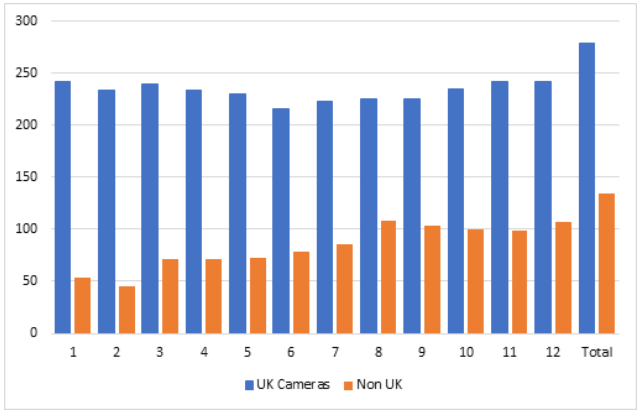

Figure 50 – Number of contributing cameras by month for UKMON.

Matches

UK cameras contributed to 132530 trajectories in 2025, about 14% of the total reported by GMN. As might be expected, the latter half of the year was more active, with December, November and August being the most active months.

As noted above, many UK stations' data matched with stations in Europe – 23708 trajectories also involved cameras from other countries. This shows the importance of a global network as many of these meteors might have been missed, or been analyzed less robustly, without contributions from across Europe.

On average, five stations were involved in each match, and generally there were more stations involved in each match than in prior years, with 90% of trajectories involving up to ten stations. Furthermore, 99 trajectories involved twenty or more stations, and the maximum number of involved stations was 36. *Figure 51* shows the number of detections on the left axis, and the number of involved stations on the horizontal axis for up to 15-station matches.

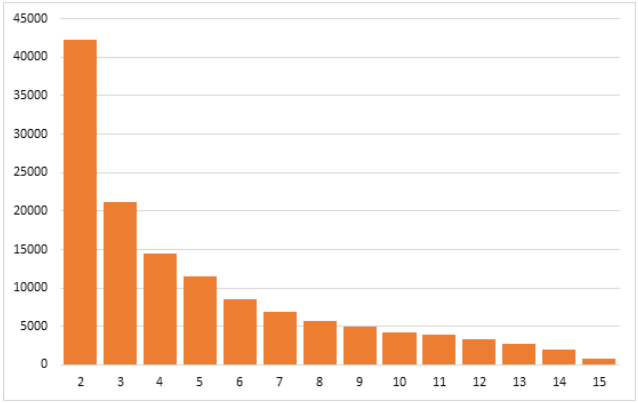

Figure 51 – Number of detections (vertical axis) and the number of involved stations in each detection (horizontal axis).

Geographic coverage

Geographic range was roughly similar to 2024, with trajectories obtained for events between 45.6 and 60.5 North, and between 12.7 West and 10.5 East, covering an area of about two million square kilometers. This equates to about six meteors per year, per ten-kilometer square. When viewed in this context, it is perhaps less surprising that two fireballs were seen a few months apart over the same general area.

Fireballs

Although only 46 fireballs were recorded by UKMON (defining a fireball as having a visual magnitude of brighter than –4), around 1000 detections had an absolute magnitude between –4 and –5, and a further 400 were brighter than this. Many of these were offshore or very distant from cameras and hence with a lower visual magnitude. Nonetheless its likely there were more meteorite-dropping events than we thought. From analysis of trajectories at least

[22] https://www.emeteornews.net/wp-content/uploads/2026/01/2025_uk.zip

three or four of the 46 visual fireballs probably dropped meteorites, though searches were unsuccessful.

Showers

41336 meteors were classified as members of 270 separate showers. 9382 of these were Geminids, 6119 were Perseids, 2711 were Quadrantids and 2123 were Orionids. Other showers had fewer than 1000 meteors each, with 120 showers having fewer than 100 detections.

Looking forward

UK camera growth seems to have peaked south of the Edinburgh-Glasgow line, where every part of the island is covered by at least two cameras, and cameras pointing offshore cover Europe, Eire and the seas around the UK.

We'd like to see more in the West and Highlands of Scotland, though the terrain makes pointing cameras more challenging, and low-elevation detections and matches are less likely. The further north regions of the UK are also a challenge due to lack of darkness in the summer, and generally less clement weather in the winter.

4.44 US – United States

The American New Mexico Meteor Array was the pioneering network of the GMN as it started to harvest meteors in December 2018 with six cameras, producing the first 497 orbits for GMN. It remained the only data provider for GMN until May 2019 when the first 3 Croatian cameras started to deliver orbits. At the end of 2019, the number of US cameras had increased to 20 when the network collected 27643 orbits that year. In 2020, the 33 operational cameras in the US collected as many as 50537 orbits. With 72 RMS cameras registering paired meteors in the US, a total of 91637 orbits were obtained in 2021.

The number of GMN cameras involved in orbit determinations had increased to 100 in 2022, good for 114054 orbits. 2023 saw a further increase in cameras resulting in 120162 orbits. With 141 operational cameras in 2024, 135819 meteor orbits were collected. In 2025 five cameras had been decommissioned, 35 new systems were installed, two resumed capturing, with 173 operational cameras 181237 orbits were collected in 2025. The all-time number of orbits for the USA is 721920. Until 2025 the USA had 17 decommissioned GMN cameras.

Figure 52 shows the GMN status like it was at the end of 2025 with 173 GMN cameras in the US, most of which belong to the New Mexico Camera Array and the Lowell Observatory in Arizona. Both networks are independent in neighboring states but have a large overlap. *Figure 54* shows the situation for the Lowell network in Arizona. The Lowell Observatory cameras also benefit coverage from other GMN cameras in the state as well as in California (*Figure 53*).

GMN camera networks are emerging at several other sites in the US (*Figure 52*). The network reaches till Alaska at 65° northern latitude. Several cameras installed near the East Coast, south of the Canadian border connect to the existing GMN network in Canada (*Figure 55*). The maps show where cameras in the US still wait for multi-station partners to set up cameras (*Figure 56*). The density of the overlap of the camera fields of view is better consulted in Google Earth with the kml file aggregated for all North American cameras[23].

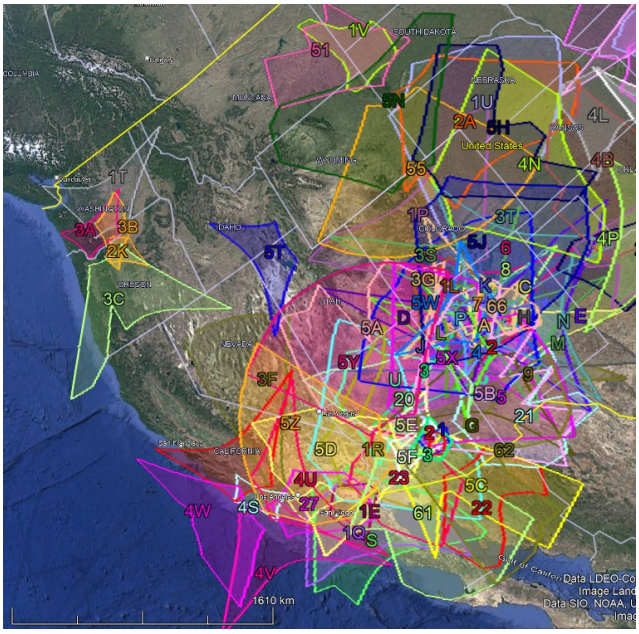

Figure 53 – GMN camera fields in 2025 intersected at 100 km elevation, for cameras in the western part of the USA.

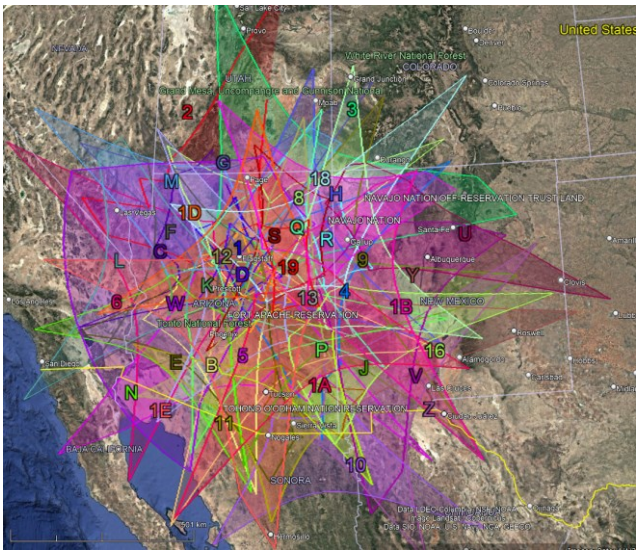

Figure 54 – GMN camera fields in 2025 intersected at 100 km elevation, for cameras of the Lowell Observatory in Arizona.

[23] https://www.emeteornews.net/wp-content/uploads/2026/01/n_america_2025.zip

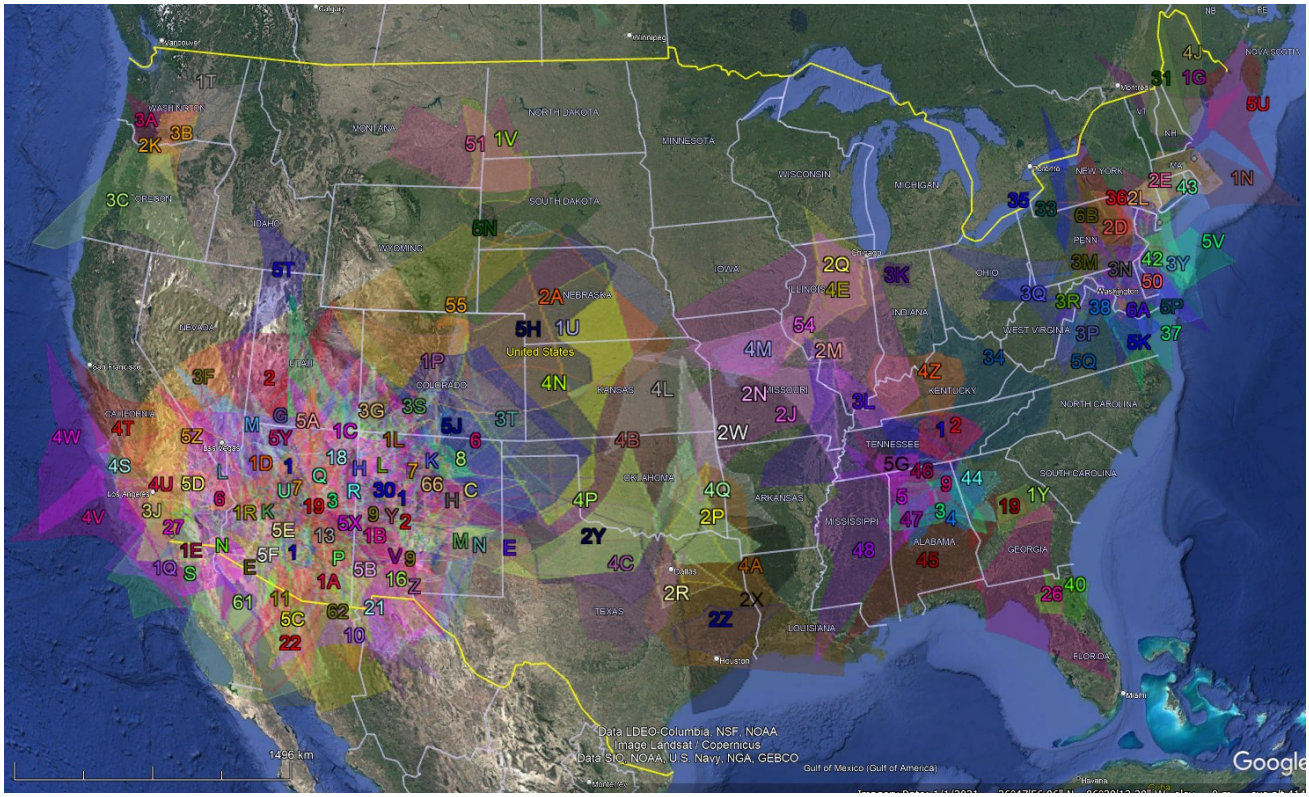

Figure 52 – GMN camera fields in 2024 intersected at 100 km elevation, for cameras in the western part of the USA.

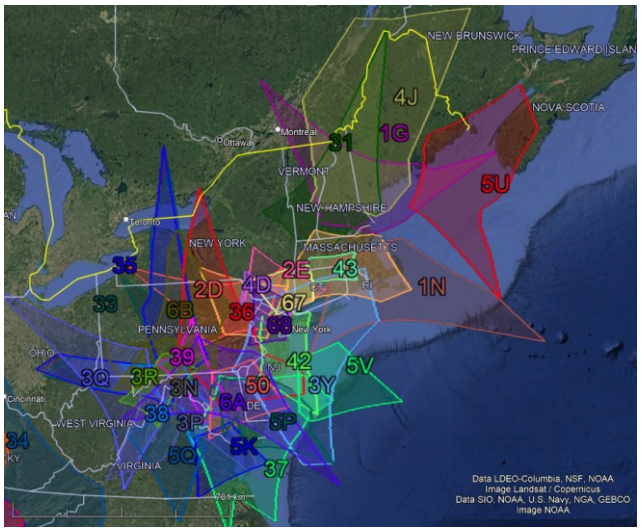

Figure 55 – GMN camera fields in 2025 intersected at 100 km elevation, for cameras in the north-eastern part of the USA.

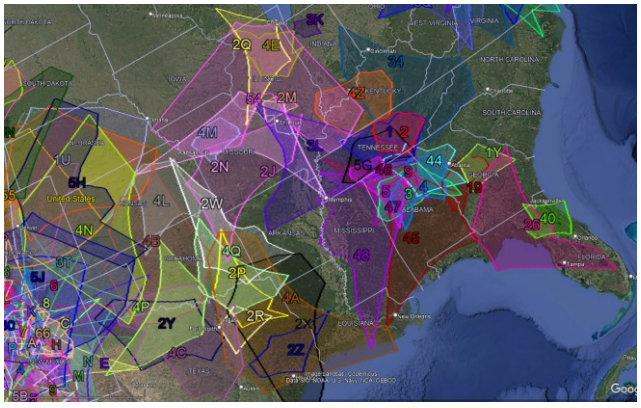

Figure 56 – GMN camera fields in 2025 intersected at 100 km elevation, for cameras in the south-eastern and central parts of the USA.

4.45 ZA – South Africa

The first two GMN cameras were installed at the end of 2022 but no paired meteors were obtained then. In 2023 the number of cameras increased to four and the first 200 orbits were obtained in South Africa. Major progress was made in 2024 when the number of operational cameras doubled and 2294 meteor orbits were recorded. In 2025 four new cameras were installed and 11396 orbits were collected (*Figure 57*). Four cameras were stationed at two schools and there is interest from several more schools giving hope to expand the number of cameras in South Africa further in 2026. The all-time total of orbits is 13890 for South Africa. The geographical position of South Africa makes this network of strategic interest for the coverage of southern hemisphere meteor activity.

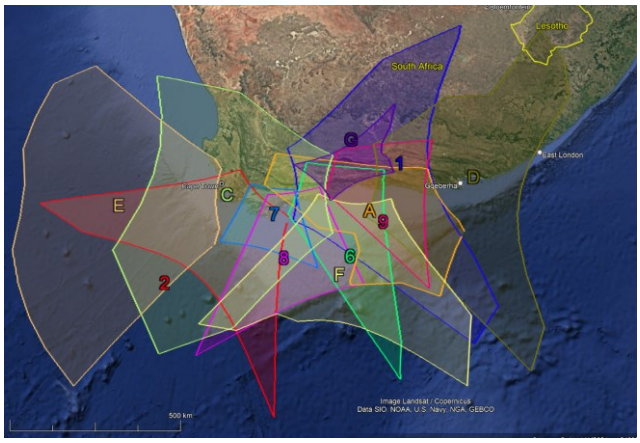

Figure 57 – GMN camera fields in 2025 intersected at 100 km elevation, for cameras active in South Africa.

5 GMN statistics 2025

When a first GMN status report was published, including all data until end October 2020, 140 operational cameras were involved and 144950 orbits had been collected (Roggemans, 2021). Now, we can compare seven years of GMN work. *Figure 58* shows the accumulated number of orbits obtained and the number of contributing cameras during each calendar month. The rapid growth of the Global Meteor Network is obvious. The number of cameras involved in collecting orbits for GMN increased from 390 in 2021 to 700 in 2022, 1066 in 2023, 1213 in 2024 and 1365 in 2025.

In 2025 GMN has installed 236 new cameras while 96 cameras that were active in 2024 did no longer have paired meteors. Twelve cameras that had stopped in 2024 resumed contributing to multi-station events. Since 2018 there have been 1621 cameras contributing to paired meteors of which 254 were decommissioned.

Table 2 shows that only 32% of all orbits are collected during the first six months of each year, while 68% is obtained in the period July to December. The fast expansion of the Global Meteor Network also means that more cameras were available towards the end of each year than at the beginning of each year, what also influenced the number of orbits obtained. The most important cause for the difference in number of orbits between the first and last six months is the meteor activity itself. Apart from the most active major meteor showers like the Perseids, Taurids, Orionids, Leonids and Geminids, the overall meteor activity is much higher during the second half of the year. This can be seen very well in *Figure 58* where the blue curve has a much steeper increase each second half of the year.

Although 1365 different cameras contributed paired meteors during 2025, only 1115 or 82% were successfully contributing during December (*Table 3*). The explanation is that this report is based on the camera IDs which occur in the orbit dataset and thus successfully recorded paired meteors. Apart from the 1115 successful cameras in December there were also a number of cameras functioning without having any paired meteors and thus not listed in the orbit dataset. Persistent unfavorable weather in winter with ice and snow sometimes prevent some cameras from getting paired meteors at the Northern Hemisphere. If a camera somehow has no calibration, no trajectories can be calculated.

Occasionally some hardware or network problem occur, if the connection with the camera board gets lost, the system may ping its camera unsuccessfully until the camera owner fixes the problem. Another frequent hardware problem is when the sd card crashes and needs replacement. To prevent loss of valuable observing data, it is strongly recommended

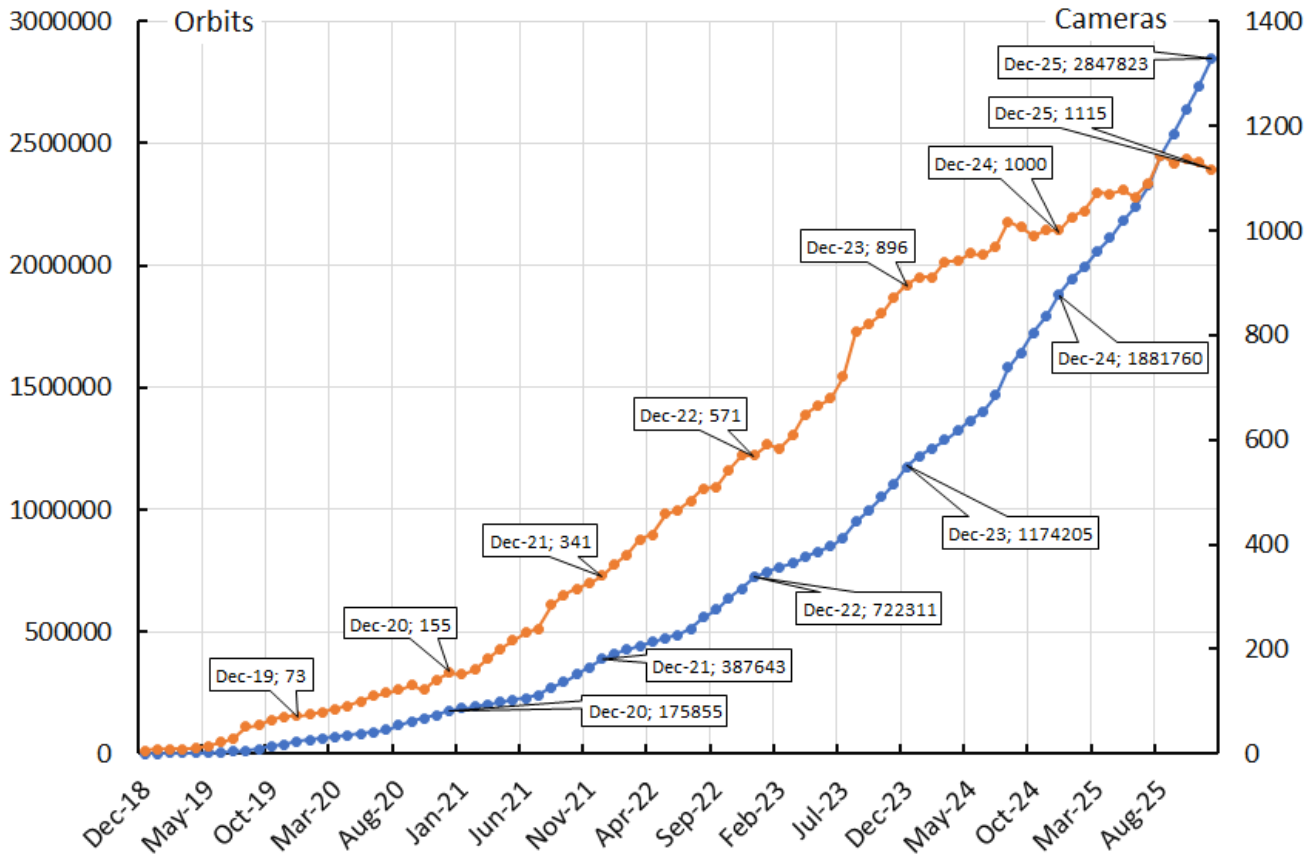

Figure 58 – The accumulated number of orbits (blue) and the actual number of operational cameras involved in triangulations (orange). The numbers at the end of each year are indicated.

Table 2 – Total number of orbits obtained by the Global Meteor Network per calendar month for each year.

	2018	2019	2020	2021	2022	2023	2024	2025	Totals
January	–	564	7539	9919	23727	23972	45613	62373	173707
February	–	1284	5330	6529	14910	18602	31316	49527	127498
March	–	537	5101	8767	15409	16310	33960	64809	144893
April	–	876	7213	9655	15658	22713	38029	55227	149371
May	–	1242	5654	10217	16951	22050	39834	67921	163869
June	–	1523	5700	7954	13463	23125	38336	55659	145760
July	–	1961	10973	11325	25226	35109	67402	88341	240337
August	–	5387	19422	31292	47300	65155	112442	125815	406813
September	–	6058	14012	21189	29984	44174	62041	88586	266044
October	–	11978	13097	31501	48360	59134	81356	96024	341450
November	–	7710	13228	30381	37895	54030	67862	93761	304867
December	497	11143	17826	33059	45785	67520	89364	118020	383214
Totals	497	50263	125095	211788	334668	451894	707555	966063	2847823

Table 3 – Total number of operational cameras with paired meteors within the Global Meteor Network per calendar month.

	2018	2019	2020	2021	2022	2023	2024	2025	Totals
January		9	75	152	363	591	910	1025	1303
February		9	80	161	380	583	911	1038	1302
March		9	86	182	410	609	940	1072	1342
April		10	91	200	418	648	942	1070	1366
May		15	101	216	458	665	956	1077	1393
June		22	111	232	466	680	953	1064	1394
July		29	117	239	483	720	969	1091	1432
August		52	122	285	507	806	1016	1144	1495
September		55	131	304	510	821	1007	1128	1497
October		65	122	316	542	842	990	1137	1499
November		71	142	326	571	873	1000	1132	1495
December	6	73	155	341	571	896	1000	1115	1518
Totals	6	76	172	390	700	1066	1213	1365	1621

to look regularly at the weblog page[24] to check if all cameras report correctly to GMN. The GMN status page is another handy tool that shows all cameras per country color coding the status of all cameras in a single view[25]. This page has additional features, including fields of view, sorting of data, presentation of daily data etc.

Table 4 lists the number of orbits obtained by the cameras per country. Meteors don't care about borders and many multi-station events are recorded by stations in different countries. In that case the orbit has been counted for each different country that provided camera data for the trajectory solution.

Table 5 lists the number of cameras active per country for each year since 2018. The number of camera IDs that contributed no paired meteors in 2025 has been also listed per country. In some cases, old devices were replaced by new, in other cases the camera owner somehow was unable to solve technical issues, had lack of time or lost interest. Unfortunately, some camera operators have died.

The number of operational devices tend to stabilize above 1100 active cameras. New cameras compensate the loss of older devices. There are still critical longitudes where global coverage of meteor activity requires more cameras, mainly at the Southern Hemisphere in South America and Southern Africa.

[24] https://globalmeteornetwork.org/weblog/

[25] https://globalmeteornetwork.org/status/

Table 4 – Total number of multi-station events contributing to an orbit result, recorded in each country for each year. The list is sorted on the country ID used in the camera ID. Subnetworks for some countries are counted in the grand total for the country.

	2018	2019	2020	2021	2022	2023	2024	2025	Totals
Austria (AT)	0	0	0	0	0	0	1702	4819	6521
Australia (AU)	0	0	0	1871	12460	40712	100044	111155	266242
Bosnia and Herzegovina (BA)	0	0	0	0	0	0	0	6153	6153
Belgium (BE)	0	921	5500	8582	23174	25443	34049	53244	150913
Bulgaria (BG)	0	0	0	419	3877	3530	15058	12297	35181
Brazil (BR)	0	0	40	1645	2760	2331	4753	9949	21478
Canada (CA)	0	3599	10815	8809	16232	15023	18508	20576	93562
Switzerland (CH)	0	0	0	3	3439	4352	2383	3808	13985
Chile (CL)	0	0	0	0	0	0	0	1907	1907
Czech Republic (CZ)	0	0	163	464	2490	11269	18248	25668	58302
Germany (DE)	0	200	3963	7009	9128	12194	23240	37570	93304
Denmark (DK)	0	0	0	0	55	1386	3360	20522	25323
Spain (ES)	0	0	1207	15113	19301	22610	16771	12599	87601
Finland (FI)	0	0	0	0	41	90	204	407	742
France (FR)	0	0	3176	5601	11990	16682	20592	27617	85658
Greece (GR)	0	0	0	0	977	3375	8998	16865	30215
Croatia (HR)	0	12221	35099	38370	31329	27721	35726	57060	237526
Hungary (HU)	0	0	0	0	2114	7872	9626	19870	39482
Ireland (IE)	0	0	120	424	3490	1954	3706	6692	16386
Israel (IL)	0	0	553	2009	975	1096	991	681	6305
Italy (IT)	0	862	5384	5447	4943	5064	6603	9249	37552
Japan (JP)	0	0	0	0	0	629	606	147	1382
South Korea (KR)	0	0	0	0	7711	34044	42477	63284	147516
Luxembourg (LU)	0	0	0	0	622	2018	2194	4133	8967
Morocco (MA)	0	0	0	0	0	0	851	1312	2163
Mexico (MX)	0	0	0	0	1769	2953	2871	1134	8727
Malasia (MY)	0	0	0	0	50	501	246	258	1055
Netherlands (NL)	0	278	4337	7605	9139	9421	17409	33566	81755
New Zealand (NZ)	0	0	0	1146	6280	47436	147831	182324	385017
Poland (PL)	0	0	35	67	398	456	1759	7486	10201
Portugal (PT)	0	0	0	0	327	3322	4413	4067	12129
Romania (RO)	0	0	0	0	0	417	4361	4426	9204
Russia (RU)	0	5715	13438	6208	5437	1992	10939	10553	54282
Slovenia (SI)	0	2753	3999	6001	5887	6789	12209	14741	52379
Slovakia (SK)	0	0	0	37	2026	5535	7532	6943	22073
Tajikistan (TJ)	0	0	0	0	0	0	411	794	1205
Ukraine (UA)	0	0	0	0	0	0	0	1896	1896
United Kingdom (UK)	0	0	1889	27430	78652	84688	95730	139838	428227
USA (US)	497	27643	50607	91901	114054	120162	135819	181237	721920
Erroneous entry (XX)	0	0	0	8	28	0	123	0	159
South Africa (ZA)	0	0	0	0	0	200	2294	11396	13890

Table 5 – Total number of operational cameras with paired meteors in each country for each year. Inactive devices and cameras without orbits are not counted. The list is sorted on the country ID used in the camera ID. Subnetworks for some countries are counted in the grand total for the country. The column 'Quit' lists the number of cameras which had paired meteors before 2025 but did not appear in the 2025 data and are therefore considered as decommissioned.

	2018	2019	2020	2021	2022	2023	2024	2025	Totals	Quit
Austria (AT)	0	0	0	0	0	0	2	2	2	0
Australia (AU)	0	0	0	12	29	66	88	82	102	20
Bosnia and Herzegovina (BA)	0	0	0	0	0	0	0	5	5	0
Belgium (BE)	0	4	4	10	20	23	28	43	45	2
Bulgaria (BG)	0	0	0	2	6	7	17	16	18	2
Brazil (BR)	0	0	2	13	20	34	37	36	52	16
Canada (CA)	0	11	17	29	51	51	46	43	77	34
Canada (CAWE)	0	0	0	0	7	8	4	6	14	8
Canada (CAWT)	0	0	0	0	0	8	1	0	8	8
Switzerland (CH)	0	0	0	1	5	5	4	4	5	1
Chile (CL)	0	0	0	0	0	0	0	2	2	0
Czech Republic (CZ)	0	0	3	4	6	20	25	28	29	1
Germany (DE)	0	4	10	12	18	19	30	32	34	2
Denmark (DK)	0	0	0	0	1	4	5	27	27	0
Spain (ES)	0	0	8	23	30	35	32	33	41	8
Finland (FI)	0	0	0	0	4	5	7	8	8	0
France (FR)	0	0	10	14	16	18	19	20	28	8
Greece (GR)	0	0	0	0	1	4	8	8	8	0
Croatia (HR)	0	23	32	48	45	41	43	50	72	22
Hungary (HU)	0	0	0	0	2	3	3	12	12	0
Ireland (IE)	0	0	2	3	5	5	6	6	9	3
Israel (IL)	0	0	3	6	5	6	7	6	9	3
Italy (IT)	0	1	1	5	5	7	7	7	10	3
Japan (JP)	0	0	0	0	0	2	2	3	3	0
South Korea (KR)	0	0	0	0	47	125	122	123	128	5
Luxembourg (LU)	0	0	0	0	1	1	1	2	2	0
Morocco (MA)	0	0	0	0	0	0	3	3	3	0
Mexico (MX)	0	0	0	0	12	15	13	11	15	4
Malasia (MY)	0	0	0	0	3	5	6	10	11	1
Netherlands (NL)	0	2	11	11	13	14	18	31	36	5
New Zealand (NZ)	0	0	0	2	28	111	152	184	191	7
Poland (PL)	0	0	1	1	3	2	4	11	13	2
Portugal (PT)	0	0	0	0	1	1	2	2	2	0
Romania (RO)	0	0	0	0	0	3	3	5	6	1
Russia (RU)	0	10	21	21	19	15	22	21	35	14
Slovenia (SI)	0	1	1	2	2	6	6	7	7	0
Slovakia (SK)	0	0	0	1	3	4	5	5	5	0
Tajikistan (TJ)	0	0	0	0	0	0	2	2	2	0
Ukraine (UA)	0	0	0	0	0	0	0	5	5	0
United Kingdom (UK)	0	0	13	97	191	261	283	279	335	56
USA (US)	6	20	33	72	100	128	141	173	190	17
USA (US0)	6	20	24	36	51	78	97	124	133	9
USA (USL)	0	0	9	36	47	45	41	41	48	7
USA (USN)	0	0	0	0	0	3	1	5	6	1
USA (USV)	0	0	0	0	2	2	2	3	3	0
Erroneous entry (XX)	0	0	0	1	1	0	1	0	1	1
South Africa (ZA)	0	0	0	0	0	4	8	12	12	0

6 Meteor showers covered by GMN

Using the Working List of Meteor Showers[26] (Jenniskens et al., 2020; Jopek and Kaňuchová, 2017; Jopek and Jenniskens, 2011; Neslušan et al., 2020) as a reference, 387 of the showers listed could be associated with orbits collected by the Global Meteor Network. The number of orbits recorded for each of these showers is listed in *Table 6* for each year since 2018.

The GMN meteor shower association was originally based on the table of Sun-centered ecliptic shower radiant positions given in Jenniskens et al. (2018). However, in May 2023 it was concluded that the list had some imperfections and therefore it was decided to make GMN's own meteor shower list and redo the meteor shower associations from the past. The new reference list contained 387 meteor showers instead of the 425 in the previous list. Meanwhile, new discovered activities and known showers that were missing in the list have been added bringing the total number of meteor showers monitored by GMN at 418. Still, many entrees of the IAU MDC Working List of Meteor Showers have no matching orbits in the GMN database and most of these meteor showers are not included in the GMN list for reasons explained below. Some of the showers are periodic and display only some activity once every few years, some showers have been detected by radar in a fainter range of magnitudes than what GMN cameras cover and others are known as daylight meteor showers. While GMN is getting better coverage at the southern hemisphere, more of the low declination meteor showers are getting covered. For many of the listed meteoroid streams their absence in the GMN orbit database can be explained because the evidence for the existence of the shower is still missing. One of the goals of the GMN project is to help to identify ghost meteor showers that should be removed from the Working List.

Table 6 serves as an inventory of what the GMN orbit database has available until end 2025. Of course, the number of shower members detected depends on the criteria used to associate a meteor with a known meteor shower radiant. The GMN shower association criterion assumes that meteors within 1° in solar longitude, within 3° in radiant, and within 10% in geocentric velocity of a shower reference location are members of that shower. Further details about the shower association are explained in Moorhead et al. (2020). This is a rather strict criterion since meteor showers often have a larger dispersion in radiant position and velocity. Therefore, using the orbit similarity criteria (Drummond, 1981; Southworth and Hawkins, 1963; Jopek, 1993) will certainly detect more shower candidates but at the risk of including sporadic orbits that fulfil similarity criteria by pure chance.

In 2025 a number of case studies on GMN meteoroid orbit data to document meteor shower activities have been published:

- New meteor shower in Cassiopeia, 4 September 2024
- New meteor shower in Ursa Minor, 23–24 September 2024
- New meteor shower in Lyra, 26–27 October 2024
- New meteor shower in Puppis
- New meteor shower in Octans
- New meteor shower in Equuleus
- New meteor shower in Indus
- June delta Pavonids (JDP#835) in 2025
- Two meteor shower outbursts with potential connection to comet 73P/Schwassmann-Wachmann
- New meteor shower in Eridanus
- Outburst of a new meteor shower in Aries
- New meteor shower in Delphinus (M2025-S1)
- M2024-S1 activity confirmed in 2025
- Epsilon-Ursae Minorids (EPU#1044) enhanced activity in 2025
- New meteor shower in Hydrus (M2025-S2)
- Delta-Horologiids (DHO#1146) in 2025
- October epsilon-Carinids (OEC#1172)
- A Carinids (842#CRN) outburst in 2025
- New meteor shower in Pegasus (M2025-U1)
- New meteor shower in Monoceros (M2025-V1)
- 29-Piscids (PIS#1046) return in 2025
- M2024-H1 activity confirmed in 2025
- M2024-N1 activity confirmed in 2025
- Eccentrids in the GMN orbit dataset

The main goal of the GMN, not to let any meteor shower activity pass unnoticed, is being achieved. Whenever some unexpected meteor activity occurs, the Global Meteor Network has good chances to cover it. Many of the existing showers monitored by GMN are still awaiting independent confirmation to be nominated by the IAU-MDC staff to get the status of an established shower.

More case studies on poorly known meteor showers are possible thanks to the statistically relevant numbers of shower meteors recorded by GMN for many of these meteoroid streams that wait to be better documented. Therefore, it is most important to keep as many cameras operational around the globe.

More information and detailed documentation about meteor showers can be found in the new reference work "Atlas of Earth's Meteor Showers" that appeared in October 2023 (Jenniskens, 2023).

[26] https://www.ta3.sk/IAUC22DB/MDC2022/Roje/roje_lista.php?corobic_roje=0&sort_roje=0

Table 6 – Total number of orbits according to the meteor shower association (IAU number + code) for each year.

IAU id	Meteor shower name	< 2021	2021	2022	2023	2024	2025	Total
Spo#-1	Sporadics	124497	145663	231788	318794	519521	707068	2047331
CAP#1	alpha-Capricornids	698	451	1147	1840	3845	4740	12721
STA#2	Southern Taurids	1603	1934	2178	3575	4564	5765	19619
SIA#3	Southern iota-Aquariids	38	39	52	116	267	271	783
GEM#4	Geminids	8206	9968	15800	19655	13814	37342	104785
SDA#5	Southern delta-Aquariids	1540	1225	3190	4138	10056	13999	34148
LYR#6	April Lyrids	561	743	1066	1451	1235	2703	7759
PER#7	Perseids	7423	11407	15126	22003	35890	32234	124083
ORI#8	Orionids	4546	4556	9576	10417	10664	12708	52467
DRA#9	October Draconids	6	7	11	6	295	19	344
QUA#10	Quadrantids	574	1216	1070	1017	2798	5535	12210
EVI#11	eta-Virginids	40	283	241	82	139	1562	2347
KCG#12	kappa-Cygnids	93	1773	85	107	180	222	2460
LEO#13	Leonids	955	953	1548	2362	2281	3443	11542
URS#15	Ursids	332	169	325	402	745	832	2805
HYD#16	sigma-Hydrids	848	1613	1263	2737	4287	3456	14204
NTA#17	Northern Taurids	923	965	1053	2397	2161	2902	10401
AND#18	Andromedids	111	920	175	216	226	333	1981
MON#19	December Monocerotids	365	593	531	1291	1438	1712	5930
COM#20	Comae Berenicids	846	680	1660	1686	2347	3169	10388
AVB#21	alpha-Virginids	117	123	142	368	394	673	1817
LMI#22	Leonis Minorids	186	193	357	436	539	789	2500
EGE#23	epsilon-Geminids	216	347	510	624	753	920	3370
NOA#25	Northern October delta-Arietids	274	183	294	437	392	725	2305
NDA#26	Northern delta-Aquariids	492	476	774	1265	1792	2300	7099
KSE#27	kappa-Serpentids	14	29	26	54	76	78	277
SOA#28	Southern October delta-Arietids	216	318	124	576	706	360	2300
ETA#31	eta-Aquariids	665	1321	2446	2575	7948	10243	25198
NIA#33	Northern iota-Aquariids	196	215	230	382	623	740	2386
ZCY#40	zeta-Cygnids	130	203	303	347	357	636	1976
DLI#47	mu-Virginids	60	33	143	205	214	188	843
TAH#61	tau-Herculids	0	1	1243	1	3	2	1250
GDE#65	gamma-Delphinids	7	27	26	36	45	72	213
SSG#69	Southern mu-Sagittariids	64	67	81	354	674	974	2214
SLY#81	September Lyncids	87	104	75	197	214	228	905
ODR#88	omicron-Draconids	21	17	46	31	53	71	239
PVI#89	January pi-Virginids	20	48	89	105	208	196	666
NCC#96	Northern delta-Cancrids	103	86	245	204	388	490	1516
SCC#97	Southern delta-Cancrids	170	104	278	272	498	674	1996
PIH#101	pi-Hydrids	206	290	469	649	1196	1437	4247
ACE#102	alpha-Centaurids	0	0	29	40	319	382	770
BTU#108	beta-Tucanids	0	0	1	28	29	3	61
AAN#110	alpha-Antliids	23	10	61	48	76	159	377
DPA#120	delta-Pavonids	0	0	0	0	0	128	128
DME#130	delta-Mensids	0	0	5	57	215	259	536
ELY#145	eta-Lyrids	46	148	209	181	289	368	1241
NOP#149	Northern May Ophiuchids	26	12	18	61	110	146	373

IAU id	Meteor shower name	< 2021	2021	2022	2023	2024	2025	Total
SOP#150	Southern May Ophiuchids	12	25	15	70	144	151	417
EAU#151	epsilon-Aquilids	99	109	230	303	563	588	1892
NOC#152	Northern Daytime omega-Cetids	6	8	9	12	13	31	79
OCE#153	Southern Daytime omega-Cetids	0	0	0	0	0	16	16
SSC#161	Southern omega-Scorpiids	17	38	21	50	102	70	298
NZC#164	Northern June Aquilids	394	304	709	1005	1966	2368	6746
SZC#165	Southern June Aquilids	93	93	226	408	1287	1229	3336
JBO#170	June Bootids	4	0	35	5	0	2	46
ARI#171	Daytime Arietids	20	32	34	46	90	113	335
JPE#175	July Pegasids	169	221	404	669	960	1048	3471
PHE#176	July Phoenicids	1	11	49	221	650	940	1872
OCY#182	omicron-Cygnids	21	20	31	34	41	67	214
PAU#183	Piscis Austrinids	38	40	52	104	352	191	777
GDR#184	July gamma-Draconids	132	66	175	127	322	413	1235
EUM#186	epsilon-Ursae Majorids	13	6	14	22	33	25	113
PCA#187	psi-Cassiopeiids	23	33	56	80	71	87	350
BPE#190	beta-Perseids	35	33	96	75	151	186	576
ERI#191	eta-Eridanids	166	183	328	642	1614	1464	4397
UCE#194	upsilon-Cetids	84	114	200	272	393	443	1506
AUD#197	August Draconids	329	320	460	714	858	1014	3695
ADC#199	August delta-Capricornids	0	0	0	0	0	1	1
AUR#206	Aurigids	79	128	152	157	265	371	1152
SPE#208	September epsilon-Perseids	305	411	310	833	865	882	3606
BAU#210	beta-Aurigids	159	159	250	340	374	609	1891
KLE#212	Daytime kappa-Leonids	6	6	7	24	12	29	84
NPI#215	Northern delta-Piscids	172	123	253	237	386	643	1814
SPI#216	Southern delta-Piscids	78	52	96	175	156	386	943
NDR#220	nu-Draconids	86	51	91	169	165	312	874
DSX#221	Daytime Sextantids	8	22	42	34	66	89	261
SOR#225	sigma-Orionids	119	118	218	310	394	463	1622
XDR#242	xi-Draconids	33	66	72	136	131	139	577
ZCN#243	zeta-Cancrids	10	22	15	26	25	23	121
NHD#245	November Hydrids	31	81	66	131	154	152	615
AMO#246	alpha-Monocerotids	47	40	73	80	138	138	516
NOO#250	November Orionids	505	821	1047	953	2127	1797	7250
ALY#252	alpha-Lyncids	7	10	16	8	15	31	87
CMI#253	December Canis Minorids	94	100	158	189	298	343	1182
PHO#254	Phoenicids	0	0	0	0	53	12	65
ORN#256	Northern chi-Orionids	242	233	376	423	611	828	2713
ORS#257	Southern chi-Orionids	432	525	688	971	1330	1671	5617
OCT#281	October Camelopardalids	37	55	149	55	163	129	588
FTA#286	omega-Taurids	153	156	492	206	537	1162	2706
DSA#288	Southern December delta-Arietids	115	111	220	259	355	579	1639
DNA#289	Northern December delta-Arietids	39	126	96	96	237	251	845
TPU#307	tau-Puppids	1	3	11	31	86	91	223
PIP#308	January pi-Puppids	35	36	66	108	321	300	866
MVE#318	mu-Velids	27	35	49	107	200	251	669
JLE#319	January Leonids	9	5	24	13	33	56	140

IAU id	Meteor shower name	< 2021	2021	2022	2023	2024	2025	Total
LBO#322	lambda-Bootids	16	29	70	56	86	81	338
XCB#323	xi-Coronae Borealids	17	31	41	65	92	54	300
EPR#324	epsilon-Perseids	12	3	12	17	17	27	88
EPG#326	epsilon-Pegasids	33	33	52	59	104	126	407
SSE#330	sigma-Serpentids	7	0	8	4	8	5	32
AHY#331	alpha-Hydrids	38	43	161	62	405	496	1205
OCU#333	October Ursae Majorids	93	150	139	295	176	296	1149
DAD#334	December alpha-Draconids	270	406	481	606	817	940	3520
XVI#335	December chi-Virginids	136	115	163	289	352	400	1455
DKD#336	December kappa-Draconids	141	293	149	423	668	309	1983
NUE#337	nu-Eridanids	657	850	1309	1849	2746	3678	11089
OER#338	omicron-Eridanids	278	308	435	718	946	1147	3832
PSU#339	psi-Ursae Majorids	55	124	62	150	291	129	811
TPY#340	theta-Pyxidids	62	63	154	194	400	451	1324
XUM#341	January xi-Ursae Majorids	22	31	50	133	135	152	523
HVI#343	h-Virginids	158	6	2	7	116	505	794
FHE#345	f-Herculids	14	30	75	49	77	157	402
XHE#346	x-Herculids	36	53	96	84	123	193	585
BPG#347	beta-Pegasids	1	7	4	5	8	19	44
ARC#348	April rho-Cygnids	91	119	232	205	175	488	1310
LLY#349	lambda-Lyrids	3	2	4	6	7	15	37
DTR#351	Daytime Triangulids	0	0	0	0	0	12	12
JMC#362	June mu-Cassiopeiids	26	56	66	44	69	81	342
PPS#372	phi-Piscids	352	354	841	952	1301	2189	5989
ALN#376	August Lyncids	16	19	31	45	49	105	265
OLP#384	October Leporids	26	36	50	74	102	109	397
OBC#386	October beta-Camelopardalids	45	71	117	115	155	177	680
CTA#388	chi-Taurids	123	195	202	288	377	394	1579
THA#390	November theta-Aurigids	315	507	387	693	947	1026	3875
NID#392	November i-Draconids	55	74	79	126	136	177	647
ACA#394	alpha-Canis Majorids	39	51	77	107	203	190	667
GCM#395	gamma-Canis Majorids	88	39	130	132	323	363	1075
GUM#404	gamma-Ursae Minorids	30	19	54	162	103	165	533
DPI#410	delta-Piscids	14	17	54	98	69	355	607
CAN#411	c-Andromedids	148	205	411	439	652	882	2737
SIC#416	September iota-Cassiopeiids	37	43	42	82	108	111	423
SOL#424	September-October Lyncids	78	77	181	178	245	439	1198
FED#427	February eta-Draconids	8	3	27	11	31	106	186
DSV#428	December sigma-Virginids	182	222	407	395	711	805	2722
ACB#429	alpha-Coronae Borealids	29	18	103	115	71	161	497
JIP#431	June iota-Pegasids	17	11	60	106	68	138	400
ZCS#444	zeta-Cassiopeiids	161	262	392	624	644	613	2696
KUM#445	kappa-Ursae Majorids	76	125	111	154	161	141	768
DPC#446	December phi-Cassiopeiids	23	71	89	40	357	54	634
AAL#448	April alpha-Librids	22	26	54	52	94	173	421
AED#450	April epsilon-Delphinids	18	27	48	49	93	127	362
CAM#451	Camelopardalids	4	2	6	6	2	7	27
MPS#456	May psi-Scorpiids	117	139	211	390	493	935	2285

IAU id	Meteor shower name	< 2021	2021	2022	2023	2024	2025	Total
JEC#458	June epsilon-Cygnids	46	61	43	128	107	99	484
JEO#459	June epsilon-Ophiuchids	67	10	47	110	90	154	478
AXC#465	August xi-Cassiopeiids	26	57	74	96	106	97	456
AOC#466	August omicron-Cetids	11	16	25	52	109	83	296
LAQ#473	lambda-Aquariids	31	23	44	104	56	189	447
ICE#476	iota-Cetids	53	32	36	60	68	128	377
TCA#480	tau-Cancrids	155	233	371	439	502	661	2361
NZP#486	November zeta-Perseids	28	17	50	43	55	80	273
NSU#488	November sigma-Ursae Majorids	27	25	53	45	77	72	299
DEL#494	December Lyncids	56	127	93	169	214	207	866
DAB#497	December alpha-Bootids	18	20	47	52	31	75	243
FPL#501	February pi-Leonids	23	30	31	52	100	99	335
DRV#502	December rho-Virginids	84	129	140	173	263	281	1070
AIC#505	August iota-Cetids	170	159	312	439	635	1035	2750
FEV#506	February epsilon-Virginids	88	115	302	360	473	532	1870
UAN#507	upsilon-Andromedids	81	87	265	211	299	420	1363
JRC#510	June rho-Cygnids	16	44	55	98	116	142	471
RPU#512	rho-Puppids	48	47	56	185	192	232	760
OMC#514	omega-Capricornids	13	16	34	120	223	358	764
OLE#515	omicron-Leonids	74	87	193	189	350	389	1282
FMV#516	February mu-Virginids	23	32	105	116	149	225	650
ALO#517	April lambda-Ophiuchids	6	25	45	30	54	106	266
AHE#518	April 102-Herculids	12	4	19	27	18	39	119
BAQ#519	beta-Aquariids	12	28	53	31	109	145	378
MBC#520	May beta-Capricornids	21	25	32	90	108	201	477
AGC#523	August gamma-Cepheids	69	72	169	103	260	363	1036
LUM#524	lambda-Ursae Majorids	25	66	108	35	148	184	566
SLD#526	Southern lambda-Draconids	33	67	68	92	101	106	467
EHY#529	eta-Hydrids	155	241	287	473	632	616	2404
ECV#530	eta-Corvids	36	47	130	211	362	434	1220
GAQ#531	gamma-Aquilids	24	60	73	94	114	188	553
JXA#533	July xi-Arietids	50	60	134	212	418	445	1319
THC#535	theta-Cetids	5	11	20	29	91	46	202
TTB#543	22-Bootids	12	9	22	16	27	52	138
JNH#544	January nu-Hydrids	17	10	33	20	58	86	224
XCA#545	xi-Cassiopeiids	7	10	29	13	24	49	132
FTC#546	43-Cassiopeiids	69	63	83	149	167	232	763
KAP#547	kappa-Perseids	204	266	462	689	900	1212	3733
FAN#549	49-Andromedids	59	77	112	156	132	248	784
PSO#552	pi6-Orionids	112	221	270	361	428	403	1795
OCP#555	October gamma-Camelopardalids	32	51	83	85	136	147	534
PTA#556	phi-Taurids	22	50	78	81	147	116	494
SFD#557	64-Draconids	82	101	111	191	202	252	939
MCB#559	beta-Canis Majorids	23	10	42	42	65	87	269
SSX#561	6-Sextantids	29	31	61	64	77	136	398
DOU#563	December omega-Ursae Majorids	56	26	96	88	177	182	625
SUM#564	61-Ursae Majorids	30	13	40	23	81	78	265
OHY#569	omicron-Hydrids	31	34	128	225	511	679	1608

IAU id	Meteor shower name	< 2021	2021	2022	2023	2024	2025	Total
FBH#570	February beta-Herculids	12	11	48	48	58	157	334
TSB#571	26-Bootids	11	11	29	28	48	108	235
SAU#575	63-Aurigids	24	19	41	60	56	79	279
CHA#580	chi-Andromedids	41	16	73	67	97	169	463
NHE#581	90-Herculids	71	88	130	190	160	304	943
JBC#582	January beta-Craterids	15	36	60	80	182	216	589
GCE#584	Cepheids-Cassiopeiids	39	50	84	102	169	193	637
THY#585	33-Hydrids	19	20	41	73	56	81	290
FNC#587	59-Cygnids	18	24	45	25	47	49	208
FCA#589	50-Cancrids	27	49	81	62	131	138	488
VCT#590	10-Canum Venaticids	6	2	14	5	30	26	83
ZBO#591	zeta-Bootids	23	28	52	49	92	102	346
PON#592	91-Piscids	13	18	30	39	61	44	205
TOL#593	28-Lyncids	35	62	77	126	117	157	574
RSE#594	Serpentids-Coronae Borealids	3	4	4	27	11	30	79
POS#599	72-Ophiuchids	48	89	156	173	256	355	1077
ICT#601	iota-Craterids	12	10	27	28	86	98	261
KCR#602	kappa-Craterids	1	21	36	37	104	85	284
FAR#608	14-Aurigids	15	38	52	64	86	49	304
TLY#613	31-Lyncids	13	61	56	104	97	84	415
THD#618	12-Hydrids	8	16	30	12	64	55	185
XCS#623	xi2-Capricornids	98	99	248	814	499	878	2636
XAR#624	xi-Arietids	239	138	370	523	286	882	2438
LTA#625	lambda-Taurids	180	132	454	492	286	1646	3190
LCT#626	lambda-Cetids	73	126	191	42	271	477	1180
NPS#627	nu-Piscids	72	158	226	122	402	463	1443
STS#628	s-Taurids	185	208	3172	258	388	5156	9367
ATS#629	A2-Taurids	208	176	326	706	228	883	2527
TAR#630	tau-Arietids	247	411	352	537	698	584	2829
DAT#631	delta-Arietids	225	374	553	227	877	1207	3463
NET#632	November eta-Taurids	222	377	179	774	682	542	2776
PTS#633	p-Taurids	193	262	246	401	692	551	2345
TAT#634	tau-Taurids	256	210	487	606	670	1096	3325
ATU#635	A1-Taurids	307	471	260	1090	969	1407	4504
MTA#636	m-Taurids	93	172	121	182	432	267	1267
FTR#637	f-Taurids	276	404	1248	663	760	3745	7096
DZT#638	December zeta-Taurids	33	39	47	97	66	150	432
AOA#640	August omicron-Aquariids	313	328	547	1117	2296	1567	6168
JLL#644	January lambda-Leonids	124	107	134	231	249	397	1242
BCO#647	beta-Comae Berenicids	48	69	99	82	117	234	649
TAL#648	22-Aquilids	88	113	216	317	431	610	1775
OAV#651	68-Virginids	50	67	128	385	273	374	1277
OSP#652	omicron-Serpentids	14	21	30	36	96	99	296
RLY#653	R-Lyrids	38	33	88	71	94	201	525
APC#655	April phi-Capricornids	3	4	4	29	63	73	176
GSG#657	gamma-Sagittariids	2	12	13	27	60	66	180
EDR#658	epsilon-Draconids	16	22	30	19	44	100	231
EPS#660	epsilon-Scorpiids	18	30	25	61	143	209	486

IAU id	Meteor shower name	< 2021	2021	2022	2023	2024	2025	Total
OTH#661	110-Herculids	11	28	32	25	45	72	213
MUC#665	May upsilon-Cygnids	24	27	35	64	58	89	297
JMP#668	June mu-Pegasids	23	16	36	52	38	61	226
MCY#671	mu-Cygnids	3	9	20	9	32	33	106
MUA#679	mu-Aquariids	11	33	32	56	91	99	322
JEA#680	June epsilon-Arietids	15	12	19	22	33	29	130
OAQ#681	omicron-Aquariids	21	17	21	48	56	120	283
JTS#683	June theta-Serpentids	8	6	5	20	21	48	108
JPS#685	June beta-Pegasids	15	9	39	37	42	74	216
JRD#686	June rho-Draconids	1	7	17	26	15	17	83
KDP#687	kappa-Delphinids	9	5	7	8	19	7	55
TAC#689	tau-Capricornids	49	31	100	160	468	510	1318
ZCE#691	zeta-Cetids	1	13	29	15	49	57	164
EQA#692	epsilon-Aquariids	134	239	373	159	1243	1056	3204
ANP#693	August nu-Perseids	61	65	158	147	208	317	956
OMG#694	omicron-Geminids	105	111	180	217	283	342	1238
APA#695	August psi-Aurigids	18	27	36	34	46	89	250
OAU#696	omicron-Aurigids	31	36	63	79	96	135	440
AET#698	August eta-Taurids	23	30	48	81	48	152	382
BCE#701	beta-Cepheids	10	7	24	37	93	91	262
ASP#702	August 78-Pegasids	13	9	17	13	23	41	116
OAN#704	omicron-Andromedids	101	107	135	197	250	316	1106
ZPI#706	zeta-Piscids	75	80	132	174	210	326	997
BPX#707	beta-Pyxidids	2	4	19	15	102	121	263
RLM#708	R-Leonis Minorids	4	24	31	46	86	61	252
FDC#712	February delta-Cygnids	9	12	19	21	20	46	127
CCR#713	chi-Cancrids	15	9	19	25	13	43	124
RPI#714	rho-Piscids	96	89	143	181	250	368	1127
ACL#715	alpha-Camelopardalids	222	286	401	557	607	758	2831
OCH#716	October chi-Andromedids	54	67	108	109	154	204	696
NGB#720	November gamma-Bootids	10	16	16	16	50	64	172
DAS#721	December alpha-Sextantids	19	38	19	23	73	49	221
FLE#722	15-Leonids	25	42	36	45	112	64	324
DEG#726	December epsilon-Geminids	55	12	85	76	119	177	524
ISR#727	iota-Serpentids	4	0	16	6	12	44	82
PGE#728	phi-Geminids	25	11	46	26	65	71	244
DCO#729	delta-Corvids	11	2	17	13	48	53	144
ATV#730	April theta-Virginids	7	1	4	7	22	26	67
FGV#732	February gamma-Virginids	15	14	33	41	27	123	253
MOC#734	March omicron-Cygnids	13	14	17	11	23	49	127
XIP#736	xi-Perseids	11	15	32	27	60	53	198
FNP#737	59-Perseids	5	2	15	4	25	25	76
RER#738	rho-Eridanids	16	31	47	78	238	119	529
LAR#739	lambda-Arietids	18	26	57	36	81	132	350
OSD#745	October 6-Draconids	25	40	66	83	84	115	413
EVE#746	e-Velids	24	123	195	942	1710	1408	4402
JKL#747	January kappa-Leonids	31	44	101	52	153	197	578
JTL#748	January theta-Leonids	22	14	95	92	139	203	565

IAU id	Meteor shower name	< 2021	2021	2022	2023	2024	2025	Total
SMV#750	Southern March gamma-Virginids	56	94	186	229	397	691	1653
KCE#751	kappa-Cepheids	59	39	78	87	109	172	544
MID#755	May iota-Draconids	4	3	11	6	5	18	47
CCY#757	chi-Cygnids	392	16	23	47	57	1209	1744
SCO#771	sigma-Columbids	3	9	9	27	25	41	114
ILU#783	iota-Lupids	0	0	0	0	0	26	26
KVE#784	kappa-Velids	2	28	103	99	404	353	989
TCD#785	theta-Carinids	0	9	41	75	343	360	828
SXP#786	6-Puppids	6	1	13	10	34	29	93
KVO#787	kappa-Volantids	0	0	0	0	0	324	324
MBE#792	March beta-Equuleids	0	2	4	6	9	4	25
KCA#793	kappa-Cancrids	8	10	30	14	53	59	174
SED#796	September epsilon-Draconids	11	29	41	34	63	78	256
ADS#802	June Aquariids	8	9	18	46	68	84	233
LSA#803	lambda-Sagittariids	7	27	54	69	200	169	526
FLO#807	February Leonids	64	61	98	126	180	405	934
XCD#810	October Cetids	17	29	63	62	62	97	330
NAA#812	November alpha-Aurigids	25	27	32	64	59	76	283
CVD#814	January Canum Venaticids	6	6	34	48	24	72	190
UMS#815	August Ursae Majorids	10	9	15	16	16	36	102
CVT#816	February Canum Venaticids	6	13	15	23	20	44	121
OAG#818	October Aurigids	15	10	21	30	28	49	153
NUT#822	nu-Taurids	4	9	18	52	108	131	322
FCE#823	56-Cetids	30	26	54	85	129	165	489
DEX#824	December Sextantids	20	13	35	45	66	77	256
XIE#825	xi-Eridanids	26	22	25	69	111	42	295
ILI#826	iota1-Librids	40	42	69	126	282	347	906
NPE#827	nu-Pegasids	18	16	31	52	90	107	314
JSP#829	July 77-Pegasids	25	54	46	113	121	130	489
SCY#830	63-Cygnids	29	20	46	46	65	84	290
GPG#831	gamma-Pegasids	13	14	30	44	61	63	225
LEP#832	Leporids	4	5	12	27	85	84	217
KOR#833	kappa-Orionids	8	13	30	34	54	43	182
ACU#834	April theta-Centaurids	2	6	6	9	57	43	123
JDP#835	June delta-Pavonids	0	0	0	0	0	79	79
ABH#836	April beta-Herculids	2	8	17	22	30	48	127
CAE#837	Caelids	2	2	19	30	20	77	150
PSR#839	phi-Serpentids	10	17	22	29	53	27	158
TER#840	tau4-Eridanids	4	8	3	17	31	37	100
DHE#841	delta-Herculids	5	16	46	25	46	79	217
CRN#842	A-Carinids	0	0	0	0	0	229	229
DMD#843	December mu-Draconids	6	5	9	13	25	37	95
DTP#844	December theta-Pyxidids	21	45	36	61	151	100	414
TSC#846	tau-Sculptorids	0	0	0	0	0	46	46
BEL#847	beta-Leonids	4	13	10	12	19	23	81
OPE#848	omicron-Perseids	6	4	9	8	2	17	46
SZE#849	September zeta-Eridanids	16	17	22	48	60	99	262
PCY#854	psi-Cygnids	18	25	67	69	71	93	343

IAU id	Meteor shower name	< 2021	2021	2022	2023	2024	2025	Total
ATD#855	August tau-Draconids	3	8	8	18	19	12	68
EMO#856	epsilon-Monocerotids	12	15	25	17	43	54	166
FPB#858	February phi-Bootids	23	15	75	81	62	113	369
MTB#859	March 12-Bootids	3	17	35	21	45	105	226
PAN#860	psi-Andromedids	3	12	28	22	15	24	104
JXS#861	June xi1-Sagittariids	10	4	15	33	26	89	177
SSR#862	16-Scorpiids	10	16	37	48	61	123	295
TLR#863	12-Lacertids	6	12	12	26	17	15	88
JSG#864	June 66-Pegasids	3	10	8	20	24	22	87
JES#865	June epsilon-Serpentids	8	3	15	25	25	40	116
ECB#866	epsilon-Coronae Borealids	7	9	8	6	17	12	59
FPE#867	52-Pegasids	13	2	38	17	44	52	166
PSQ#868	psi3-Aquariids	6	2	8	23	29	38	106
UCA#869	upsilon1-Cassiopeiids	10	5	25	29	65	98	232
JPG#870	July eta-Pegasids	11	8	11	10	27	45	112
DCD#871	delta-Cepheids	9	5	11	11	18	43	97
ETR#872	epsilon-Triangulids	11	16	32	39	84	42	224
OMI#873	omicron-Cetids	13	12	26	21	39	91	202
PXS#874	September xi-Perseids	57	45	75	113	82	186	558
TEI#875	tau9-Eridanids	6	13	19	24	42	42	146
ROR#876	rho-Orionids	20	20	49	43	79	131	342
OHD#877	omega-Hydrids	12	21	25	41	19	45	163
OEA#878	October epsilon-Aurigids	7	2	9	23	21	33	95
ATI#879	alpha-Taurids	18	28	35	58	56	64	259
YDR#880	Y-Draconids	25	28	40	50	42	87	272
TLE#881	theta-Leonids	2	21	19	9	19	22	92
PLE#882	phi-Leonids	10	10	20	20	25	21	106
NBP#884	November beta-Pyxidids	4	1	15	29	61	49	159
DEV#885	December epsilon-Virginids	15	7	32	16	69	74	213
ACV#886	alpha-Corvids	8	11	48	24	104	135	330
DZB#887	December zeta-Bootids	16	15	25	13	37	85	191
SCV#888	6-Corvids	2	10	10	21	43	46	132
YOP#889	Y-Ophiuchids	1	2	8	6	10	14	41
ESU#890	eta-Scutids	6	3	6	10	5	19	49
FSL#891	February sigma-Leonids	19	9	55	44	38	184	349
MCN#892	March Centaurids	0	3	9	5	22	24	63
EOP#893	eta-Ophiuchids	19	25	42	71	100	173	430
OTA#896	130-Taurids	32	11	42	61	41	119	306
OUR#897	October alpha-UrsaeMinorids	11	21	28	10	49	31	150
SGP#898	September gamma-Piscids	15	19	10	30	50	43	167
EMC#899	epsilon-Microscopiids	1	3	13	29	72	109	227
BBO#900	beta-Bootids	18	40	109	44	155	105	471
TLC#901	34-Lyncids	11	7	19	21	22	37	117
DCT#902	delta-Cetids	28	24	36	86	83	104	361
OAT#903	October alpha-Triangulids	20	7	25	35	51	61	199
OCO#904	omicron-Columbids	4	14	5	50	56	26	155
MXD#905	March xi-Draconids	7	6	7	11	7	22	60
ETD#906	eta-Draconids	13	18	34	27	17	99	208

IAU id	Meteor shower name	< 2021	2021	2022	2023	2024	2025	Total
MCE#907	mu-Cepheids	6	11	21	17	26	12	93
BTC#910	beta2-Cygnids	15	19	32	26	35	91	218
TVU#911	21-Vulpeculids	13	29	57	49	80	141	369
BCY#912	beta-Cygnids	18	23	39	46	74	92	292
DNO#915	delta-Normids	1	2	6	41	45	167	262
TAG#918	theta-Aurigids	14	17	41	18	37	70	197
ICN#919	iota-Centaurids	2	4	3	17	126	223	375
XSC#920	xi-Scorpiids	14	25	43	53	137	163	435
JLC#921	July lambda-Capricornids	18	6	22	27	48	116	237
SAN#924	62-Andromedids	4	20	5	26	16	6	77
EAN#925	eta-Andromedids	6	4	23	23	14	31	101
OCR#1033	omega-Carinids	0	0	0	6	19	14	39
EPU#1044	epsilon-Ursae Minorids	0	0	0	0	0	150	150
TVL#1055	35-Vulpeculids	0	0	0	0	0	13	13
SCE#1070	77-Cetids	0	0	0	0	0	244	244
IHD#1071	iota-Hydrusids	0	0	0	0	0	60	60
GAD#1106	gamma-Draconids	0	0	0	0	0	51	51
IHR#1108	July iota-Hydrusids	0	0	0	0	0	17	17
ARD#1130	Arids	0	6	0	1	2	0	9
OZP#1131	October zeta-Perseids	0	6	1	0	0	0	7
OEC#1172	October epsilon-Carinids	0	0	0	0	0	161	161
M23K1	M2023-K1	0	0	0	0	0	21	21
M24H1	M2024-H1	0	0	0	0	0	17	17
M24N1	M2024-N1	0	0	0	0	0	42	42
M24S1	M2024-S1	0	0	0	0	0	28	28
M25F1	M2025-F1	0	0	0	0	0	124	124
M25K1	M2025-K1	0	0	0	0	0	35	35
M25L1	M2025-L1	0	0	0	0	0	55	55
M25L2	M2025-L2	0	0	0	0	0	46	46
M25O1	M2025-O1	0	0	0	0	0	69	69
M25O2	M2025-O2	0	0	0	0	0	48	48
M25P1	M2025-P1	0	0	0	0	0	70	70
M25S1	M2025-S1	0	0	0	0	0	132	132
M25S2	M2025-S2	0	0	0	0	0	466	466
M2025U1	M2025-U1	0	0	0	0	0	152	152
M25Y1	M2025-Y1	0	0	0	0	0	395	395
	Totals	175855	211788	334668	451894	707555	966063	2847823

Acknowledgments

This report is based on the data of the Global Meteor Network which is released under the CC BY 4.0 license[27]. We thank all the 927 participants in the Global Meteor Network project for their contribution and perseverance, operators whose cameras provided the data used in this work and contributors who made important code contributions The Global Meteor Network results were obtained thanks to the efforts of the following volunteers. (list cut-off date as it was at the end of 28 January 2026).

In memory of Global Meteor Network members:

Dr. Daniel A. Klinglesmith III (d. 2019)
Martin Richmond-Hardy (d. 2023)
Rajko Susanj (d. 2023)
Zoran Dragic (d. 2025)
Romke Schievink (d. 2025)
Seppe Canonaco (d. 2025)

Memento mori
Each of us, a fleeting flame
Yet our paths remain.

A. Campbell, Adam Mullins, Aden Walker, Adrian Bigland, Adriana Roggemans, Adriano Fonseca, Aksel Askanius, Al Foster, Alain Marin, Alaistar Brickhill, Alan Beech, Alan Maunder, Alan Pevec, Alan Pickwick, Alan Decamps, Alan Cowie, Alan Kirby, Alan Senior, Alastair Emerson, Aled Powell, Alejandro Barriuso, Aleksandar Merlak, Aleksei Blokhin, Alex Bell, Alex Haislip, Alex Hodge, Alex Jeffery, Alex Kichev, Alex McConahay, Alex Pratt, Alex Roig, Alex Aitov, Alex McGuinness, Alexander Wiedekind-Klein, Alexander Kasten, Alexandre Alves, Alexandru Tudorica, Alfredo Dal' Ava Júnior, Alison Scott, Amy Barron, Anatoly Ijon, Andre Rousseau, Andre Bruton, Andrea Storani, Andrei Marukhno, Andres Fernandez, Andrew Campbell-Laing, Andrew Challis, Andrew Cooper, Andrew Fiamingo, Andrew Heath, Andrew Moyle, Andrew Washington, Andrew Fulher, Andrew Robertson, Andy Stott, Andy Sapir, Andy Shanks, Ange Fox, Angel Sierra, Angélica López Olmos, Anna Johnston, Anne van Weerden, Anoop Chemencherry, Ansgar Schmidt, Anthony Hopkinson, Anthony Pitt, Anthony Kesterton, Anton Macan, Anton Yanishevskiy, Antony Crowther, Anzhari Purnomo, Ari Paulechen Jr, Arie Blumenzweig, Arie Verveer, Arnaud Leroy, Arne Krueger, Artem Oskolkov, Attila Nemes, Barry Findley, Bart Dessoy, Bela Szomi Kralj, Ben Poulton, Bence Kiss, Bernard Côté, Bernard Hagen, Bev M. Ewen-Smith, Bill Cooke, Bill Wallace, Bill Witte, Bill Carr, Bill Thomas, Bill Kraimer, Bob Evans, Bob Greschke, Bob Hufnagel, Bob Marshall, Bob Massey, Bob Zarnke, Bob Guzik, Branko Zubić, Brenda Goodwill, Brendan Cooney, Brendon Reid, Brian Chapman, Brian Murphy, Brian Rowe, Brian Hochgurtel, Wyatt Hochgurtel, Brian Mitchell, Bridgend Astronomical Society, Bruno Bonicontro, Bruno Casari, Callum Potter, Carl Elkins, Carl Mustoe, Carl Panter, Cesar Domingo Pardo, Charles Thody, Charlie McCormack, Chris Baddiley, Chris Blake, Chris Dakin, Chris George, Chris James, Chris Ramsay, Chris Reichelt, Chris Chad, Chris O'Neill, Chris White, Chris Jones, Chris Sale, Chris Raynerd, Christian Wanlin, Christine Ord, Christof Zink, Christophe Demeautis, Christopher Coomber, Christopher Curtis, Christopher Tofts, Christopher Brooks, Christopher Matthews, Chuck Goldsmith, Chuck Pullen, Ciaran Tangney, Claude Boivin, Claude Surprenant, Clive Sanders, Clive Hardy, Colin Graham, Colin Marshall, Colin Nichols, Con Stoitsis, Craig Young, Creina Beaman, Daknam Al-Ahmadi, Dale Hooper, Damien Lemay, Damien McNamara, Damir Matković, Damir Šegon, Damjan Nemarnik, Dan Klinglesmith, Dan Pye, Daniel Duarte, Daniel J. Grinkevich, Daniela Cardozo Mourão, Danijel Reponj, Danko Kočiš, Dario Zubović, Dave Jones, Dave Mowbray, Dave Newbury, Dave Smith, David Akerman, David Attreed, David Bailey, David Brash, David Castledine, David Hatton, David Leurquin, David Price, David Rankin, David Robinson, David Rollinson, David Strawford, David Taylor, David Rogers, David Banes, David Johnston, David Rees, David Cowan, David Greig, David Hickey, David Colthorpe, David Straer, David Harding, David Furneaux, David Teissier, David Lynch, David M. Goldie, Dean Moore, Debbie Godsiff, Denis Bergeron, Denis St-Gelais, Dennis Behan, Derek Poulton, Derek Baker, Didier Walliang, Dimitris Georgoulas, Dino Čaljkušić, Dmitrii Rychkov, Dominique Guiot, Don Anderson, Don Hladiuk, Dorian Božičević, Dougal Matthews, Douglas Sloane, Douglas Stone, Dustin Rego, Dylan O'Donnell, Ed Breuer, Ed Harman, Edd Stone, Edgar Mendes Merizio, Edison José Felipe Pérezgómez Álvarez, Edson Valencia Morales, Eduardo Fernandez Del Peloso, Eduardo Lourenço, Edward Cooper, Egor Gustov, Ehud Behar, Eleanor Mayers, Emily Barraclough, Enrico Pettarin, Enrique Arce, Enrique Chávez Garcilazo, Eric Lopez, Eric Toops, Eric O' Toole, Eric Ronney, Errol Balks, Erwin van Ballegoij, Erwin Harkink, Eugene Potapov, Ewan Richardson, Fabricio Borges, Fabricio Colvero, Fabrizio Guida, Felipe P. Leitzke, Felix Bettonvil, Ferenc-Levente Juhos, Fernando Dall'Igna, Fernando Jordan, Fernando Requena, Filip Matković, Filip Mezak, Filip Parag, Fiona Cole, Firuza Rahmat, Florent Benoit, Francis Rowsell, François Simard, Frank Lyter, Frans Lowiessen, Frantisek Bilek, Gabor Sule, Gaétan Laflamme, Gareth Brown, Gareth Lloyd, Gareth Oakey, Garry Dymond, Gary Parker, Gary Eason, Gavin Martin, Gene Mroz, Geoff Scott, Georges Attard, Georgi Momchilov, Gerald Engwell, Gerard Van Os, Germano Soru, Gert Jan Netjes, Gilberto Sousa, Gilton Cavallini, Gino Robert, Glen Shennan, Gordon Hudson, Graeme Hanigan, Graeme McKay, Graham Stevens, Graham Winstanley, Graham Henstridge, Graham Atkinson, Graham Palmer, Graham Cann, Graham Mallin, Grant Salmond, Greg Michael, Greg Parker, Guillaume Poulizac, Gulchehra Kokhirova, Gustav Frisholm, Gustavo Silveira B. Carvalho, Guy Létourneau, Guy Williamson, Guy Lesser, Hamish Barker, Hamish McKinnon, Hanson Du, Haris Jeffrey, Harri Kiiskinen,

[27] https://creativecommons.org/licenses/by/4.0/

Hartmut Leiting, Heather Petelo, Henk Bril, Henning Letmade, Heriton Rocha, Hervé Lamy, Herve Roche, Holger Pedersen, Horst Meyerdierks, Howard Edin, Hugo González, Iain Drea, Ian Enting Graham, Ian Lauwerys, Ian Parker, Ian Pass, Ian A. Smith, Ian Williams, Ian Hepworth, Ian Collins, Ian Cattermole, Igor Duchaj, Igor Henrique, Igor Macuka, Igor Pavletić, Ilya Jankowsky, Ioannis Kedros, Ivan Gašparić, Ivan Sardelić, Ivica Ćiković, Ivica Skokić, Ivo Dijan, Ivo Silvestri, Jack Barrett, Jacques Masson, Jacques Walliang, Jacqui Thompson, Jake Turner, James Davenport, James Farrar, James Scott, James Stanley, James Dawson, James Lloyd, James Malley, Jamie Allen, Jamie Cooper, Jamie McCulloch, Jamie Olver, Jamie Shepherd, Jan Hykel, Jan Wisniewski, Jan Tromp, Janis Russell, Janusz Powazki, Jasminko Mulaomerović, Jason Burns, Jason Charles, Jason Gill, Jason van Hattum, Jason Sanders, Javor Kac, Jay Shaffer, Jayce Dowell, Jean Francois Larouche, Jean Vallieres, Jean Brunet, Jean-Baptiste Kikwaya, Jean-Bruno Desrosiers, Jean-Fabien Barrois, Jean-Louis Naudin, Jean-Marie Jacquart, Jean-Paul Dumoulin, Jean-Philippe Barrilliot, Jeff Holmes, Jeff Huddle, Jeff Wood, Jeff Devries, Jeffrey Legg, Jenifer Millard, Jeremy Taylor, Jeremy Spink, Jesse Stayte, Jesse Lard, Jessica Richards, Jim Blackhurst, Jim Cheetham, Jim Critchley, Jim Fordice, Jim Gilbert, Jim Rowe, Jim Seargeant, Jim Fakatselis, João Mattei, Joaquín Albarrán, Jochen Vollsted, Jocimar Justino, Joe Zender, Joe Farragher, Johann Swanepoel, John W. Briggs, John Drummond, John Hale, John Kmetz, John Maclean, John Savage, John Thurmond, John Tuckett, John Waller, John Wildridge, John Bailey, John Thompson, John Martin, John Yules, John Burrin, John Huberd, Jon Bursey, Jonathan Alexis Valdez Aguilar, Jonathan Eames, Jonathan Mackey, Jonathan Whiting, Jonathan Wyatt, Jonathan Pettingale, Jonathon Kambulow, Jorge Augusto Acosta Bermúdez, Jorge Oliveira, Jose Carballada, Jose Galindo Lopez, José María García, José-Luis Martín, Josef Scarantino, Joseph Jones, Josip Belas, Josip Krpan, Jost Jahn, Juan Luis Muñoz, Juergen Neubert, Julián Martínez, Julien Roy, Jure Zakrajšek, Jürgen Dörr, Jürgen Ketterer, Justin Zani, Kamel Nechma, Karen Smith, Karl Browne, Kath Johnston, Kees Habraken, Keith Maslin, Keith Biggin, Keith Christie, Keith Scorrar, Keith Butterworth, Kelvin Richards, Ken Jamrogowicz, Ken Lawson, Ken Gledhill, Ken Kirvan, Ken Whitnall, Kevin Gibbs-Wragge, Kevin Morgan, Kevin Faure, Kevin Nielsen, Klaas Jobse, Korado Korlević, Kyle Francis, Lachlan Gilbert, Larry Groom, Lars Rombi, Laurent Brunetto, Laurent Reix, Laurie Stanton, Lawrence Saville, Lee Hill, Lee Brady, Leith Robertson, Len North, Les Rowe, Leslie Kaye, Lev Pustil'Nik, Lexie Wallace, Lisa Holstein, Llewellyn Cupido, Logan Carpenter, Lorna McCalman, Louw Ferreira, Lovro Pavletić, Lubomir Moravek, Luc Turbide, Luc Busquin, Lucia Dowling, Luciano Miguel Diniz, Ludger Börgerding, Luis Fabiano Fetter, Luis Santo, Maciej Reszelsk, Maciej Kwinta, Magda Wisniewska, Manel Colldecarrera, Marc Corretgé Gilart, Marcel Berger, Marcelo Domingues, Marcelo Zurita, Marcio Malacarne, Marco Verstraaten, Marcus Rigo, Margareta Gumilar, Marián Harnádek, Mario Sandri, Mariusz Adamczyk, Mark Fairfax, Mark Gatehouse, Mark Haworth, Mark McIntyre, Mark Phillips, Mark Robbins, Mark Spink, Mark Suhovecky, Mark Williams, Mark Ward, Mark Bingham, Mark Fechter, Mark Severance, Marko Šegon, Marko Stipanov, Marshall Palmer, Marthinus Roos, Martin Breukers, Martin Richmond-Hardy, Martin Robinson, Martin Walker, Martin Woodward, Martin Connors, Martin Kobliha, Martyn Andrews, Martyn Kinder, Martyn Hunter-Wyatt, Mary Waddingham, Mary Hope, Mason McCormack, Mat Allan, Máté Pintér, Matej Mihelčić, Matt Cheselka, Matt McMullan, Matthew Howarth, Matthew Finch, Matthew Terracciano, Max Schmid, Megan Gialluca, Megan Spencer-Young, Mia Boothroyd, Michael Cook, Michael Mazur, Michael O'Connell, Michael Krocil, Michael Camilleri, Michael Kennedy, Michael Lowe, Michael Atkinson, Michael Rainbow, Michał Warchoł, Michel Saint-Laurent, Mielke Sarkol, Miguel Diaz Angel, Miguel Preciado, Miguel Ángel Rapado, Mike Breimann, Mike Hutchings, Mike Read, Mike Shaw, Mike Ball, Mike Youmans, Milan Kalina, Milen Nankov, Miles Eddowes, Minesh Patel, Miranda Clare, Mirjana Malarić, Motohito Mizusaw, Muhammad Luqmanul Hakim Muharam, Murray Forbes, Murray Singleton, Murray Thompson, Myron Valenta, Nalayini Brito, Nawaz Mahomed, Ned Smith, Nedeljko Mandić, Nedim Mujić, Neil Graham, Neil Papworth, Neil Waters, Neil Petersen, Neil Allison, Nelson Moreira, Neville Vann, Nial Bruce, Nicholas Hill, Nicholas Ruffier, Nick Howarth, Nick James, Nick Moskovitz, Nick Norman, Nick Primavesi, Nick Quinn, Nick Russel, Nick Powell, Nick Wiffen, Nicola Masseroni, Nigel Bubb, Nigel Evans, Nigel Owen, Nigel Harris, Nigen Harris, Nikola Gotovac, Nikolay Gusev, Nikos Sioulas, Noah Simmonds, Norman Izsett, Olaf Jakubzik Reinartz, Ole Alexander, Ollie Eisman, Pablo Canedo, Pablo Domingo Escat, Paraksh Vankawala, Pat Devine, Patrick Franks, Patrick Poitevin, Patrick Geoffroy, Patrick Onesty, Patrik Kukić, Paul Cox, Paul Dickinson, Paul Haworth, Paul Heelis, Paul Kavanagh, Paul Ludick, Paul Prouse, Paul Pugh, Paul Roche, Paul Roggemans, Paul Stewart, Paul Huges, Paul Breck, Paul Volman, Paul Jenkinson, Paul D. Clarke, Pedro Augusto de Jesus Castro, Penko Yordanov, Pete Graham, Pete Lynch, Peter G. Brown, Peter Campbell-Burns, Peter Davis, Peter Eschman, Peter Gural, Peter Hallett, Peter Jaquiery, Peter Kent, Peter Lee, Peter McKellar, Peter Meadows, Peter Stewart, Peter Triffitt, Peter Leigh, Peter Felhofer, Péter Molnár, Peter Murray, Peter Watts, Pető Zsolt, Phil James, Philip Gladstone, Philip Norton, Philippe Schaak, Phillip Wilhelm Maximilian Grammerstorf, Pierre Gamache, Pierre de Ponthière, Pierre-Michael Micaletti, Pierre-Yves Pechart, Pieter Dijkema, Predrag Vukovic, Przemek Nagański, Radim Stano, Rajko Sušanj, Raju Aryal, Ralph Brady, Raoul van Eijndhoven, Raul Truta, Raul Elias-Drago, Raymond Shaw, Rebecca Starkey, Reinhard Kühn, Reinier Ott, Rembert Melman, Remi Lacasse, Renato Cássio Poltronieri, René Tardif, Richard Abraham, Richard Bassom, Richard Croy, Richard Davis, Richard Fleet, Richard Hayler, Richard Johnston, Richard Kacerek, Richard Payne, Richard Stevenson, Richard Severn, Richard Bates, Rick Fischer, Rick Hewett, Rick James, Rick

Olupot, Ricky Bassom, Rob Agar, Rob de Corday Long, Rob Saunders, Rob Smeenk, Rob Musquetier, Robert Longbottom, Robert McCoy, Robert Saint-Jean, Robert D. Steele, Robert Veronneau, Robert Peledie, Robert Haas, Robert Kiendl, Robert Vallone, Robert Bungener, Robert Lucas, Robin Boivin, Robin Earl, Robin Rowe, Robin Leadbeater, Roel Gloudemans, Roger Banks, Roger Morin, Roger Conway, Roland Idaczyk, Rolf Carstens, Roman Moryachkov, Romke Schievink, Romulo Jose, Ron James Jr, Ron Paine, Ronal Kunkel, Roslina Hussain, Ross Skilton, Ross Dickie, Ross Welch, Ross Hortin, Russell Jackson, Russell Brunton, Ruud Oskam, Ryan Frazer, Ryan Harper, Ryan Kinnett, Ryan Thompson, Salvador Aguirre, Sam Green, Sam Hemmelgarn, Sam Leaske, Sandy Allan, Sarah Tonorio, Scott Kaufmann, Sean Lavigne, Sebastiaan de Vet, Sebastian Klier, Seppe Canonaco, Seraphin Feller, Serge Bergeron, Sergei Pavlov, Sergio Mazzi, Sergiy Ivanchenko, Sevo Nikolov, Simon Cooke-Willis, Simon Holbeche, Simon Maidment, Simon McMillan, Simon Minnican, Simon Parsons, Simon Saunders, Simon Fidler, Simon Oosterman, Simon Peterson, Simon lewis, Simon Lewis, Simon van Leverink, Simon Andersson, Slava Ilyin, Sofia Ulrich, Srivishal Sudharsan, Stacey Downton, Stan Nelson, Stanislav Korotkiy, Stanislav Tkachenko, Stef Vancampenhout, Stefan Frei, Stephane Zanoni, Stephen Grimes, Stephen Nattrass, Stephen M. Pereira, Steve Berry, Steve Bosley, Steve Carter, Steve Dearden, Steve Homer, Steve Kaufman, Steve Lamb, Steve Rau, Steve Tonkin, Steve Trone, Steve Welch, Steve Wyn-Harris, Steve Matheson, Steve Daniels, Steven Shanks, Steven Tilley, Stewart Doyle, Stewart Ball, Stewart Clark, Stuart Brett, Stuart Land, Stuart McAndrew, Sue Baker Wilson, Sylvain Cadieux, Tammo Jan Dijkema, Ted Cline, Terry Pundiak, Terry Richardson, Terry Simmich, Terry Young, Terry Meldrum, Theodor Feldbaumer, Thiago Paes, Thilo Mies, Thomas Blog, Thomas Schmiereck, Thomas Stevenson, Thomas Duff, Tihomir Jakopčić, Tim Burgess, Tim Claydon, Tim Cooper, Tim Gloudemans, Tim Havens, Tim Polfliet, Tim Frye, Tioga Gulon, Tobias Westphal, Tobias Hinse, Tom Warner, Tom Bell, Tomi Simola, Tommy McEwan, Tommy B. Nielsen, Torcuill Torrance, Tosh White, Tracey Snelus, Travis Shao, Trevor Clifton, Ubiratan Borges, Urs Wirthmueller, Uwe Glässner, Vasilii Savtchenko, Ventsislav Bodakov, Victor Acciari, Viktor Toth, Vincent McDermott, Vitor Jose Pereira, Vladimir Jovanović, Vladimir Usanin, Waily Harim, Warley Souza, Warwick Latham, Washington Oliveira, Wayne Metcalf, Wenceslao Trujillo, William Perkin, William Schauff, William Stewart, William Harvey, William Hernandez, Wullie Mitchell, Yakov Tchenak, Yanislav Ivanov, Yfore Scott, Yleana Ceballos, Yohsuke Akamatsu, Yong-Ik Byun, Yozhi Nasvadi, Yuri Stepanychev, Zach Steele, Zané Smit, Zbigniew Krzeminski, Željko Andreić, Zhuoyang Chen, Zoran Dragić, Zoran Knez, Zoran Novak, Zouhair Benkhaldoun, Łukasz Sanocki, Łukasz Łyjak, Alexander-von-Humboldt-Gymnasium (Germany), Asociación de Astronomía de Marina Alta (Spain), Costa Blanca Astronomical Society (Spain), Friedrich-Schiller-Gymnasium Preetz (Germany), HUN-REN Institute of Earth Physics and Space Science (Hungary), Haagar Observatory (Norway), Laingsburg High School (South Africa), Perth Observatory Volunteer Group (Australia), Phillips Academy Andover (United States), Royal Astronomical Society of Canada Calgary Centre (Canada), Touwsrivier Primary School (South Africa).

The following cameras contributed to triangulations with a valid meteor trajectory and meteoroid orbit in 2025. The camera id is given with the total number of orbits in brackets:

AT0002 (878), AT0004 (3989), AU0001 (470), AU0002 (7836), AU0003 (5143), AU000A (5061), AU000B (2012), AU000C (4557), AU000D (11267), AU000F (4425), AU000G (4080), AU000J (5), AU000K (13), AU000L (767), AU000Q (1187), AU000R (3936), AU000S (2948), AU000T (2316), AU000U (3705), AU000V (6323), AU000W (6099), AU000X (8008), AU000Y (6024), AU000Z (1886), AU0010 (3586), AU001A (10930), AU001B (7427), AU001C (1760), AU001D (1523), AU001E (4760), AU001F (5387), AU001G (167), AU001K (4424), AU001L (7449), AU001M (103), AU001N (2744), AU001P (8722), AU001Q (9180), AU001R (5897), AU001S (11719), AU001T (154), AU001U (4342), AU001V (5236), AU001W (8368), AU001X (4360), AU001Y (4658), AU001Z (2877), AU0028 (1409), AU0029 (2561), AU002A (1157), AU002B (3630), AU002C (829), AU002D (1249), AU002E (1047), AU002F (769), AU0030 (7805), AU0031 (42), AU0034 (62), AU0035 (4), AU003C (507), AU003E (5454), AU003F (37), AU003G (2397), AU003H (6387), AU003J (4762), AU003K (2), AU0040 (642), AU0041 (1354), AU0042 (1755), AU0043 (960), AU0044 (11), AU0045 (756), AU0046 (2696), AU0047 (2851), AU0048 (2277), AU004A (283), AU004B (1220), AU004H (541), AU004J (1207), AU004K (1080), AU004L (3167), AU004M (501), AU004Q (1646), AU004R (216), BA0001 (959), BA0002 (1401), BA0003 (2499), BA0004 (2095), BA0005 (1122), BE0001 (3017), BE0002 (1553), BE0003 (1155), BE0004 (1549), BE0005 (2843), BE0006 (3183), BE0007 (2208), BE0008 (2342), BE0009 (2028), BE000A (1600), BE000B (2456), BE000C (3814), BE000D (2220), BE000E (2739), BE000G (3825), BE000H (675), BE000J (1014), BE000K (2750), BE000L (5110), BE000M (1826), BE000P (4408), BE000Q (5525), BE000R (3275), BE000S (3295), BE000T (4492), BE000U (2594), BE000V (5168), BE000W (4090), BE000X (2380), BE000Y (652), BE000Z (1463), BE0010 (1884), BE0011 (1742), BE0012 (1774), BE0013 (1823), BE0014 (2607), BE0015 (1778), BE0016 (1487), BE0017 (2072), BE0018 (2313), BE0019 (1576), BE001A (1326), BE001B (103), BG0001 (1759), BG0002 (620), BG0003 (5772), BG0004 (632), BG0005 (1002), BG0008 (321), BG0009 (970), BG000A (674), BG000B (4213), BG000C (2525), BG000E (67), BG000F (220), BG000G (3027), BG000H (576), BG000J (569), BG000K (1116), BR0001 (45), BR0002 (924), BR0003 (89), BR0004 (85), BR0005 (137), BR000A (149), BR000F (1463), BR000G (2815), BR000H (1), BR000M (93), BR000Q (1260), BR000R (85), BR000S (537), BR000T (825), BR000Y (726), BR0013 (65), BR0015 (244), BR0016 (68), BR0019 (6), BR001F (390), BR001G (41),

BR001H (245), BR001M (1320), BR001Q (313), BR001R (2365), BR001S (9), BR001T (992), BR001U (514), BR001W (808), BR001X (12), BR001Z (188), BR0021 (1), BR0029 (983), BR002A (906), BR002B (933), BR002C (1367), CA0003 (1), CA000C (10), CA000E (888), CA000L (836), CA000P (977), CA000Q (2200), CA000R (1939), CA000U (1679), CA000V (1511), CA000Y (983), CA001F (205), CA001G (925), CA001H (607), CA001J (401), CA001N (66), CA001R (2508), CA001Z (251), CA0022 (2185), CA0023 (1110), CA0026 (1007), CA002F (1435), CA002H (73), CA002J (720), CA002K (1900), CA002L (1792), CA002N (797), CA002P (269), CA002Q (4), CA002R (2164), CA002U (2296), CA002V (2064), CA0031 (3077), CA0032 (1590), CA0035 (3421), CA0036 (66), CA0037 (406), CA003A (2055), CA003B (199), CA003C (253), CA003D (1921), CA003E (37), CA003V (559), CA003W (269), CAWEC1 (68), CAWEC2 (147), CAWEC3 (34), CAWEC4 (16), CAWEC5 (22), CAWEC6 (36), CH0002 (1244), CH0003 (1335), CH0004 (939), CH0005 (2084), CL0002 (1907), CL0003 (1907), CZ0001 (552), CZ0002 (1985), CZ0003 (827), CZ0004 (1019), CZ0006 (929), CZ0007 (1470), CZ0008 (1029), CZ0009 (1508), CZ000A (2518), CZ000B (1139), CZ000C (1228), CZ000E (2190), CZ000F (900), CZ000G (1108), CZ000H (4056), CZ000J (1054), CZ000K (2966), CZ000L (1960), CZ000M (3380), CZ000N (1310), CZ000P (2187), CZ000Q (2926), CZ000R (2428), CZ000U (784), CZ000V (815), CZ000W (1091), CZ000X (833), CZ000Y (1472), DE0001 (3034), DE0002 (86), DE0003 (111), DE0004 (1746), DE0005 (2263), DE0006 (1638), DE0007 (1370), DE0008 (1863), DE0009 (1205), DE000B (4307), DE000C (651), DE000G (146), DE000H (213), DE000J (1922), DE000K (1846), DE000M (1009), DE000P (727), DE000Q (2474), DE000R (835), DE000S (4216), DE000V (486), DE000W (4043), DE000X (3370), DE000Y (1995), DE0011 (2860), DE0012 (1650), DE0013 (4422), DE0014 (1598), DE0015 (1698), DE0016 (3136), DE0017 (650), DE0018 (40), DK0001 (2882), DK0002 (1539), DK0003 (2957), DK0004 (2327), DK0005 (711), DK0006 (2015), DK0007 (3689), DK0008 (2611), DK0009 (2120), DK000A (1919), DK000B (1248), DK000C (2233), DK000D (3168), DK000E (481), DK000F (2201), DK000G (2406), DK000H (300), DK000J (1592), DK000K (2330), DK000L (859), DK000M (710), DK000N (295), DK000P (1358), DK000Q (1662), DK000R (2244), DK000S (2021), DK000T (2020), ES0001 (299), ES0002 (1), ES0003 (39), ES0004 (455), ES0005 (532), ES0006 (125), ES0009 (589), ES000C (1420), ES000D (1250), ES000E (484), ES000F (345), ES000H (695), ES000L (147), ES000M (128), ES000N (25), ES000P (36), ES000Q (1691), ES000T (852), ES000U (1794), ES000V (603), ES000W (34), ES000X (143), ES000Z (443), ES0011 (61), ES0013 (1149), ES0016 (1891), ES0019 (1368), ES001A (1722), ES001B (2), ES001D (690), ES001F (2113), ES001G (934), ES001H (392), FI0001 (20), FI0002 (63), FI0003 (61), FI0004 (158), FI0005 (231), FI0007 (128), FI0008 (25), FI0009 (46), FR0003 (758), FR0006 (3172), FR000A (1998), FR000G (787), FR000L (21), FR000M (129), FR000P (140), FR000R (1878), FR000U (588), FR000V (1338), FR000X (3820), FR000Y (5187), FR000Z (4077), FR0011 (3287), FR0012 (2396), FR0013 (3704), FR0014 (1279), FR0015 (381), FR0016 (2393), FR0017 (214), GR0002 (4050), GR0003 (4054), GR0004 (2926), GR0005 (1032), GR0006 (6275), GR0007 (3246), GR0008 (3319), GR0009 (7218), HR0001 (1849), HR0002 (2132), HR0004 (95), HR0006 (2186), HR0007 (5452), HR0008 (1431), HR000D (326), HR000H (989), HR000J (653), HR000K (58), HR000M (61), HR000P (1839), HR000Q (998), HR000S (2061), HR000U (295), HR000V (1672), HR000W (389), HR000Z (54), HR0015 (1298), HR0016 (687), HR001D (1312), HR001E (4162), HR001J (768), HR001K (550), HR001L (208), HR001M (230), HR001N (294), HR001P (336), HR001Q (789), HR001R (346), HR001X (1575), HR001Z (8740), HR0021 (10), HR0024 (1524), HR0025 (1859), HR0027 (2143), HR002D (8307), HR002E (4313), HR002F (5247), HR002G (5106), HR002H (5892), HR002J (9308), HR002K (2729), HR002M (2031), HR002T (3184), HR002U (99), HR002V (5715), HR002W (4021), HR002X (5033), HR002Y (1754), HU0001 (2309), HU0002 (5181), HU0003 (5869), HU0004 (2753), HU0005 (3786), HU0006 (1481), HU0007 (1402), HU0008 (819), HU0009 (1736), HU000A (2966), HU000B (5935), HU000C (373), IE0004 (3259), IE000G (654), IE000H (445), IE000J (1340), IE000M (794), IE000N (848), IL0001 (61), IL0002 (613), IL0003 (16), IL0004 (295), IL0009 (82), IL000A (332), IT0001 (2650), IT0004 (3801), IT0007 (57), IT0008 (2409), IT000A (240), IT000B (1034), IT000C (7), JP0001 (147), JP0002 (58), JP0003 (89), KR0001 (479), KR0002 (5616), KR0003 (354), KR0004 (6333), KR0005 (1203), KR0006 (502), KR0007 (584), KR0008 (409), KR0009 (1745), KR000A (5252), KR000B (4154), KR000C (2244), KR000D (3339), KR000E (3680), KR000F (2392), KR000G (1995), KR000H (5112), KR000J (4585), KR000K (4050), KR000L (2840), KR000M (3173), KR000N (4895), KR000P (3349), KR000Q (1779), KR000R (3030), KR000S (3048), KR000Y (2), KR000Z (2603), KR0010 (2764), KR0011 (2829), KR0012 (1900), KR0013 (2434), KR0014 (366), KR0015 (819), KR0016 (864), KR0017 (1417), KR0018 (1328), KR0019 (3947), KR001A (1526), KR001B (3200), KR001C (3134), KR001D (2470), KR001E (2386), KR001F (1338), KR001G (1969), KR001H (2573), KR001J (1761), KR001K (909), KR001L (486), KR001M (783), KR001N (573), KR001P (957), KR001Q (1371), KR001R (463), KR001S (707), KR001T (974), KR001U (1980), KR001V (1301), KR001W (1633), KR001X (1066), KR001Y (716), KR001Z (741), KR0020 (1333), KR0021 (1149), KR0022 (3294), KR0023 (3184), KR0024 (3651), KR0025 (2320), KR0026 (2006), KR0027 (2305), KR0028 (2826), KR0029 (2412), KR002A (1183), KR002B (1455), KR002C (2354), KR002D (2353), KR002E (2056), KR002F (1892), KR002G (1947), KR002H (1168), KR002J (1387), KR002K (499), KR002L (1739), KR002M (1527), KR002N (1182), KR002P (1433), KR002Q (1489), KR002R (997), KR002S (1377), KR002T (1344), KR002U (50), KR002V (31), KR002W (22), KR002X (13), KR002Y (18), KR002Z (45), KR0030 (32), KR0036 (2793), KR0037 (1841), KR0038 (863), KR0039 (2398), KR003A (1748), KR003B (1412), KR003C (987), KR003D (793), KR003E (359), KR003F (429), KR003G

(1335), KR003H (1399), KR003J (3386), KR003K (2327), KR003L (2598), KR003M (3385), KR003N (4903), KR003P (3579), KR003Q (3275), KR003R (3312), KR003S (3481), KR003T (4507), KR003U (2186), KR003V (1723), KR003W (2791), KR003X (3531), LU0001 (2423), LU0002 (1783), MA0001 (862), MA0002 (540), MA0003 (1312), MX0001 (53), MX0003 (76), MX0004 (3), MX0006 (165), MX0009 (92), MX000A (1), MX000B (41), MX000C (20), MX000D (775), MX000E (221), MX000F (88), MY0001 (4), MY0002 (106), MY0004 (26), MY0005 (15), MY0006 (82), MY0008 (122), MY000B (8), MY000C (93), MY000D (5), MY000E (62), NL0001 (1835), NL0006 (1226), NL0009 (3363), NL000A (1197), NL000B (623), NL000C (3383), NL000D (1287), NL000G (1425), NL000K (1811), NL000L (90), NL000M (2518), NL000N (2711), NL000P (2752), NL000Q (2907), NL000R (3295), NL000S (3774), NL000T (2494), NL000U (3429), NL000W (1290), NL000Z (3807), NL0010 (2853), NL0011 (2421), NL0013 (3183), NL0014 (2908), NL0017 (2244), NL0019 (1962), NL001A (704), NL001B (644), NL001D (427), NL001E (441), NL001F (475), NZ0001 (3274), NZ0002 (4674), NZ0003 (3427), NZ0004 (5571), NZ0007 (4955), NZ0008 (1970), NZ0009 (4333), NZ000A (67), NZ000B (2443), NZ000C (477), NZ000D (5158), NZ000F (661), NZ000G (2531), NZ000H (2708), NZ000J (432), NZ000K (1564), NZ000L (776), NZ000M (2989), NZ000N (2598), NZ000P (396), NZ000Q (1248), NZ000R (1272), NZ000S (3854), NZ000T (887), NZ000U (1712), NZ000V (2364), NZ000W (2560), NZ000X (1107), NZ000Y (2727), NZ000Z (4586), NZ0010 (2312), NZ0011 (4920), NZ0012 (7040), NZ0013 (1238), NZ0014 (6484), NZ0015 (2999), NZ0016 (2153), NZ0017 (4886), NZ0018 (7676), NZ0019 (4572), NZ001A (3513), NZ001B (57), NZ001C (324), NZ001D (1326), NZ001E (1701), NZ001G (3814), NZ001H (2632), NZ001J (3084), NZ001K (296), NZ001L (2872), NZ001N (2625), NZ001P (5617), NZ001Q (2235), NZ001R (3674), NZ001S (5356), NZ001V (4951), NZ001W (1878), NZ001X (2908), NZ001Y (1312), NZ001Z (2407), NZ0020 (4256), NZ0021 (2656), NZ0022 (4850), NZ0023 (4973), NZ0024 (3626), NZ0025 (359), NZ0026 (5438), NZ0027 (6888), NZ0028 (1266), NZ0029 (5926), NZ002C (10194), NZ002D (2191), NZ002E (3430), NZ002F (5798), NZ002G (3377), NZ002H (3621), NZ002J (1772), NZ002K (4193), NZ002L (2649), NZ002M (94), NZ002N (7437), NZ002P (4959), NZ002Q (5316), NZ002R (7191), NZ002S (4250), NZ002T (6121), NZ002U (2095), NZ002V (3058), NZ002W (4518), NZ002X (7571), NZ002Y (2861), NZ002Z (5709), NZ0030 (7998), NZ0032 (4195), NZ0033 (7503), NZ0034 (6610), NZ0035 (2794), NZ0036 (6766), NZ0037 (7140), NZ0038 (3721), NZ0039 (382), NZ003A (5405), NZ003B (2927), NZ003C (7407), NZ003E (6754), NZ003G (2039), NZ003H (6407), NZ003K (8395), NZ003L (262), NZ003M (263), NZ003N (5643), NZ003Q (2627), NZ003R (7407), NZ003S (2885), NZ003T (4489), NZ003U (6400), NZ003V (6291), NZ003W (5593), NZ003X (4113), NZ003Y (8119), NZ003Z (7757), NZ0040 (10839), NZ0041 (4723), NZ0042 (7056), NZ0043 (163), NZ0044 (4772), NZ0045 (5466), NZ0046 (5866), NZ0047 (1063), NZ0048 (303), NZ0049 (3284), NZ004A (5337), NZ004B (5727), NZ004C (3878), NZ004D (6104), NZ004E (3447), NZ004H (4478), NZ004J (7026), NZ004L (7976), NZ004M (2965), NZ004N (7926), NZ004R (9115), NZ004S (2769), NZ004T (4700), NZ004U (4039), NZ004V (3882), NZ004W (2213), NZ004X (1980), NZ004Y (8053), NZ004Z (2516), NZ0051 (10011), NZ0059 (8159), NZ005A (3994), NZ005B (4531), NZ005C (7080), NZ005D (5931), NZ005E (6241), NZ005F (3318), NZ005G (1086), NZ005H (600), NZ005J (557), NZ005K (997), NZ005L (793), NZ005M (2200), NZ005N (5160), NZ005Q (486), NZ005R (279), NZ005S (290), NZ005T (400), NZ005U (446), NZ005Y (2384), NZ005Z (3514), NZ0061 (4318), NZ0063 (2361), NZ0065 (1021), NZ0066 (835), NZ0067 (970), NZ0068 (1512), NZ0069 (1446), NZ006F (18), NZ006G (11), NZ006H (2), NZ006J (7), NZ006K (16), PL0005 (1372), PL0006 (280), PL0008 (2321), PL0009 (1311), PL000A (1048), PL000B (1248), PL000C (256), PL000D (182), PL000E (384), PL000F (571), PL000G (359), PT0002 (3527), PT0003 (541), RO0001 (3522), RO0002 (3310), RO000A (218), RO000B (10), RO000C (69), RU0001 (798), RU0003 (3161), RU0004 (659), RU0008 (1963), RU0009 (1356), RU000E (1174), RU000F (962), RU000M (1010), RU000N (2575), RU000Q (580), RU000T (251), RU000V (170), RU000Y (127), RU000Z (124), RU0016 (867), RU0017 (1547), RU0018 (632), RU0019 (2185), RU001A (892), RU001C (892), RU001D (142), SI0001 (986), SI0002 (5534), SI0003 (1503), SI0004 (942), SI0005 (3549), SI0006 (3273), SI0007 (615), SK0002 (892), SK0003 (276), SK0004 (1954), SK0005 (1838), SK0006 (2391), TJ0001 (794), TJ0002 (794), UA0001 (1536), UA0002 (1536), UA0003 (360), UA0005 (107), UA0006 (253), UK0001 (3432), UK0002 (645), UK0004 (1864), UK0006 (6660), UK0008 (1887), UK0009 (4602), UK000B (244), UK000D (3687), UK000F (5574), UK000H (5618), UK000J (1114), UK000P (1375), UK000R (95), UK000S (5852), UK000T (3034), UK000U (805), UK000Y (2437), UK000Z (633), UK001E (188), UK001H (832), UK001K (2491), UK001L (6244), UK001M (758), UK001Q (310), UK001R (271), UK001S (2135), UK001T (284), UK001U (91), UK001W (27), UK001Z (4597), UK0020 (789), UK0021 (1522), UK0022 (4615), UK0024 (3576), UK0025 (3243), UK0026 (4454), UK0029 (565), UK002D (655), UK002F (7087), UK002J (2715), UK002K (4278), UK002L (1369), UK002Q (3182), UK002W (788), UK002X (1096), UK002Y (1153), UK002Z (4129), UK0030 (1423), UK0031 (4247), UK0032 (1281), UK0034 (2334), UK0035 (3028), UK0039 (366), UK003B (643), UK003C (2119), UK003D (1879), UK003E (1898), UK003F (709), UK003K (294), UK003N (4280), UK003T (3029), UK003U (3854), UK003V (1574), UK003W (2473), UK003X (4846), UK003Y (1233), UK003Z (2597), UK0041 (3604), UK0042 (4448), UK0045 (2785), UK0049 (2132), UK004A (74), UK004B (3517), UK004C (1977), UK004D (4163), UK004E (3677), UK004F (3498), UK004G (3184), UK004H (689), UK004J (2149), UK004L (315), UK004M (1678), UK004N (1412), UK004R (451), UK004U (658), UK004V (1951), UK004X (133), UK0050 (3914), UK0051 (1971), UK0055 (485),

UK0057 (2428), UK005C (1187), UK005E (1011), UK005G (3873), UK005H (3191), UK005J (722), UK005L (2047), UK005M (3258), UK005N (2633), UK005P (1838), UK005R (822), UK005S (1607), UK005U (1022), UK005V (922), UK005Y (592), UK0060 (1264), UK0061 (1325), UK0062 (614), UK0066 (1012), UK0067 (2687), UK0069 (11), UK006A (193), UK006B (576), UK006C (3286), UK006D (3233), UK006E (870), UK006G (2146), UK006H (1391), UK006J (1486), UK006L (2042), UK006P (4713), UK006R (297), UK006S (789), UK006T (2014), UK006U (1266), UK006V (3057), UK006X (996), UK006Z (82), UK0070 (2539), UK0072 (36), UK0073 (993), UK0074 (1118), UK0077 (1106), UK0078 (2204), UK0079 (3085), UK007A (4125), UK007B (3582), UK007C (377), UK007G (1773), UK007H (2904), UK007J (1007), UK007P (4090), UK007Q (3772), UK007R (4188), UK007U (2294), UK007V (1099), UK007Y (4676), UK007Z (2537), UK0080 (2067), UK0081 (1948), UK0082 (693), UK0083 (2962), UK0084 (4633), UK0085 (832), UK0086 (1125), UK0087 (2118), UK0088 (1447), UK0089 (2980), UK008A (1761), UK008B (3149), UK008C (3130), UK008D (1906), UK008E (3), UK008F (6420), UK008G (3355), UK008H (902), UK008J (2635), UK008K (394), UK008M (790), UK008Q (3330), UK008R (638), UK008S (2452), UK008T (3398), UK008U (2321), UK008V (2360), UK008X (4475), UK008Z (2382), UK0090 (1542), UK0092 (3459), UK0096 (812), UK0098 (5740), UK0099 (5489), UK009A (553), UK009B (405), UK009C (2774), UK009D (3855), UK009F (1342), UK009G (4546), UK009J (3472), UK009K (4778), UK009L (4245), UK009M (2139), UK009P (5657), UK009Q (1980), UK009R (1470), UK009S (4078), UK009T (666), UK009U (1097), UK009V (2539), UK009W (5008), UK009X (5442), UK00A0 (2972), UK00A1 (3472), UK00A2 (2008), UK00A3 (3198), UK00A4 (5542), UK00A5 (5816), UK00A6 (2437), UK00A7 (475), UK00AA (4030), UK00AB (4325), UK00AD (1989), UK00AE (2674), UK00AF (3557), UK00AG (945), UK00AJ (3437), UK00AK (3828), UK00AL (5809), UK00AM (5088), UK00AN (4560), UK00AP (2092), UK00AQ (1413), UK00AS (1242), UK00AT (4027), UK00AU (5214), UK00AV (324), UK00AZ (520), UK00B0 (5950), UK00B1 (5728), UK00B2 (3970), UK00B5 (3912), UK00B6 (2132), UK00B7 (478), UK00BA (5310), UK00BB (2011), UK00BC (59), UK00BD (487), UK00BF (3481), UK00BH (1226), UK00BJ (4775), UK00BK (6055), UK00BL (1331), UK00BN (1006), UK00BQ (1362), UK00BW (6334), UK00C0 (845), UK00C1 (2199), UK00C2 (2957), UK00C3 (433), UK00C4 (325), UK00C6 (1475), UK00C7 (4658), UK00C9 (2935), UK00CA (3321), UK00CC (4772), UK00CD (2206), UK00CE (2821), UK00CH (2366), UK00CJ (3753), UK00CK (1938), UK00CQ (3574), UK00CS (2643), UK00CT (1450), UK00CU (1464), UK00CV (1893), UK00CZ (2289), UK00D6 (1528), UK00D7 (2362), UK00D9 (2065), UK00DA (1261), UK00DB (1749), UK00DC (305), UK00DD (476), UK00DE (1660), UK00DF (435), UK00DG (1826), UK00DH (1787), UK00DJ (1274), UK00DN (230), US0001 (6284), US0002 (4469), US0003 (10960), US0004 (6148), US0005 (11910), US0006 (7019), US0007 (3184), US0008 (6654), US0009 (3906), US000C (10351), US000D (5623), US000E (7596), US000G (7754), US000H (16294), US000J (17744), US000K (5867), US000L (7689), US000M (6793), US000N (5736), US000P (4764), US000R (4718), US000S (4149), US000U (7445), US000V (3040), US0019 (420), US001E (235), US001G (1165), US001L (2548), US001N (303), US001P (3710), US001Q (2238), US001R (4984), US001U (1879), US001V (2005), US001Y (116), US0020 (3088), US0021 (1445), US0022 (1058), US0023 (1738), US0026 (90), US0027 (765), US002A (2916), US002D (1535), US002E (1100), US002J (41), US002L (1599), US002M (152), US002N (336), US002P (1694), US002Q (1633), US002R (1720), US002W (1076), US002X (4265), US002Y (2342), US002Z (352), US0030 (92), US0031 (121), US0035 (2605), US0036 (2458), US0037 (1526), US0038 (3180), US0039 (3208), US003G (5967), US003K (2), US003M (1730), US003N (4671), US003P (3041), US003Q (459), US003R (1676), US003S (1987), US003T (4229), US003Y (1474), US0040 (85), US0043 (90), US0044 (1581), US0045 (251), US0046 (868), US0047 (794), US0048 (156), US004A (800), US004B (3208), US004C (4787), US004D (1277), US004E (610), US004J (2108), US004L (401), US004M (129), US004N (4230), US004P (4255), US004Q (4786), US004S (6), US004U (545), US004V (159), US0050 (1922), US0051 (2008), US0054 (1514), US0055 (2704), US0059 (329), US005A (4089), US005B (4651), US005C (2279), US005D (3866), US005E (4910), US005F (1225), US005G (1028), US005H (2546), US005J (2331), US005K (432), US005N (574), US005P (1121), US005Q (1029), US005U (126), US005V (211), US005W (4101), US005X (10320), US005Y (9982), US005Z (7618), US0061 (3454), US0062 (4265), US0066 (4164), US0067 (559), US0068 (738), US006A (1248), US006B (801), USL001 (2358), USL002 (3284), USL003 (584), USL004 (3344), USL005 (3461), USL006 (2), USL007 (2856), USL008 (3306), USL009 (1269), USL00A (1397), USL00B (2490), USL00C (1742), USL00D (2961), USL00E (558), USL00F (5776), USL00G (6128), USL00J (3864), USL00K (3997), USL00L (6076), USL00M (9444), USL00N (3365), USL00P (11069), USL00Q (11958), USL00X (317), USL00Y (8), USL00Z (533), USL010 (329), USL011 (812), USL012 (1575), USL013 (3375), USL014 (6174), USL015 (2611), USL016 (1374), USL017 (7786), USL018 (5806), USL019 (2512), USL01A (4040), USL01B (5781), USL01C (2795), USL01D (5267), USL01E (5227), USN001 (880), USN002 (528), USN003 (1535), USN004 (1103), USN009 (517), USV001 (3957), USV002 (2990), USV003 (3973), ZA0001 (1450), ZA0002 (1610), ZA0006 (4098), ZA0007 (4291), ZA0008 (6254), ZA0009 (413), ZA000A (190), ZA000C (5001), ZA000D (202), ZA000E (43), ZA000F (124), ZA000G (15).

References

Dijkema T. J. (2022). “Visualizing meteor ground tracks on the meteor map”. *eMetN Meteor Journal*, **7**, 73–75.

Drummond J. D. (1981). “A test of comet and meteor shower associations”. *Icarus*, **45**, 545–553.

Gural P. and Šegon D. (2009). “A new meteor detection processing approach for observations collected by the Croatian Meteor Network (CMN)”. *WGN, the Journal of the IMO*, **37**, 28–32.

Harman E., Eschman P., Massey B., and Olivera W. (2023). “Using GUI RMS on Linux to support multiple cameras”. *eMetN Meteor Journal*, **8**, 185–196.

Jenniskens P., Baggaley J., Crumpton I., Aldous P., Pokorny P., Janches D., Gural P. S., Samuels D., Albers J., Howell A., Johannink C., Breukers M., Odeh M., Moskovitz N., Collison J., Ganju S. (2018). “A survey of southern hemisphere meteor showers”. *Planetary and Space Science*, **154**, 21–29.

Jenniskens P., Jopek T.J., Janches D., Hajduková M., Kokhirova G.I., Rudawska R. (2020). “On removing showers from the IAU Working List of Meteor Showers”. *Planetary and Space Science*, **182**, id. 104821.

Jenniskens P. (2023). Atlas of Earth’s Meteor Showers. Elsevier, USA, ISBN: 978-0-443-23577-1, 824 pages.

Jopek T. J. (1993). “Remarks on the meteor orbital similarity D-criterion”. *Icarus*, **106**, 603–607.

Jopek T. J. and Jenniskens P. M. (2011). “The Working Group on Meteor Showers Nomenclature: A History, Current Status and a Call for Contributions”. In Meteoroids: The Smallest Solar System Bodies, *Proceedings of the Meteoroids Conference* held in Breckenridge, Colorado, USA, May 24-28, 2010. Edited by W.J. Cooke, D.E. Moser, B.F. Hardin, and D. Janches, NASA/CP-2011-216469., 7–13.

Jopek T. J. and Kaňuchová Z. (2017). “IAU Meteor Data Center - the shower database: A status report”. *Planetary and Space Science*, **143**, 3–6.

Kalina M. (2024). “Meteorview – new meteor visualizing tool for the Global Meteor Network”. *eMetN Meteor Journal*, **9**, 406–409.

Moorhead A. V., Clements T. D., Vida D. (2020). “Realistic gravitational focusing of meteoroid streams”. *Monthly Notices of the Royal Astronomical Society*, **494**, 2982–2994.

Mroz E. J. (2021). “Optimizing Camera Orientation for the New Mexico Meteor Array”. *eMetN Meteor Journal*, **6**, 562–567.

Neslušan L., Poručan V., Svoreň J., Jakubík M. (2020). “On the new design othe IAU MDC portal”. *WGN, Journal of the International Meteor Organization*, **48**, 168–169.

Roggemans P., Campbell-Burns P., McIntyre M., Šegon D. and Vida D. (2023). “Global Meteor Network report 2022”. *eMetN Meteor Journal*, **8**, 77–98.

Roggemans P., Campbell-Burns P., Kalina M., McIntyre M., Scott J. M., Šegon D., Stano R., Vida D. (2024). “Global Meteor Network report 2023”. *eMetN Meteor Journal*, **9**, 56–89.

Roggemans P., Campbell-Burns P., Kalina M., McIntyre M., Scott J. M., Šegon D., Vida D. (2025a). “Global Meteor Network report 2024”. *eMetN Meteor Journal*, **10**, 67–101.

Roggemans P., Šegon D., Vida D. (2025b). “June delta Pavonids (JDP#835) in 2025”. *eMetN Meteor Journal*, **10**, 269–274.

Roggemans P., Vida D., Šegon D. (2025c). “M2024-S1 activity confirmed in 2025”. *eMetN Meteor Journal*, **10**, 353–359.

Roggemans P., Vida D., Šegon D. (2025d). “Epsilon-Ursae Minorids (EPU#1044) enhanced activity in 2025”. *eMetN Meteor Journal*, **10**, 360–367.

Roggemans P., Šegon D., Vida D., Scott J. M., Wood J. (2025e). “Delta-Horologiids (DHO#1146) in 2025”. *eMetN Meteor Journal*, **10**, 378–383.

Roggemans P., Vida D., Šegon D., Scott J. M., Wood J. (2026a). “October epsilon-Carinids (OEC#1172)”. *eMetN Meteor Journal*, **11**, 1-7.

Roggemans P., Vida D., Šegon D., Scott J. M., Wood J. (2026b). “A Carinids (842#CRN) outburst in 2025”. *eMetN Meteor Journal*, **11**, 8–15.

Roggemans P., Vida D., Šegon D., Scott J. M., Wood J. (2026c). “29-Piscids (PIS#1046) return in 2025”. *eMetN Meteor Journal*, **11**, 31–41.

Roggemans P., Vida D., Šegon D., Scott J. M., Wood J. (2026d). “M2024-H1 activity confirmed in 2025”. *eMetN Meteor Journal*, **11**, 42–46.

Roggemans P., Vida D., Šegon D., Scott J. M., Wood J. (2026e). “M2024-N1 activity confirmed in 2025”. *eMetN Meteor Journal*, **11**, 47–51.

Roggemans P. (2026f). “Eccentrids in the GMN orbit dataset”. *eMetN Meteor Journal*, **11**, 60–62.

Šegon D., Vida D., Roggemans P. (2025a). “New meteor shower in Cassiopeia, 4 September 2024”. *eMetN Meteor Journal*, **10**, 5–11.

Šegon D., Vida D., Roggemans P. (2025b). “New meteor shower in Ursa Minor, 23–24 September 2024”. *eMetN Meteor Journal*, **10**, 12–19.

Šegon D., Vida D., Roggemans P. (2025c). “New meteor shower in Lyra, 26–27 October 2024”. *eMetN Meteor Journal*, **10**, 22–26.

Šegon D., Vida D., Roggemans P. (2025d). “New meteor shower in Puppis”. *eMetN Meteor Journal*, **10**, 165–169.

Šegon D., Vida D., Roggemans P. (2025f). “New meteor shower in Eridanus”. *eMetN Meteor Journal*, **10**, 282–286.

Šegon D., Vida D., Roggemans P. (2025g). “Outburst of a new meteor shower in Aries”. *eMetN Meteor Journal*, **10**, 287–292.

Šegon D., Vida D., Roggemans P. (2025h). “New meteor shower in Delphinus (M2025-S1)”. *eMetN Meteor Journal*, **10**, 348–352.

Šegon D., Vida D., Roggemans P., Scott J. M., Wood J. (2025i). “New meteor shower in Hydrus (M2025-S2)”. *eMetN Meteor Journal*, **10**, 368–377.

Šegon D., Vida D., Roggemans P., Scott J. M., Wood J. (2026a). “New meteor shower in Pegasus (M2025-U1)”. *eMetN Meteor Journal*, **11**, 16–22.

Šegon D., Vida D., Roggemans P., Scott J. M., Wood J. (2026b). “New meteor shower in Monoceros (M2025-V1)”. *eMetN Meteor Journal*, **11**, 23–30.

Southworth R. R. and Hawkins G. S. (1963). “Statistics of meteor streams”. *Smithson. Contrib. Astrophys.*, **7**, 261–286.

Vida D., Zubović D., Šegon D., Gural P. and Cupec R. (2016). “Open-source meteor detection software for low-cost single-board computers”. In: Roggemans A. and Roggemans P., editors, *Proceedings of the International Meteor Conference*, Egmond, the Netherlands, 2-5 June 2016. International Meteor Organization, pages 307–318.

Vida D., Gural P., Brown P., Campbell-Brown M., Wiegert P. (2020a). “Estimating trajectories of meteors: an observational Monte Carlo approach - I. Theory”. *Monthly Notices of the Royal Astronomical Society*, **491**, 2688–2705.

Vida D., Gural P., Brown P., Campbell-Brown M., Wiegert P. (2020b). “Estimating trajectories of meteors: an observational Monte Carlo approach - II. Results”. *Monthly Notices of the Royal Astronomical Society*, **491**, 3996–4011.

Vida D., Šegon D., Gural P. S., Brown P. G., McIntyre M. J. M., Dijkema T. J., Pavletić L., Kukić P., Mazur M. J., Eschman P., Roggemans P., Merlak A., Zubrović D. (2021). “The Global Meteor Network – Methodology and first results”. *Monthly Notices of the Royal Astronomical Society*, **506**, 5046–5074.

Vida D., Blaauw Erskine R. C., Brown P. G., Kambulow J., Campbell-Brown M., Mazur M. J. (2022). “Computing optical meteor flux using global meteor network data”. *Monthly Notices of the Royal Astronomical Society*, **515**, 2322–2339.

Vida D., Šegon D., Roggemans P. (2025a). “New meteor shower in Octans”. *eMetN Meteor Journal*, **10**, 218–222.

Vida D., Šegon D., Roggemans P. (2025b). “New meteor shower in Equuleus”. *eMetN Meteor Journal*, **10**, 259–263.

Vida D., Šegon D., Roggemans P. (2025c). “New meteor shower in Indus”. *eMetN Meteor Journal*, **10**, 264–268.

Vida D., Šegon D., Roggemans P. (2025d). “Two meteor shower outbursts with potential connection to comet 73P/Schwassmann-Wachmann”. *eMetN Meteor Journal*, **10**, 275–281.

Zubović D., Vida D., Gural P. and Šegon D. (2015). “Advances in the development of a low-cost video meteor station”. In: Rault J.-L. and Roggemans P., editors, *Proceedings of the International Meteor Conference*, Mistelbach, Austria, 27-30 August 2015. International Meteor Organization, pages 94–97.

Iota-Lupids (ILU#783) activity in 2025

Paul Roggemans[1], **Denis Vida**[2,3], **Damir Šegon**[4,5], **James M. Scott**[6], **Jeff Wood**[7]

[1] **Pijnboomstraat 25, 2800 Mechelen, Belgium**

[2] **Department of Physics and Astronomy, University of Western Ontario, Richmond Street, London, N6A 3K7, Ontario, Canada**

[3] **Institute for Earth and Space Exploration, University of Western Ontario, Perth Drive, London, N6A 5B8, Ontario, Canada**
denis.vida@gmail.com

[4] **Astronomical Society Istra Pula, Park Monte Zaro 2, 52100 Pula, Croatia**

[5] **Višnjan Observatory, Istarska 5, 52463 Višnjan, Croatia**

[6] **Department of Geoscience, Aarhus University, Høegh-Guldbergs Gade 2. DK-8000 Aarhus C, Denmark**
jscott@geo.au.dk

[7] **PO Box 162, Willetton, Western Australia 6955, Australia**

An activity source identified as the iota-Lupids has been detected between the 17th and 21st of December 2025 from a radiant at R.A. = 214.1° and Decl.= –42.2°, with a geocentric velocity of 41.5 km/s. This case study confirms the existence of this annual meteor shower and the shower fulfils the criteria to be nominated for established status by the IAU-MDC.

1 Introduction

A small but distinct group of radiants appeared on the Global Meteor Network radiant density maps between the 17th and 21st of December 2025 (*Figure 1*). A first preliminary analysis failed to identify this activity source with any known meteor shower in the IAU-MDC Working List of Meteor Shower. This activity was initially monitored as a possible new meteor shower.

Before reporting this source to the IAU-MDC as a possible new meteor shower another checkup was done based upon the orbit data and that resulted in a positive match although rather weak correlation with similarity criteria D_{SH} ~0.15 and D_D ~0.1. The shower is known as the iota-Lupids (ILU#783)[28] which was discovered by Pokorný et al. (2017) during a meteoroid stream search on data of the Southern

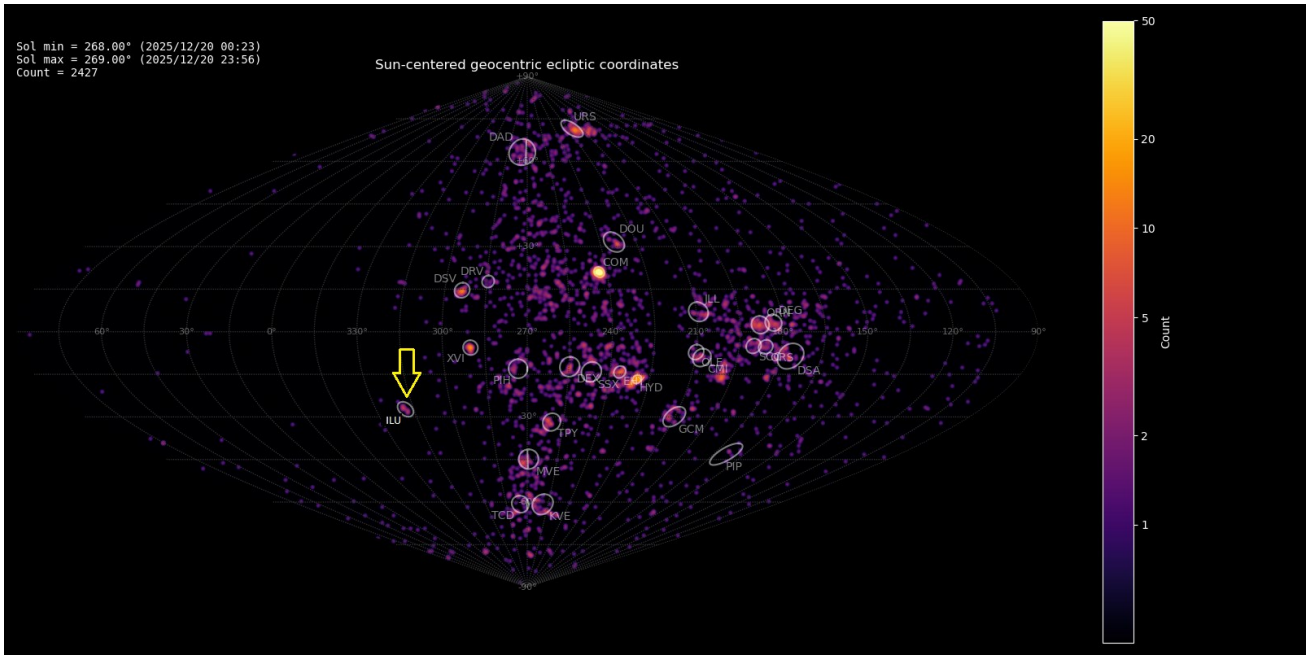

Figure 1 – Radiant density map with 2427 radiants obtained by the Global Meteor Network during 20–21 December, 2025. The position of the iota-Lupids in Sun-centered geocentric ecliptic coordinates is marked with a yellow arrow.

[28] https://www.ta3.sk/IAUC22DB/MDC2022/Roje/pojedynczy_obiekt.php?lporz=01690&kodstrumienia=00783

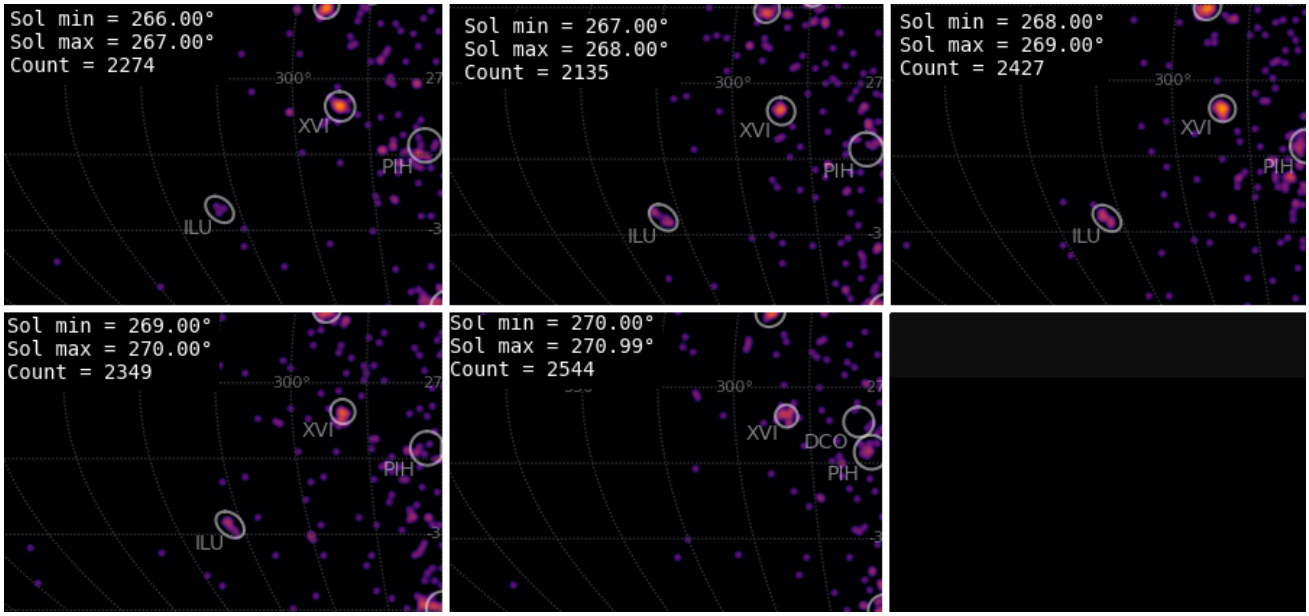

Figure 2 – Changes in the radiant appearance during the activity period.

Argentina Agile MEteor Radar (SAAMER) between 2012–2015.

2 Shower classification based on radiants

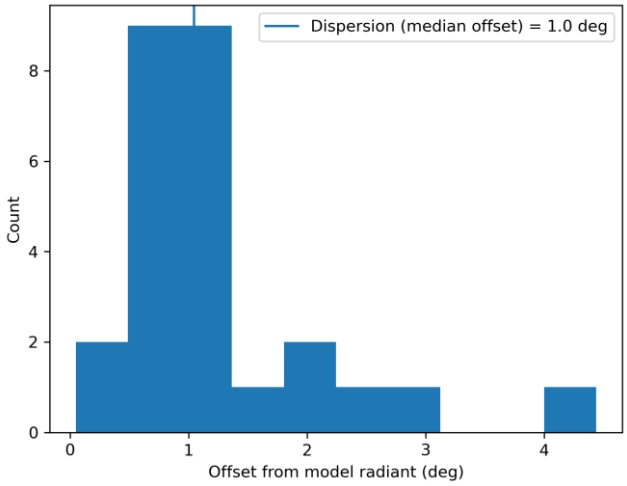

Figure 3 – Dispersion median offset on the radiant position.

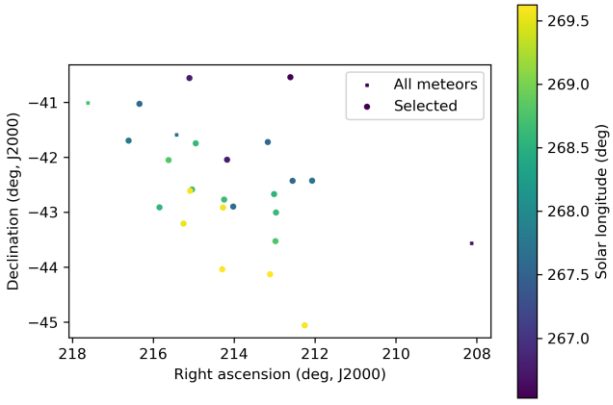

Figure 4 – The radiant distribution during the solar-longitude interval 266.5° – 269.5° in equatorial coordinates.

The GMN shower association criteria assume that meteors within 1° in solar longitude, within 2.5° in radiant in this case, and within 10% in geocentric velocity of a shower reference location are members of that shower. Further details about the shower association are explained in Moorhead et al. (2020). Using these meteor shower selection criteria, 23 orbits have been identified as iota-Lupids by 80 GMN cameras installed in Australia, New Zealand and the United States. The final results have been listed in *Table 1*.

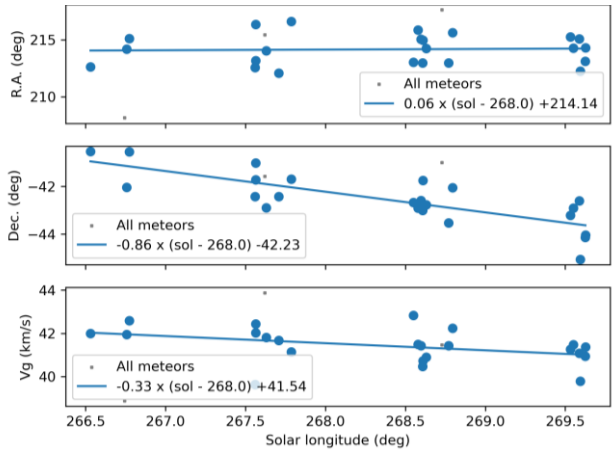

Figure 5 – The radiant drift.

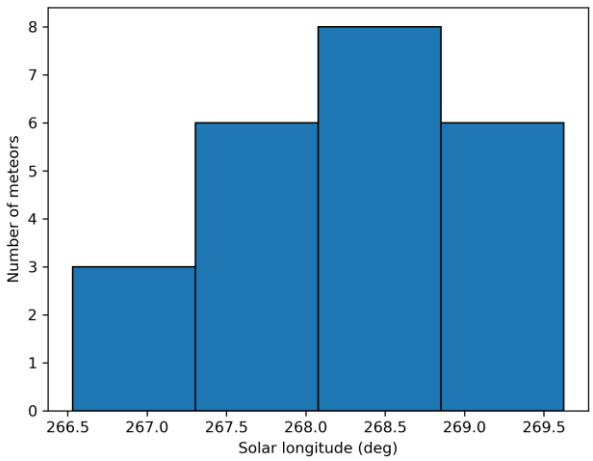

Figure 6 – The uncorrected number of shower meteors recorded per degree in solar longitude.

3 Shower classification based on orbits

A complete independent meteoroid stream search has been applied based upon orbit data for confirmation. This method has been described in a separate publication (Roggemans, 2026). The mean orbit was computed by the method of Jopek et al. (2006) for all orbits that fit the thresholds $D_{SH} < 0.15$ & $D_D < 0.06$ & $D_J < 0.15$ (Southworth and Hawkins, 1963; Drummond, 1981; Jopek, 1993). The results have been listed in *Table 1*.

Twenty iota-Lupids were identified in common by both methods, three were found by the radiant identification method but not confirmed by the orbit method and four were identified by the orbit identification but not detected by the radiant method.

The radiant plots in equatorial coordinates (*Figure 7*) and in Sun-centered ecliptic coordinates (*Figure 8*) show a distinct concentration in a generally sparse distributed sporadic background. The radiant drift listed in *Table 1* is rather uncertain due to the small number of shower meteors.

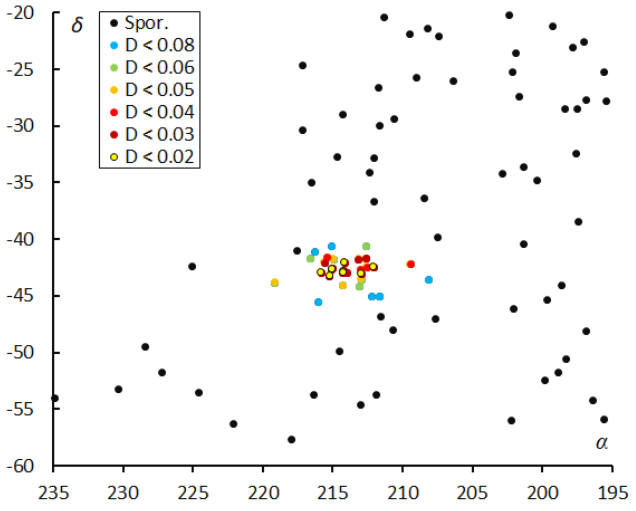

Figure 7 – The radiant distribution during the solar-longitude interval 265° – 273° in equatorial coordinates, color-coded for different threshold values of the D_D orbit similarity criterion.

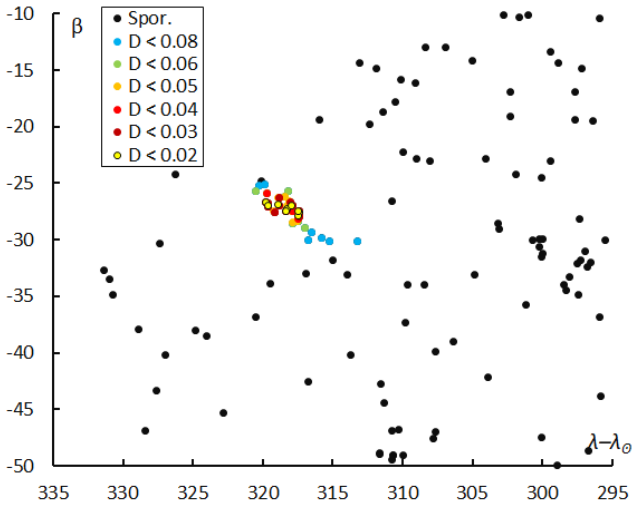

Figure 8 – The radiant distribution during the solar-longitude interval 265° – 273° in Sun-centered geocentric ecliptic coordinates, color-coded for different threshold values of the D_D orbit similarity criterion.

4 Orbit and parent body

The only previously known record for the iota-Lupids orbit has been obtained from radar observations (Pokorný et al., 2017) and the orbital parameters differ mainly because of the significant lower geocentric velocity measured by radar. The radar results are included in *Table 1* for comparison. Radar meteor observations cover another population in meteoroid streams than low-light optical cameras. It is not clear if the difference in velocity and consequent shorter orbit observed by radar is due to the fact that the radar detects mainly fainter meteors and thus much smaller particles, or if the difference is instrumental.

Table 1 – Comparing solutions derived by two different methods, radiant based method and orbit based menthod for $D_D < 0.06$, both compared to Pokorný (2017).

	Radiant method	Orbit method $D_D < 0.06$	Pokorný (2017)
$\lambda_\odot$ (°)	268.6	268.6	271.0
$\lambda_{\odot b}$ (°)	266.0	265.4	267.0
$\lambda_{\odot e}$ (°)	270.0	272.9	272.0
α_g (°)	214.1	214.2	213.0
δ_g (°)	–42.2	–42.6	–46.1
$\Delta\alpha_g$ (°)	+0.06	+0.86	+1.58
$\Delta\delta_g$ (°)	–0.86	–0.39	–0.36
v_g (km/s)	41.5	41.4	37.0
H_b (km)	97.4	97.4	–
H_e (km)	85.9	86.2	–
H_p (km)	89.3	90.1	–
Mag_{Ap}	–0.5	–0.3	–
λ_g (°)	226.62	226.9	227.4
$\lambda_g - \lambda_\odot$ (°)	318.62	318.2	316.4
β_g (°)	–26.83	–27.2	–30.7
a (A.U.)	1.337	1.339	1.05
q (A.U.)	0.233	0.234	0.268
e	0.826	0.826	0.744
i (°)	72.9	72.9	66.2
ω (°)	226.7	226.8	225.1
Ω (°)	88.4	88.3	91.0
Π (°)	315.0	315.1	316.1
T_j	4.06	4.06	5.21
N	23	24	185

Looking at the diagram of inclination versus longitude of perihelion, we found a concentration amid a scarce populated space (*Figure 9*). It appears there are very few meteoroids in this range of inclination and longitude of perihelion, with mainly iota-Lupid meteoroids in this diagram.

The distribution of the perihelion distance versus the inclination (*Figure 10*) shows a concentration near what looks like the edge for short perihelion distances.

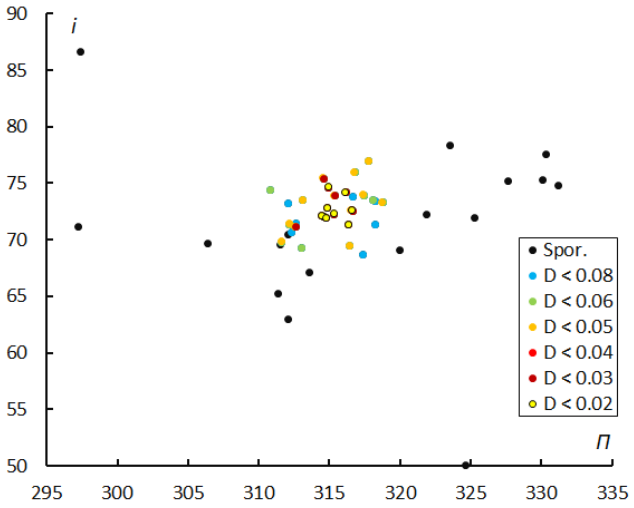

Figure 9 – The diagram of the inclination i against the longitude of perihelion Π color-coded for different classes of D criteria thresholds, for $\lambda_\odot$ between 265° and 273°.

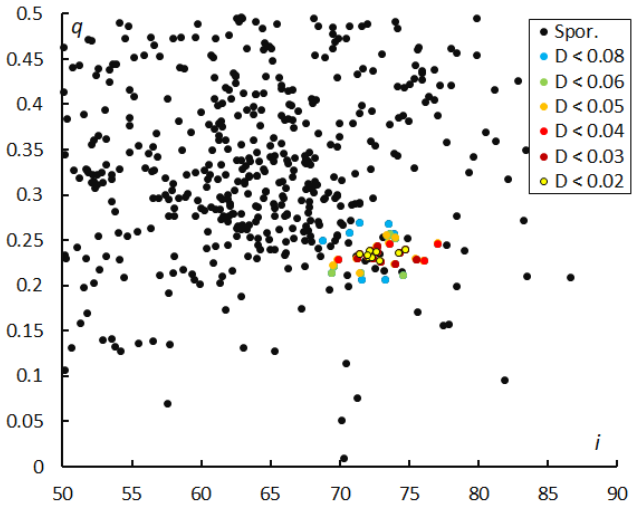

Figure 10 – The diagram of the perihelion distance q against the inclination i color-coded for different classes of D criteria thresholds, for $\lambda_\odot$ between 265° and 273°.

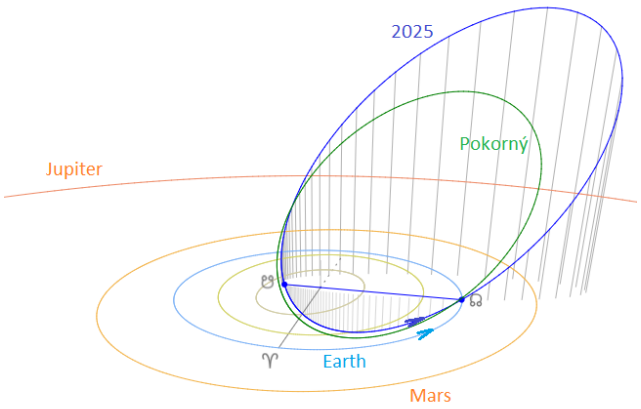

Figure 11 – Comparing the mean orbits for the solutions for the iota-Lupids based on the radiant shower identification (blue), to the radar orbit (green) published by Pokorný et al. (2017), close-up at the inner Solar System. (Plotted with the Orbit visualization app provided by Pető Zsolt).

The iota-Lupids encounter the Earth at their ascending node (*Figure 11*). The position of the descending node is far inside the orbit of planet Mercury, which means that the meteoroids are exposed to extreme thermal stress due to intense Solar radiation. The orbit determined by radar observations is plotted in green and represents mainly smaller particles far inside the orbit (blue) determined by the low-light cameras of the Global Meteor Network.

The Tisserand relative to Jupiter, with $T_J = 4.06$, indicates an asteroidal orbit type and close approaches to the Sun with perihelion distance far inside the orbit of planet Mercury explains why this meteoroid stream can be called a Sun-skirter.

The original discovery of this meteoroid stream mentioned 2012MS4 as possible parent object. However, this object does not appear in the top-10 of best fitting orbits of minor bodies, all of which have poor similarity far above the minimal threshold of $D_D < 0.105$ (*Table 2*). The parent body, if still preserved, is therefore unknown.

Table 2 – Top ten matches of a search for possible parent bodies with $D_D < 0.35$

Name	D_D
C/1905 X1 (Giacobini)	0.249
(620071) 2011 WN_{15}	0.293
2019 UU_{13}	0.306
2004 WK_1	0.312
C/2002 X_5 (Kudo-Fujikawa)	0.315
(177651) 2004 XM_{14}	0.323
2022 YN_7	0.331
2019 WM_3	0.334
C/2019 Y4-D (ATLAS)	0.336
C/1844 Y1 (Great comet)	0.337

5 Past activity

Searching previous years of Global Meteor Network data, twelve iota-Lupids orbits were found in 2024, fourteen in 2023, four in 2022 and one in 2020, none in 2021 or 2019. The expansion of GMN at the Southern Hemisphere in recent years explains the increase in detected orbits from this shower in recent years. The SonotaCo Net and EDMOND meteoroid orbit datasets had zero iota-Lupids, as these networks cover mainly the Northern Hemisphere. The CAMS dataset covers 2010–2016 and had one iota-Lupid in 2015 and two in 2016.

Verification of visual records from the past did not result in any findings and it appears there has never been a potential detection by anyone until Pokorný and his team in 2017. The iota-Lupids appear to be an annual minor shower and its observations depend upon the detection capacity at the Southern Hemisphere.

Acknowledgments

This report is based on the data of the Global Meteor Network (Vida et al., 2020a; 2020b; 2021) which is released

AU0002, AU000U, AU000V, AU001A, AU001B, AU001E, AU001Q, AU001R, AU001S, AU001U, AU001V, AU001W, AU002B, AU002E, AU0030, AU003E, AU0046, NZ000B, NZ000D, NZ000G, NZ000T, NZ0011, NZ0014, NZ0016, NZ0017, NZ001A, NZ001N, NZ001P, NZ001R, NZ0022, NZ0025, NZ0026, NZ0028, NZ0029, NZ002C, NZ002D, NZ002G, NZ002H, NZ002K, NZ002N, NZ002R, NZ002V, NZ002X, NZ0030, NZ0033, NZ0034, NZ0035, NZ0037, NZ0038, NZ003A, NZ003C, NZ003K, NZ0040, NZ0043, NZ0044, NZ0048, NZ004A, NZ004C, NZ004N, NZ004U, NZ0059, NZ005B, NZ005C, NZ005D, NZ005E, NZ005F, NZ005H, NZ005J, NZ005N, NZ005Q, NZ005R, NZ005T, NZ005U, NZ005Z, NZ0061, NZ0063, NZ0067, NZ0068, US003G, US005W.

References

Drummond J. D. (1981). “A test of comet and meteor shower associations”. *Icarus*, **45**, 545–553.

Jopek T. J. (1993). “Remarks on the meteor orbital similarity D-criterion”. *Icarus*, **106**, 603–607.

Jopek T. J., Rudawska R. and Pretka-Ziomek H. (2006). “Calculation of the mean orbit of a meteoroid stream”. *Monthly Notices of the Royal Astronomical Society*, **371**, 1367–1372.

Moorhead A. V., Clements T. D., Vida D. (2020). “Realistic gravitational focusing of meteoroid streams”. *Monthly Notices of the Royal Astronomical Society*, **494**, 2982–2994.

Pokorný P., Janches D., Brown P. G., Hormaechea J. L. (2017). “An orbital meteoroid stream survey using the Southern Argentina Agile MEteor Radar (SAAMER) based on a wavelet approach”. *Icarus*, **290**, 162–182.

Roggemans P., Vida D., Šegon D., Scott J.M. (2026). “Meteoroid orbit shower identification”. *eMetN Meteor Journal*, **11**, To be published.

Roggemans P., Campbell-Burns P., Kalina M., McIntyre M., Scott J. M., Šegon D., Vida D. (2026b). “Global Meteor Network report 2025”. *eMetN Meteor Journal*, **11**, 89–129.

Southworth R. B. and Hawkins G. S. (1963). “Statistics of meteor streams”. *Smithsonian Contributions to Astrophysics*, **7**, 261–285.

Vida D., Gural P., Brown P., Campbell-Brown M., Wiegert P. (2020a). “Estimating trajectories of meteors: an observational Monte Carlo approach - I. Theory”. *Monthly Notices of the Royal Astronomical Society*, **491**, 2688–2705.

Vida D., Gural P., Brown P., Campbell-Brown M., Wiegert P. (2020b). “Estimating trajectories of meteors: an observational Monte Carlo approach - II. Results”. *Monthly Notices of the Royal Astronomical Society*, **491**, 3996–4011.

Vida D., Šegon D., Gural P. S., Brown P. G., McIntyre M. J. M., Dijkema T. J., Pavletić L., Kukić P., Mazur M. J., Eschman P., Roggemans P., Merlak A., Zubrović D. (2021). “The Global Meteor Network – Methodology and first results”. *Monthly Notices of the Royal Astronomical Society*, **506**, 5046–5074.

[29] https://creativecommons.org/licenses/by/4.0/

2025 outburst of the Volantids (VOL#758)

Paul Roggemans[1], **Denis Vida**[2,3], **Damir Šegon**[4,5], **James M. Scott**[6], **Jeff Wood**[7]

[1] **Pijnboomstraat 25, 2800 Mechelen, Belgium**

[2] **Department of Physics and Astronomy, University of Western Ontario, Richmond Street, London, N6A 3K7, Ontario, Canada**

[3] **Institute for Earth and Space Exploration, University of Western Ontario, Perth Drive, London, N6A 5B8, Ontario, Canada**
denis.vida@gmail.com

[4] **Astronomical Society Istra Pula, Park Monte Zaro 2, 52100 Pula, Croatia**

[5] **Višnjan Observatory, Istarska 5, 52463 Višnjan, Croatia**

[6] **Department of Geoscience, Aarhus University, Høegh-Guldbergs Gade 2. DK-8000 Aarhus C, Denmark**

[7] **PO Box 162, Willetton, Western Australia 6955, Australia**

An outburst of the Volantids has been detected between the 23rd of December 2025 and the 4th of January 2026 from a radiant at R.A. = 125.4° and Decl.= –72.0°, with a geocentric velocity of 30.3 km/s. This case study confirms the existence of this episodic meteor shower with a five-year periodicity. The KVO#787 and VOL#758 entries in the MDC list were found to be the same shower on the basis of our observations, we recommend merging them with VOL#758 in the MDC list. The shower fulfils the criteria to be nominated for established status by the IAU-MDC.

1 Introduction

On 30 December 2025 the GMN radiant density map revealed that an optical outburst of the kappa-Volantids was ongoing. The first results matched the orbit of the kappa-Volantids (KVO#787)[30] with D-criteria thresholds of $D_{SH} < 0.038$ & $D_D < 0.015$ & $D_J < 0.038$. Another positive match with the Volantids (VOL#758) had worse similarity thresholds and therefore the outburst was identified in first instance as the kappa-Volantids.

The shower appeared to have been active several days earlier and lasted until 4 January 2026. It was monitored by 202 GMN cameras installed in Australia, Brazil, Chile, New Zealand and South Africa. A CBET was issued to report the outburst (Vida et al., 2026). This publication also covered the results by the CAMS-network on this shower, identified as the Volantids (VOL#758)[31] by Jenniskens et al. (2026). Both showers in the IAU-MDC list refer to the same activity and should be moved under a single entry.

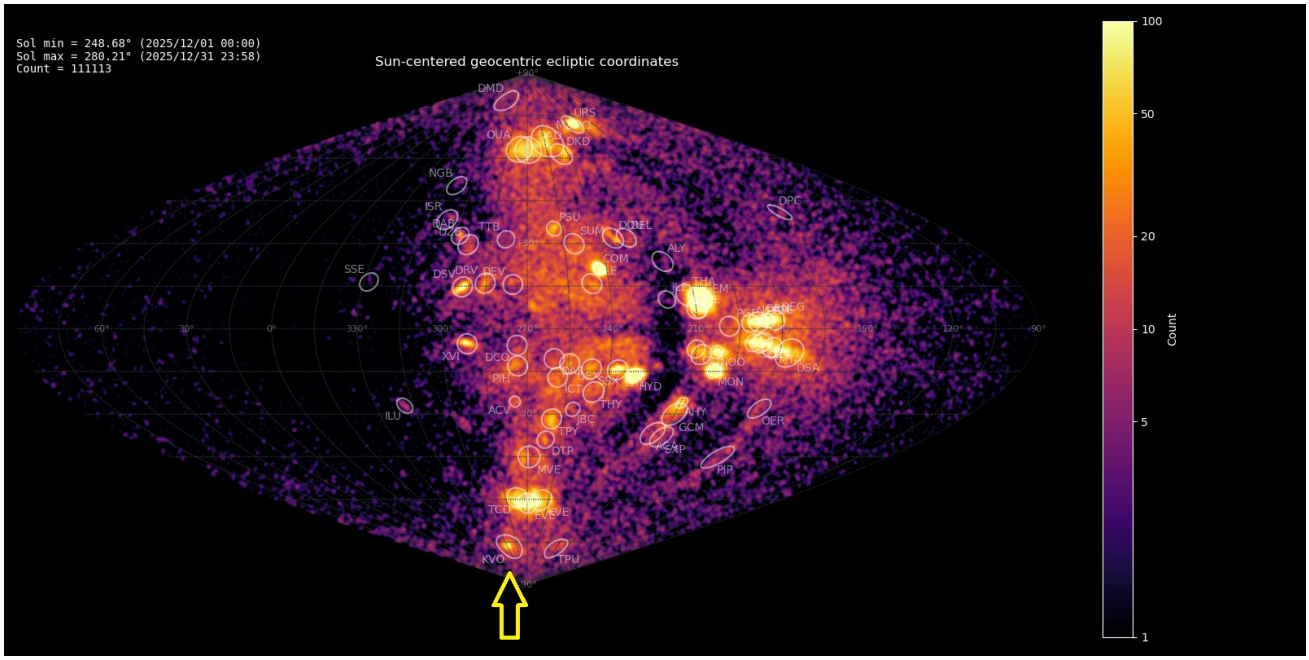

Figure 1 – Radiant density map with 111113 radiants obtained by the Global Meteor Network during December, 2025. The position of the kappa-Volantids in Sun-centered geocentric ecliptic coordinates is marked with a yellow arrow.

[30] https://www.ta3.sk/IAUC22DB/MDC2022/Roje/pojedynczy_obiekt.php?lporz=01699&kodstrumienia=00787

[31] https://www.ta3.sk/IAUC22DB/MDC2022/Roje/pojedynczy_obiekt.php?lporz=01662&kodstrumienia=00758

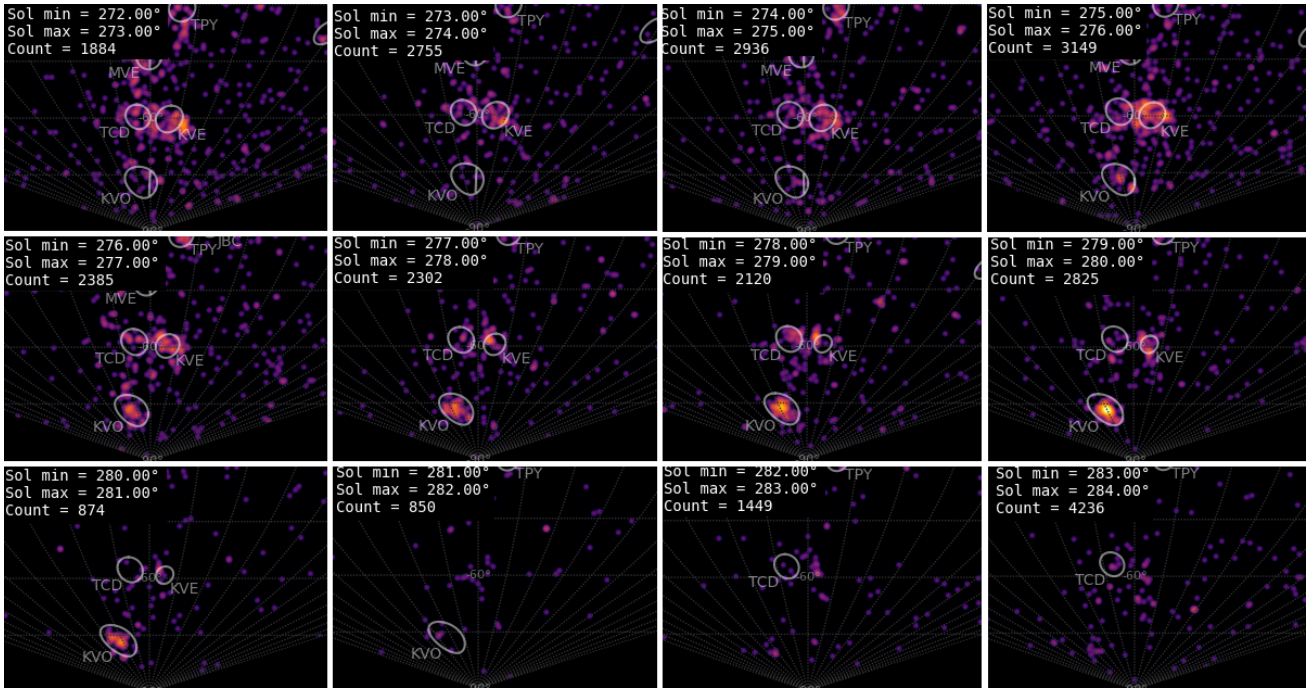

Figure 2 – Changes in the radiant appearance of the kappa-Volantids during the activity period.

2 Shower classification based on radiants

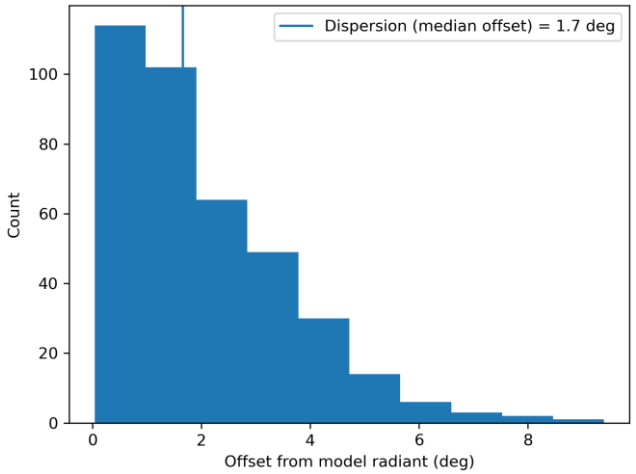

Figure 3 – Dispersion median offset on the radiant position.

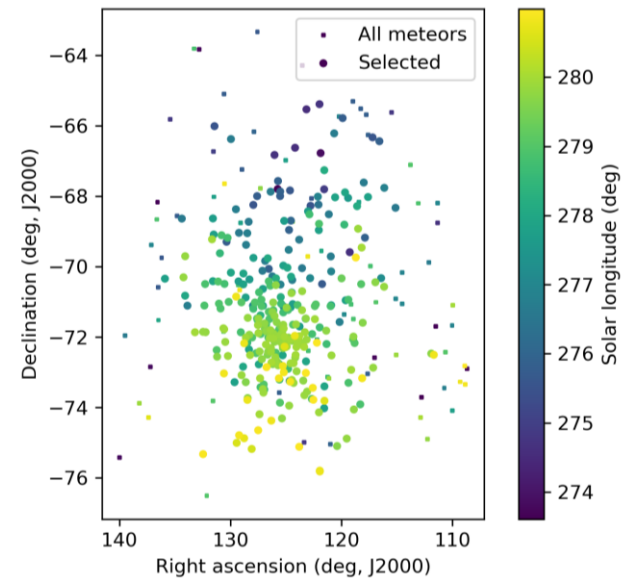

Figure 4 – The radiant distribution during the solar-longitude interval 274° – 281° in equatorial coordinates.

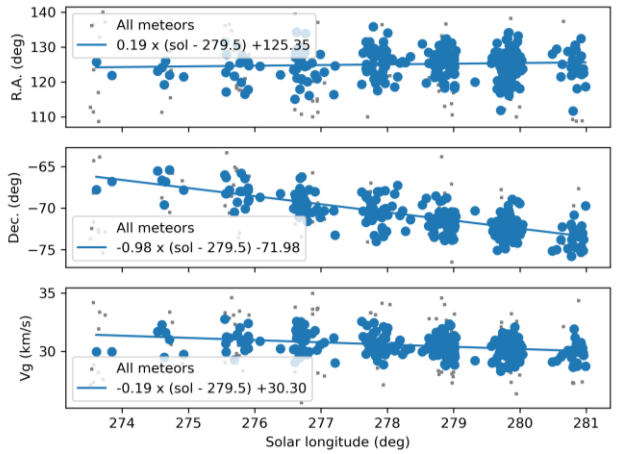

Figure 5 – The radiant drift.

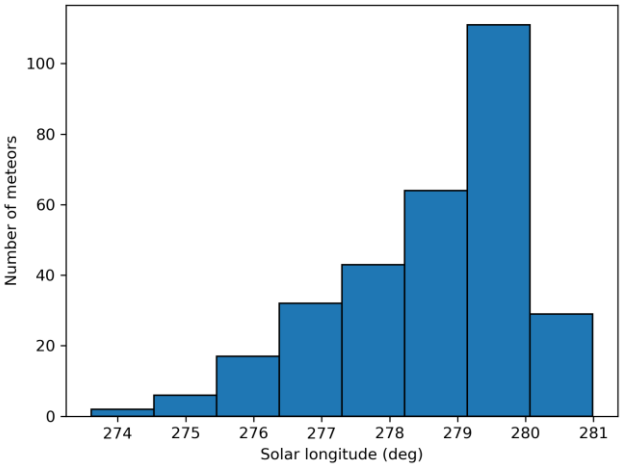

Figure 6 – The uncorrected number of shower meteors recorded per degree in solar longitude.

The GMN shower association criteria assume that meteors within 1° in solar longitude, within 3.3° in radiant in this case, and within 10% in geocentric velocity of a shower reference location are members of that shower. Further

details about the shower association are explained in Moorhead et al. (2020). Using these meteor shower selection criteria, 304 orbits have been identified as kappa-Volantids. The final results have been listed in *Table 1*.

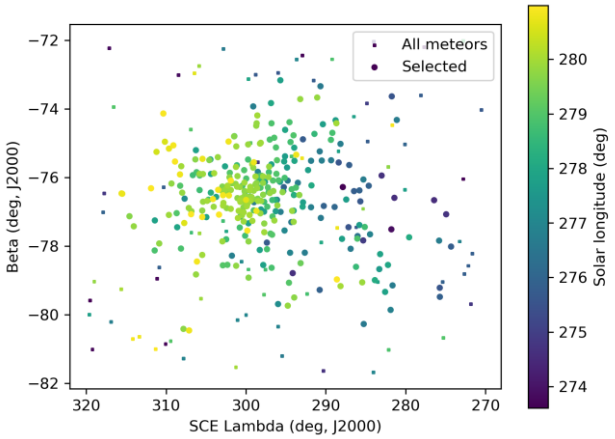

Figure 7 – The radiant distribution during the solar-longitude interval 274° – 281° in Sun centered geocentric ecliptic coordinates.

3 Shower classification based on orbits

A complete independent meteoroid stream search has been applied for confirmation based upon orbit data. This method has been described in a separate publication (Roggemans, 2026). The mean orbit has been computed by the method of Jopek et al. (2006) for all 293 orbits that fit the thresholds $D_{SH} < 0.125$ & $D_D < 0.05$ & $D_J < 0.125$ (Southworth and Hawkins, 1963; Drummond, 1981; Jopek, 1993). The results have been listed in *Table 1*.

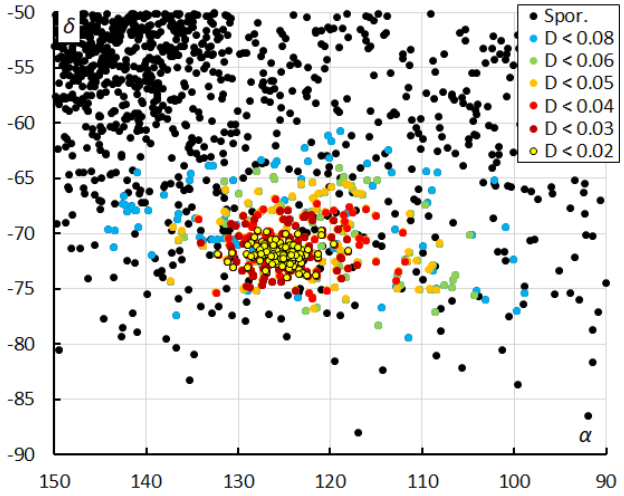

Figure 8 – The radiant distribution during the solar-longitude interval 270° – 285° in equatorial coordinates, color-coded for different classes of D-criteria thresholds.

The radiant plots in equatorial coordinates (*Figure 8*) and in Sun-centered ecliptic coordinates (*Figure 9*) show a distinct concentration stretched out because of the projection near the poles in both equatorial as ecliptic coordinates. The dense concentration in the upper left corner of *Figure 8* is mainly due to the kappa-Velids (KVE#784), another shower that had its maximum activity a bit earlier than the kappa-Volantids outburst. These kappa-Velid radiants are also visible in the upper right corner of *Figure 9*. GMN detected as many as 230 kappa-Velids in December 2025.

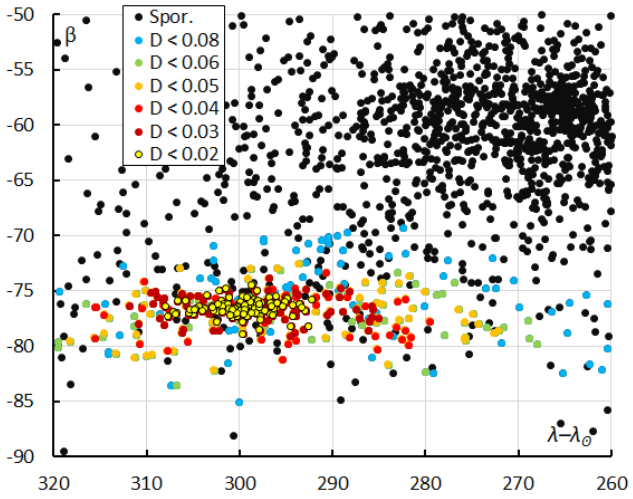

Figure 9 – The radiant distribution during the solar-longitude interval 270° – 285° in Sun-centered geocentric ecliptic coordinates, color-coded for different classes of D-criteria thresholds.

4 Activity based on the two methods

256 kappa-Volantids were identified in common by both methods. 48 were found by the radiant identification method but not found by the orbit method. 37 were identified by the orbit identification but not detected by the radiant method. The radiant classification method counts all possible kappa-Volantids if their radiants fit within a given radiant size, regardless deviant orbits. The orbit classification method counts all possible kappa-Volantids if their orbits fit with the mean orbit within chosen similarity thresholds, regardless the radiant position. The percentage of KVO-meteors relative to the total number of meteors recorded at the Southern Hemisphere, counted in time bins of one degree every 0.25° in Solar Longitude results in the skew activity profile in *Figure 10* for both methods. Orbit classification indicates longer activity duration starting earlier than $\lambda_\odot = 274°$ and lasting longer than $\lambda_\odot = 281°$.

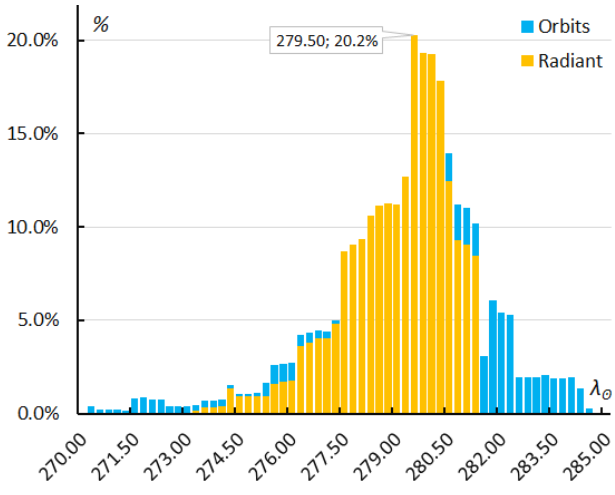

Figure 10 – The percentage of KVO-meteors relative to the total number of meteors recorded by cameras at the Southern Hemisphere. Orange is the result for the radiant shower classification, blue for the orbit classification method.

5 Orbit and parent body

The final orbits obtained by the two classifications are listed in *Table 1* and compared to the results obtained by radar (Pokorný, 2017) and the CAMS-network (Jenniskens, 2023). The radiant method had 84% of its meteors in common with the orbit method and the orbit method 87% of its meteors in common with the radiant method. Despite the differences in selection of the KVO-meteors, the resulting mean orbits computed by the method of Jopek et al. (2006) are in excellent agreement. The 2025 result of GMN is also in very good agreement with Pokorný et al. (2017), reason why the outburst was identified as the kappa-Volantids. The CAMS-result differs quite a lot in eccentricity but the other elements are in good agreement. The CAMS results were listed as Volantids (VOL#758) although this is the same activity as the kappa-Volantids.

Table 1 – Comparing solutions derived by the radiant based method and the orbit orbit based menthod for $D_D < 0.05$, both compared to Pokorný et al. (2017) and Jenniskens (2023).

	Radiant method	Orbit method	Pokorný (2017)	CAMS (2023)
$\lambda_\odot$ (°)	279.5	279.0	280.0	279.3
$\lambda_{\odot b}$ (°)	273.0	270.6	274	276
$\lambda_{\odot e}$ (°)	281.0	284.2	283	283
α_g (°)	125.4	125.2	121.1	123.4
δ_g (°)	–72.0	–71.7	–72.7	–72.1
$\Delta\alpha_g$ (°)	+0.19	–0.12	–1.42	–0.96
$\Delta\delta_g$ (°)	–0.98	–0.84	–0.64	–0.88
v_g (km/s)	30.3	30.3	29.6	30.4
H_b (km)	94.5	94.7	–	–
H_e (km)	82.6	82.2	–	–
H_p (km)	87.1	86.8	–	–
Mag_{Ap}	+0.1	+0.0	–	–
λ_g (°)	219.49	218.4	223.58	220.48
$\lambda_g - \lambda_\odot$ (°)	299.99	298.8	303.58	301.1
β_g (°)	–76.53	–76.6	–77.76	–77.2
a (A.U.)	2.628	2.65	2.72	2.81
q (A.U.)	0.973	0.973	0.973	0.973
e	0.630	0.633	0.642	0.654
i (°)	50.9	50.6	49.1	50.5
ω (°)	347.6	347.8	346.7	347.1
Ω (°)	98.7	98.7	100	99.3
Π (°)	86.3	86.5	86.7	86.4
T_j	2.68	2.67	2.64	2.57
N	304	293	398	205

Looking at the diagram of inclination versus longitude of perihelion, we can see a distinct concentration of KVO-meteors (*Figure 11*). The dense concentration at the top are mainly Quadrantids, the concentration at right are the Ursids. The spread on the blue dots indicates that the thresholds with $D_{SH} < 0.20$ & $D_D < 0.08$ & $D_J < 0.20$ are contaminated with sporadics and too tolerant for orbit classification. There is a slight decreasing trend in the inclination (*Figure 12*) and in the longitude of perihelion (*Figure13*) during the activity period. The other orbital elements, semi-major axis a, perihelion distance q and eccentricity e, show no changes during the activity period.

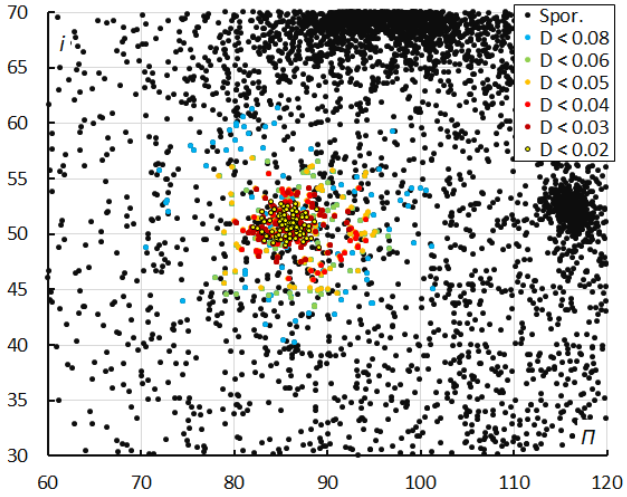

Figure 11 – The diagram of the inclination i versus the longitude of perihelion Π color-coded for different classes of D-criteria thresholds, for $\lambda_\odot$ between 270° and 285°.

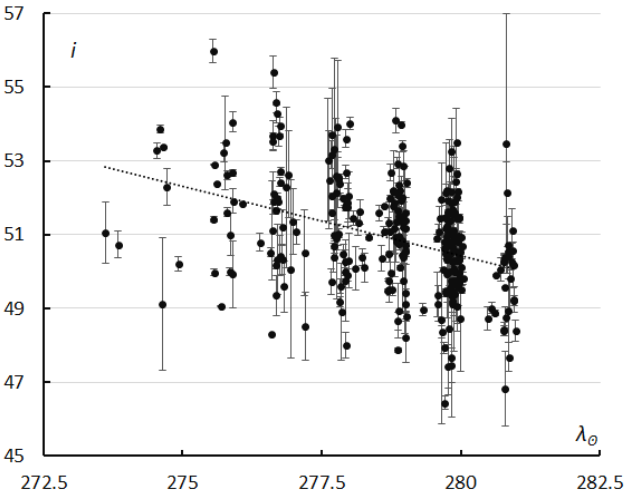

Figure 12 – The evolution of the inclination i in function of the solar longitude $\lambda_\odot$ for the kappa-Volantids 2025–2026.

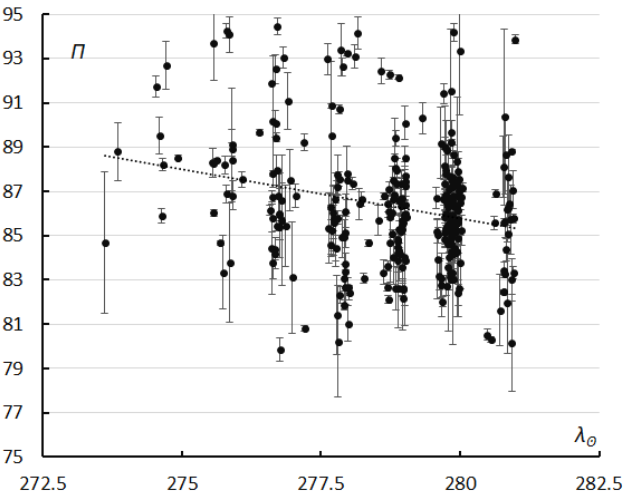

Figure 13 – The evolution of the longitude of perihelion Π in function of the solar longitude $\lambda_\odot$ for the kappa-Volantids 2025–2026.

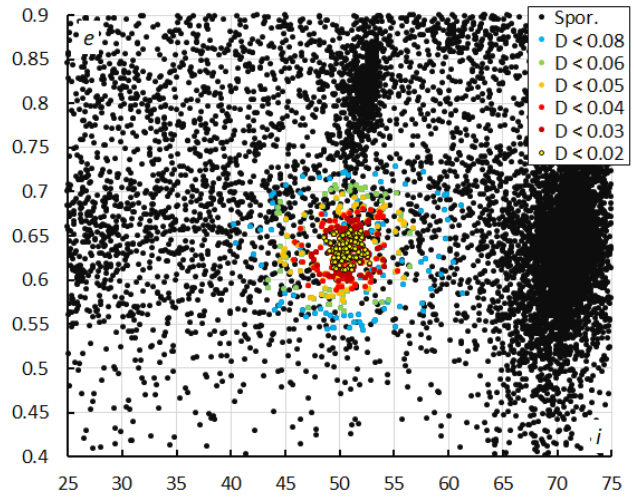

Figure 14 – The diagram of the eccentricity e versus the inclination i color-coded for different classes of D-criteria thresholds, for $\lambda_\odot$ between 270° and 285°.

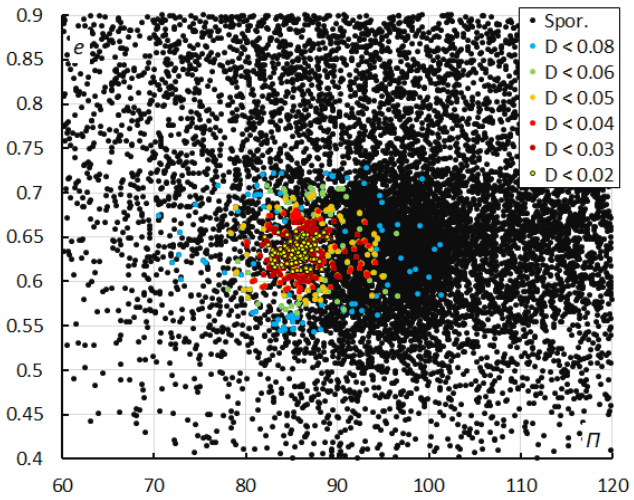

Figure 15 – The diagram of the inclination e versus the longitude of perihelion Π color-coded for different classes of D-criteria thresholds, for $\lambda_\odot$ between 270° and 285°.

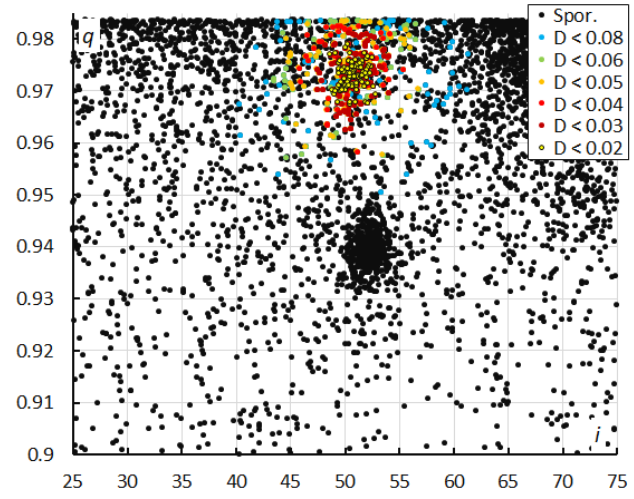

Figure 16 – The diagram of the perihelion distance q versus the inclination i color-coded for different classes of D-criteria thresholds, for $\lambda_\odot$ between 270° and 285°.

The distribution of the eccentricity e versus inclination i displays the KVO-meteors as a dense concentration (*Figure 14*). The dense concentration above the KVO-meteors are the Ursids, the concentration at right are the Quadrantids and the kappa-Velids. The distribution of the eccentricity e versus longitude of perihelion Π displays the KVO-meteors as a dense concentration just left of a dense concentration caused by the Quadrantids (*Figure 15*). The distribution of the perihelion distance q versus the inclination i shows the concentration of KVO-meteors, the dense concentration in the middle of the plot are the Ursids (*Figure 16*).

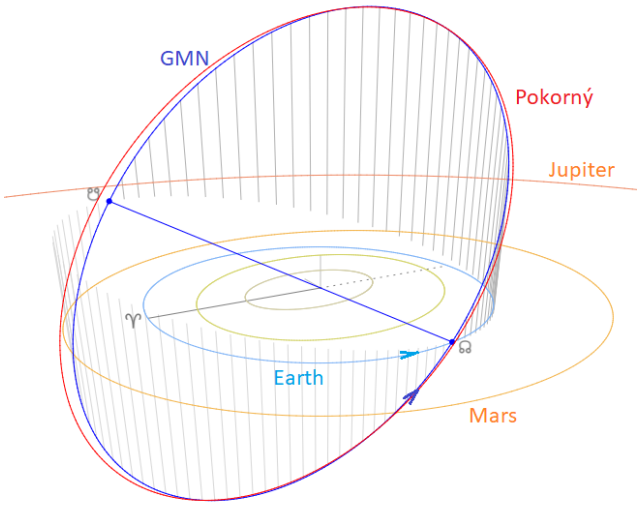

Figure 17 – Comparing the GMN solutions (blue) for the kappa-Volantids 2025 with the solution obtained by Pokorný et al. (2017) (red), close-up at the inner Solar System. (Plotted with the Orbit visualization app provided by Pető Zsolt).

The kappa-Volantids encounter the Earth at their ascending node Ω on an orbit steep to the ecliptic plane. *Figure 17* shows the agreement between the GMN result for 2025 and the radar result for 2015. The Tisserand value relative to Jupiter with $T_J = 2.68$ is typical for a Jupiter-family comet type orbit. A parent body search did not reveal any convincing candidate. Either the meteoroid streams' parent has still to be discovered or orbit integrations may reveal the connection between some known object and the meteoroid dust. The ten best matches are listed in *Table 2*.

Table 2 – Top ten matches of a search for possible parent bodies with $D_D < 0.17$

Name	D_D
2017 YN_3	0.116
2022 WC_{12}	0.127
2022 BJ_3	0.14
2018 AG	0.149
2020 WS_5	0.151
2024 AA_2	0.152
2018 AG_{13}	0.157
2019 AW_7	0.159
2017 XH_2	0.16
2002 AA_2	0.162

6 Past activity

The shower has been first noticed on 31 December 2015 by CAMS-New Zealand (Jenniskens et al., 2016) and was confirmed by radar observations by Younger et al. (2016). The activity was recorded during several days until 2 January 2016. The same radiant appears in the orbital meteoroid stream survey of the SAAMER meteor radar data (Pokorný et al., 2017) which was added to the IAU-MDC Working List of Meteor Showers as the kappa-Volantids (KVO#787) while the CAMS results were included as Volantids (VOL#758). The next few years the shower didn't produce any activity until 2020.

The shower reoccurred on 27–28 December 2020 (Jenniskens, 2021). The activity was detected until 3 January 2021 and the final orbital parameters for 2020–2021 CAMS data by Jenniskens and Cooper (2021) are in better agreement with the 2025–2026 GMN results than the 2015–2016 CAMS results based on a much smaller number of meteors.

Global Meteor Network obtained good coverage at the Southern Hemisphere since 2022, but no activity from this radiant has been observed in previous years. A search through available visual observations from the Southern Hemisphere revealed no records of any activity in the past.

7 Conclusion

The Global Meteor Network detected a meteor shower outburst near the Southern Hemisphere pole during 30–31 December 2025. The activity was identified as the kappa-Volantids (VKO#787) as best matching meteoroid stream listed in the IAU-MDC Working List of Meteor Showers. Another matching meteoroid stream listed as the Volantids (VOL#758), had a positive match but with a much weaker correlation. The 2025–2026 activity has been also observed by CAMS, confirming the observations by GMN, but identified as the Volantids (VOL#758) (Jenniskens et al., 2026).

The confirmation of the kappa-Volantids (KVO#787) by GMN in 2025–2026 with an independent solution reported to the IAU-MDC, fulfils the criteria[32] to be nominated for established status. The confusion created by using two different identifications for the same shower should be resolved. This coincidence between both listed showers has been documented before by Masahiro Koseki (2023) who made a detailed evaluation of the IAU-MDC Working List with many suggestions for corrections.

Meteoroid stream identification by GMN is based solely on the latest status of the IAU-MDC Working List of Meteor Showers. Literature searches for specific case studies often reveal very interesting data that is not cited in the IAU-MDC Working List. Such sources may be cited in the case study, but any initial identifications are based solely upon the IAU-MDC Working List as universal reference source.

The final decision about the naming of meteor showers is at the discretion of the IAU Commission F1 working group. During the review period of this paper the IAU-MDC staff has communicated the following proposal. "*If a shower is found to be a duplicate of another shower, its parameters will be moved to the earlier discovered shower as a further solution, and only a single (the first given) name will be retained. The discovery date of a shower is considered to be the date it was submitted to the MDC or, where applicable, the date it was announced in the CBET. This implies that we should keep the earlier discovered shower, VOL#758 (Jenniskens, 2016), and add to it both solutions of the KVO#787 (Pokorny et al., 2017 and Roggemans et al., 2026); the shower KVO#787 (kappa-Volantids) will be moved to the List of removed shower data, with links to the publications where it is identified as a duplicate shower of VOL#758 (Volantids)*". To facilitate future literature consultations, the authors refer to the Volantids in the title, abstract and metadata while the content of the case study has been left unchanged referring to the kappa-Volantids like the data were originally analyzed. This way this paper documents how the two shower names were merged under Volantids (VOL#758).

Acknowledgments

This report is based on the data of the Global Meteor Network (Vida et al., 2020a; 2020b; 2021) which is released under the CC BY 4.0 license[33]. We thank all 927 participants in the Global Meteor Network project for their contribution and perseverance. A list with the names of the volunteers who contribute to GMN has been published in the 2025 annual report (Roggemans et al., 2026). The following 202 cameras recorded kappa-Volantids that have been used in this study:

AU0002, AU000A, AU000B, AU000C, AU000D, AU000F, AU000G, AU000L, AU000R, AU000T, AU000U, AU000V, AU000W, AU000X, AU000Y, AU000Z, AU0010, AU001A, AU001B, AU001C, AU001D, AU001E, AU001F, AU001K, AU001L, AU001N, AU001P, AU001Q, AU001R, AU001S, AU001U, AU001V, AU001W, AU001X, AU001Y, AU001Z, AU0028, AU0029, AU002A, AU002B, AU002C, AU002D, AU0030, AU003E, AU003G, AU003H, AU0040, AU0046, AU004H, AU004L, AU004M, AU004Q, AU004R, BR000F, BR000Y, BR001H, BR002C, CL0002, CL0003, NZ0001, NZ0003, NZ0004, NZ0007, NZ0008, NZ000B, NZ000D, NZ000G, NZ000H, NZ000M, NZ000N, NZ000P, NZ000Q, NZ000S, NZ000T, NZ000X, NZ000Y, NZ000Z, NZ0010, NZ0011, NZ0012, NZ0014, NZ0015, NZ0016, NZ0017, NZ0018, NZ0019, NZ001C, NZ001E, NZ001G, NZ001J, NZ001L, NZ001N, NZ001P, NZ001R, NZ001S, NZ001V, NZ001W, NZ001X, NZ0020, NZ0021, NZ0022, NZ0023, NZ0024, NZ0025, NZ0026, NZ0027, NZ0028, NZ0029, NZ002C, NZ002D, NZ002E, NZ002F, NZ002G, NZ002J, NZ002K, NZ002L, NZ002N, NZ002P, NZ002Q, NZ002R, NZ002S,

[32] https://www.ta3.sk/IAUC22DB/MDC2022/Dokumenty/shower_nomenclature.php

[33] https://creativecommons.org/licenses/by/4.0/

NZ002T, NZ002U, NZ002W, NZ002X, NZ002Y, NZ002Z, NZ0030, NZ0033, NZ0034, NZ0036, NZ0037, NZ0038, NZ003A, NZ003B, NZ003C, NZ003E, NZ003K, NZ003N, NZ003Q, NZ003R, NZ003S, NZ003U, NZ003V, NZ003W, NZ003Y, NZ003Z, NZ0040, NZ0041, NZ0042, NZ0044, NZ0046, NZ0049, NZ004A, NZ004B, NZ004C, NZ004D, NZ004H, NZ004J, NZ004L, NZ004M, NZ004N, NZ004R, NZ004T, NZ004U, NZ004V, NZ004W, NZ004Y, NZ004Z, NZ0051, NZ0059, NZ005A, NZ005B, NZ005C, NZ005D, NZ005E, NZ005F, NZ005G, NZ005J, NZ005K, NZ005L, NZ005M, NZ005N, NZ005R, NZ005S, NZ005T, NZ005Y, NZ005Z, NZ0061, NZ0063, NZ0065, NZ0066, NZ0068, NZ0069, NZ006F, NZ006K, ZA0002, ZA0006, ZA0007, ZA000C, ZA000F and ZA000G.

References

Drummond J. D. (1981). “A test of comet and meteor shower associations”. *Icarus*, **45**, 545–553.

Jenniskens P., Baggaley J., Crumpton I., Aldous P., Gural P. S., Samuels D., Albers J., Soja R. (2016). “A surprise southern hemisphere meteor shower on New-Year's Eve 2015: the Volantids (IAU#758, VOL)”. *WGN, Journal of the International Meteor Organization*, **44**, 35–41.

Jenniskens P. (2021). “Return of Volantid meteor shower, expected to peak on New Year’s Eve”. *eMetN Meteor Journal*, **6**, 22–23.

Jenniskens P., Cooper T. (2021). “The 2020 return of the Volantids (VOL#758)”. *eMetN Meteor Journal*, **6**, 262–263.

Jenniskens P., Lauretta D. S., Baggaley J., Scott J., Devillepoix H. A. R., Rollinson D. (2026). “Volantid meteors 2025-2026”. CBET 5653, 2026 January 7, D.W.E. Green, editor.

Jopek T. J. (1993). “Remarks on the meteor orbital similarity D-criterion”. *Icarus*, **106**, 603–607.

Jopek T. J., Rudawska R. and Pretka-Ziomek H. (2006). “Calculation of the mean orbit of a meteoroid stream”. *Monthly Notices of the Royal Astronomical Society*, **371**, 1367–1372.

Koseki M. (2023). “Grading evaluation of meteor showers’ report in the IAU Meteor Data Center Shower Database”. *eMetN Meteor Journal*, **8**, 337–367.

Moorhead A. V., Clements T. D., Vida D. (2020). “Realistic gravitational focusing of meteoroid streams”. *Monthly Notices of the Royal Astronomical Society*, **494**, 2982–2994.

Pokorný P., Janches D., Brown P. G., Hormaechea J. L. (2017). “An orbital meteoroid stream survey using the Southern Argentina Agile MEteor Radar (SAAMER) based on a wavelet approach”. *Icarus*, **290**, 162–182.

Roggemans P., Vida D., Šegon D., Scott J.M. (2026). “Meteoroid orbit shower identification”. *eMetN Meteor Journal*, **11**, To be published.

Roggemans P., Campbell-Burns P., Kalina M., McIntyre M., Scott J. M., Šegon D., Vida D. (2026). “Global Meteor Network report 2025”. *eMetN Meteor Journal*, **11**, 89–129.

Southworth R. B. and Hawkins G. S. (1963). “Statistics of meteor streams”. *Smithsonian Contributions to Astrophysics*, **7**, 261–285.

Younger J., Reid I., Murphy D. (2016). “Radar observations of the Volantids meteor shower”. In, Roggemans A., Roggemans P., editors, *Proceedings of the International Meteor Conference*. Egmond, the Netherlands, 2-5 June 2016. IMO ISBN 978-2-87355-030-1, 352–357.

Vida D., Gural P., Brown P., Campbell-Brown M., Wiegert P. (2020a). “Estimating trajectories of meteors: an observational Monte Carlo approach - I. Theory”. *Monthly Notices of the Royal Astronomical Society*, **491**, 2688–2705.

Vida D., Gural P., Brown P., Campbell-Brown M., Wiegert P. (2020b). “Estimating trajectories of meteors: an observational Monte Carlo approach - II. Results”. *Monthly Notices of the Royal Astronomical Society*, **491**, 3996–4011.

Vida D., Šegon D., Gural P. S., Brown P. G., McIntyre M. J. M., Dijkema T. J., Pavletić L., Kukić P., Mazur M. J., Eschman P., Roggemans P., Merlak A., Zubrović D. (2021). “The Global Meteor Network – Methodology and first results”. *Monthly Notices of the Royal Astronomical Society*, **506**, 5046–5074.

Vida D., Šegon D., Roggemans P., Wood J., Scott J., Cooke W.J., Vriezelaar A. (2026). “Volantid meteors 2025-2026”. CBET 5653, 2026 January 7, D.W.E. Green, editor.

62-Andromedids (SAN#924) and 1998 ST_{27}

Paul Roggemans[1], **Denis Vida**[2,3], **Damir Šegon**[4,5], **James M. Scott**[6], **Jeff Wood**[7]

[1] **Pijnboomstraat 25, 2800 Mechelen, Belgium**

[2] **Department of Physics and Astronomy, University of Western Ontario, Richmond Street, London, N6A 3K7, Ontario, Canada**

[3] **Institute for Earth and Space Exploration, University of Western Ontario, Perth Drive, London, N6A 5B8, Ontario, Canada**
denis.vida@gmail.com

[4] **Astronomical Society Istra Pula, Park Monte Zaro 2, 52100 Pula, Croatia**

[5] **Višnjan Observatory, Istarska 5, 52463 Višnjan, Croatia**

[6] **Department of Geoscience, Aarhus University, Høegh-Guldbergs Gade 2. DK-8000 Aarhus C, Denmark**
jscott@geo.au.dk

[7] **PO Box 162, Willetton, Western Australia 6955, Australia**

A case study based on Global Meteor Network data is presented for the 62-Andromedids, which is determined to have a radiant at R.A. = 38.2°, Decl.= +46.3° and a geocentric velocity of 17.0 km/s active around $\lambda_{\odot}$ = 197°. This analysis confirms the existence of this annual meteor shower and the shower fulfils the criteria to be nominated for established status by the IAU-MDC. The Aten-class object 1998 ST_{27} is confirmed as the most likely parent object.

1 Introduction

A paper on the Eccentrids of the Mars family by Terentjeva and Bakanas (2026) and the request to lookup very short orbits in the GMN meteoroid orbit dataset revealed the occurrence of 62-Andromedids activity (Roggemans, 2026). This shower has an unusual short period orbit of 0.74 years or 271 days, a perihelion between the orbits of the planets Mercury and Venus and an aphelion within the orbit of the planet Mars. The shower was discovered by Jenniskens et al. (2018) based upon 19 orbits triangulated by CAMS. Jenniskens suggested 363027 (1998 ST_{27}), a primitive asteroid, as likely parent body (Jenniskens, 2023).

The shower activity is barely detectable in the GMN data with only one orbit in 2019, three in 2020, 20 in 2021, five in 2022, 26 in 2023, 16 in 2024 and only six in 2025, 77 in total. As such, it can be hardly seen on the radiant density map of October 2023 (*Figure 1*). Its detection strongly depends upon the camera coverage during the Solar Longitude interval 196°–198° (*Figure 2*). In 2025 this coverage was poor due to bad weather.

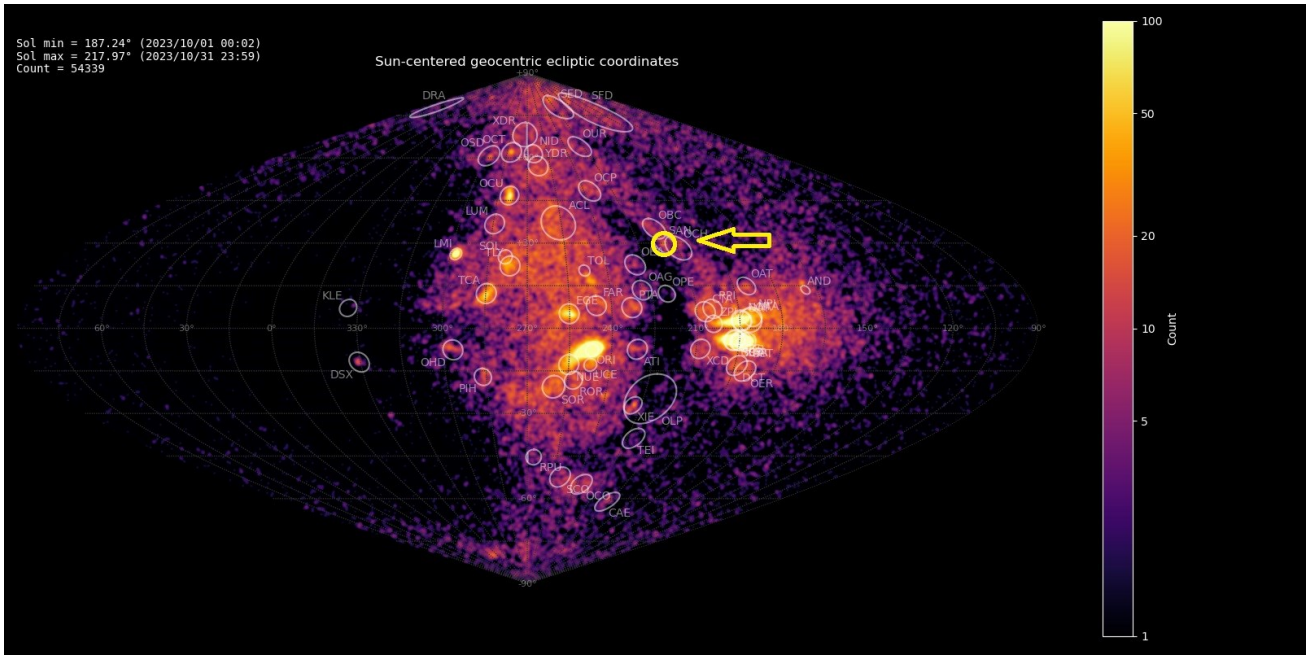

Figure 1 – Radiant density map with 54339 radiants obtained by the Global Meteor Network in October, 2023. The position of the 62-Andromedids (SAN#924) in Sun-centered geocentric ecliptic coordinates is marked with a yellow arrow.

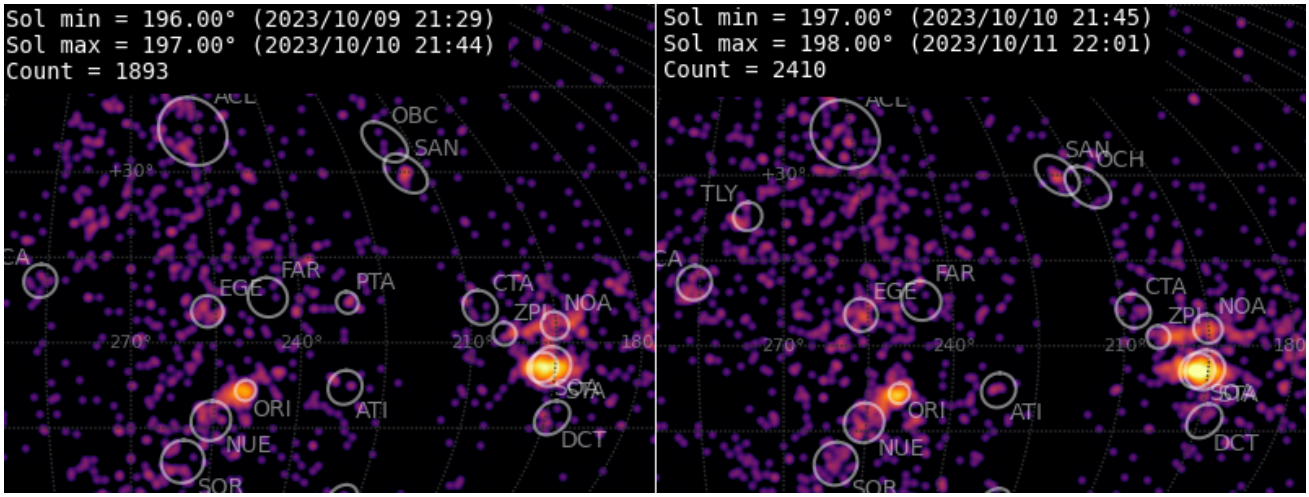

Figure 2 – Radiant density maps for 9–10–11 October 2023. The shower is labeled SAN.

2 Shower classification based on radiants

The GMN shower association criteria assume that meteors within 1° in Solar Longitude, within 1.0° in radiant in this case, and within 10% in geocentric velocity of a shower reference location are members of that shower. Further details about the shower association are explained in Moorhead et al. (2020). Using these meteor shower selection criteria, 76 orbits have been identified as 62-Andromedids in the years 2019–2025 by 186 GMN cameras installed in Australia, Belgium, Canada, Croatia, Czech Republic, Germany, France, Hungary, Italy, Netherlands, New Zealand, Slovenia, South Korea, Spain, Switzerland, United Kingdom and the United States. The weak activity of this shower requires a high-performance camera network to sample the 62-Andromedid meteoroid orbits. The camera coverage of the GMN is useful for detecting and documenting this kind of minor showers. The final results are listed in *Table 1*.

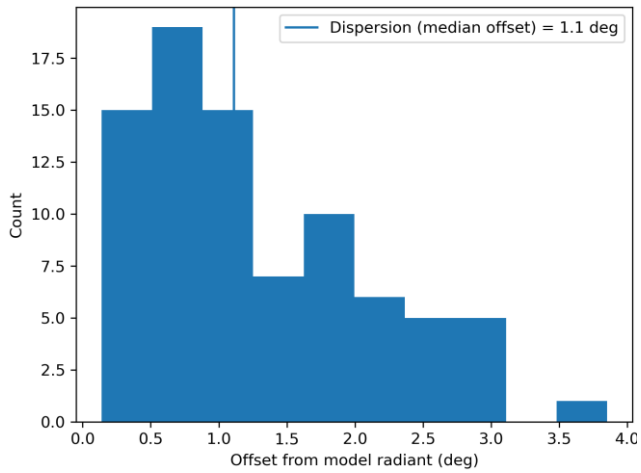

Figure 3 – Dispersion median offset on the radiant position.

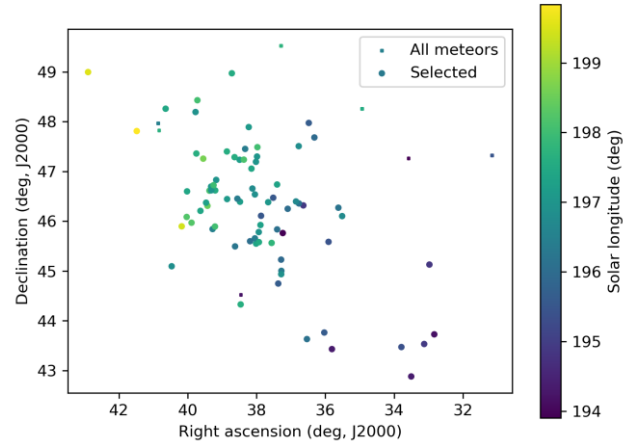

Figure 4 – The radiant distribution during the solar-longitude interval 194° – 200° in equatorial coordinates.

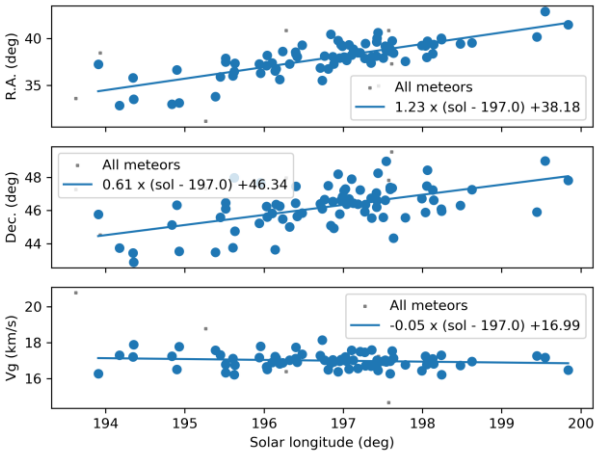

Figure 5 – The radiant drift.

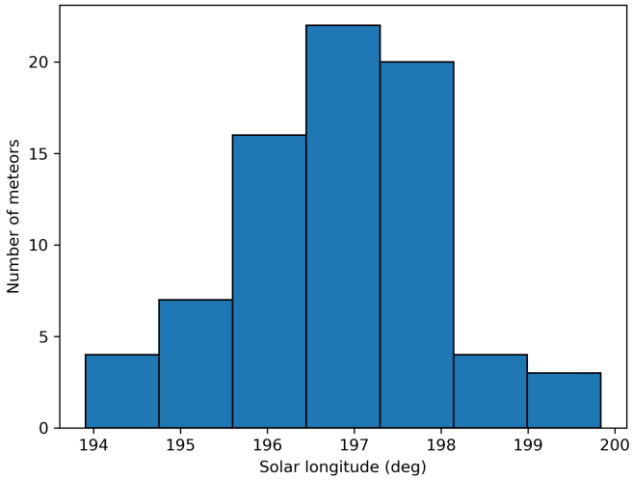

Figure 6 – The uncorrected number of shower meteors recorded per degree in solar longitude.

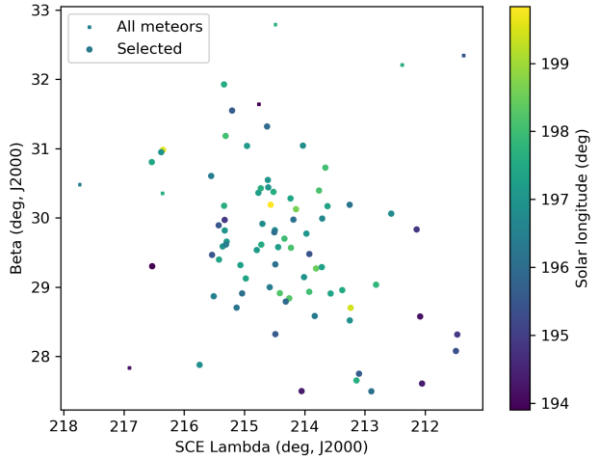

Figure 7 – The radiant distribution during the solar-longitude interval 194° – 200° in Sun-centered geocentric ecliptic coordinates.

3 Shower classification based on orbits

A complete independent meteoroid stream search has been applied based upon orbit data for confirmation. This method has been described in a separate publication (Roggemans and Vida, 2026). The mean orbit was computed by the method of Jopek et al. (2006) for all orbits that fit the thresholds $D_{SH} < 0.075$ & $D_D < 0.03$ & $D_J < 0.075$ (Southworth and Hawkins, 1963; Drummond, 1981; Jopek, 1993). The results have been listed in *Table 1*.

The 62-Andromedid radiant occurs next to other meteor activity (see *Figure 2*). The October beta-Camelopardalids (OBC#386) have a rather dispersed radiant immediately north of the 62-Andromedids in *Figures 8 and 9*. Right next to the 62-Andromedids are the October chi-Andromedids (OCH#716) in both coordinate systems. The presence of these two other meteor showers presents a challenge for identifying the shower association based upon the radiant position with the key difference being in geocentric velocity, which allows proper identification of the 62-Andromedids as very slow meteors with 17 km/s, while the October chi-Andromedids with 41 km/s and the October beta-Camelopardalids with 44 km/s are significant faster.

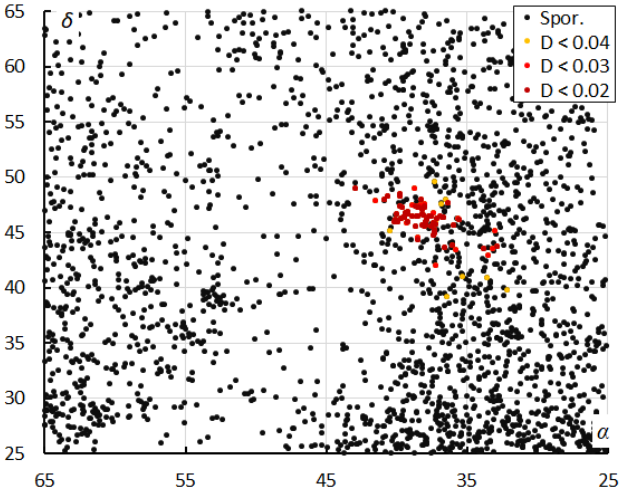

Figure 8 – The radiant distribution during the solar-longitude interval 193° – 201° in equatorial coordinates, color-coded for different threshold values of the D_D orbit similarity criterion.

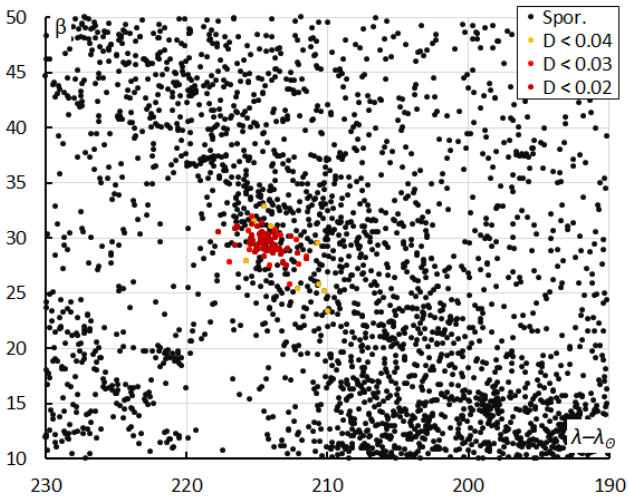

Figure 9 – The radiant distribution during the solar-longitude interval 193° – 201° in Sun-centered geocentric ecliptic coordinates, color-coded for different threshold values of the D_D orbit similarity criterion.

The 62-Andromedid radiant appears as a distinct concentration in both coordinate systems (*Figures 8 and 9*). Counting the numbers of 62-Andromedid meteors and the total number of meteors per degree in Solar Longitude in steps of 0.25 degree, enables expression of the 62-Andromedid activity as a percentage of the total activity. Despite the very low activity level of 4 permille at best, an acceptable activity profile emerges with best rates around $\lambda_\odot = 197.0°$ (*Figure 10*).

Seventy-three 62-Andromedids were identified in common by both methods, with three found by the radiant identification method but not confirmed by the orbit method and three that were identified by the orbit identification but not detected by the radiant method. Both methods produce the same results.

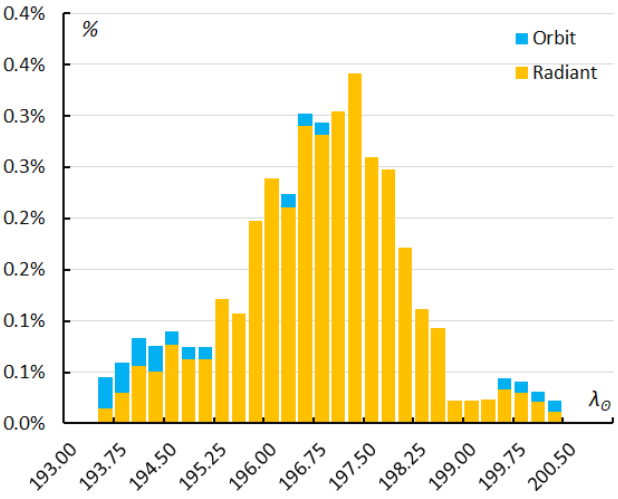

Figure 10 – The percentage of SAN-meteors relative to the total number of meteors. Orange is the result for the radiant shower classification, blue for the orbit classification method.

4 Orbit and parent body

The only previously known record for the 62-Andromedids orbit has been obtained by CAMS (Jenniskens, 2023) and

the orbital parameters are in excellent agreement with the GMN results (*Table 1*).

Table 1 – Two solutions for the 62-Andromedids derived by two different methods, radiant based method and orbit based menthod for $D_D < 0.03$, both compared to Jenniskens (2023) and 1998 ST_{27}[34].

	Radiant method	Orbit method	CAMS	1998 ST_{27}
$\lambda_\odot$ (°)	197.0	197.0	196.5	–
$\lambda_{\odot b}$ (°)	193.9	193.9	190	–
$\lambda_{\odot e}$ (°)	199.9	199.9	200	–
α_g (°)	38.2	38.1	37.9	–
δ_g (°)	+46.3	+46.3	+46.3	–
$\Delta\alpha_g$ (°)	+1.23	+1.11	+1.18	–
$\Delta\delta_g$ (°)	+0.61	+0.64	+0.28	–
v_g (km/s)	17.0	17.0	16.9	–
H_b (km)	87.0	87.0	–	–
H_e (km)	72.2	72.2	–	–
H_p (km)	78.5	78.5	–	–
Mag_{Ap}	+0.7	+0.6	–	–
λ_g (°)	51.37	51.4	51.1	–
$\lambda_g - \lambda_\odot$ (°)	214.37	214.4	214.6	–
β_g (°)	+29.61	+29.6	+29.6	–
a (A.U.)	0.819	0.818	0.82	0.8194
q (A.U.)	0.394	0.393	0.395	0.386
e	0.519	0.520	0.518	0.5299
i (°)	21.3	21.3	20.9	21.06
ω (°)	320.5	320.6	320.7	322.49
Ω (°)	196.9	196.8	196.5	197.53
Π (°)	157.4	157.4	157.6	160.02
T_j	6.99	6.99	6.99	6.98
N	76	76	79	–

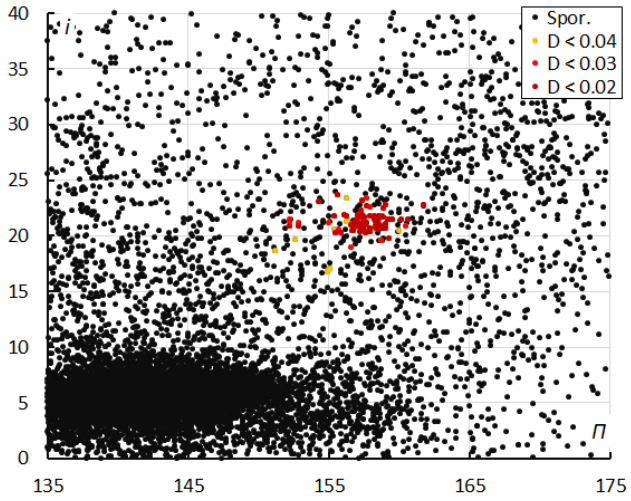

Figure 11 – The diagram of the inclination i versus the longitude of perihelion Π color-coded for different classes of D-criteria thresholds, for $\lambda_\odot$ between 193° and 201°.

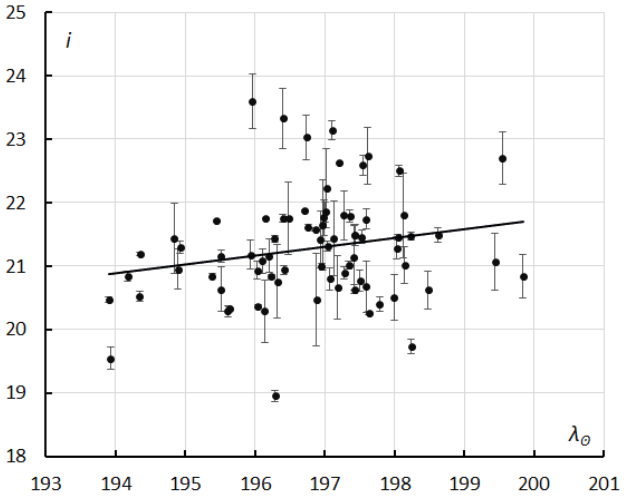

Figure 12 – The evolution of the inclination i in function of the solar longitude $\lambda_\odot$ for the 62-Andromedids 2019–2025.

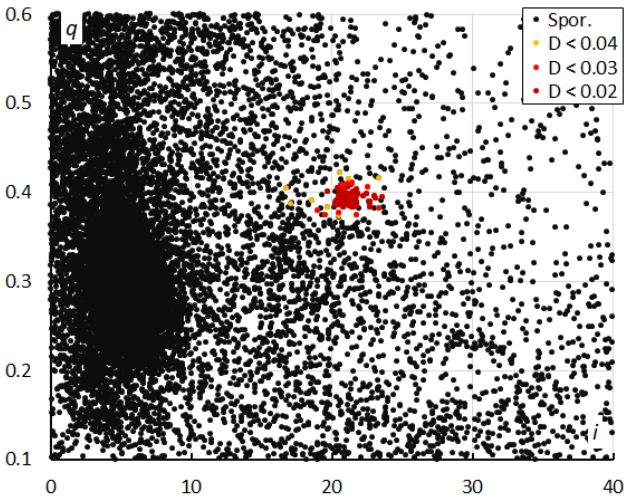

Figure 13 – The diagram of the perihelion distance q versus the inclination i color-coded for different classes of D-criteria thresholds, for $\lambda_\odot$ between 193° and 201°.

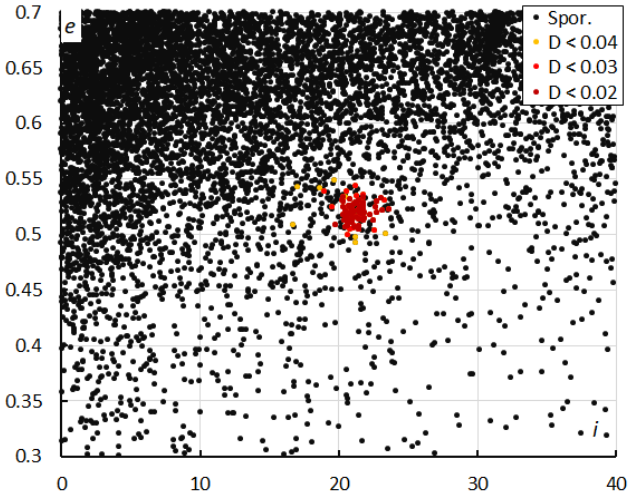

Figure 14 – The diagram of the eccentricity e versus the inclination i color-coded for different classes of D-criteria thresholds, for $\lambda_\odot$ between 193° and 201°.

The diagram of inclination versus longitude of perihelion (*Figure 11*) shows a clear concentration of 62-Andromedid

[34] https://www.spacereference.org/asteroid/363027-1998-st27

orbits in inclination and longitude of perihelion. The large dense concentration at the bottom left are mainly Southern Taurids (STA#2) and some other ecliptic meteoroid streams. The inclination *i* displays a slight trend to increase during the activity period (*Figure 12*). All the other Kepler elements remain constant during the activity.

The diagram with perihelion distance *q* versus inclination *i* shows a very strong concentration of 62-Andromedid orbits (*Figure 13*). This diagram also shows several other concentrations caused by other meteoroid streams. In the diagram with the eccentricity *e* versus the inclination *i* (*Figure 14*), the 62-Andromedids appear as very dense cluster at the edge of what appears like a very densely populated distribution with several meteoroid streams and sporadics with the 62-Andromedids as a border case.

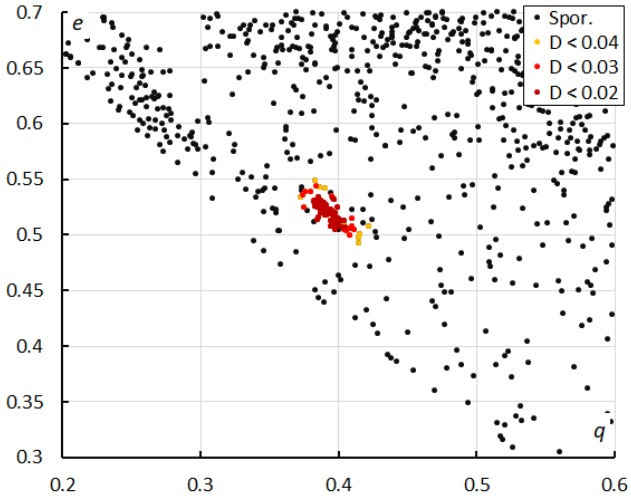

Figure 15 – The diagram of the eccentricity *e* versus the perihelion distance *q* color-coded for different classes of D-criteria thresholds, for $\lambda_\odot$ between 193° and 201°.

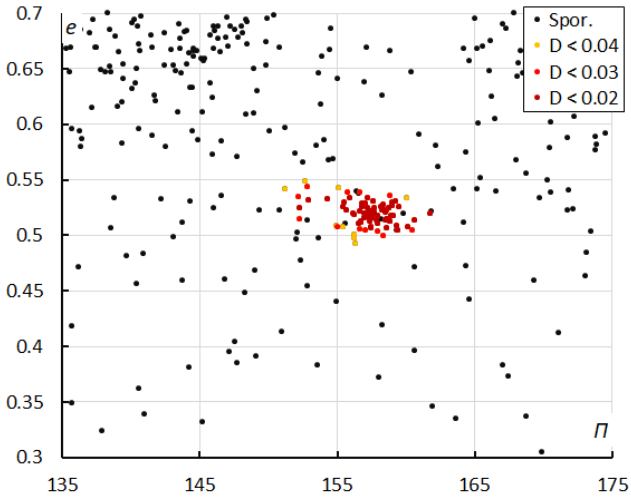

Figure 16 – The diagram of the eccentricity *e* versus the longitude of perihelion *Π* color-coded for different classes of D-criteria thresholds, for $\lambda_\odot$ between 193° and 201°.

The distribution of the eccentricity *e* versus the perihelion distance *q* shows the cluster of 62-Andromedid orbits close to the limit beyond which meteoroids cannot encounter Earth, the white space in *Figure 15*. The distribution eccentricity *e* versus longitude of perihelion *Π* also reveals the shower as a dense cluster within a sparsely scattered distribution (*Figure 16*).

The 62-Andromedids cross the ecliptic at their descending node (☋) at the Earth orbit (*Figure 17*). The orbit is among the shortest in period among known meteoroid streams. A search for possible parent bodies has one positive match that is most likely the parent body for this shower, (363027) 1998 ST_{27} with $D_D = 0.016$ (*Table 2*). Jenniskens (2023) also associated this shower with this parent object. 1998 ST_{27} was discovered by LINEAR in September, 1998, and has a diameter of 0.58±0.23 km. It is a triple system and the largest satellite has a diameter of about 100 meters and a period of more than seven days around the main object. Goldstone radar imaging has revealed a second satellite having less than 50m in diameter. 1998 ST_{27} is an Aten-class object with an orbital period of 0.74 years. The perihelion distance is a relatively low with 0.385 AU. 1998 ST_{27} made a flyby near Earth in 2024 which was the closest since 1958 and for more than 500 years into the future. The Minor Planet Center has designated this object as a Potentially Hazardous Asteroid.[35]. A triple system may indicate that more small fragments remain undetected and that we are dealing with a breaking up body that produced a meteoroid stream. 1998 ST_{27} is a very dark object with an albedo of only 0.059±0.066 according to NASA's NEOWISE mission. The spectral data, combined with a low albedo, suggest the surface composition is most consistent with CM2 or CI1-type carbonaceous chondrites (Abell et al., 2006). Obtaining spectra from 62-Andromedids may confirm the relationship but is a challenge seen the low activity level of this meteor shower. The Tisserand value relative to Jupiter with $T_J = 6.99$ indicates an asteroid type orbit but does not exclude a Jupiter-family comet origin.

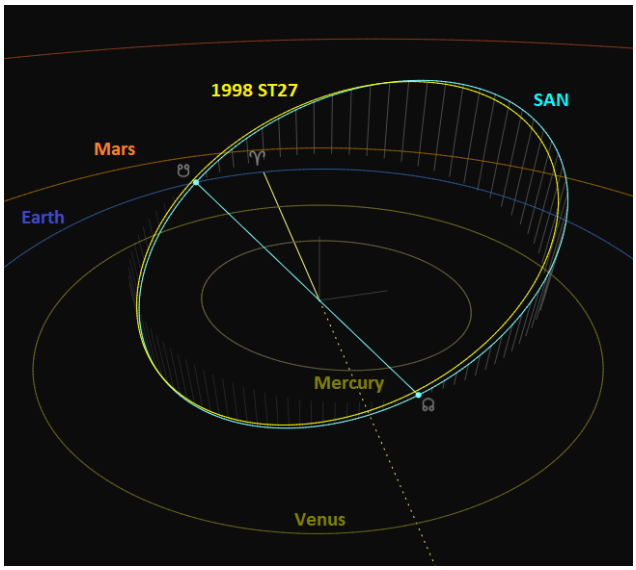

Figure 17 – Comparing the GMN solutions (blue) for the 62-Andromedids with the orbit of the most likely parent body 1998 ST_{27} (yellow), close-up at the inner Solar System. (Plotted with the Orbit visualization app provided by Pető Zsolt).

[35] https://echo.jpl.nasa.gov/asteroids/oct2024.goldstone.planning.html

Table 2 – Top ten matches of a search for possible parent bodies with $D_D < 0.12$.

Name	D_D
(363027) 1998 ST_{27}	0.016
(337248) 2000 RH_{60}	0.077
2019 TL_6	0.092
2016 VA	0.096
2014 QE_{365}	0.101
2009 UM_1	0.107
(614134) 2008 TC_4	0.11
2019 PM_2	0.112
2017 TG_5	0.112
(475534) 2006 TS_7	0.113

The 62-Andromedids penetrate very deep into the atmosphere before ablating with a beginning height of 87 km and an ending height of 72 km. The particles in this meteoroid stream are most of the time exposed to thermal stresses while moving far within the Earth and the Venus orbits. This exposure is very destructive for fragile cometary material, nevertheless, Jenniskens derived a fragile meteoroid density from CAMS data (Jenniskens, 2023). The nature of these meteoroids and the decisive association with the likely parent body may be obtained from spectral meteor observations.

5 Conclusion

The confirmation of the existence of the 62-Adromedids (SAN#924) by GMN data from 2019–2025 with an independent solution reported to the IAU-MDC, fulfils the criteria[36] to be nominated for established status. The GMN solution has been double checked by using two independent shower identification methods as a two-factor authentication for the validation of the analyses.

We confirm the earlier suggestion by Jenniskens et al. (2018) these meteoroids are derived from the Aten-class object (363027) 1998 ST_{27}.

Acknowledgments

This report is based on the data of the Global Meteor Network (Vida et al., 2020a; 2020b; 2021) which is released under the CC BY 4.0 license[37]. We thank all 927 participants in the Global Meteor Network project for their contribution and perseverance. A list with the names of the volunteers who contribute to GMN has been published in the 2025 annual report (Roggemans et al., 2026). The following 186 cameras recorded 62-Andromedids that have been used in this study:

AU0006, AU000D, AU0028, AU002A, AU002B, AU0030, AU003J, BE0001, BE0003, BE0004, BE0005, BE0006, BE0007, BE0008, BE000A, BE000B, BE000C, BE000D, BE000E, BE000G, CA000D, CA000E, CA000P, CA0022, CA0026, CA002F, CH0002, CH0003, CH0005, CZ0002, CZ000F, DE0005, DE0006, DE0008, DE000B, DE000X, ES0007, ES0008, ES000D, ES000F, ES000H, ES000K, ES000N, ES000T, ES000W, ES000Z, ES0019, FR0008, FR000A, FR000X, FR000Z, FR0012, FR0014, HR0001, HR0006, HR000M, HR000Q, HR000S, HR000V, HR001A, HR0024, HR002E, HU0001, HU0002, IT0001, KR000B, KR000F, KR000P, KR000S, KR0011, KR001G, KR001H, KR0024, KR002U, KR002W, KR003G, KR003H, NL0002, NL000K, NL000M, NZ0018, NZ0022, NZ0023, NZ002B, NZ002X, SI0001, SI0005, UK000D, UK000F, UK000H, UK000P, UK000U, UK001L, UK001P, UK001T, UK0025, UK0026, UK002J, UK002K, UK002X, UK0030, UK0031, UK003U, UK0045, UK004D, UK004N, UK0050, UK005S, UK0067, UK006C, UK006S, UK007E, UK007G, UK007N, UK007V, UK0080, UK0082, UK0083, UK0085, UK0086, UK0087, UK0089, UK008W, UK008X, UK0090, UK0098, UK0099, UK009A, UK009V, UK00A5, UK00AB, UK00AE, UK00AK, UK00B2, UK00BQ, US0001, US0003, US0005, US0006, US0007, US0008, US000A, US000C, US000E, US000G, US000H, US000J, US000K, US000L, US000M, US000N, US000P, US0038, US003G, US003N, US003P, US004B, US004C, US004P, US005Q, USL001, USL002, USL003, USL004, USL005, USL007, USL008, USL009, USL00A, USL00B, USL00C, USL00D, USL00E, USL00F, USL00G, USL00H, USL00J, USL00K, USL00M, USL00P, USL00Q, USL00V, USL014, USL017, USL01A and USL01D.

References

Abell P. A., Gaffey M. J., Hardersen P. S., Reddy V., Kumar S. (2006). "Compositions of binary near-Earth objects: implications for their internal structure". *Spacecraft Reconnaissance of Asteroid and Comet Interiors*. 3024.pdf.

Drummond J. D. (1981). "A test of comet and meteor shower associations". *Icarus*, **45**, 545–553.

Jenniskens P., Baggaley J., Crumpton I., Aldous P., Pokorny P., Janches D., Gural P. S., Samuels D., Albers J., Howell A., Johannink C., Breukers M., Odeh M., Moskovitz N., Collison J., Ganju S. (2018). "A survey of southern hemisphere meteor showers". *Planetary and Space Science*, **154**, 21–29.

Jenniskens P. (2023). Atlas of Earth's meteor showers. Elsevier, Cambridge, United states. ISBN 978-0443-23577-1. Page 203.

Jopek T. J. (1993). "Remarks on the meteor orbital similarity D-criterion". *Icarus*, **106**, 603–607.

Jopek T. J., Rudawska R. and Pretka-Ziomek H. (2006). "Calculation of the mean orbit of a meteoroid

[36] https://www.ta3.sk/IAUC22DB/MDC2022/Dokumenty/shower_nomenclature.php

[37] https://creativecommons.org/licenses/by/4.0/

stream". *Monthly Notices of the Royal Astronomical Society*, **371**, 1367–1372.

Moorhead A. V., Clements T. D., Vida D. (2020). "Realistic gravitational focusing of meteoroid streams". *Monthly Notices of the Royal Astronomical Society*, **494**, 2982–2994.

Roggemans P. (2026). "Eccentrids in the GMN orbit dataset". *eMetN Meteor Journal*, **11**, 60–62.

Roggemans P., Vida D., Šegon D., Scott J.M. (2026). "Meteoroid orbit shower identification". *eMetN Meteor Journal*, **11**, to be published.

Roggemans P., Campbell-Burns P., Kalina M., McIntyre M., Scott J. M., Šegon D., Vida D. (2026). "Global Meteor Network report 2025". *eMetN Meteor Journal*, **11**, 89–129.

Southworth R. B. and Hawkins G. S. (1963). "Statistics of meteor streams". *Smithsonian Contributions to Astrophysics*, **7**, 261–285.

Terentjeva A., Bakanas E. (2026). "The Eccentrids of the Mars family in the minor bodies system". *eMetN Meteor Journal*, **11**, 56–59.

Vida D., Gural P., Brown P., Campbell-Brown M., Wiegert P. (2020a). "Estimating trajectories of meteors: an observational Monte Carlo approach - I. Theory". *Monthly Notices of the Royal Astronomical Society*, **491**, 2688–2705.

Vida D., Gural P., Brown P., Campbell-Brown M., Wiegert P. (2020b). "Estimating trajectories of meteors: an observational Monte Carlo approach - II. Results". *Monthly Notices of the Royal Astronomical Society*, **491**, 3996–4011.

Vida D., Šegon D., Gural P. S., Brown P. G., McIntyre M. J. M., Dijkema T. J., Pavletić L., Kukić P., Mazur M. J., Eschman P., Roggemans P., Merlak A., Zubrović D. (2021). "The Global Meteor Network – Methodology and first results". *Monthly Notices of the Royal Astronomical Society*, **506**, 5046–5074.

Proposed changes to the IAU-MDC Working List

John Greaves

A selection of published meteor shower candidates is tested against the Global Meteor Network's database for orbits only for dates subsequent to their publication date and resulting failed candidates highlighted. Candidates still viably part of the Working List are also noted.

1 Introduction

Suggested showers based on the publicly available optical multi-station meteor orbit databases of the time that have been published in Greaves (2020a; 2020b; 2022a; 2022b; 2022c; 2022d; 2024) are examined against the Global Meteor Network (GMN) database e.g. Vida et al. (2021) for dates subsequent to the dates of publication for those papers.

This analysis solely used the GMN database it being the only publicly available dataset for optical multi-station derived orbital data which is both global, thus covering most longitudes and thus night time zones' coverage, and having predominantly homogeneous equipment and processing methodologies.

2 Methodology

The showers tested here as listed (at the time of writing the Dec 11th 2025 updated version) in the current Working List of the International Astronomical Union Meteor Data Centre (IAU-MDC e.g. Neslusan et al. (2020) are, in order of publication date, 42-Draconids (FTD, 1041) (Greaves, 2020a), May ε-Draconids (MED, 1037), 69-Draconids (SND, 1038), 45-Draconids (FFD, 1039) and September ψ^1-Draconids (SPD, 1040) (Greaves, 2020b), M2022-Q2 (Greaves, 2022a). Published showers that are fully analyzed but not drafted into the IAU MDC lists include the 41-Arietids, 59-Arietids (Greaves, 2022b), a potential shower in Lepus associated with C/2022 R2 Atlas subsequent to its apparition (Greaves, 2022c) and a potential shower associated with 501P Rankin = P/2024 L4 Rankin dubbed the α-Canis Minorids (Greaves, 2024). The comet 197P LINEAR's proposed association with the May ι-Draconids (MID, 755) is also reassessed (Greaves, 2022d) and references therein.

The published orbital meteor shower data are tested one by one against the subsets of post-publication GMN data using the Jopek (1993) version of the D criterion with a stricter than usual upper cutoff threshold of $D_J = 0.080$. The resultant matches are assessed based simply upon the number per shower. Shower candidates that are not viable are listed in *Table 1*. Shower candidates that are borderline, neither confirmed due to insufficient number of meteoroid orbits per shower nor having sufficiently low enough number of meteoroid orbits per shower to reject them are listed in *Table 2* and can likely remain in the Working List pending further data in years to come.

3 Results

Table 1 – Candidate showers from the IAU-MDC Working List and elsewhere needing full rejection or ignoring.

Shower	Orbits
SND, 1038	15
FFD, 1039	23
SPD, 1040	22
M2022-Q2	21
C/2022 R2	5

Table 2 – Candidate showers from the IAU-MDC Working List that can remain or be added thereto.

Shower	Orbits	Note
MED, 1037	68	1
FTD, 1041	70	2
41-Arietids	70	3
59-Arietids	68	3
α-CMi	58	3,4,5

Notes:

1) Associated with near Earth asteroid 1999 LT1.
2) Associated with Near Earth asteroid 2018 LF5.
3) Not currently listed in the IAU-MDC shower lists.
4) Associated with comet 501P Rankin = P/2024 L4 Rankin.
5) Although the number of matched orbits is not large the post-publication data for this candidate shower only amounts to one year's worth, namely 2025.

Periodic comet 197P LINEAR and the shower MID (755) are also tested, both separately and with their respective output matched orbits against each other, remembering that only GMN data and a D_J threshold limit of 0.08 are used. It should be noted that perturbations due to Jupiter during this comet's aphelion can cause the perihelion distance to occasionally shift slightly taking perihelion farther away then nearer to Earth's orbit over time, potentially making meteoroids likely less available after some past and future perihelion passages of the comet.

Table 3 – Number of orbits matching 197P LINEAR, MID (755) and the number of orbits common to both.

Identify	Orbits
197P LINEAR	87
MID, 755	113
197P and MID	41

4 Conclusion

Candidate meteor showers proposed in the past by the current author are tested using D criterion against GMN meteor orbits observed since their dates of publication. False positive showers in need of being rejected from the IAU-MDC Working List, and one not included in said and not needing to be included, are noted.

Showers still not confirmed by newer data but with sufficient number of meteor orbit matches to still be possible showers and thus suitable for remaining in the IAU-MDC Working List are also noted, as well as three published showers never listed in the Working List that need to be added to it due to their potential viability, which may lead to them being confirmed after several years more data.

Periodic comet 197P LINEAR is also tentatively affirmed as a source of meteors with their mutual D_J testing giving orbits common to both it and the May ι-Draconids of Segon et al. (2015).

Acknowledgment

The public meteor orbit data used herein to test the above published meteor shower orbits is made available by the Global Meteor Network under CC BY 4.0 license. Gratitude is extended for not only the availability but also the ease of access of these data.

References

Greaves J. (2020a). “Meteors and 2018 LF5”. *eMetN Meteor Journal*, **5**, 290–294.

Greaves J. (2020b). “Some Near Earth Objects and meteor associations”. *eMetN Meteor Journal*, **5**, 295–299.

Greaves J. (2022a). “A potential new summer shower in Lacerta”. *eMetN Meteor Journal*, **7**, 195–198.

Greaves J. (2022b). “Three showers in Aries, two new and one known, or just one?”. *eMetN Meteor Journal*, **7**, 246–249.

Greaves J. (2022c). “Will C/2022 R2 Atlas lead to meteors leaping from Lepus in late November?”. *eMetN Meteor Journal*, **7**, 379–380.

Greaves J. (2022d). “Discovery of a shower associated with comet 197P/LINEAR in UKMON Meteor Orbit Data”. *eMetN Meteor Journal*, **7**, 188–194.

Greaves J. (2024). “A note on meteor association with the orbit of P/2024 L4 Rankin”. *eMetN Meteor Journal*, **9**, 288–290.

Jopek T. J. (1993). “Remarks on the meteor orbital similarity D-criterion”. *Icarus*, **106**, 603–607.

Neslušan L., Poručan V., Svoreň J., Jakubík M. (2020). “On the new design of the IAU MDC portal”. *Journal of the International Meteor Organization*, **48**, 168–169.

Šegon D., Gural P., Andreic Ž., Vida D., Skokić I., Novoselnik F. (2015). “Four possible new high-declination showers”. *Journal of the International Meteor Organization*, **43**, 147–150.

Vida D., Šegon D., Gural P. S., Brown P. G., McIntyre M. J. M., Dijkema T. J., Pavletić L., Kukić P., Mazur M. J., Eschman P., Roggemans P., Merlak A., Zubrović D. (2021). “The Global Meteor Network – Methodology and first results”. *Monthly Notices of the Royal Astronomical Society*, **506**, 5046–5074.

Independent confirmation of meteor shower candidates from the Southern Argentine Agile Meteor Radar

John Greaves

Radar meteor showers published in 2017 using data from the Southern Argentine Agile Meteor Radar are reassessed using publicly available data from the same source for the years 2020 to 2023.

1 Introduction

Suggested showers derived using data sourced from the Southern Argentine Agile Meteor Radar (SAAMER), e.g. Janches (2000), before 2017 were published in Pokorný (2017). These are reassessed here via the Jopek (1993) variation of the dissimilarity criterion, D_J, in a temporally independent manner such that SAAMER data is still used but the data are from January 2020 to October 2023, as sourced from the holdings of the 2025 version of the International Astronomical Union Meteor Data Centre (IAU-MDC) database server (Neslušan, 2020).

2 Methodology

The SAAMER radar meteor orbits from 2020 to 2023 were tested against the Pokorný (2017) showers using $D_J < 0.08$. The published suggested upper threshold value for D_J is 0.105 but 0.080 was used here to remove as many outliers as possible, as the smaller the value the better the confirmation. The 2020 to 2023 SAAMER dataset contains just over 11 million radar meteor orbits covering most of four years so only the top three well matching results with large numbers of matches and relatively small standard deviation (such that the value of the standard deviation was < 1% of 360° for Right Ascension, Declination and Solar Longitude) were selected for confirmation.

New mean, median, standard deviation and modal values were then calculated from the newer 2020 to 2023 SAAMER data matches as well as the maximum and minimum range values for each of Right Ascension, Declination, Solar Longitude, Perihelion Distance, orbital eccentricity, orbital Inclination, Argument of Perihelion and Longitude of the Ascending Node.

Each shower then had all the SAAMER 2020 to 2023 radar meteors selected in two dimensions with regions of Right Ascension and Declination ranging ±30° for both axes centered upon the approximate mean radiant position, and for one shower also included the mean Solar Longitude for three dimensions used for illustrative purposes. The showers chosen as suitable for confirmation are also checked against optical meteor orbits.

3 Results

The three confirmed showers, all with $D_J < 0.08$, are the January μ-Velids (JMV, 789), the κ-Velids (KVE, 784) and the ψ-Phoenicids (PPH, 769) with 416, 500 and 899 radar meteor matches respectively. Their particulars are given in *Tables 1, 2 and 3* respectively.

Figures 1, 2 and 3 respectively give plots for regions of sky ranging from around 30° either side of the mean radiant given for the January μ-Velids, the κ-Velids and the ψ-Phoenicids respectively, illustrating the density of the detected meteors relative to the background sporadic population at the time. Note that the January μ-Velids and the κ-Velids lie spatially adjacent upon the sky and are also relatively close to each other in time but have quite distinct orbital elements. *Figure 4* shows a three-dimension plot for the ψ-Phoenicids, including the Solar Longitude, for illustrative purposes in order to affirm the compact nature of this shower relative to the background radar meteors with each axis ranging 30° either side of the three axes centers. Unfortunately, there were insufficient shower meteors for the other two radiants for the plots to work for those, it not being an ideal image even for the larger number of meteors found for the ψ-Phoenicids.

Table 1 – Radiant and orbital element details for the January μ-Velids.

	α (°)	δ (°)	$\lambda_\odot$ (°)	q (A.U.)	e	i (°)	ω (°)	Ω (°)
mean	165.48	–51	287.194	0.78	0.118	72.97	170.23	106.9
median	165.41	–50.94	287.02	0.782	0.117	72.96	170.2	106.73
σ	2.45	1.21	1.995	0.036	0.023	1.72	13.56	2
mode	165.08	–50.62	289.492	0.782	0.126	73.52	168.75	103.3
max	171.31	–47.71	291.416	0.861	0.168	76.75	203.65	111.11
min	159.87	–54.56	282.88	0.702	0.067	68.89	135.44	102.6

Table 2 – Radiant and orbital element details for the κ-Velids.

	α (°)	δ (°)	$\lambda\odot$ (°)	q (A.U.)	e	i (°)	ω (°)	Ω (°)
mean	140.8	-50.77	276.077	0.963	0.531	72.98	19.63	95.77
median	140.78	-50.75	276.004	0.963	0.53	72.92	19.84	95.7
σ	2.39	1.39	1.716	0.007	0.031	1.93	3.58	1.72
mode	139.73	-50.29	278.777	0.963	0.519	74.12	23.27	96.79
max	146.63	-47.91	280.285	0.977	0.612	77.3	27.06	100.01
min	135.33	-54.42	272.079	0.946	0.46	68.67	10.88	91.77

Table 3 – Radiant and orbital element details for the ψ-Phoenicids.

	α (°)	δ (°)	$\lambda\odot$ (°)	q (A.U.)	e	i (°)	ω (°)	Ω (°)
mean	29.92	-47.16	111.368	0.888	0.295	74.48	63.65	291.06
median	29.91	-47.25	111.297	0.888	0.294	74.38	63.67	290.99
σ	2.25	1.35	1.818	0.022	0.032	1.69	5.7	1.82
mode	29.76	-48.02	109.633	0.896	0.284	73.74	56.23	290.73
max	35.82	-43.63	115.66	0.941	0.364	79.08	77.97	295.34
min	24.14	-50.4	106.969	0.834	0.222	70.5	49.18	286.64

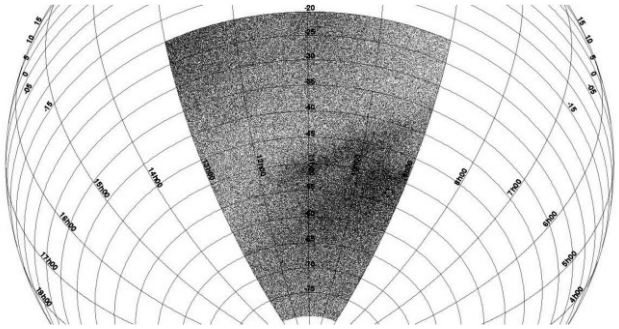

Figure 1 – Individual meteor radiants are plotted for ±30° of Right Ascension and Declination from the mean radiant position of the January μ-Velids, note the κ-Velids can also be seen, distinct and discrete to them, to the lower right.

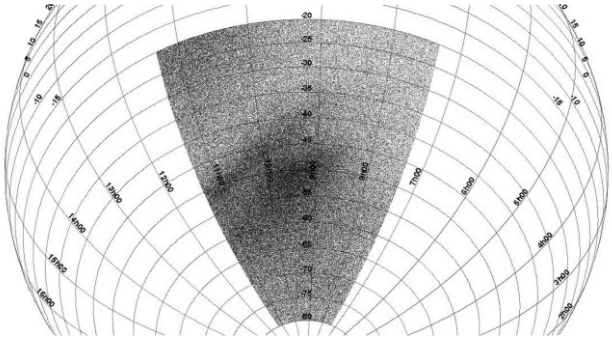

Figure 2 – Individual meteor radiants are plotted for ±30° of Right Ascension and Declination from the mean radiant position of the κ-Velids, note the January μ-Velids can also be seen, distinct and discrete to them, to the upper left.

Each of the three showers gave as little as one to around half a dozen matches when tested against optical meteor orbit database sources that summed to a total of nearly four million optical meteor orbits dating up to November 2025 inclusive.

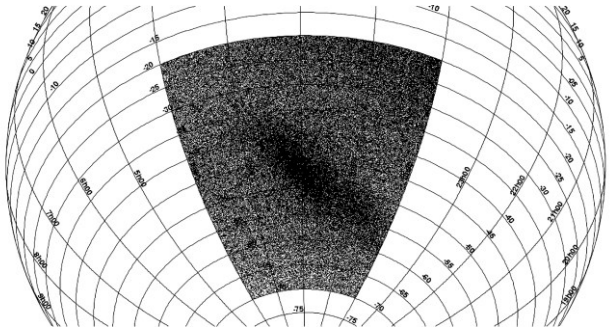

Figure 3 – Individual meteor radiants are plotted for ±30° of Right Ascension and Declination from the mean radiant position of the ψ-Phoenicids.

4 Conclusion

A set of candidate radar meteor showers from prior to 2017 are reassessed against a time independent set of later individual radar meteor orbit data generated by the same observatory for 2020 to 2023 using dissimilar orbit criterion.

Three showers are found to have a good number of well-matched radar meteor orbits from a source of 11 million whilst incredibly low number matches occurred if tested against optical meteor orbits amounting to nearly four million. They are therefore effectively radar meteor showers with no optical expression.

The showers January μ-Velids (JMV, 789), κ-Velids (KVE, 784) and ψ-Phoenicids (PPH, 769) are suitable for promotion from the IAU MDC Working List (Neslušan, 2020) and upgraded as Established List showers.

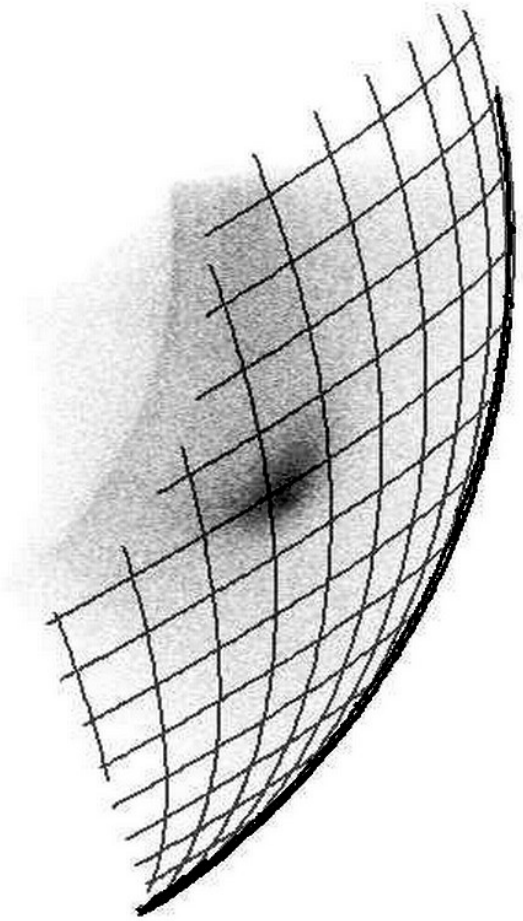

Figure 4 – Individual meteor radiants are plotted for ±30° of Right Ascension, Declination and Solar Longitude from the mean radiant position and date of the ψ-Phoenicids

Acknowledgment

TOPCAT[38] was used for figure generation.

References

Janches D., Bruzzone J. S., Weryk R. J., Hormaechea J. L., Wiegert P., Brunini C. (2020). "Observations of an Unexpected Meteor Shower Outburst at High Ecliptic Southern Latitude and Its Potential Origin". *The Astrophysical Journal*, **895**, L25.

Jopek T. J. (1993). "Remarks on the meteor orbital similarity D-criterion". *Icarus*, **106**, 603–607.

Neslušan L., Poručan V., Svoreň J., Jakubík M. (2020). "On the new design of the IAU MDC portal". *Journal of the International Meteor Organization*, **48**, 168–169.

Pokorný P., Janches D., Brown P. G., Hormaechea J. L. (2017). "An orbital meteoroid stream survey using the Southern Argentina Agile MEteor Radar (SAAMER) based on a wavelet approach". *Icarus*, **290**, 162–182.

[38] https://www.star.bris.ac.uk/~mbt/topcat/

A calcium-enriched meteor from Vesta: Spectroscopic and dynamical identification of a Eucrite

Yury Harachka

Minsk, Belarus
astronominsk@gmail.com

On 16 January 2024, the cameras of the Belarusian Meteor Network recorded a meteor spectrum with exceptionally intense calcium emission lines. The calculated Tisserand parameter with respect to Jupiter, $T_j = 3.53 \pm 0.15$, suggests an association with asteroid (4) Vesta. Spectroscopic analysis confirms the meteoroid's affiliation with the HED clan (Howardites–Eucrites–Diogenites), most likely classifying it as a eucrite.

1 Event description

On 16 January 2024 at $22^h57^m31^s$ UTC, a meteor with a peak magnitude of -3^m was recorded by the Belarusian Meteor Network (*Figure 1*). The trajectory was observed over Lithuania from two stations in Belarus, located 300–350 km from the event. The specifications of the cameras used are given in *Table 1*. The camera at the Minsk_24 station captured only a segment of the trajectory without an ending. In contrast, the Derazhnoye_30 station, equipped with a diffraction grating, recorded the complete trajectory of the meteor and obtained its emission spectrum.

This meteor had an average velocity, ignited smoothly, and faded out fairly quickly at the end of its flight. No flashes indicating fragmentation processes were observed. A faint, rapidly disappearing tail was observed in the middle part of the trajectory. *Figure 2* shows individual frames from the video with an interval of 250 ms.

The obtained spectrum is highly anomalous. Detailed analysis indicates that the event was produced by a rare meteoroid with significant calcium enrichment. To date, this spectrum remains unique within the database of the Belarusian Meteor Network, which comprises over 480 meteor spectra collected during approximately four years of observations.

Table 1 – Detailed information about the cameras that recorded the meteor.

Camera ID	Minsk_24	Derazhnoye_30
Type of camera	AHD IMX327 (color)	USB ZWO ASI 290MM mini (mono)
Resolution (pix)	1920×1080	1936×1096
FOV (°)	88.6×49.8	89.6×50.7
fps	30	20
Diffraction grating (lines/mm)	–	1000
Geographical coordinates	53.9384 27.5925	53.6860 26.5162

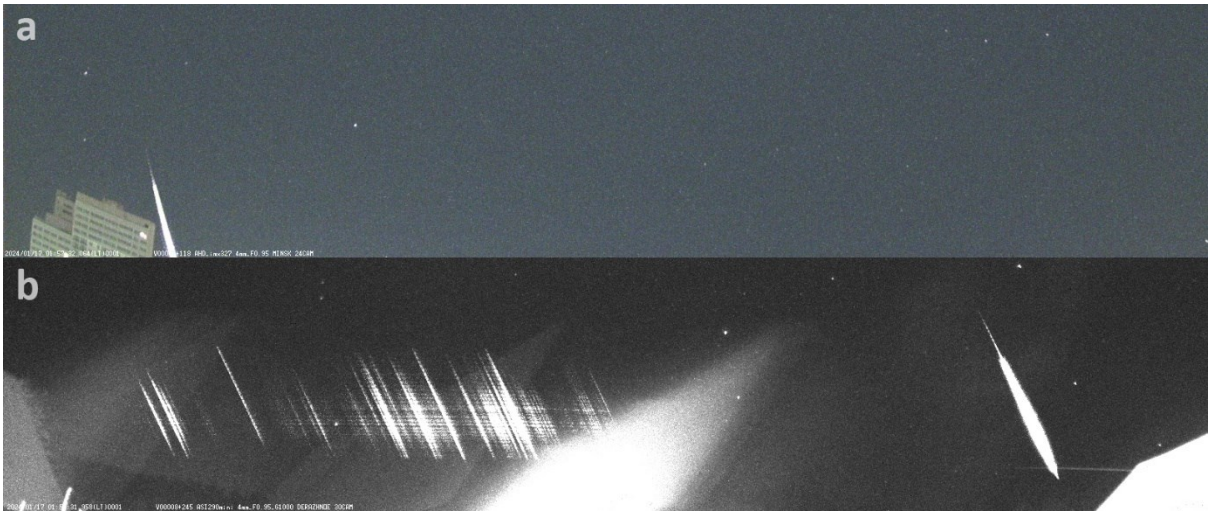

Figure 1 – Images of the meteor captured by the Minsk_24 camera (a) and the Derazhnoye_30 spectral camera (b), which shows the original image with a first-order diffraction spectrum. The spectral image also shows diffraction grating-induced stray light from a bright terrestrial object (illuminated rooftop).

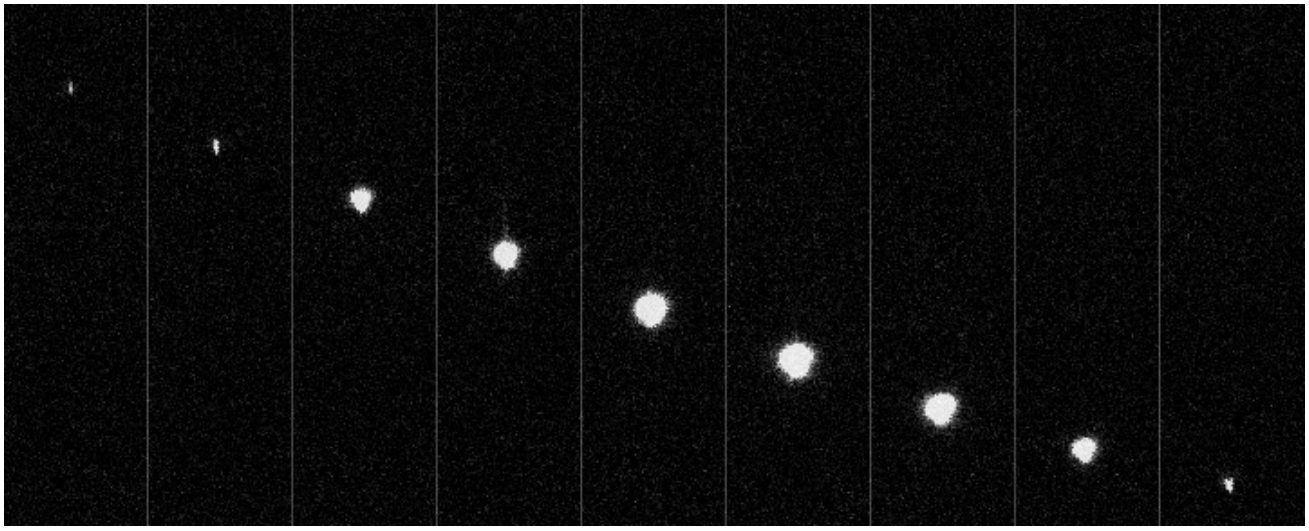

Figure 2 – Individual frames from the Derazhnoye_30 camera show the head of the meteor in motion at intervals of 250 ms.

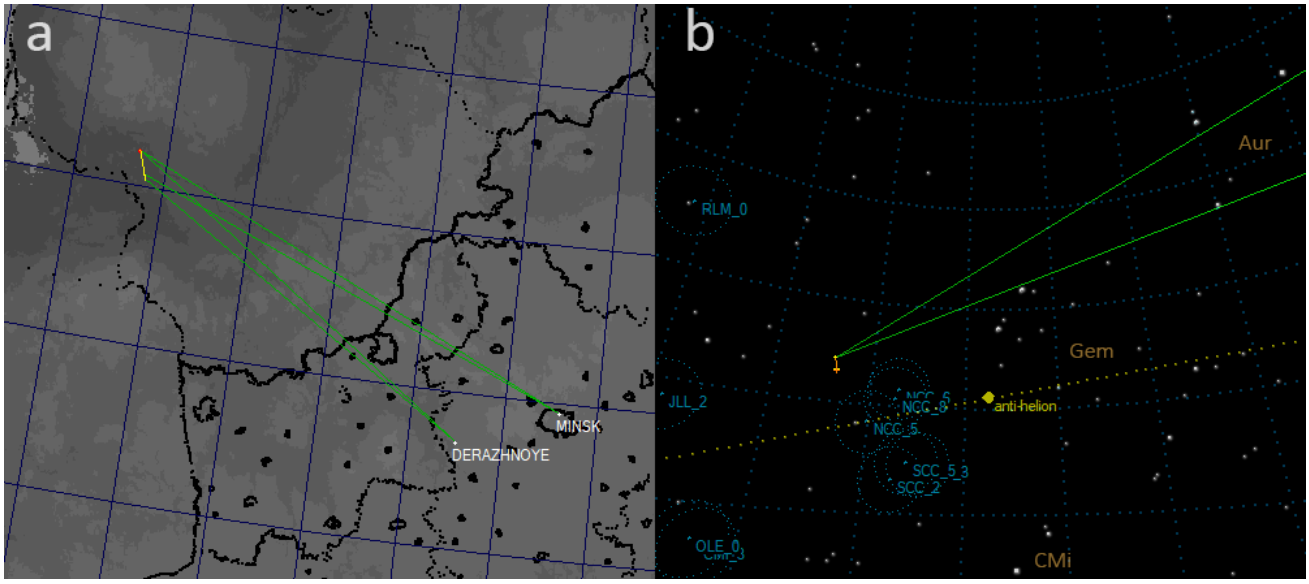

Figure 3 – Stations and meteor trajectory in projection on the Earth's surface (a) and at the celestial sphere (b).

2 Trajectory and Orbit

Video data processing and astrometric measurements were conducted using UFOAnalyzer[39] software. The orbital elements were subsequently calculated with UFOOrbit[1]. Both recording cameras utilize rolling shutters; therefore, to enhance the accuracy of the derived orbital parameters, a correction for the rolling shutter effect was applied during orbit calculation.

The meteor was classified as sporadic, with its radiant situated in the anti-helion source region (*Figure 3*). The meteoroid entered the Earth's atmosphere at an entry angle of 58°. The luminous phase initiated at an altitude of 87.6 km and terminated at 34.3 km, covering a total atmospheric path of 62.7 km over a duration of 2.26 seconds. To minimize the effects of atmospheric drag on the orbital solution, only the initial segment of the trajectory (above 54 km altitude) was used for the calculation of heliocentric orbital elements. The resulting orbital parameters are presented in *Table 2*.

Table 2 – Unified radiant and orbit elements.

Apparent right ascension (°)	134.0 ± 2.4
Apparent declination (°)	24.1 ± 1.6
Pre-atmospheric velocity (km/s)	30.7 ± 1.2
Geocentric right ascension (°)	133.7 ± 2.5
Geocentric declination (°)	23.0 ± 1.7
Geocentric velocity (km/s)	28.5 ± 1.3
Semimajor axis (AU)	1.8240 ± 0.3915
Eccentricity	0.8149 ± 0.0302
Perihelion distance (AU)	0.338 ± 0.033
Inclination (°)	6.46 ± 2.23
Argument of perihelion (°)	297.57 ± 4.88
Longitude of the ascending node (°)	295.98
Tisserand's parameter, Tj	3.53 ± 0.15

[39] SonotaCo, www.sonotaco.com

Analysis of the derived orbital elements reveals that the meteoroid moved on a low-inclination orbit ($i = 6.46°$) with an aphelion situated between the orbits of Mars and Jupiter (*Figure 4*). A key dynamical result is the close match between the Tisserand parameter with respect to Jupiter (T_j) for meteoroid sp205 ($T_j = 3.53306$) and that of asteroid (4) Vesta ($T_j = 3.53394$). This dynamical affinity strongly suggests a genetic link between sp205 and the Vesta family.

This conclusion is robustly supported by the spectral data. Meteorites of the HED clan (howardites, eucrites, diogenites), which are linked to Vesta (McSween et al., 2013), are characteristically enriched in calcium. Consequently, the exceptionally intense calcium emission observed in the spectrum of sp205 provides independent, compositional confirmation of its origin on Vesta and its classification within the HED meteorite clan.

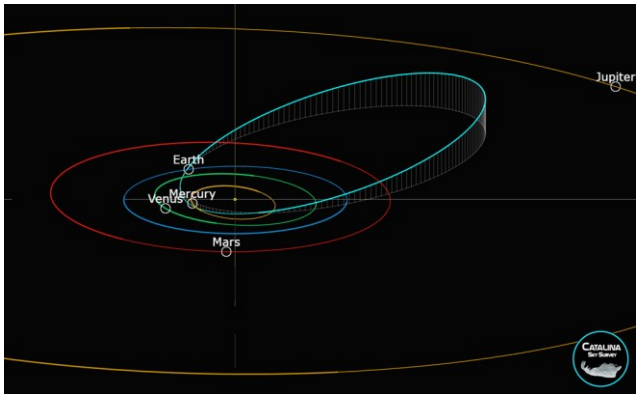

Figure 4 – The plotting of the orbits was made using the CSS Orbit View application[40].

3 Spectrum

Spectral data processing and analysis

The spectral recording from the Derazhnoye_30 station was affected by stray light, an artifact caused by a street lamp reflecting off a snow-covered rooftop. To mitigate its impact, a background subtraction procedure was applied. Frames for the final composite spectrum were stacked using only the initial segment of the meteor's trajectory. This segment was selected based on two criteria: the absence of pixel saturation in the spectral image and the minimal influence of the aforementioned stray light artifact.

The processed spectral image was analyzed using a non-linear calibration method. Calibration, analysis, and line identification were performed with the RSpec software, referencing atomic line data from the NIST database (Ralchenko et al., 2006).

Spectral characteristics of sp205

The resulting spectrum of meteoroid sp205 (*Figure 5*) exhibits both common meteor features and distinct anomalies. It shows standard emission lines from neutral magnesium (Mg I), iron (Fe I), and sodium (Na I), though their relative intensities are notably subdued (as quantified in the following section). The most prominent feature is the exceptionally intense emission from neutral calcium (Ca I).

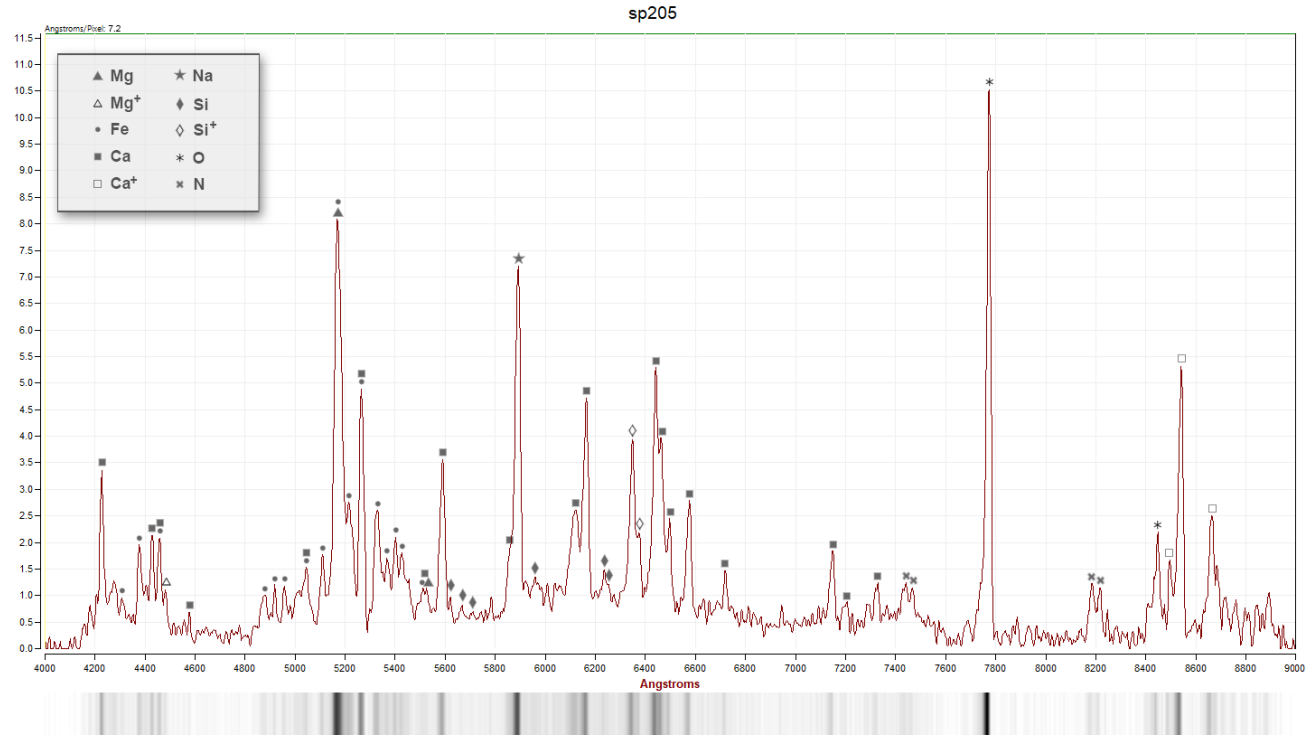

Figure 5 – Calibrated spectral profile of meteoroid sp205 (Derazhnoye_30 station, 16 January 2024). The first-order diffraction spectrum, covering 4000–9000 Å, has been corrected for the instrumental response. Identified emission lines are marked with their corresponding atomic species.

[40] CSS Orbit View, https://neofixer.arizona.edu/css-orbit-view

Prominent spectral features of meteoroid sp205

The most intense calcium emissions are manifested in the following spectral regions:

- The blue region: a distinct line at 4227 Å (Ca I, multiplet 2).
- The yellow-green region (~5590 Å): a bright peak in the 5590 Å region (Ca I – 21), consisting of a series of not resolved Ca I lines.
- The red region (6100–6600 Å): a group of intense peaks (Ca I, multiplets 3, 18, 19, 20).
- The near-infrared region: prominent lines of ionized calcium (Ca II) at 8498 Å, 8542 Å, and 8662 Å.

Additionally, the spectrum exhibits unusually intense lines of ionized silicon (Si II) at 6347 Å and 6371 Å. These lines are typically pronounced only in high-velocity meteors (v > 50 km/s), making their distinct presence in sp205 (v ~ 30 km/s) highly anomalous.

Calcium is a refractory element that rarely produces bright emissions in the visible meteor plasma spectrum. At low spectral resolution, its weak lines often blend with other features. The high-temperature Ca II H and K lines in the near-UV (3934, 3968 Å) were not recorded due to the camera's low sensitivity below 4000 Å. Notably, calcium emission was absent even in recent laboratory simulations of meteorite ablation (Matlovič et al., 2024), underscoring the challenge of its detection in meteor spectra.

Therefore, the exceptional intensity of both neutral and ionized calcium lines in the spectrum of sp205 unambiguously indicates an anomalously high calcium abundance in the meteoroid's composition. This specific geochemical signature is a definitive characteristic of meteorites from the HED clan (howardites, eucrites, diogenites).

4 Method for subgroup classification within the HED clan

To approximately classify the meteoroid within the HED clan (eucrite, howardite, diogenite), a comparative spectral analysis method was employed. The method is based on comparing two ratios:

1. The observed intensity ratio of calcium lines in the sp205 spectrum to that in a reference spectrum of chondritic composition.
2. The known ratio of calcium weight fractions in HED meteorites to that in ordinary chondrites, as measured in laboratory samples.

This comparative approach assumes that the relative spectral line intensity of a major element correlates with its relative abundance in the parent body.

Reference spectrum selection

The spectrum of meteor sp037 (STA, #00002), recorded on 2 November 2022 during the Southern Taurid shower, was used as the chondritic reference. This choice was based on two key criteria:

- Compositional typicality: Southern Taurid meteors are spectroscopically classified as "normal type", corresponding to a typical chondritic composition.

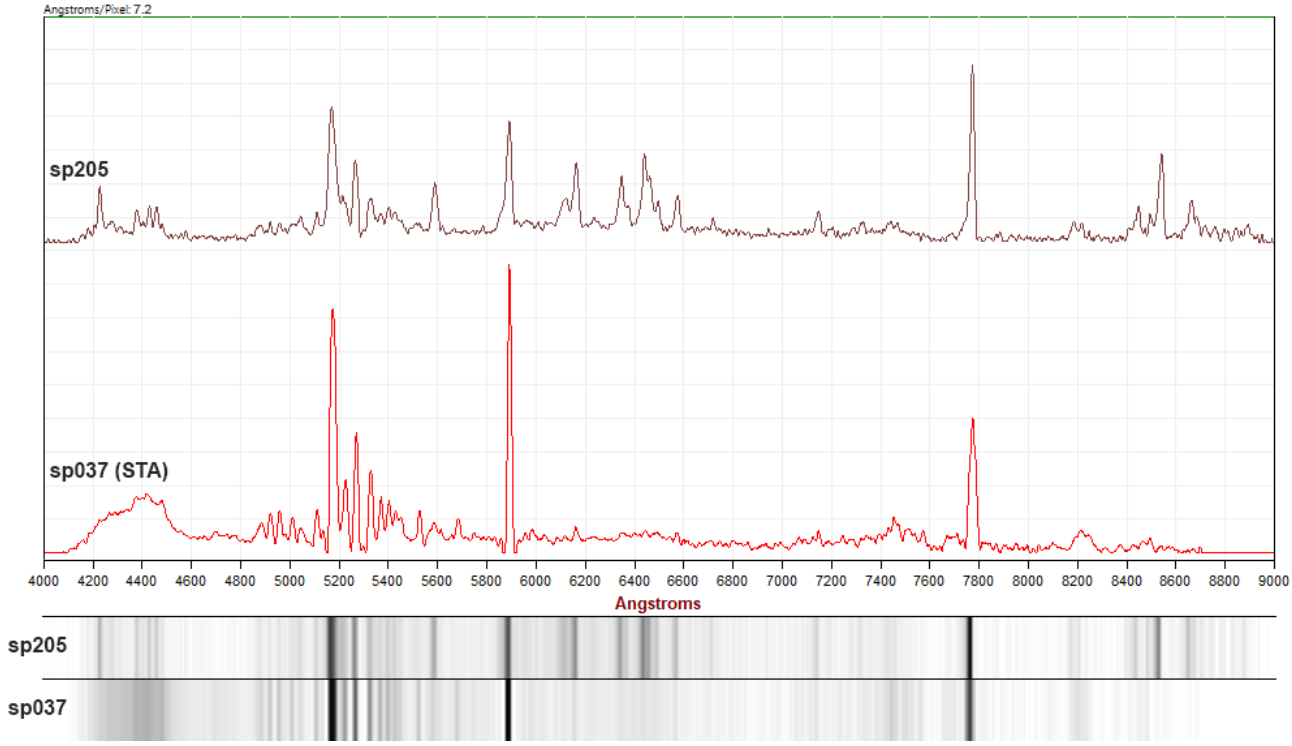

Figure 6 – Comparison of spectra of sp205 and sp037 (STA) in the range 4000–9000 Å. Displayed spectral profiles were corrected for the spectral sensitivity of the camera.

Comparable observational parameters: Meteor sp037 had a similar peak magnitude (~ -3^m) and initial velocity (v_0 = 30.0 km/s) to the studied meteor sp205 (v_0 = 30.7 km/s). Similar velocities help minimize biases related to the excitation conditions of the meteor plasma.

Both spectra are presented for comparison in *Figure 6*.

Methodological assumptions and their justification

The comparative analysis rests on two fundamental simplifications:

1. Spectrum normalization via the oxygen line: The intensity of the neutral oxygen triplet (O I 7774 Å) is primarily a function of meteor velocity (Vojáček et al., 2022). For two meteors with similar velocities and magnitudes, the O I 7774 Å intensities can be considered equivalent. This line was therefore used as an internal standard to normalize the intensity scales of both spectra.

2. Linear abundance-intensity relationship: It is assumed that the intensity of a spectral line is directly proportional to the abundance of its parent element in the meteoroid. This is valid for an optically thin plasma, where self-absorption is negligible. Meteor plasma is typically treated as optically thin, allowing radiation to escape freely.

These assumptions enable a direct comparison between the observed calcium line ratio (sp205 / sp037) and the known calcium abundance ratio (HED meteorites / ordinary chondrites) from laboratory data.

Limitations and caveats

These assumptions are significant simplifications. The intensity of the O I 7774 Å line can be influenced by additional factors, including the meteoroid's bulk composition, density, and the atmospheric parameters at the ablation altitude. Furthermore, even spectra classified as "normal type" (like the Southern Taurid reference) exhibit natural variability in the Mg-Fe-Na ratios, which could introduce noise into the comparison.

Despite these limitations, the method provides a robust first-order approximation. For the purpose of an initial classification of meteoroid sp205 within the HED clan subgroups, the comparative analysis is justified and offers a meaningful assessment of its likely composition.

5 Comparative compositional analysis

Chemical composition data

Data on the bulk chemical composition of ordinary chondrites and HED meteorites were taken from the literature ([1] D'iakonova et al., 1979; [2] Matlovič et al., 2024). These data, presented in *Table 3*, were used to calculate the ratio of element weight percentages (wt%) in HED meteorites relative to their chondritic abundances.

Spectral processing and intensity measurement

The spectra of sp205 and the reference meteor sp037 were corrected for instrumental response and normalized to the intensity of the O I 7774 Å line, which was set to 100 relative intensity units. Following normalization, the integrated intensities of the Ca I, Mg I (multiplet 2), Na I (multiplet 1), and Fe I (multiplet 15) lines were measured in both spectra by calculating the area under each peak above the local continuum. For consistency, only Ca I lines unambiguously present in both spectra were selected for analysis. The results of these measurements are presented in *Table 4*.

Results of the comparative method

The ratios of the measured line intensities (sp205 / sp037) for calcium, sodium, and magnesium are plotted in *Figure 7* alongside the corresponding ratios of their bulk abundances (HED / chondrite) from laboratory data. Iron was excluded from this comparison, as its abundance is similar across HED materials (*Table 3*). While calcium is the primary element of interest, sodium and magnesium were included to validate the methodological assumptions; agreement between spectral and bulk ratios for these elements would support the reliability of the approach for calcium.

Table 3 – Bulk composition of elements in chondrites and HED clan meteorites, wt%.

Meteorite	Type	Ca (wt%)	Mg (wt%)	Na (wt%)	Fe (wt%)	Source
Chondrite (avg)	LL, L, H	1.3	14.49	0.65	23.75	[1]
Stannern	Eucrite	7.61	4.21	0.43	13.93	[2]
Pomozdino	Eucrite	7.64	5.98	0.3	11.4	[1]
–	Eucrite (averaged)	7.625	5.095	0.365	12.665	–
Sariçiçek	Howardite	5.34	9.94	0.255	14.4	[2]
Brient	Howardite	6.13	6.76	0.18	13.28	[1]
Erevan	Howardite	4.86	10.18	0.2	12.08	[1]
–	Howardite (averaged)	5.44	8.96	0.212	13.253	–
Bilanga	Diogenite	0.5	18	0.009	12.2	[2]

Table 4 – Measured peak intensities in the sp205 and sp037 (STA) spectra in relative units. The intensity of the O I 7774 Å line is taken as 100.

Element	Peak, Å	Lines, Å	Multiplets	Intensity (sp205)	Intensity (sp037)
Ca I	4227	4227	2	16.1	1.3
Ca I	4429	4425, 4435	4	8.6	1.5
Mg I	5174	5167, 5173, 5184	2	104.8	184.5
Fe I	5269-5449	5269, 5328, 5371, 5404, 5431, 5449	15	138.4	202
Ca I	5589	5582, 5589, 5590, 5595, 5599, 5601, 5603	21	33.3	5.1
Na I	5892	5890, 5896	1	69.4	134.8
Ca I	6122	6103, 6122	3	26.9	2.9
Ca I	6164	6161, 6162, 6164, 6166, 6169, 6170	3, 20	42.7	8.2
Ca I	6439-6472	6439,6450, 6456, 6463, 6472	18, 19	69.5	2.8
Ca I	6496	6494, 6500	18	11.4	1.8
Ca I	6573	6573	1	20	5.9
Ca I	7148	7148	30	13	8.6
O I	7774	7772, 7774, 7775	1	100	100
Ca I (total)	—	—	—	241.5	38.1

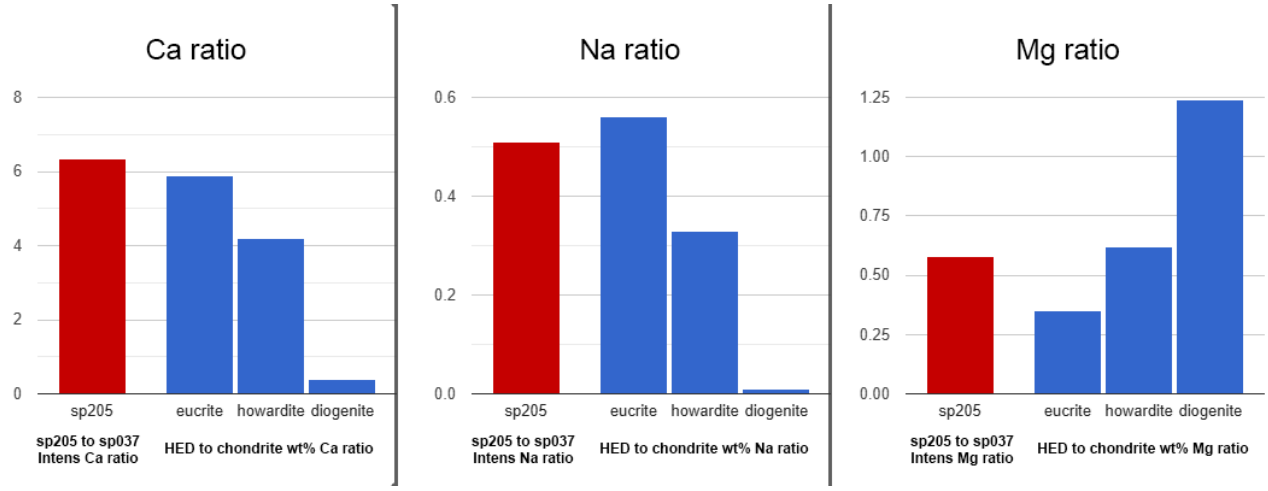

Figure 7 – The ratios of calcium, sodium, and magnesium line intensities in the sp205 spectrum under study relative to the sp037 control spectrum (STA) are highlighted in red, and the ratios of the weight fractions of these elements in HED clan meteorites relative to chondrites are highlighted in blue.

Subgroup Classification of sp205

The comparative analysis yields the following classification based on individual elements:

- **Calcium**: The intensity ratio indicates a calcium abundance ~6 times higher than in the chondritic reference. This value aligns sp205 with the eucrite subgroup within the HED clan.

- **Sodium**: The observed depletion (factor of ~2) relative to chondrites also supports a eucrite classification.

- **Magnesium**: The magnesium intensity ratio suggests a depletion factor of ~2, which is more characteristic of howardites rather than eucrites. This result is inconsistent with the classifications based on calcium and sodium.

Interpretation and final assessment

The discrepancy observed for magnesium likely stems from the methodological limitations outlined earlier (e.g., sensitivity to atmospheric conditions, natural variability in reference spectra) or could be attributed to technical artifacts such as local saturation of the bright Mg I lines in the spectra. Despite this single inconsistency, the primary and most robust diagnostic — the exceptionally high calcium signature — provides compelling evidence.

Therefore, based on the dominant spectral evidence and its agreement with the sodium trend, we classify meteoroid sp205 as a likely eucrite.

6 Conclusion

The meteoroid sp205, observed on 16 January 2024, exhibits a unique spectrum dominated by exceptionally intense calcium emission, unprecedented in the multi-year database of the Belarusian Meteor Network.

Its calculated Tisserand parameter with respect to Jupiter ($T_j = 3.53$) dynamically links it to the (4) Vesta asteroid family. Comparative spectroscopic analysis confirms its compositional affiliation with the HED (howardite-eucrite-diogenite) clan of meteorites. The diagnostic calcium enrichment, supported by sodium depletion, allows its classification most specifically as a eucrite.

This event demonstrates the value of precise meteor spectroscopy coupled with orbital analysis for identifying the asteroidal sources of individual meteoroids and for detecting rare compositional types within the Solar System's minor body population.

Acknowledgment

The author thanks all operators and volunteers of the Belarusian Meteor Network for their dedicated work in maintaining the observations. The author also thanks Paul Roggemans for his helpful support in drafting this article.

References

D'iakonova M. I., Kharitonova V. I., Iavnel A. A. (1979). Khimicheskii sostav meteoritov [Chemical composition of meteorites]. Moscow: Nauka.

Matlovič P., Pisarčíková A., Pazderová V., Loehle S., Tóth J., Ferrière L., Čermák P., Leiser D., Vaubaillon J., Ravichandran R. (2024). "Spectral properties of ablating meteorite samples for improved meteoroid composition diagnostics". *Astronomy & Astrophysics*, **689**, A323.

McSween H. Y. Jr., Binzel R. P., De Sanctis M. C., Ammannito E., Prettyman T. H., Beck A. W., Reddy V., Le Corre L., Gaffey M. J., McCord T. B., Raymond C. A., Russell C. T. and the Dawn Science Team (2013). "Dawn; the Vesta–HED connection; and the geologic context for eucrites, diogenites, and howardites". *Meteoritics & Planetary Science*, **48**, 2090–2104.

Ralchenko Y., Jou F., Kelleher D., Kramida A., Musgrove A., Reader J., Wiese W., and Olsen K. (2006). "NIST Atomic Spectra Database (version 3.1.0)". http://physics.nist.gov/asd3 (Accessed October 27, 2025).

Vojáček V., Borovička J. and Spurný P. (2022). "Oxygen line in fireball spectra and its application to satellite observations". *Astronomy & Astrophysics*, **668**, A102.

Ursids 2025 by worldwide radio meteor observations

Hiroshi Ogawa

The International Project for Radio Meteor Observations
h-ogawa@iprmo.org

Global radio meteor observations caught an unusual activity in 2025. The activity level reached AL=1.1±0.3 at $\lambda_\odot = 270.38°$ (December 22, 08^h30^m UT). This activity was possibly mixed with a traditional annual activity and a predicted encounter with a dust filament. The activity was estimated as AL=0.9 at $\lambda_\odot = 270.38°$.

1 Introduction

The Ursids is one of the major annual meteor showers. The shower reaches a maximum with a *ZHR* = 10 at $\lambda_\odot = 270.7°$ in visual observations (Rendtel, 2024). Although it usually shows a weak activity level in ordinary years, some activity outburst caused by dust trails and filaments have been detected in the past.

With radio meteor observations it is possible to obtain a complete activity profile even during bad weather and daytime. Therefore, the International Project for Radio Meteor Observations[41] (IPRMO) has been organized in 2001 to analyze a complete meteor shower activity without any radiant problem (Ogawa et al., 2001). In past research, activity profiles were derived from worldwide radio data from Radio Meteor Observation Bulletin[42] (RMOB).

A long-term study of the Ursids by radio meteor observations has clearly established the annual activity profile. IPRMO concluded that the peak of the Ursids occurred at $\lambda_\odot = 270.5°$ with a peak Activity Level Index (AL) of 0.4 using worldwide data during the period of 2004–2024. Radio meteor observations registered also some unusual activities. For example, in recent years enhanced activity was observed twice in 2020 and 2021 (Ogawa and Sugimoto, 2021; 2022). Ogawa and Steyaert (2017) reported outburst activities in 2008, 2009 ,2014 and 2016.

In 2025, some researchers had computed some possible encounters with dust filaments (Rendtel, 2024). This paper reports the result for the Ursids 2025 using worldwide radio meteor observations.

2 Data

Data from 52 observers in 12 countries has been used in this analysis. These data were provided by the following observers who reported to RMOB and Japanese observers: *Johan Bogaerts* (Belgium), *Chris Steyaert* (Belgium), *Felix Verbelen* (Belgium), *Lucas Frederic* (France), *Philippe Rainard* (France), *Pierre Heinz* (France), *Pierre Terrier* (France), *SAT00 Observatoire_SAT00* (France), *Bernd Wallbaum* (Germany), *Klaus Henning* (Germany), *WHS Essen* (Germany), *Istvan Tepliczky* (Hungary), *Observatory Szeged (Hungary), Vilmos Keresztesi (Hungary), GABB .IT* (Italy), *Licei Lunigianesi* (Italy), *APA Latina* (Italy), *Mario Bombardini* (Italy), *Hirofumi Sugimoto* (Japan), *Hironobu Shida* (Japan), *Hiroshi Suzuki* (Japan), *Kenji Fujito* (Japan), *Koichiro Okuno* (Japan), *Mai Wakita* (Japan), *Masahiko Matsuda* (Japan), *Masaki Kano* (Japan), *Masaki Tsuboi* (Japan), *Nobuo Katsura* (Japan), *Norihiro Nakamura* (Japan), *Yasufumi Yoshikawa* (Japan), *Jean-Claude Thibaut* (Luxembourg), *Aguirre Salvador* (Mexico), *Michal Biernacki* (Poland), *MAR JEN* (Poland), *Joan Figueras* (Spain), *Jochen Richert* (Switzerland), *Philip Norton* (United Kingdom), *Philip Norton Vert* (United Kingdom), *Philip Rourke* (United Kingdom), *Stephen Grimes* (United Kingdom), *Mike Otte* (United States of America), *Stanley Nelson* (United States of America).

3 Method

The meteor activity is calculated by the “Activity Level Index: *AL*(t)” (Ogawa et al., 2001) to analyze the worldwide radio meteor observation data. The activity profile was estimated using the Lorentz activity profile (Jenniskens et al., 2000).

4 Results

Figure 1 shows the result of the Activity Level Index. A clear peak was observed at $\lambda_\odot = 270.38°$ (December 22, 8^h30^m UT) with $AL = 1.1 \pm 0.3$. The beginning of increase was around $\lambda_\odot = 270.25°$ (December 22, 5^h00^m UT). After that, the activity level dropped back to the level of the annual activity profile (gray line in *Figure 1*) around $\lambda_\odot = 270.5°$ (December 22, 11^h00^m UT).

[41] https://www.iprmo.org/

[42] https://www.rmob.org/

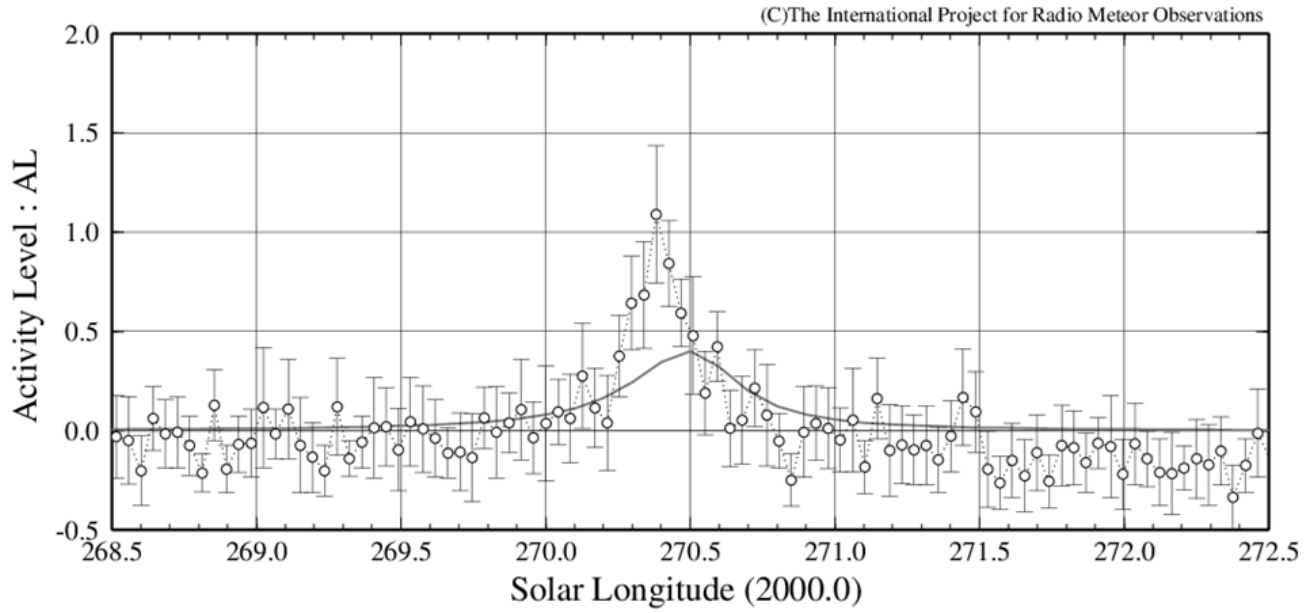

Figure 1 –Activity Level Index of the Ursids 2025 (gray line: average for the period of 2004–2024).

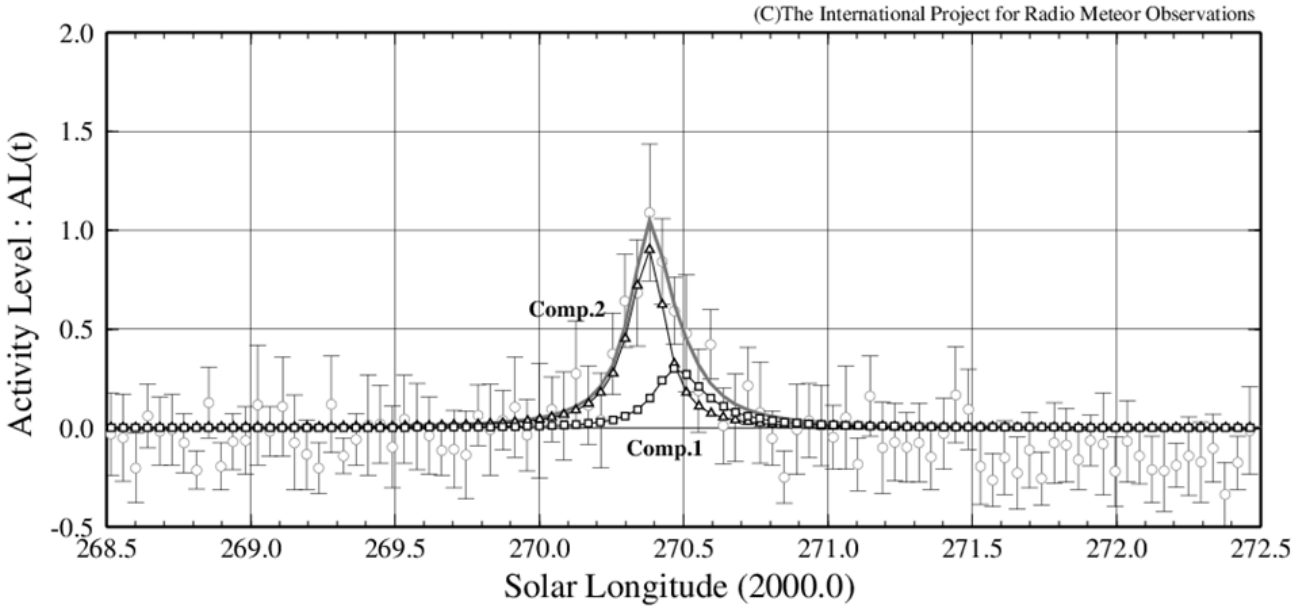

Figure 2 – The Activity Level Index: the estimated components using the Lorentz Profile (solid line: total activity of Comp1–Comp3).

The activity level *AL* of the Ursids 2025 displays two estimated components using the Lorentz profile (*Figure 2* and *Table 1*). One component corresponds to the traditional annual activity. The peak occurred at $\lambda_\odot$ = 270.47° (December 22, 10^h30^m UT). This is a similar result as in ordinary years ($\lambda_\odot$ = 270.5°).

The other component indicates an unusual activity that has *AL* = 0.9 at $\lambda_\odot$ = 270.38° (December 22, 08^h30^m UT). The Full Width of Half Maximum (FWHM) has a –2.0 hours and + 1.5 hours.

Table 1 – Comparison between the estimated components by IPRMO and the predictions.

Source	$\lambda_{\odot\,(max)}$	Activity	Comments
Comp.1	270.47°	AL = 0.3	–
Comp.2	270.38°	AL = 0.9	–
IPRMO	270.5°	AL = 0.4	ave.(2004–2024)
IMO	270.7°	ZHR 10	traditional activity
Jenniskens	270.26°	ZHR 25	filament
Vaubaillon	270.7°	–	densest section

5 Discussion

Table 1 compares the estimated components by IPRMO and published information. Comp.1 in *Figure 2* was the same result as the traditional annual activity by IPRMO. However, it requires discussion to explain Comp.2.

Jenniskens (2006) described a possible encounter with the filament at $\lambda_\odot$ = 270.26°. However, the densest section was indicated by Vaubaillon at $\lambda_\odot$ = 270.7° (*Table 1*). The peak time of Comp.2 was slightly earlier than Vaubaillon, but slightly later than Jenniskens. The Activity Level was about three times higher, which was close to the *ZHR* given by

Jenniskens. Therefore, it is possible that the encounter with the filament predicted by Jenniskens occurred later than predicted.

6 Conclusion

The worldwide radio meteor observers caught an unusual activity around $\lambda_{\odot}$ =270.38° for the Ursids in 2025. The Activity Level reached $AL = 0.9$. It is possible that this activity was caused by the encounter with a dust filament.

Acknowledgment

The worldwide data were provided by the Radio Meteor Observation Bulletin (RMOB).

We wish to thank *Pierre Terrier* for developing and hosting rmob.org. A very special thank you to *Paul Roggemans* for proofreading this article.

References

Jenniskens P., Crawford C., Butow S. J., Nugent D., Koop M., Holman D., Houston J., Jobse K., Kronk G., and Beatty K. (2000). "Lorentz shaped comet dust trail cross section from new hybrid visual and video meteor counting technique imprications for future Leonid storm encounters". *Earth, Moon and Planets*, **82–83**, 191–208.

Jenniskens P. (2006). "Meteor showers and their parent comets". *Cambr. Univ. Press.*

Ogawa H., Toyomasu S., Ohnishi K., and Maegawa K. (2001). "The Global Monitor of Meteor Streams by Radio Meteor Observation all over the world". In, Warmbein Barbara, editor, Proceeding of the Meteoroids 2001 Conference, 6-10 August 2001, Swedish Institute of Space Physics, Kiruna, Sweden. ESA Publications Division, European Space Agency, Noordwijk, The Netherlands, 189–191.

Ogawa H. and Steyaert C. (2017). "Major and Daytime Meteor Showers using Global Radio Meteor Observations covering the period 2001-2016". *WGN, Journal of the IMO*, **45**, 98–106.

Ogawa H. and Sugimoto H. (2021). "Ursids 2020 with Worldwide Radio Meteor Observations". *eMetN Meteor Journal*, **6**, 19–21

Ogawa H. and Sugimoto H. (2022). "A strong activity of the Ursids in 2021 by worldwide radio meteor observations". *eMetN Meteor Journal*, **7**, 32–33

Ogawa H. (2022). "Long-Term Studies of Major and Daytime Meteor Showers using Worldwide Radio Meteor Observations". *WGN, Journal of the IMO*, **50**, 148–157.

Rendtel J. (2024). "2025 Meteor Shower Calendar". International Meteor Organization.

December 2025 CARMELO report

Mariasole Maglione[1], **Lorenzo Barbieri**[2]

[1] **GAV, Gruppo Astrofili Vicentini, Italy**
mariasole@astrofilivicentini.it

[2] **CARMELO network and AAB: Associazione Astrofili Bolognesi, Italy**
carmelometeor@gmail.com

The CARMELO network (Cheap Amateur Radio Meteor Echoes LOgger) is a collaboration of SDR radio receivers aimed at detecting meteor echoes. This report presents the data for December 2025.

1 Introduction

December is the month of the Geminids (GEM), a meteor shower originating from asteroid 3200 Phaethon. The peak of the Geminids' activity was recorded by the CARMELO network on the night between December 13 and 14. On the other hand, no particularly high activity was recorded from the Ursids, in line with visual observers.

2 Methods

The CARMELO network consists of SDR radio receivers. In them, a microprocessor (Raspberry) performs three functions simultaneously:

- By driving a dongle, it tunes the frequency on which the transmitter transmits and tunes like a radio, samples the radio signal and through the FFT (Fast Fourier Transform) measures frequency and received power.
- By analyzing the received data for each packet, it detects meteor echoes and discards false positives and interference.
- It compiles a file containing the event log and sends it to a server.

The data are all generated by the same standard, and are therefore homogeneous and comparable. A single receiver can be assembled with a few devices whose total current cost is about 210 euros.

To participate in the network read the instructions on this page[43].

3 December data

In the plots that follow, all available at this page[44], the abscissae represent time, which is expressed in UT (Universal Time) or in solar longitude (Solar Long), and the ordinates represent the hourly rate, calculated as the total number of events recorded by the network in an hour divided by the number of operating receivers.

In *Figure 1*, the trend of signals detected by the receivers for the month of December.

4 Geminids

In December, the most important shower is the one of the Geminids (GEM), that is evolving very rapidly and will probably disappear completely in less than a hundred years.

Figure 1 – December 2025 data trend.

[43] http://www.astrofiliabologna.it/about_carmelo

[44] http://www.astrofiliabologna.it/graficocarmelohr

Figure 2 – Image by Davide Alboresi Lenzi, member of AAB (Associazione Astrofili Bolognesi), taken in Medelana (BO, Italy) on 14/12/2025. 355 exposures of 1 minute each, ISO 1600. F = 16 mm, f/3.5.

The Geminids are a unique case among meteor showers: their origin is not linked to a comet, but to an asteroid, 3200 Phaethon (Jenniskens, 2006). Discovered in 1983 by the IRAS satellite (Infrared Astronomical Satellite), 3200 Phaethon is an Apollo-type asteroid with a highly elliptical orbit that crosses those of Mars, Earth, Venus and Mercury, bringing it closer to the Sun than any other known asteroid. This close passage generates extremely high temperatures, exceeding 750°C, enough to cause the sublimation of some surface materials and the release of debris. These debris are precisely the material that gives rise to the Geminids.

Models suggest that significant amounts of debris are produced at each close passage of the asteroid near the Sun and are distributed along its orbit in a compact, well-defined trail.

The Geminids are usually active from December 2 to 19. In recent years, the ZHR (Zenithal Hourly Rate) has remained steady at around 120–150 meteors per hour, with a peak of activity between December 13 and 14.

The radiant of the shower, that is, the point in the sky from which the meteors appear to originate, is located in the constellation Gemini, near the bright star Castor. For skies in the Northern Hemisphere, it rises around 18^h00^m and sets around 09^h00^m local time.

The radiant, located near the star Castor, is positioned at the point where the photographic sequence began, that is around 19^h30^m local time. From that moment it rises in the sky until it passes almost at the zenith, and then descends again toward the morning.

During the predicted peak of activity of the Geminids, an initial reading of the CARMELO network data might suggest an underestimation of the activity compared to expectations. In reality, this apparent discrepancy is mainly attributable to the current geometric configuration of the receiver network.

At present, the CARMELO network shows a distribution strongly concentrated over Italian territory, with a substantially homogeneous observational point of view. This results in a sampling of the sky that is not isotropic, but strongly dependent on the reception geometry with respect to the position of the shower radiant. The international expansion of the network, currently being implemented with the entry of new observers in other European countries, will in the future allow for a more uniform coverage and a better three-dimensional reconstruction of meteor activity.

In the specific case of the Geminids, the radiant is located near the star Castor, with equatorial coordinates R.A. = $07^h34^m36^s$ and Dec. = +31°53’19”. On the nights between December 12 and 14, for Italian latitudes the radiant transited the meridian at a declination close to 80°, therefore near the zenith.

The receivers currently operating within the CARMELO network have an observational field centered on average around a declination of about 40°, with an angular aperture of ±30°. As a result, the geometric sensitivity of the network to the Geminid shower was optimal during the early and late phases of the night, while it was greatly reduced around the

meridian transit of the radiant, that is, during the central part of the night.

The trend of the recorded hourly rate, shown in *Figure 3*, reflects this configuration well: an increase is observed in the early evening hours, followed by a gradual decrease until the middle of the night, with a behavior compatible with a sinusoidal dependence on the incidence angle of the radiant with respect to the receivers' field of view, and then a new increase toward the morning hours.

On the basis of this geometric distribution, it is possible to hypothesize that the true value of the hourly rate at the time of maximum was significantly higher than what was directly measured by the network (the arrow in *Figures 3 and 4*), in agreement with what has been reported by radio and visual observations on a global scale.

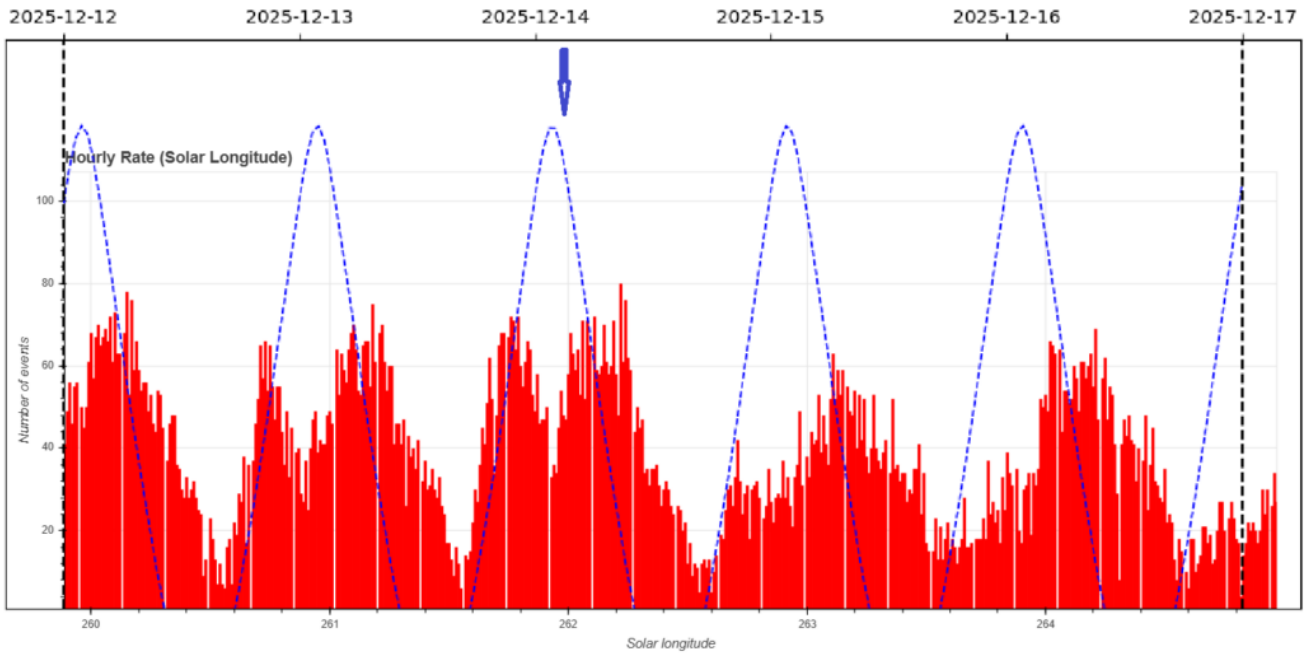

Figure 3 – Hourly rate of recorded events between December 12 and 17, as a function of solar longitude. In blue, the altitude of the radiant in the sky. The arrow indicates the likely maximum peak.

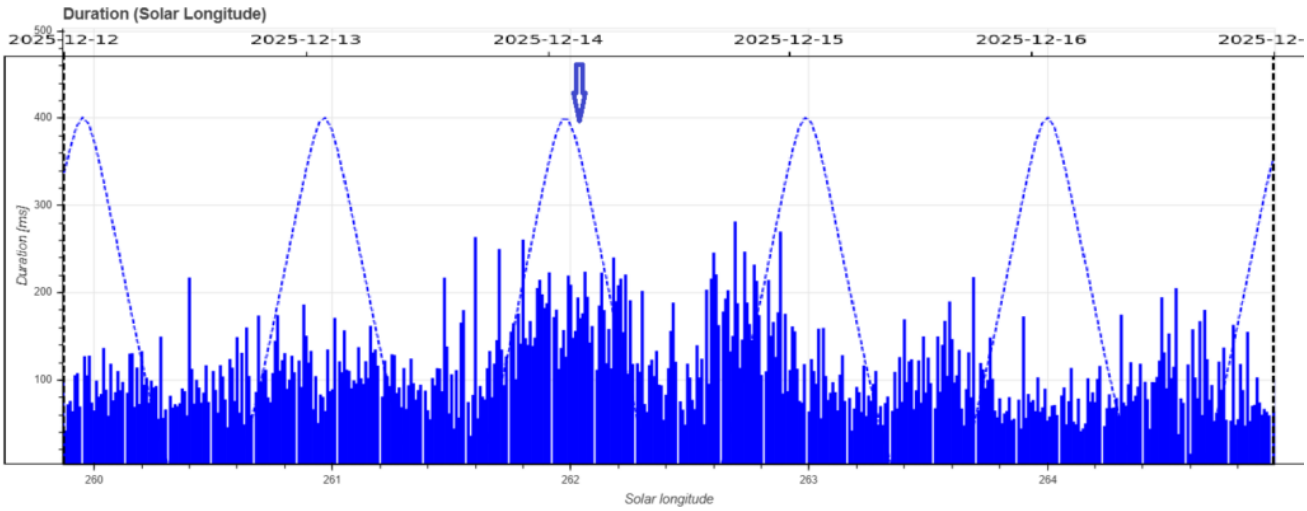

Figure 4 – Duration of the events recorded between December 12 and 17, as a function of solar longitude. In blue, the altitude of the radiant in the sky. The arrow indicates the likely maximum peak.

5 A comparison with 2024

This is the first bulletin of the second year of monthly reports on the activity recorded by the CARMELO network and on the qualitative analysis of the results. We can therefore proceed with a brief comparison with the results reported in the December 2024 bulletin (Maglione and Barbieri, 2024).

Visually, the difference between the two graphs of the recorded hourly rates (*Figure 5*) is immediately evident, due not to the number of events recorded, but to the different method of temporal sampling. In 2024 the hourly

rates were calculated over one-hour intervals, whereas in the last months of this year the resolution was changed to 15-minute intervals. The peaks therefore appear narrower and less averaged, but the overall intensity of the Geminid shower remains comparable to that of last year when integrated on an hourly basis (taking into account the considerations previously discussed regarding the detections).

One element that does show a real difference compared to 2024 is the number of counts recorded in the days before and after the shower maximum (again *Figure 5*), largely dominated by the sporadic component. In 2025 this background is noticeably higher, mainly for three reasons:

- Increase in the number of operational stations in the network;
- Introduction of the new P5 processors in the latest-generation receivers;
- Improvement of the detection and classification algorithms in the software.

These factors have led to an increase in the overall sensitivity of the system and to a greater ability to detect weaker echoes.

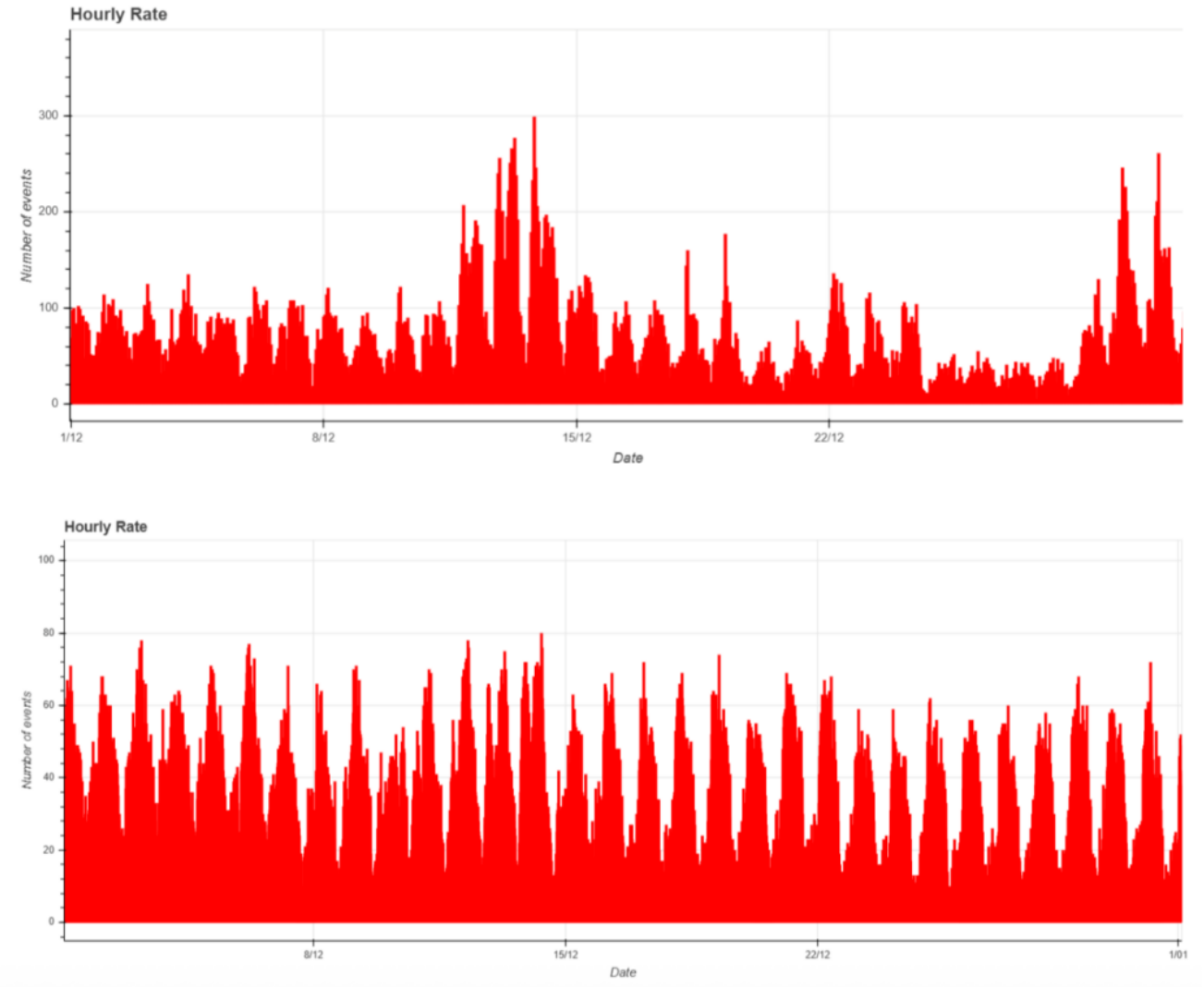

Figure 5 – Above: trend in December 2024. Below: trend in December 2025.

6 The CARMELO network

The network currently consists of 14 receivers, 12 of which are operational, located in Italy, the UK, Croatia and the USA. The European receivers are tuned to the Graves radar station frequency in France, which is 143.050 MHz. Participating in the network are:

- Lorenzo Barbieri, Budrio (BO) ITA;
- Associazione Astrofili Bolognesi, Bologna ITA;
- Associazione Astrofili Bolognesi, Medelana (BO) ITA;
- Paolo Fontana, Castenaso (BO) ITA;
- Paolo Fontana, Belluno (BL) ITA;
- Associazione Astrofili Pisani, Orciatico (PI) ITA;
- Gruppo Astrofili Persicetani, San Giovanni in Persiceto (BO) ITA;
- Roberto Nesci, Foligno (PG) ITA;
- MarSEC, Marana di Crespadoro (VI) ITA;
- Gruppo Astrofili Vicentini, Arcugnano (VI) ITA;

- Associazione Ravennate Astrofili Theyta, Ravenna (RA) ITA;
- Mike German a Hayfield, Derbyshire UK;
- Mike Otte, Pearl City, Illinois USA.

The authors' hope is that the network can expand both quantitatively and geographically, thus allowing the production of better-quality data.

References

Jenniskens P. (2006). Meteor showers and their parent comets. Cambridge University Press, pages 397–422.

Maglione M., Barbieri L. (2024). "Bollettino delle radiometeore di dicembre 2024".

January 2026 CARMELO report

Mariasole Maglione[1], **Lorenzo Barbieri**[2]

[1] **GAV, Gruppo Astrofili Vicentini, Italy**
mariasole@astrofilivicentini.it

[2] **CARMELO network and AAB: Associazione Astrofili Bolognesi, Italy**
carmelometeor@gmail.com

The CARMELO network (Cheap Amateur Radio Meteor Echoes LOgger) is a collaboration of SDR radio receivers aimed at detecting meteor echoes. This report presents the data for January 2026.

1 Introduction

January opened with the peak of the Quadrantids, which is the main and dominant shower for the entire month. The peak of the Quadrantids occurred between January 3 and 4.

2 Methods

The CARMELO network consists of SDR radio receivers. In them, a microprocessor (Raspberry) performs three functions simultaneously:

- By driving a dongle, it tunes the frequency on which the transmitter transmits and tunes like a radio, samples the radio signal and through the FFT (Fast Fourier Transform) measures frequency and received power.
- By analyzing the received data for each packet, it detects meteor echoes and discards false positives and interference.
- It compiles a file containing the event log and sends it to a server.

The data are all generated by the same standard, and are therefore homogeneous and comparable. A single receiver can be assembled with a few devices whose total current cost is about 210 euros.

To participate in the network read the instructions on this page[45].

3 January data

In the plots that follow, all available at this page[46], the abscissae represent time, which is expressed in UT (Universal Time) or in solar longitude (Solar Long), and the ordinates represent the hourly rate, calculated as the total number of events recorded by the network in an hour divided by the number of operating receivers.

In *Figure 1*, the trend of signals detected by the receivers for the month of January.

4 Quadrantids

Among the annual meteor showers, the January Quadrantids usually stand out for their intensity, reaching peaks of activity between 60 and 200 meteors per hour. Despite this, they remain less well known than other more famous showers, such as the Perseids or Geminids. Their less notoriety is also due to the very short peak of activity, which lasts about 24 hours.

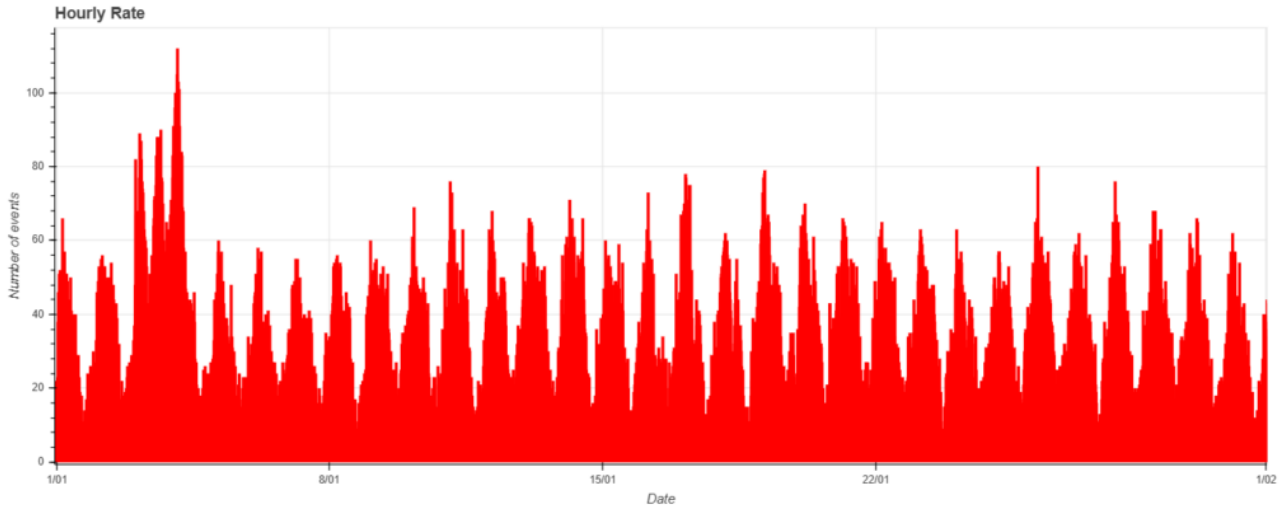

Figure 1 – January 2026 data trend.

[45] http://www.astrofiliabologna.it/about_carmelo

[46] http://www.astrofiliabologna.it/graficocarmelohr

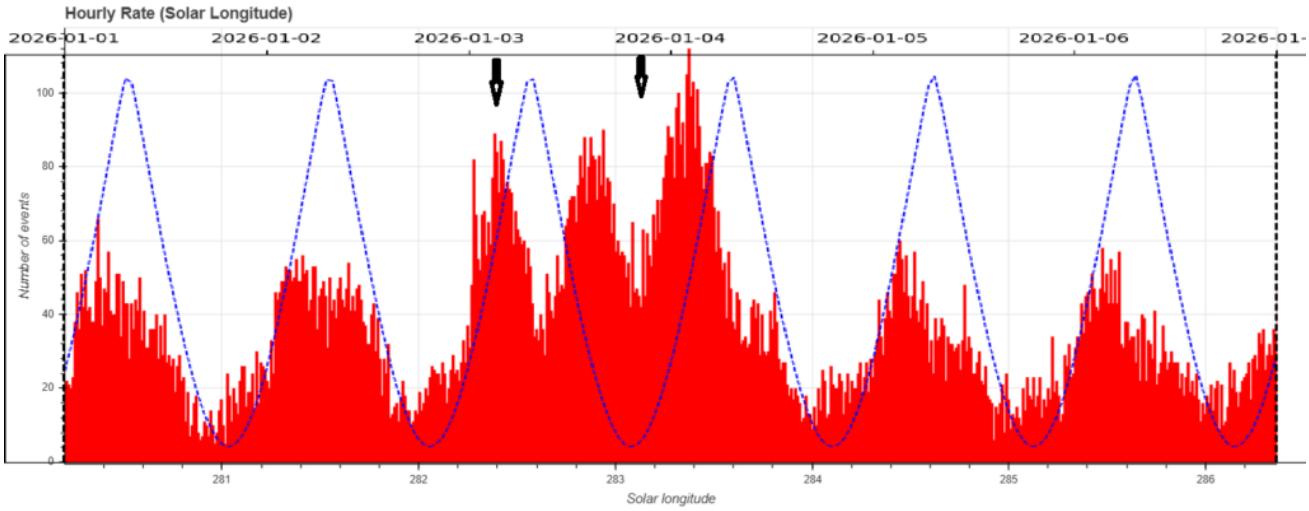

Figure 2 – Hourly rate of events recorded between January 1 and 7, based on solar longitude. In blue, the height of the radiant in the sky. The two arrows indicate the maximum at two different filaments.

The radiant of the Quadrantids is located in the Bootes constellation, in a rather low position in the northern sky, between the head of the Dragon and the helm of the Big Dipper. The name is derived from Quadrans Muralis, an ancient constellation created in 1795 by the French astronomer Jérôme Lalande that included parts of Bootes and the Dragon, and which is not on the list of 88 constellations drawn up by the International Astronomical Union (IAU) in 1922 and published in 1930 (Delporte, 1930).

The origin of this swarm remains a debated topic. In 2003, following an observational campaign on minor bodies in the Solar System, astronomer Peter Jenniskens found a possible progenitor body of the Quadrantids in the Near Earth (196256) asteroid 2003 EH_1, a hypothesis that would make them one of the few meteor showers arising from an asteroid and not a comet, similar to the Geminids in December (Jenniskens, 2004). Since then, 2003 E_1 has been considered the most likely progenitor body of the Quadrantids. It may itself be a fragment of comet C/1490 Y1, which was observed by Chinese, Japanese and Korean astronomers just over 500 years ago in 1490 (Ki-Won Lee et al., 2009).

This year, visual observations of the Quadrantids were hampered by the presence of the Full Moon, and radio observation was penalized by the fact that the peak of the shower's activity occurred just when the radiant was on the horizon. In the plot in *Figure 2*, which shows the hourly rate on the days when the Quadrantids were most active, a first filament is clearly visible, reaching its maximum at a solar longitude of about 282.4° (first black arrow), while the second and much more consistent maximum is expected at a solar longitude of about 283. 1° (second black arrow). This maximum occurs with the minimum height of the radiant in the early evening of January 3. The double filament also confirms the observations of January 2025 (Maglione and Barbieri, 2025).

The passage of the shower is also visible in the measurement of the average power of the signals received (see *Figure 3*), which shows an increase during the night

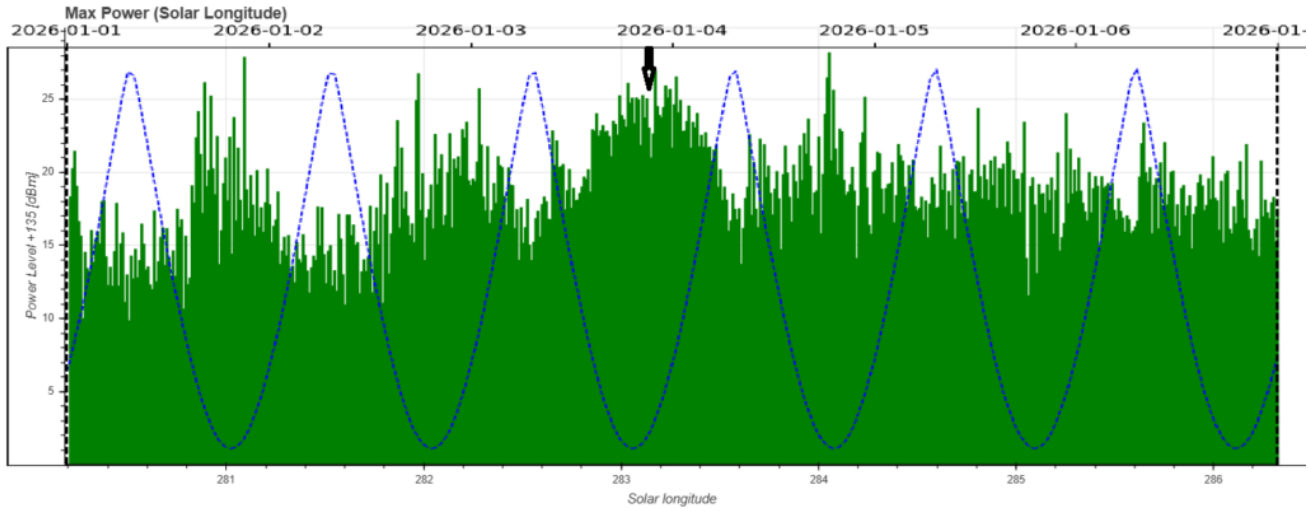

Figure 3 – Average power of signals recorded between January 1 and 7, as a function of solar longitude. In blue, the height of the radiant in the sky. The arrow indicates the maximum value, centered at a solar longitude of approximately 283.1°, corresponding to the second filament.

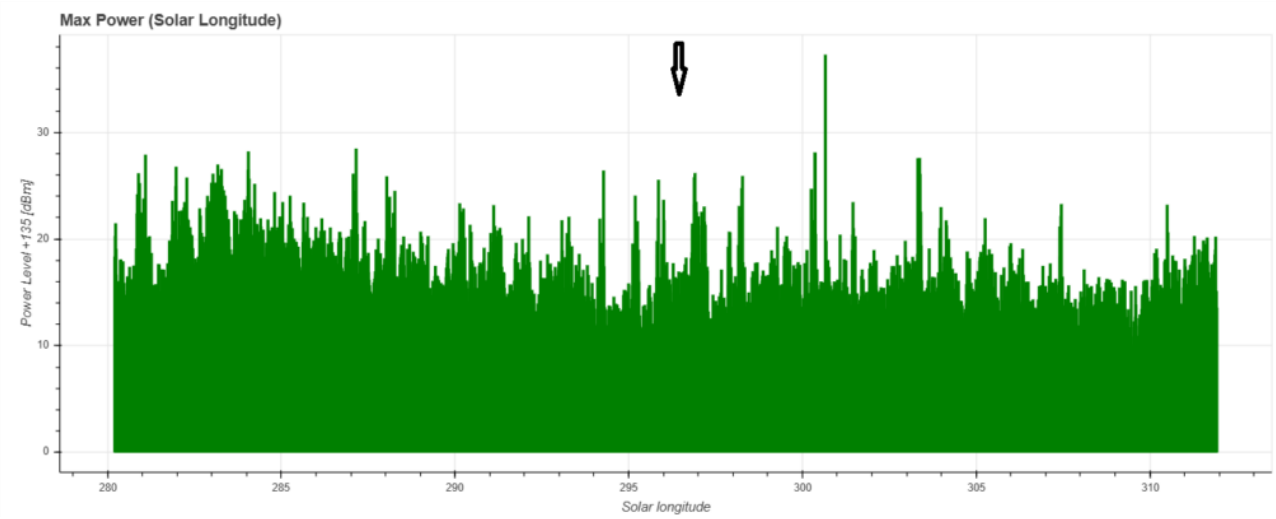

Figure 4 – Average power of signals recorded between solar longitude 280° and 312° approximately, with a peak indicated by the black arrow between 9^h UT and 16^h UT on January 17.

between January 3 and 4, with a maximum value centered at a solar longitude of approximately 283.1°. The data for the first filament, on the other hand, is much lower, a result that suggests a different mass index, with smaller and lighter meteors than the main filament.

Furthermore, throughout the day on January 17, from 9^h UT to 16^h UT, the CARMELO network recorded a slight increase in the average power of the signals received (see *Figure 4*). This average increase can be associated with weak daylight showers activity, therefore without observational counterparts in the visible spectrum. Among these, considering observations from previous years, we could mention Serpentis-Coronae Borealis (RSE#594) or γ-Ursae Minoris (GUM#404).

5 The CARMELO network

The network currently consists of 14 receivers, 12 of which are operational, located in Italy, the UK, Croatia and the USA. The European receivers are tuned to the Graves radar station frequency in France, which is 143.050 MHz. Participating in the network are:

- Lorenzo Barbieri, Budrio (BO) ITA;
- Associazione Astrofili Bolognesi, Bologna ITA;
- Associazione Astrofili Bolognesi, Medelana (BO) ITA;
- Paolo Fontana, Castenaso (BO) ITA;
- Paolo Fontana, Belluno (BL) ITA;
- Associazione Astrofili Pisani, Orciatico (PI) ITA;
- Gruppo Astrofili Persicetani, San Giovanni in Persiceto (BO) ITA;
- Roberto Nesci, Foligno (PG) ITA;
- MarSEC, Marana di Crespadoro (VI) ITA;
- Gruppo Astrofili Vicentini, Arcugnano (VI) ITA;
- Associazione Ravennate Astrofili Rheyta, Ravenna (RA) ITA;
- Mike German a Hayfield, Derbyshire UK;
- Mike Otte, Pearl City, Illinois USA.
- Yuri Malagutti, Comano (TI) CH.

The authors' hope is that the network can expand both quantitatively and geographically, thus allowing the production of better-quality data.

References

Delporte E. (1930). "IAU: Délimitation Scientifique des Constellations". At the University Press.

Jenniskens P. (2004). "2003 EH_1 and the Quadrantid shower". *WGN, Journal of the International Meteor Organization*, **32**, 7–10.

Lee K.-W., Yang H.J., Park M.-G. (2009). "Orbital Elements of Comet C/1490 Y1 and the Quadrantid shower". *Monthly Notices of the Royal Astronomical Society*, **400**, 1389–1393.

Maglione M., Barbieri L. (2025). "Bollettino delle radiometeore di gennaio 2025".

Radio meteors December 2025

Felix Verbelen

Vereniging voor Sterrenkunde & Volkssterrenwacht MIRA, Grimbergen, Belgium
felix.verbelen@gmail.com

An overview of the radio observations during December is given.

1 Introduction

The graphs show both the daily totals (*Figure 1 and 2*) and the hourly numbers (*Figure 3 and 4*) of "all" reflections counted automatically, and of manually counted "overdense" reflections, overdense reflections longer than 10 seconds and longer than 1 minute, as observed here at Kampenhout (BE) on the frequency of our VVS-beacon (49.99 MHz) during the month of December 2025.

The hourly numbers, for echoes shorter than 1 minute, are weighted averages derived from:

$$N(h) = \frac{n(h-1)}{4} + \frac{n(h)}{2} + \frac{n(h+1)}{4}$$

No lightning activity was detected, and local interference and unidentified noise remained low throughout the month.

The highlights were, of course, the Geminids, which reached their peak on December 13–14; the long-duration 'overdense' echoes clearly peaked later than the 'underdense' ones. The Ursids were also interesting, with their maximum on December 22nd. Attached you will find a few screenshots of both the Geminids (*Figure 5*) and the Ursids (*Figure 6*).

On December 26th, there was another minor surge of 'overdense' reflections, likely the omega and sigma-Serpentids.

Throughout the entire month, 7 reflections lasting longer than one minute were recorded here. A selection of some notable or strong reflections is shown in *Figures 7 to 15*. Many more are available upon request.

In addition to the usual graphs, you will also find the raw counts in cvs-format[47] from which the graphs are derived. The table contains the following columns: day of the month, hour of the day, day + decimals, solar longitude (epoch J2000), counts of "all" reflections, overdense reflections, reflections longer than 10 seconds and reflections longer than 1 minute, the numbers being the observed reflections of the past hour.

[47] https://www.emeteornews.net/wp-content/uploads/2026/01/202512_49990_FV_rawcounts.csv

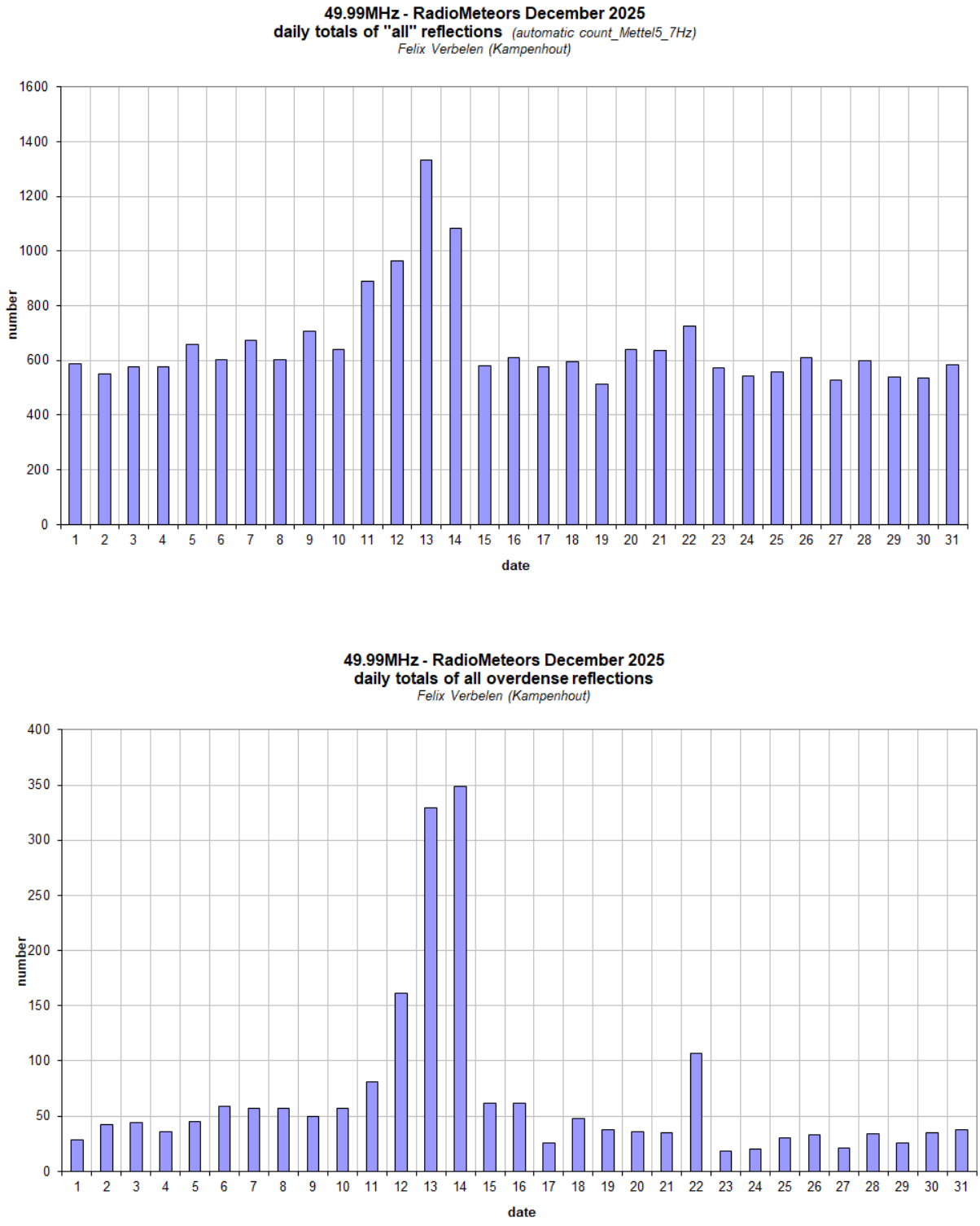

Figure 1 – The daily totals of "all" reflections counted automatically, and of manually counted "overdense" reflections, as observed here at Kampenhout (BE) on the frequency of our VVS-beacon (49.99 MHz) during December 2025.

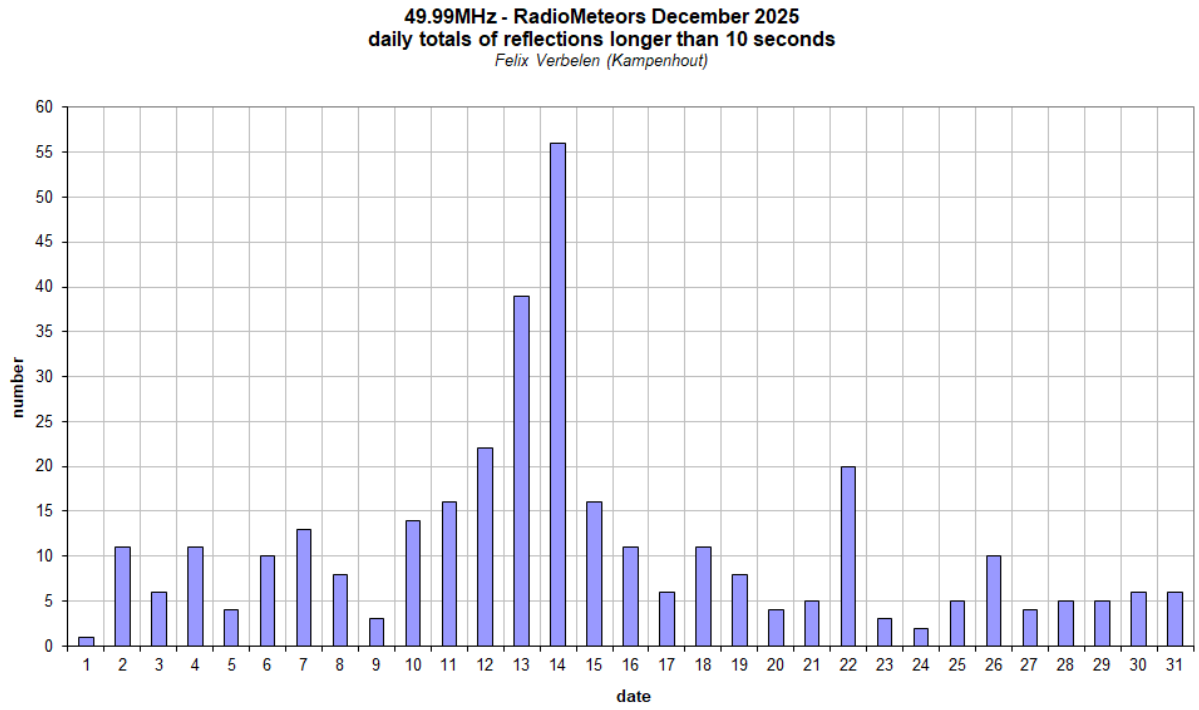

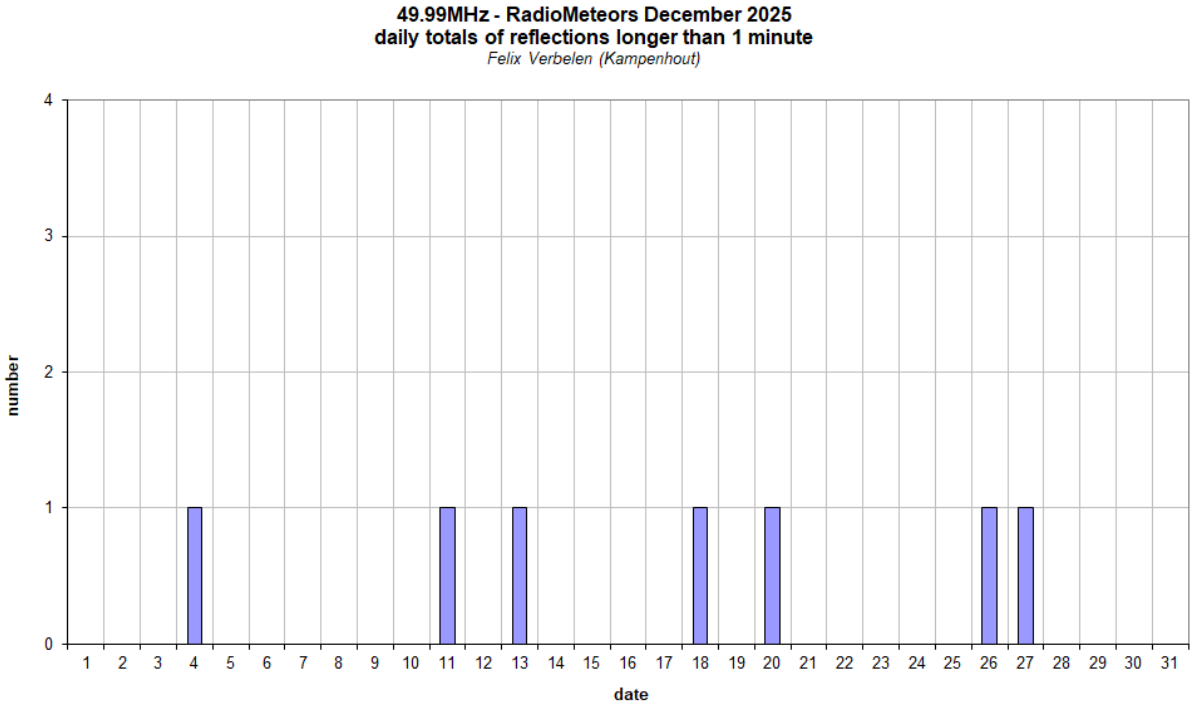

Figure 2 – The daily totals of overdense reflections longer than 10 seconds and longer than 1 minute, as observed here at Kampenhout (BE) on the frequency of our VVS-beacon (49.99 MHz) during December 2025.

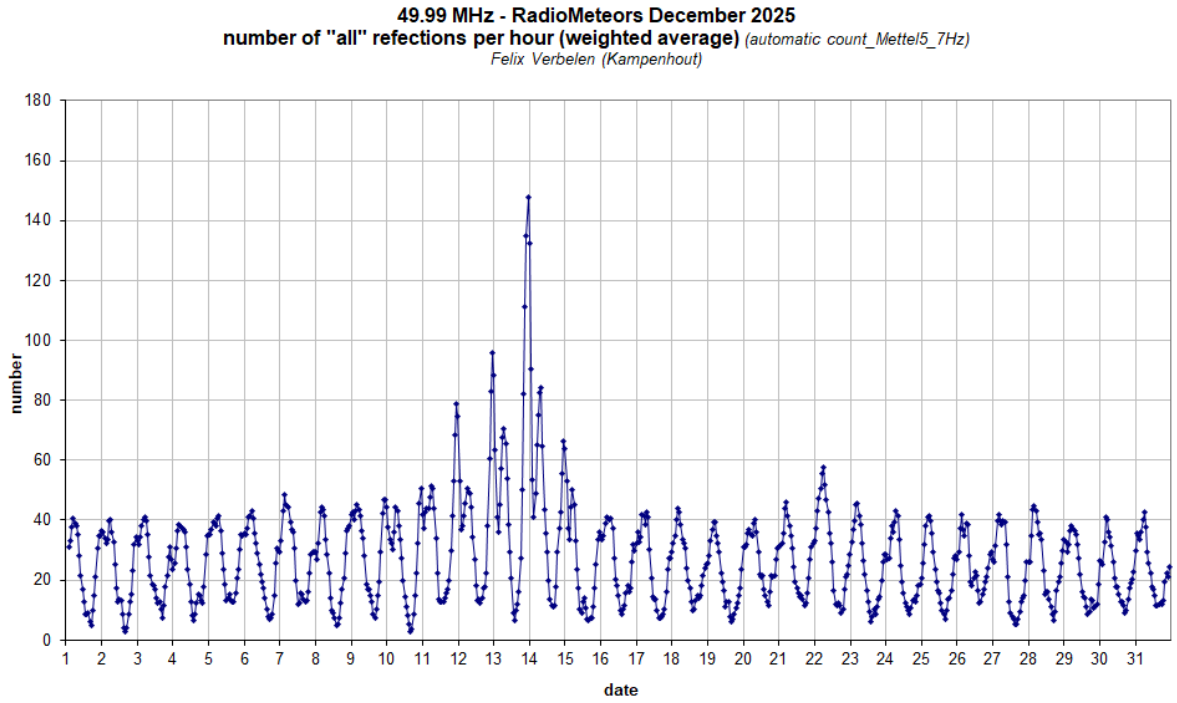

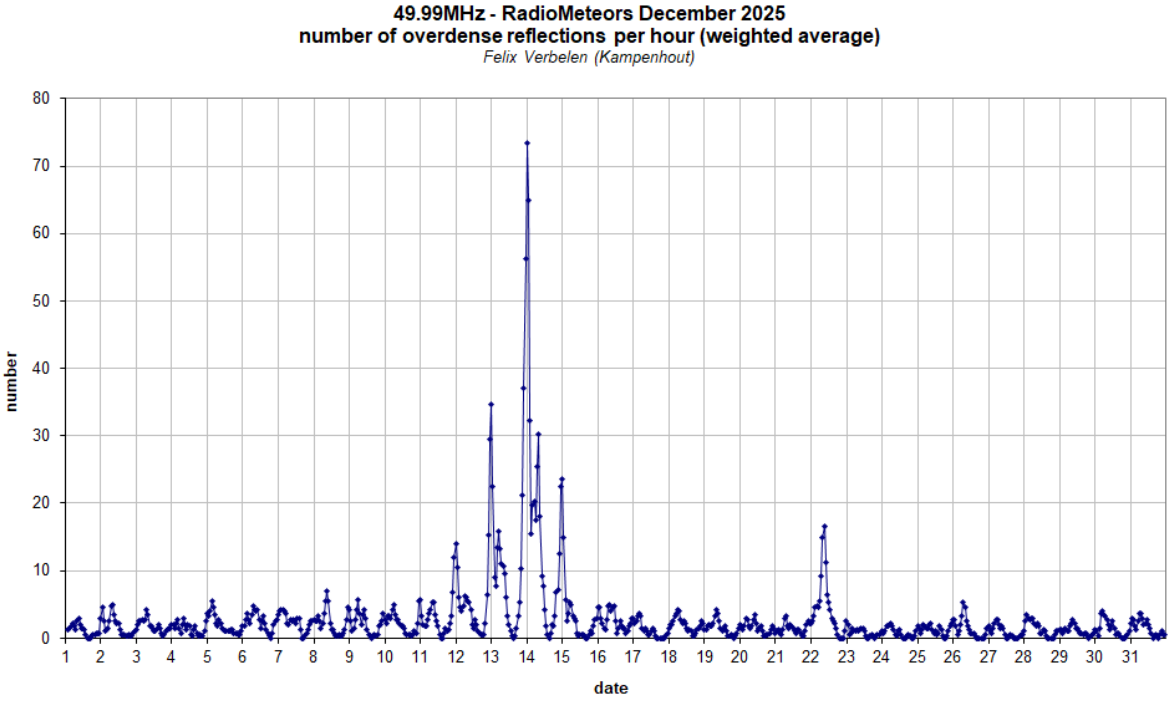

Figure 3 – The hourly numbers of "all" reflections counted automatically, and of manually counted "overdense" reflections, as observed here at Kampenhout (BE) on the frequency of our VVS-beacon (49.99 MHz) during December 2025.

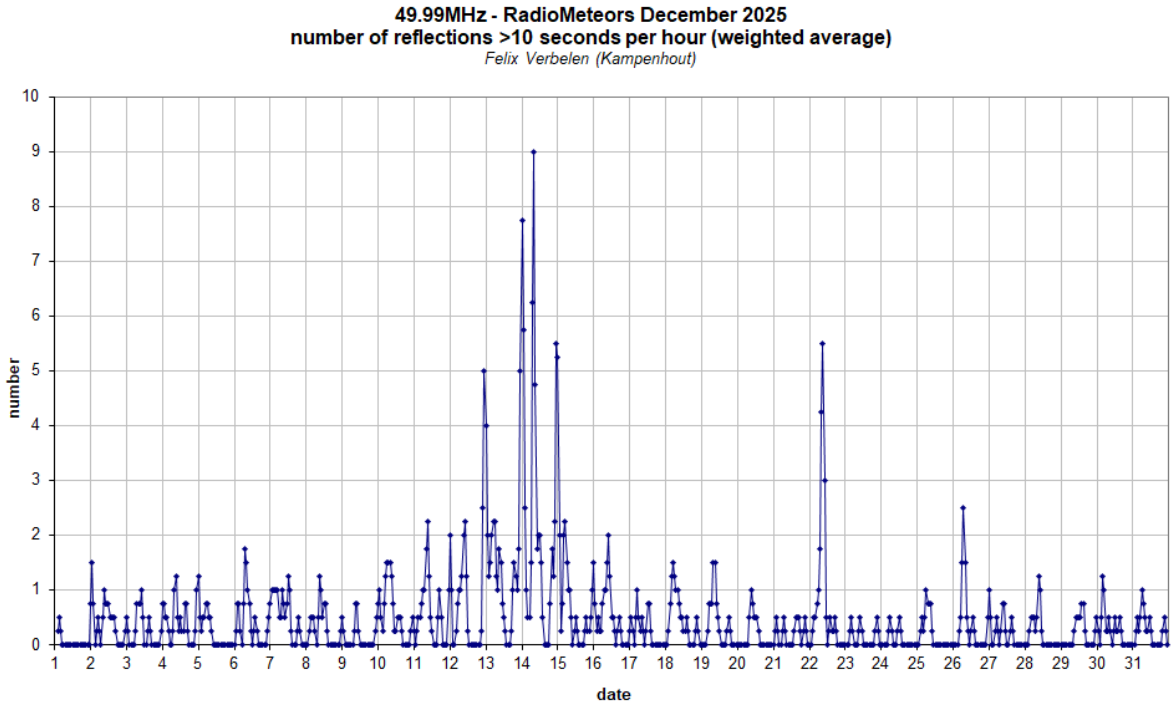

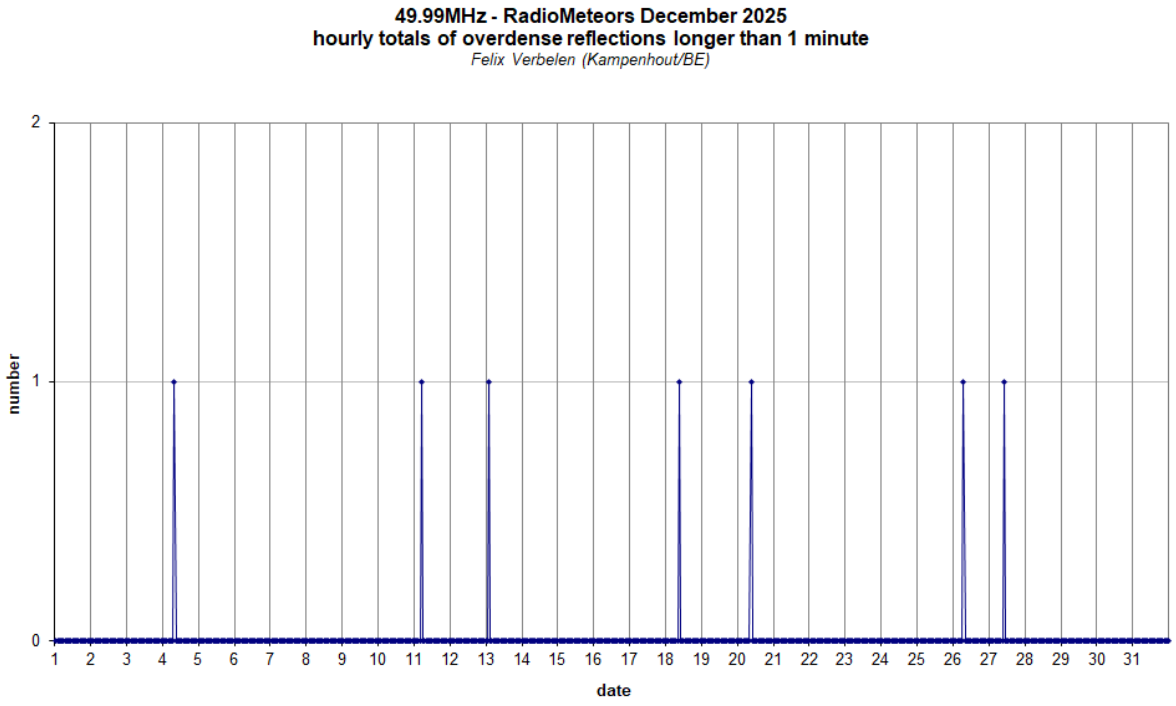

Figure 4 – The hourly numbers of overdense reflections longer than 10 seconds and longer than 1 minute, as observed here at Kampenhout (BE) on the frequency of our VVS-beacon (49.99 MHz) during December 2025.

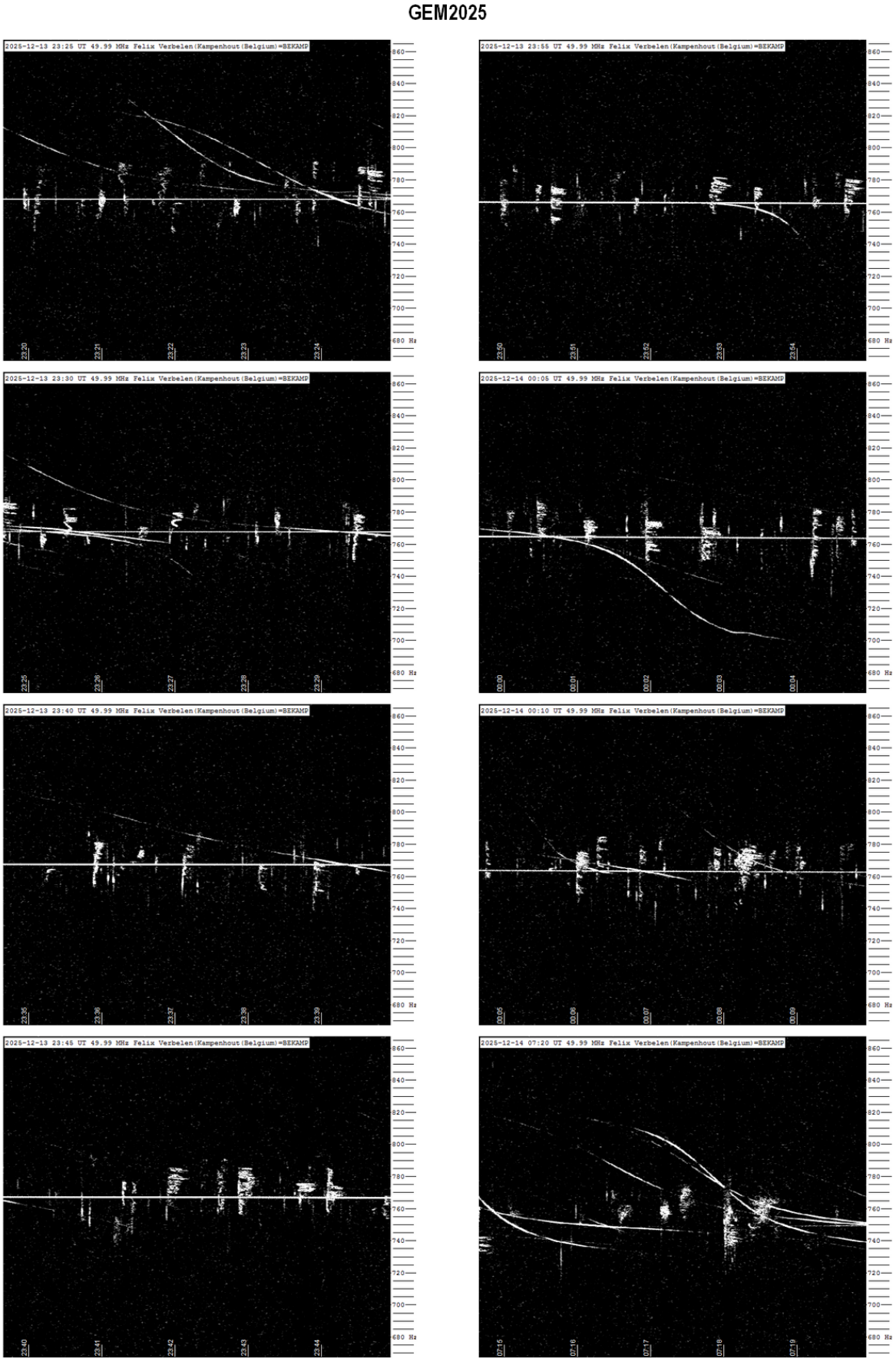

Figure 5 – Selection of meteor radio echoes during the Geminids 2025.

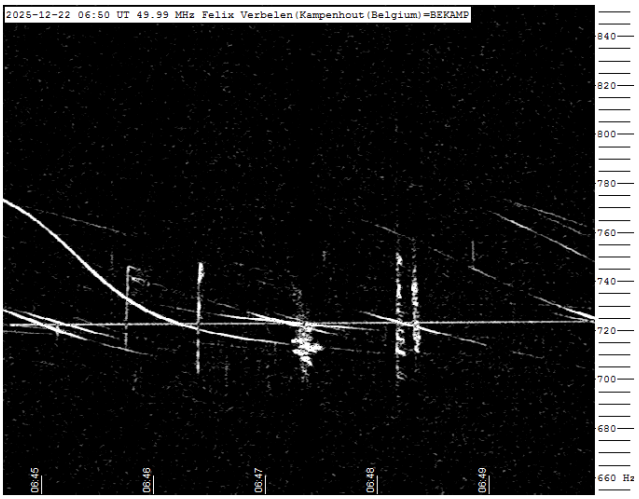

Figure 6 – Selection of meteor radio echoes during the Ursids 2025.

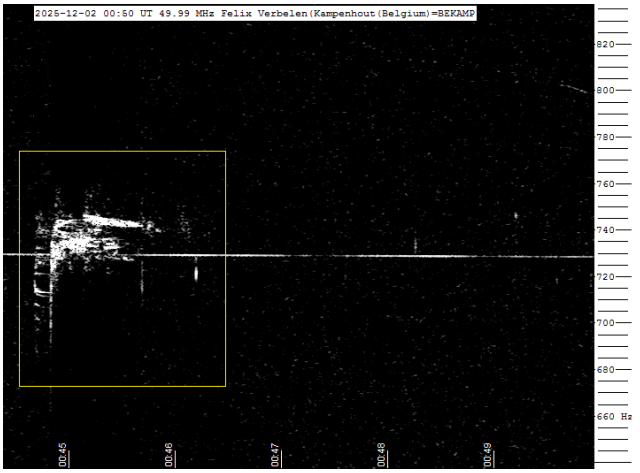

Figure 7 – Meteor echoes December 02, 00^h50^m UT.

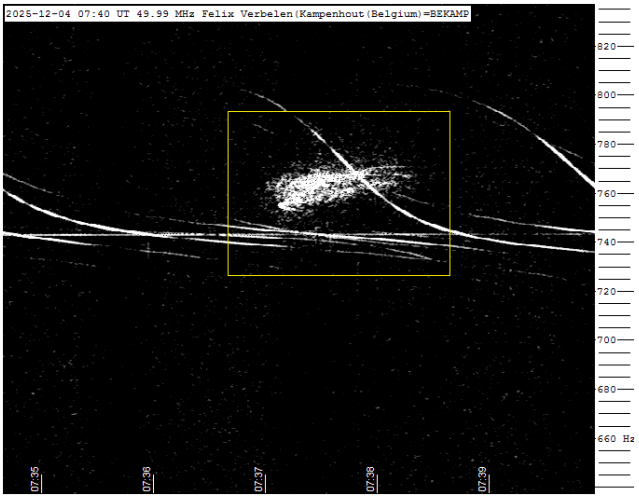

Figure 8 – Meteor echoes December 04, 07^h40^m UT.

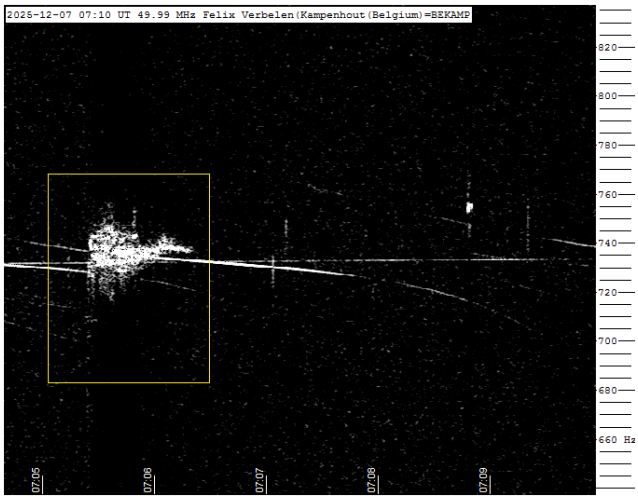

Figure 9 – Meteor echoes December 07, 07^h10^m UT.

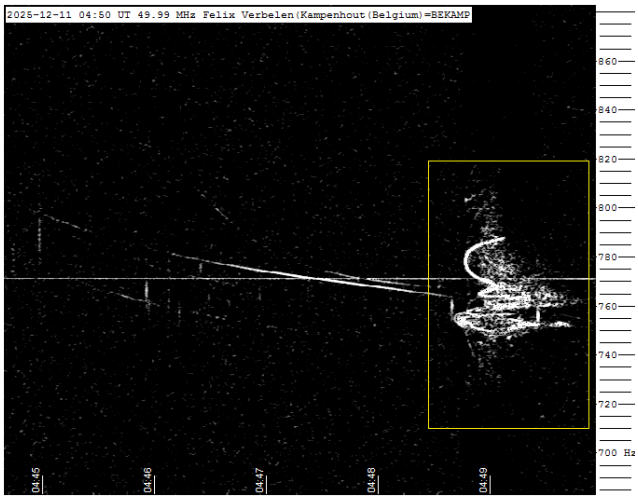

Figure 10 – Meteor echoes December 11, 04^h50^m UT.

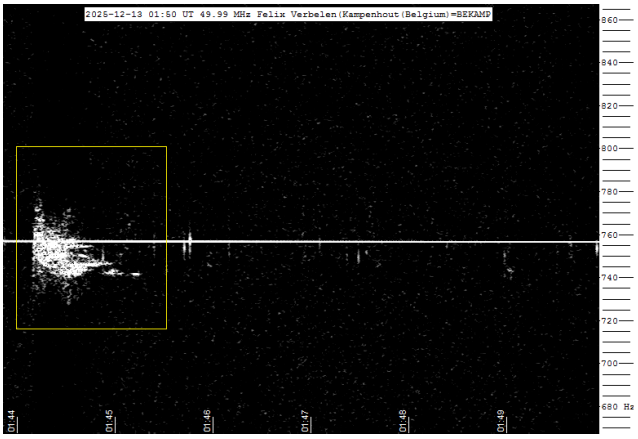

Figure 11 – Meteor echoes December 13, 01^h50^m UT.

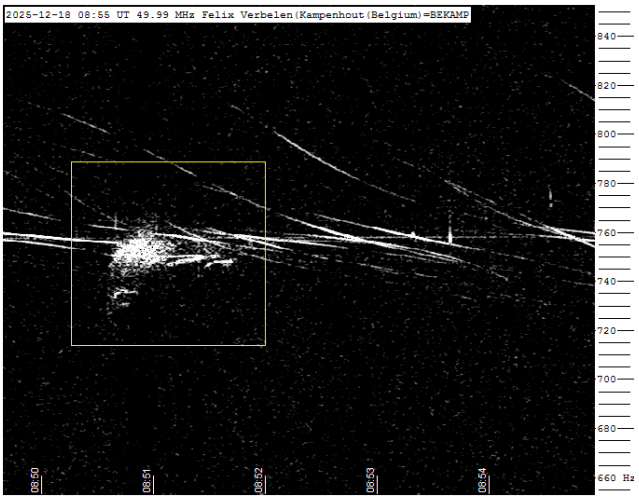

Figure 12 – Meteor echoes December 18, 08^{h}55^{m} UT.

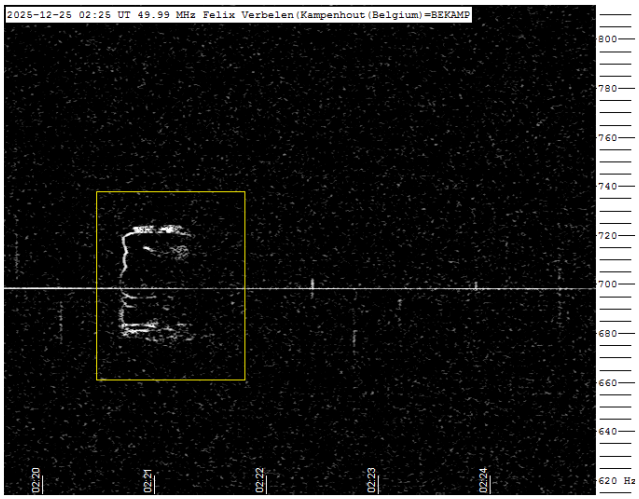

Figure 14 – Meteor echoes December 25, 02^{h}25^{m} UT.

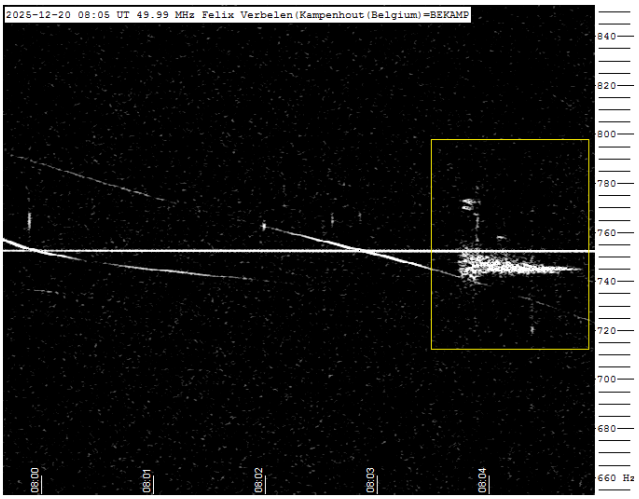

Figure 13 – Meteor echoes December 20, 08^{h}05^{m} UT.

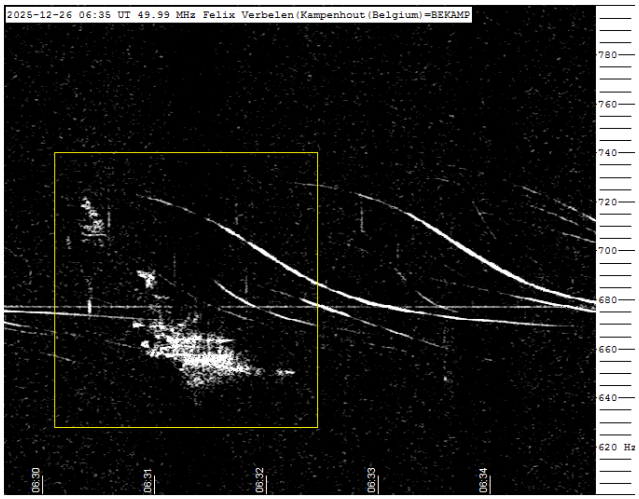

Figure 15 – Meteor echoes December 26, 06^{h}35^{m} UT.

Radio meteors January 2026

Felix Verbelen

Vereniging voor Sterrenkunde & Volkssterrenwacht MIRA, Grimbergen, Belgium
felix.verbelen@gmail.com

An overview of the radio observations during January is given.

1 Introduction

The graphs show both the daily totals (*Figure 1 and 2*) and the hourly numbers (*Figure 3 and 4*) of "all" reflections counted automatically, and of manually counted "overdense" reflections, overdense reflections longer than 10 seconds and longer than 1 minute, as observed here at Kampenhout (BE) on the frequency of our VVS-beacon (49.99 MHz) during the month of January 2026.

The hourly numbers, for echoes shorter than 1 minute, are weighted averages derived from:

$$N(h) = \frac{n(h-1)}{4} + \frac{n(h)}{2} + \frac{n(h+1)}{4}$$

Local interference and unidentified noise remained weak, and no significant lightning activity was recorded.

The highlights of the month were, of course, the Quadrantids, which reached their peak intensity here on January 4th between 04^h00^m and 05^h00^m UT, though they were also very active on January 3rd. After the maximum, Quadrantid activity declined rapidly, but remained clearly noticeable for several days. Attached are some SpecLab images that provide an indication of the shower's intensity. (*Figure 5*).

Several smaller showers were active during the month, in particular around January 18–20, but the rest of the month was, as usual, fairly quiet.

This month, 5 reflections longer than 1 minute were observed here. A selection of some notable or strong reflections is shown in *Figures 6 to 14*. Many more are available upon request.

In addition to the usual graphs, you will also find the raw counts in cvs-format[48] from which the graphs are derived. The table contains the following columns: day of the month, hour of the day, day + decimals, solar longitude (epoch J2000), counts of "all" reflections, overdense reflections, reflections longer than 10 seconds and reflections longer than 1 minute, the numbers being the observed reflections of the past hour.

[48] https://www.emeteornews.net/wp-content/uploads/2026/02/202601_49990_FV_rawcounts.csv

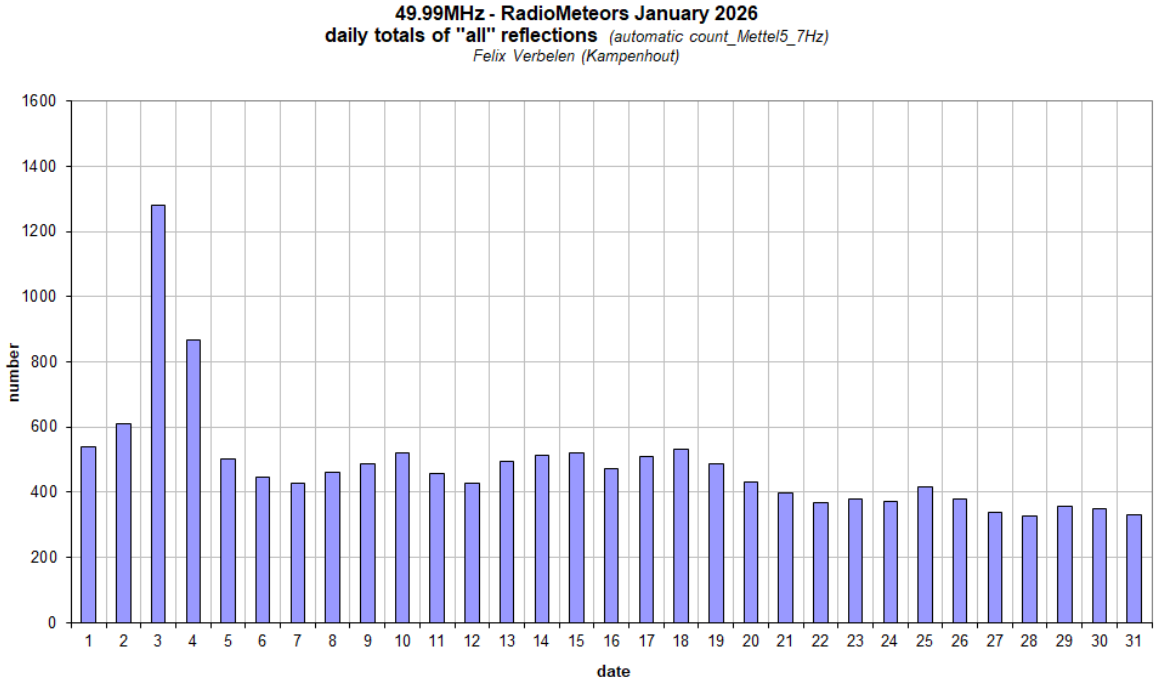

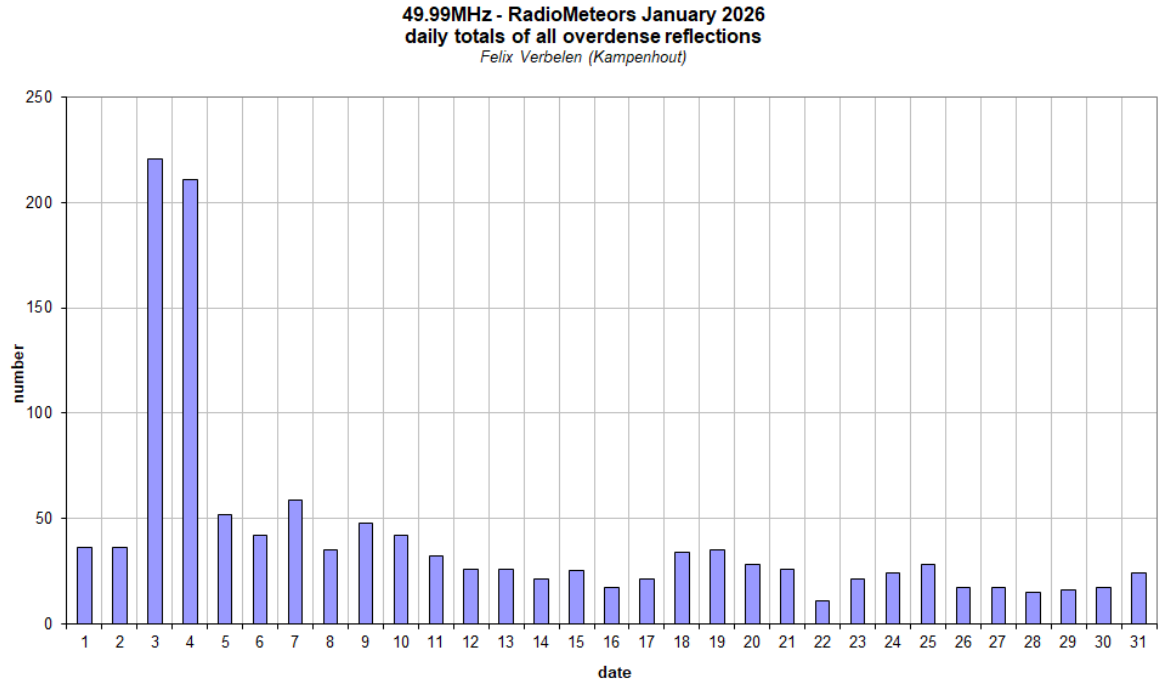

Figure 1 – The daily totals of "all" reflections counted automatically, and of manually counted "overdense" reflections, as observed here at Kampenhout (BE) on the frequency of our VVS-beacon (49.99 MHz) during January 2026.

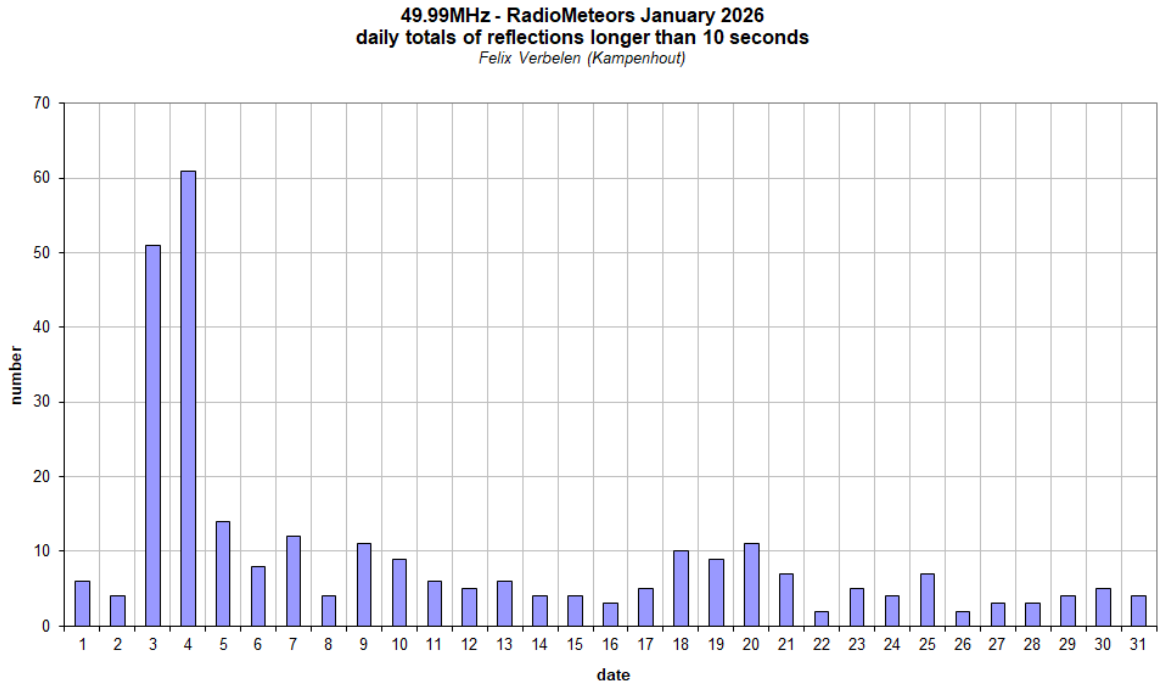

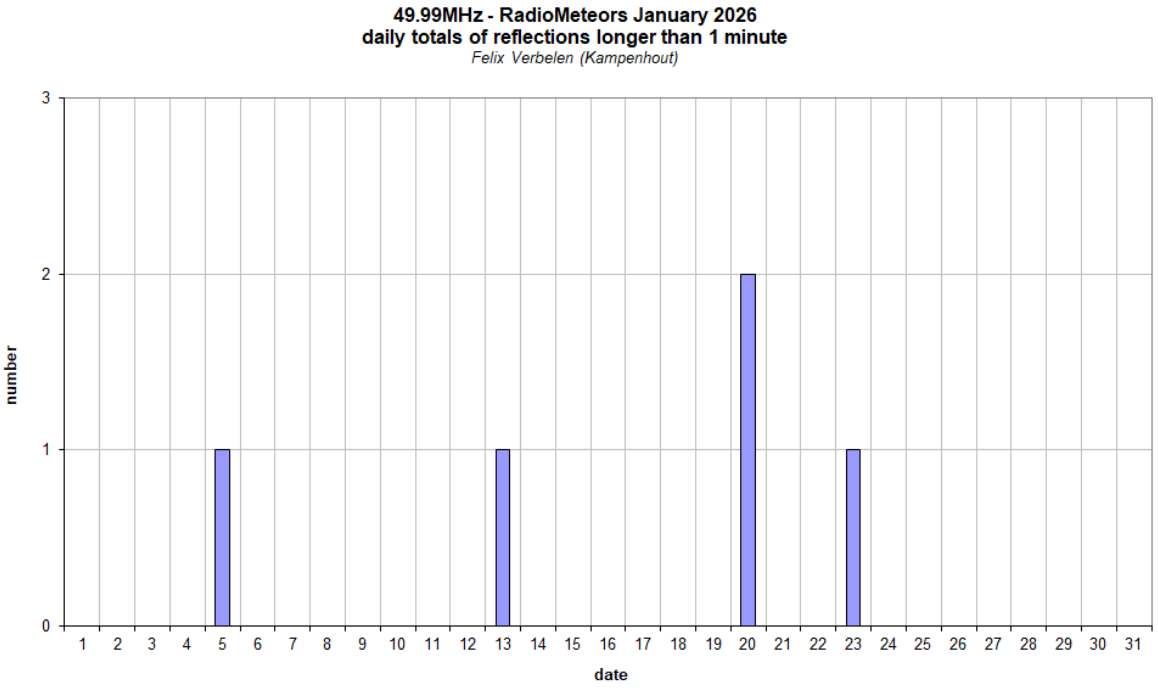

Figure 2 – The daily totals of overdense reflections longer than 10 seconds and longer than 1 minute, as observed here at Kampenhout (BE) on the frequency of our VVS-beacon (49.99 MHz) during January 2026.

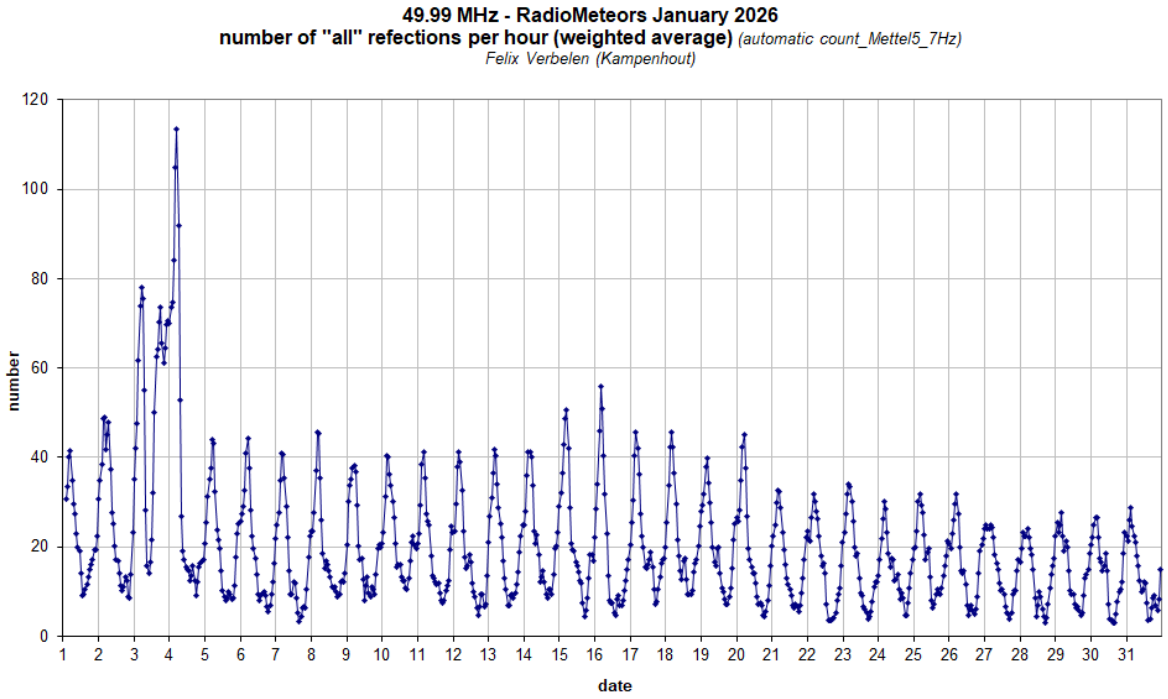

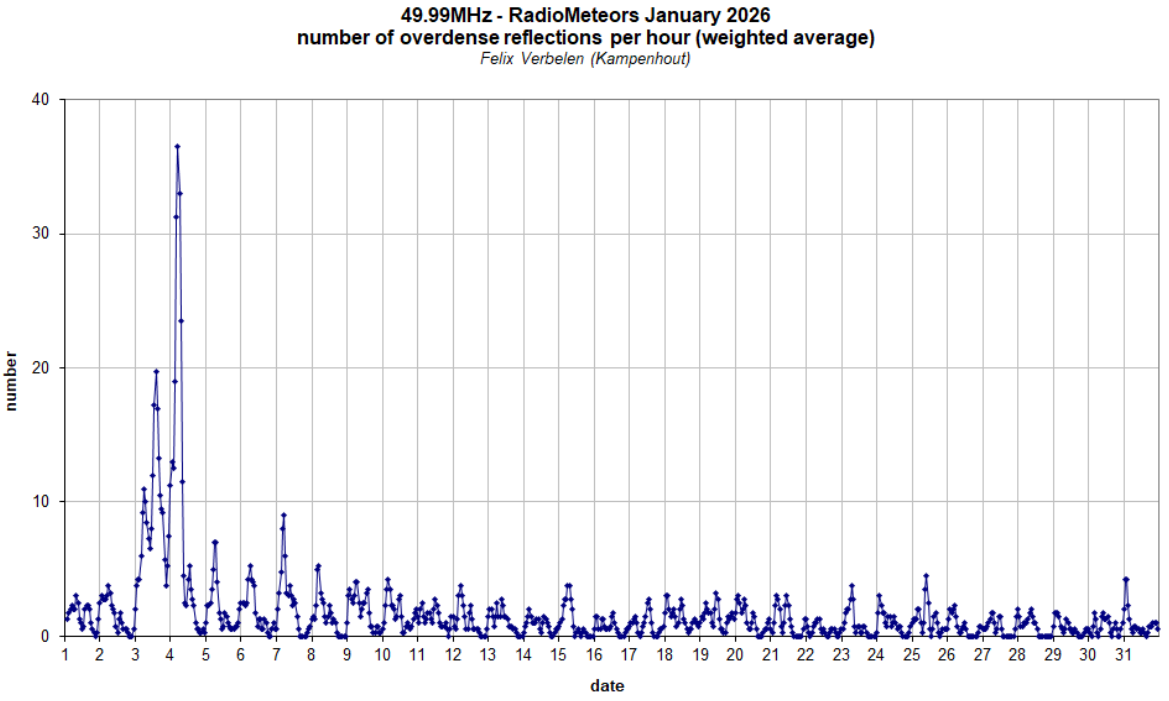

Figure 3 – The hourly numbers of "all" reflections counted automatically, and of manually counted "overdense" reflections, as observed here at Kampenhout (BE) on the frequency of our VVS-beacon (49.99 MHz) during January 2026.

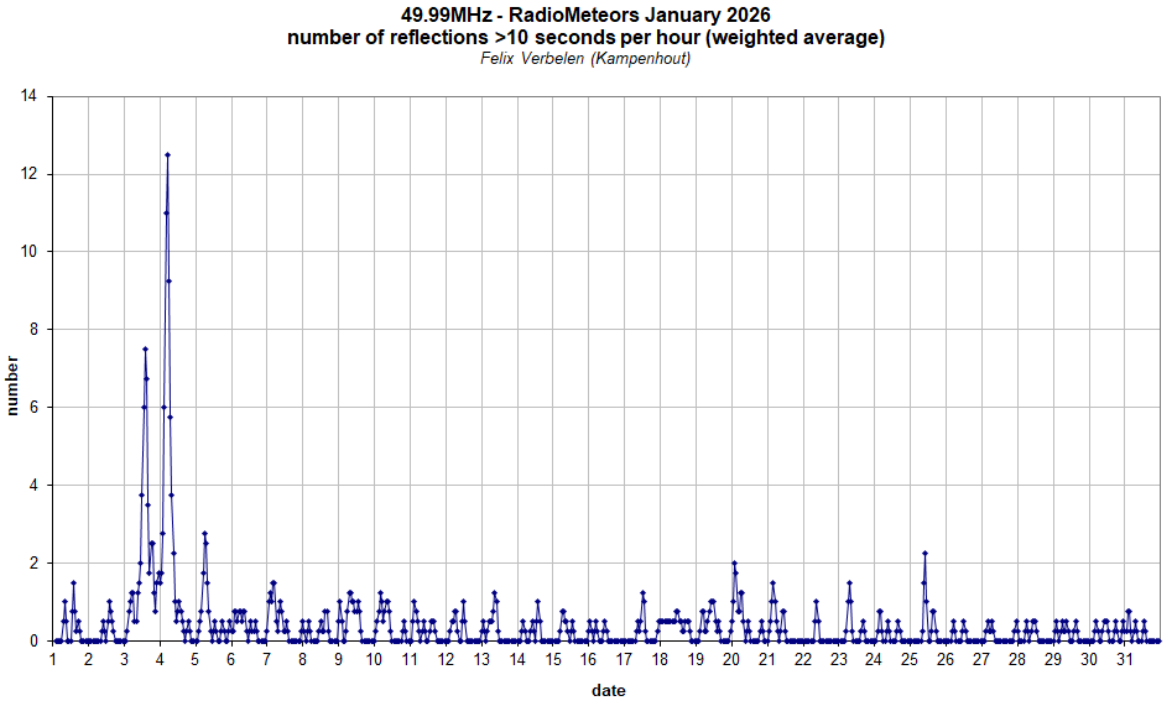

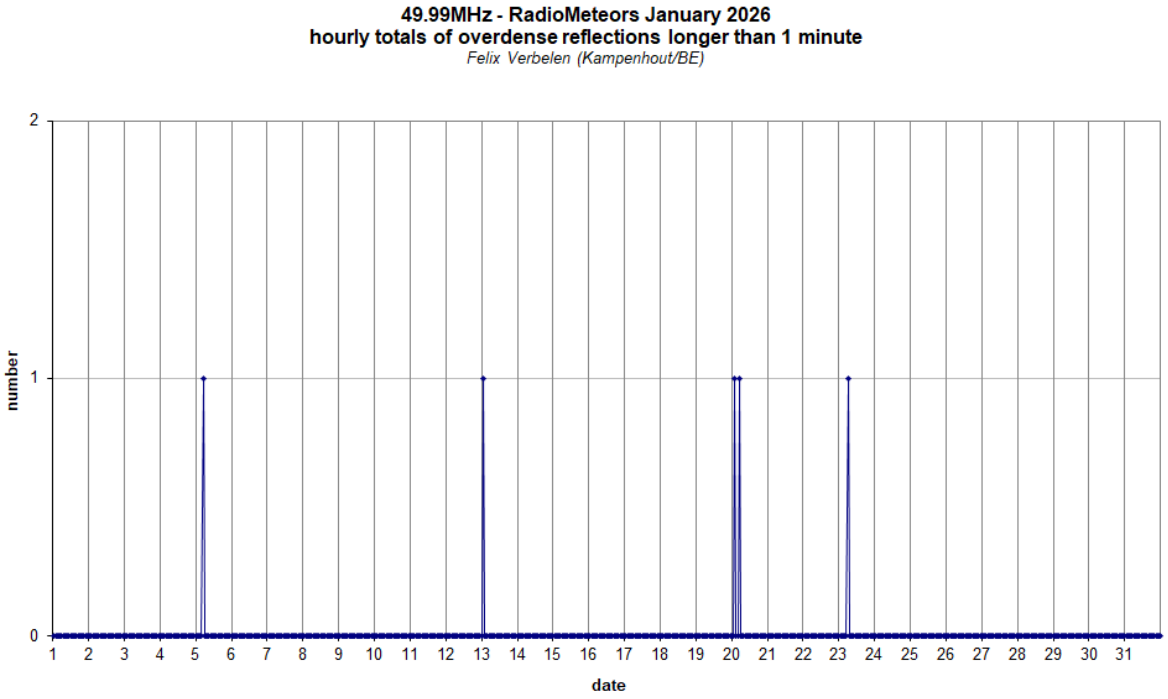

Figure 4 – The hourly numbers of overdense reflections longer than 10 seconds and longer than 1 minute, as observed here at Kampenhout (BE) on the frequency of our VVS-beacon (49.99 MHz) during January 2026.

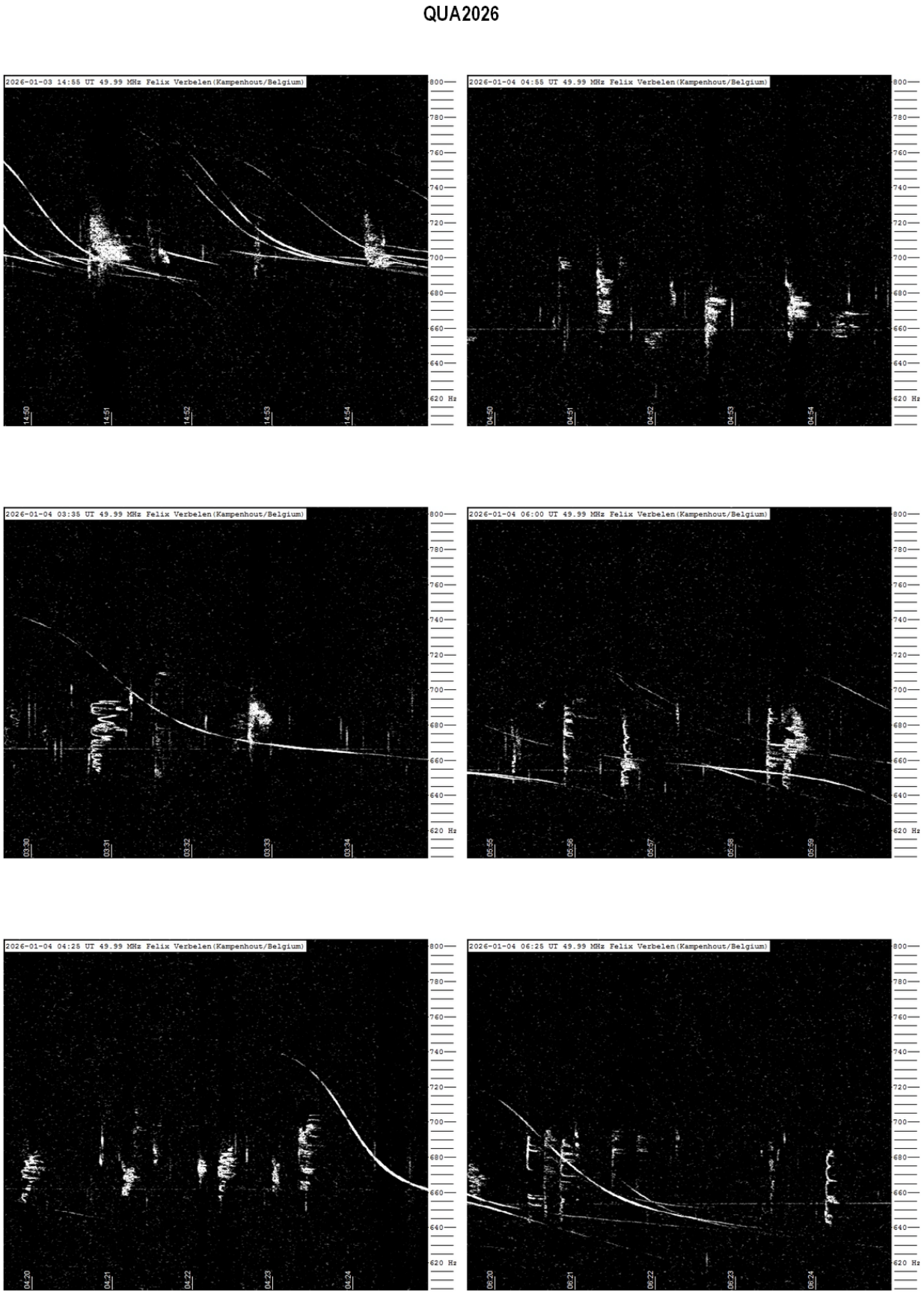

Figure 5 – Selection of meteor radio echoes during the Quadrantids 2026.

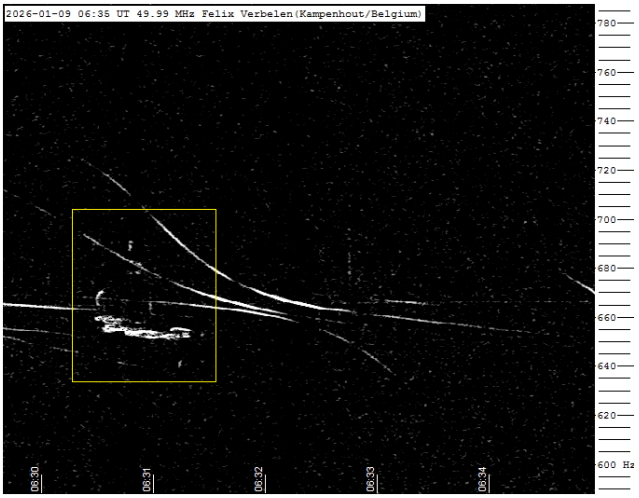

Figure 6 – Meteor echo January 09, 06^{h}35^{m} UT.

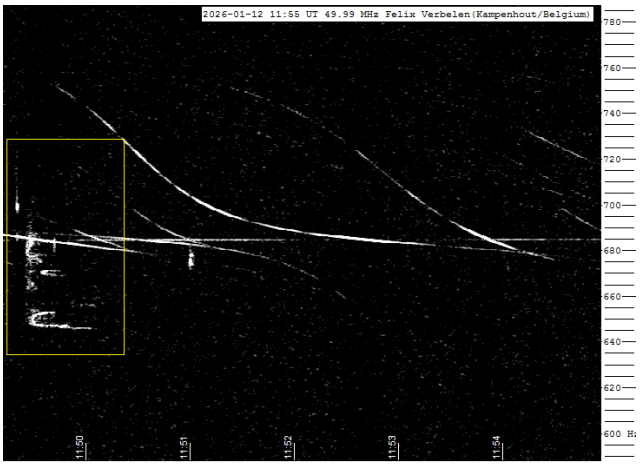

Figure 7 – Meteor echo January 12, 11^{h}55^{m} UT.

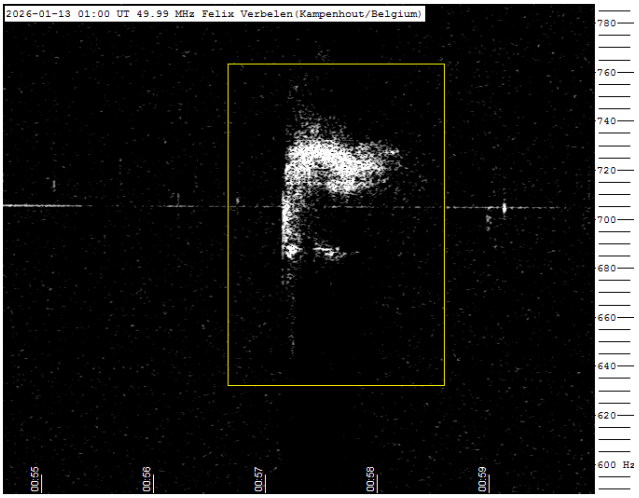

Figure 8 – Meteor echo January 13, 01^{h}00^{m} UT.

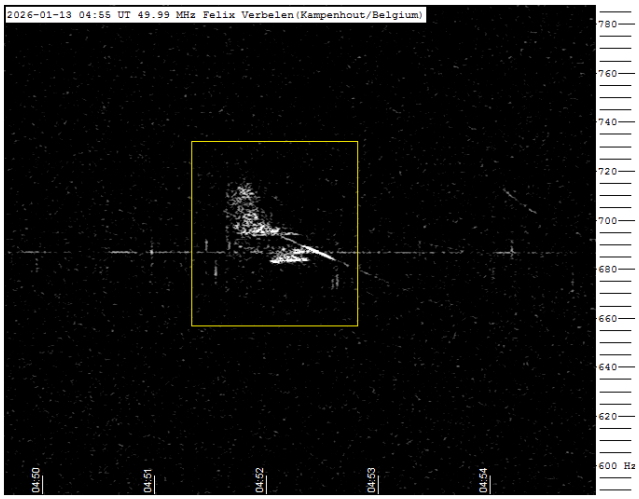

Figure 9 – Meteor echo January 13, 04^{h}55^{m} UT.

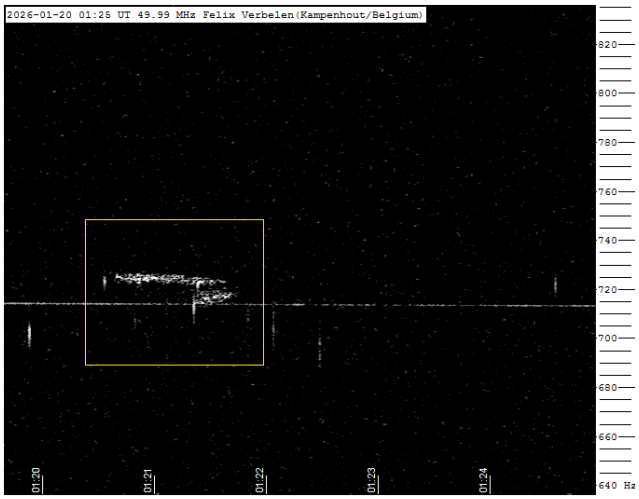

Figure 10 – Meteor echo January 20, 01^{h}25^{m} UT.

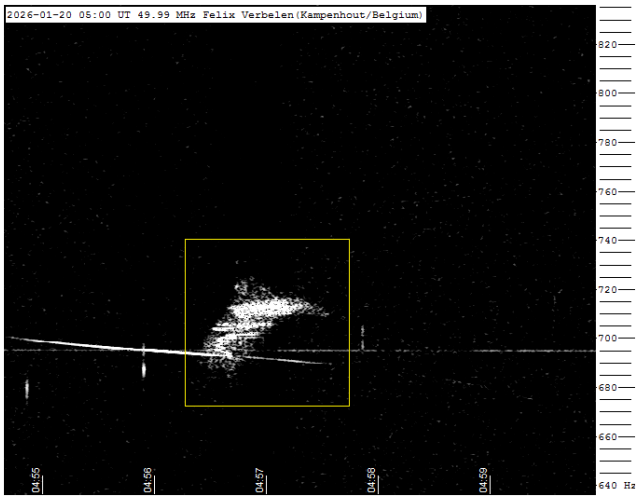

Figure 11 – Meteor echo January 20, 05^{h}00^{m} UT.

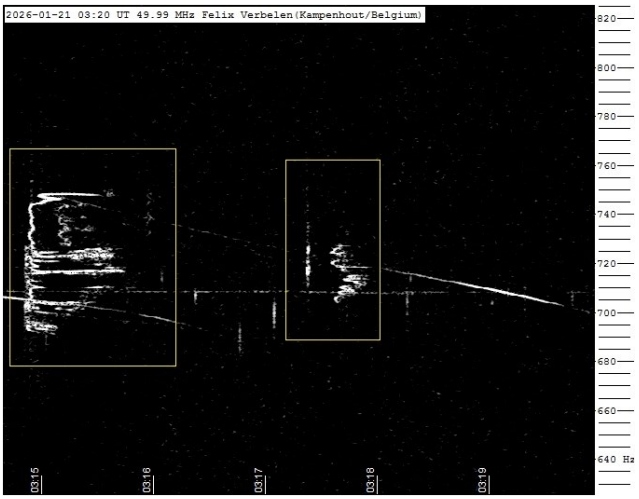

Figure 12 – Meteor echo January 21, 03^{h}20^{m} UT.

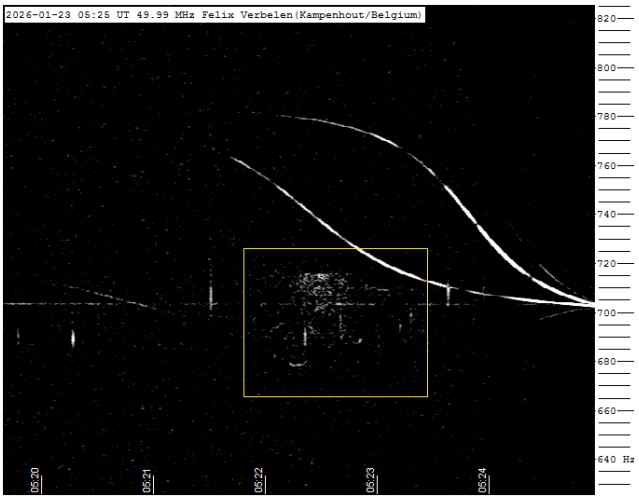

Figure 13 – Meteor echo January 23, 05^{h}25^{m} UT.

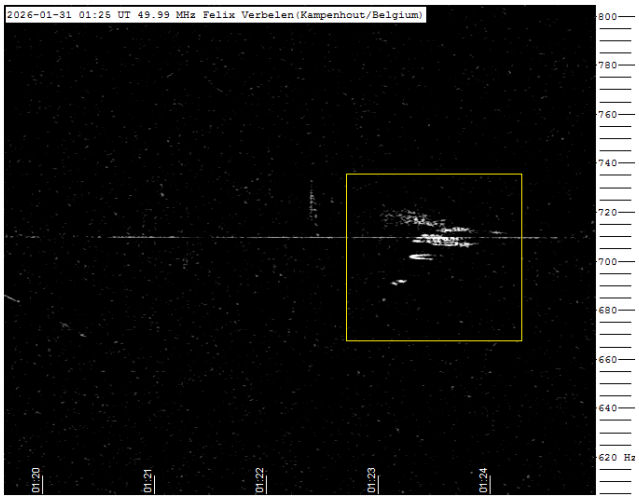

Figure 14 – Meteor echo January 31, 01^{h}25^{m} UT.

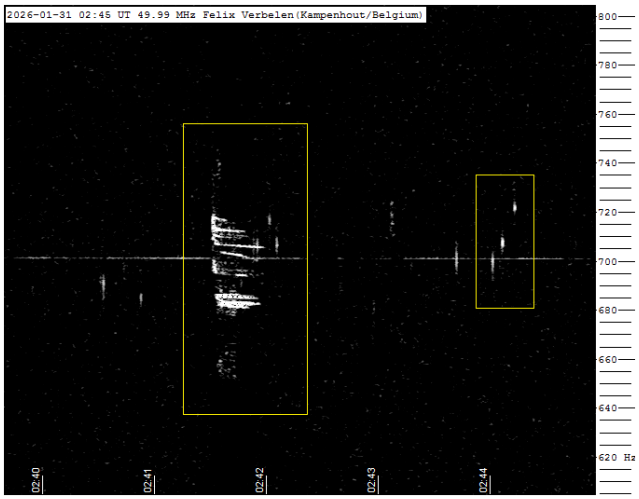

Figure 15 – Meteor echo January 21, 02^{h}45^{m} UT.

eMetN METEOR JOURNAL

Since 2016 the mission of eMetN Meteor Journal is to offer meteor news to a global audience and to provide a swift exchange of information in all fields of active amateur meteor work. eMetN Meteor Journal is freely available without any fees. eMetN Meteor Journal is independent from any country, society, observatory or institute. Articles are abstracted and archived with ADS Abstract Service: https://ui.adsabs.harvard.edu/search/q=eMetN

You are welcome to contribute to eMetN Meteor Journal on a regular or casual basis, if you wish to. Anyone can become an author or editor, for more info read: https://www.emeteornews.net/writing-content-for-emeteornews/

Articles for eMetN Meteor Journal should be submitted to: paul.roggemans@gmail.com

Contact: info@emeteornews.net

Contributors:

- Barbieri L.
- Campbell-Burns P.
- Greaves J.
- Harachka Y.
- Kalina M.
- Maglione M.
- McIntyre M.
- Ogawa H.
- Roggemans P.
- Scott J.M.
- Šegon D.
- Verbelen F.
- Vida D.
- Wood J.

Online publication https://www.emeteornews.net and https://www.emetn.net
ISSN 3041-4261, publisher: Paul Roggemans, Pijnboomstraat 25, 2800 Mechelen, Belgium